Inhibition Studies on Hypoxia-Inducible Factor (HIF) Hydroxylases

A thesis submitted to the Board of the Faculty of Physical Sciences of the University of Oxford in partial fulfilment of the requirements for the degree of Doctor of Philosophy

Mun Chiang Chan
Department of Chemical Biology
St Cross College, Oxford
Trinity Term 2014

Abstract

The hypoxia-inducible factor (HIF) is a key regulator of transcriptional responses to hypoxia in animals. As part of the cellular response to decreased oxygen concentrations, the transcriptional activity of a heterodimeric complex consisting of HIFα and HIFβ activates the expression of hundreds of target genes, including those involved in cellular growth, apoptosis, energy metabolism and angiogenesis. HIFα prolyl hydroxylation, as catalysed by the HIF prolyl hydroxylases (PHDs), leads to subsequent HIFα polyubiquitination and proteasomal degradation. HIFα asparaginyl hydroxylation as catalysed by factor inhibiting HIF (FIH), blocks the binding of HIFα to the co-activators CBP/p300, leading to reduced HIF transcriptional activity. The activities of the HIF hydroxylases (the PHDs and FIH) can be suppressed under limiting oxygen, resulting in the stabilisation of HIFα and activation of the HIF pathway. The development of PHD inhibitors in order to mimic aspects of the natural hypoxic response has been reported, although the selectivity of the inhibitors has not been investigated. Identification of selective small molecule inhibitors for the PHDs would enable further investigations into the differential role of the HIF hydroxylases in mediating the transcriptional response to hypoxia. Both the PHDs and FIH are part of the Fe(II) and 2-oxoglutarate (2OG)-dependent dioxygenase family, which includes histone and nucleic acid demethylases that are involved in gene regulation. The transcriptional response to hypoxia and/or the effects of non-selective PHD inhibitors could thus be mediated by their effects on these closely related enzymes. In the work described in this thesis, *in vitro* hydroxylation assays for PHD2 were developed for the identification of PHD inhibitors and determination of their inhibitory potencies. The development of a cellular assay for HIF levels is also described and used to measure the efficacy of PHD inhibitors. The utilisation of these assays led to the identification of potent, selective and cell-permeable PHD inhibitors suitable for use as chemical probes to study the biological roles of the PHDs. To aid in selectivity studies with the PHD isoforms, a cellular model system was developed by the re-expression of individual PHD isoforms in PHD-null mouse embryonic fibroblast cells. PHD inhibitors, including one of the PHD chemical probes identified, were used in a pan-genomic study of the transcriptional response by hypoxia in human breast cancer MCF-7 cells. The results reveal that inhibition of the PHDs, together with FIH, does not fully induce the full set of hypoxia upregulated genes, suggesting that the activation of HIF transcriptional activity alone may not be sufficient to invoke the transcriptional response to hypoxia.

Mun Chiang Chan
St Cross College

Trinity Term 2014

Acknowledgements

My utmost gratitude is extended to my supervisor, Prof. Chris Schofield for giving me the opportunity to work on my D. Phil project in his laboratory, for being a great mentor and for all the encouragements he has given me throughout the years. I will forever be indebted to him for shaping me to be the scientist I am today. I would also like to thank my co-supervisor, Dr. Emily Flashman for all the supervision and helpful discussions over the years. I am especially thankful for her critical reading of my thesis and for all the constructive comments.

I am enormously grateful to Prof. Sir Peter Ratcliffe and Prof. Chris Pugh, for being my informal supervisors throughout the extensive collaborative work carried out in their laboratories at the Centre of Cellular and Molecular Physiology (CCMP). I truly appreciate them for welcoming me warmly, for treating me as part of their research group and for all the advice and constructive criticisms I have received during my D. Phil years.

My deepest appreciation also goes to Dr. Ya-Min Tian and Dr. Akane Kawamura for providing me with day-to-day supervision, guidance and all the help in various experiments. Special thanks also to Dr. Nathan Rose, for his guidance in the early part of my D. Phil project, and Dr. Kar Kheng Yeoh, for being a supportive friend and colleague. I am thankful to all the current and previous members of the Schofield and Ratcliffe/Pugh laboratories, with whom I have the great opportunity to work with over the past three years. In addition to that, I am really appreciative of the various assistance and support from Jenny Houlsby and Catherine King. I am also thankful to all the collaborators within and outside of Oxford who were involved in my projects.

I acknowledge the kind financial support from the Khazanah Foundation in Malaysia, for awarding me a full scholarship to pursue my D. Phil studies.

This work is dedicated to my parents, for blessing me with their love and continuous support throughout my life. Thank you also to Debbie for being there for me.

Abbreviations

(S/B)	signal-to-background ratio
(P/N)	ratio of mean positive signal over mean negative signal
β_2AR	β2-adrenergic receptor
2OG	2-oxoglutarate
ADM	adrenomedullin
ALPHA	amplified luminescent proximity homogeneous assay
ARD	ankyrin repeat domain
ARNT	aryl hydrocarbon receptor nuclear translocator
AS	AlphaScreen
Asn	asparagine
Asp	aspartic acid
ATF4	activating transcription factor 4
ATP	adenosine triphosphate
BBOX	γ-butyrobetaine hydroxylase
bHLH	basic helix-loop-helix
BIQ	2-(1-chloro-4-hydroxyisoquinoline-3-carboxamido) acetic acid
BMAL1	brain and muscle ARNT-like 1
BNS	bicyclic naphthalenylsulfone
BSA	bovine serum albumin
C	Celcius
C-P4H	collagen prolyl 4-hydroxylase
CA9	carbonic anhydrase IX
CAD	*C*-terminal transactivation domain
CBP	CREB-binding protein
cDNA	complementary DNA
Cep192	Centrosomal protein of 192 kDa
CLK2	CDC-like kinase 2
CLOCK	circadian locomoter output cycles protein kaput
CODD	*C*-terminal oxygen degradation domain
CTAD	*C*-terminal transactivation domain
Da	Dalton
DCMS	dynamic-combinatorial chemistry linked to mass spectrometry
DFO	deferoxamine
DM-NOFD	dimethyl *N*-oxalyl-*D*-phenylalanine
DMOG	dimethyloxalylglycine
DMSO	dimethyl sulfoxide
DNA	deoxyribonucleic acid
Dox	doxycycline
DSBH	double-stranded β-helix
EC_{50}	half-maximal effective concentration
EDTA	ethylenediaminetetraacetic acid
ELISA	enzyme-linked immunosorbent assay
EPO	erythropoietin
ER	endoplasmic reticulum
ESI-MS	electrospray ionisation mass spectrometry
FACS	fluorescence-activated cell sorting
FIH	factor-inhibiting HIF

FPKM	fragments per kilobase of transcript per million mapped reads
FTO	fat mass and obesity associated protein
GFP	green fluorescent protein
Glu	glutamine
GST	glutathione-S-transferase
h	hour
HEPES	4-(2-hydroxyethyl)-1-piperazineethanesulfonic acid
HDM	histone demethylase
HIF	hypoxia-inducible factor
His	histidine
HRE	hypoxia responsive element
HRP	horseradish peroxidase
Hx	hypoxia
HyPro	hydroxyproline
HyAsn	hydroxyasparagine
IκKβ	IκB kinase-β
IC_{50}	half-maximal inhibitory concentration
IGFBP3	insulin-like growth factor binding protein 3
IgG	immunoglobulin G
IRES	internal ribosome entry site
JmjC	Jumonji-C
K_D	dissociation constant
KEGG	Kyoto Encyclopaedia of Genes and Genomes
K_M	Michaelis constant
L	litre
LC-MS	liquid chromatography coupled to mass spectrometry
l.e.	long exposure
LOCI	luminescent oxygen channelling immunoassay
M	molar
MALDI-TOF	matrix-assisted laser-desorption/ionisation-time of flight
MEF	mouse embryonic fibroblast
Met	methionine
min	minute
mM	millimolar
MOP3	member of PAS protein 3
mRNA	messenger RNA
MS	mass spectrometry
MSD	Meso Scale Discovery
NDRG1	N-myc downstream regulated gene 1
NFκB	nuclear factor enhancing kappa light-chain gene expression in B cells
NODD	*N*-terminal oxygen degradation domain
NOFD	*N*-oxalyl-*D*-phenylalanine
nm	nanometer
nM	nanomolar
NMR	nuclear magnetic resonance
NOG	*N*-oxalylglycine

NTAD	*N*-terminal transactivation domain
Nx	normoxia
ODD	oxygen degradation domain
p300	E1A binding protein p300
P4H-TM	transmembrane prolyl 4-hydroxylase
PAGE	polyacrylamide gel electrophoresis
PAS	Per-Arnt-Sim
PCR	polymerase chain reaction
PDB	protein data bank
Per	period circadian protein
PH-4	transmembrane prolyl 4-hydroxylase
PHD	prolyl-hydroxylase domain containing protein
PKM2	pyruvate kinase isoenzyme type M2
Pro	proline
PVDF	polyvinylidene difluoride
pVHL	von Hippel-Lindau tumor suppressor protein
qRT-PCR	real-time quantitative PCR
Rbp1	RNA-binding protein 1
RIPA	radioimmunoprecipitation assay
RNA	ribonucleic acid
RNA-seq	RNA-sequencing
SDS	sodium dodecyl sulfate
sec	second
Sim	single-minded protein
siRNA	small interfering RNA
TAD	transactivation domain
Tet	tetracycline
TKO	triple PHD knockout
tPHD2	PHD2 (residues 181-426)
TRPA1	transient receptor potential cation channel subfamily A member 1
TR-FRET	time-resolved fluorescence resonance energy transfer
TPA	triproprylamine
Trp	tryptophan
Tyr	tyrosine
USD	urea-SDS
VCB	pVHL-Elongin C-Elongin B

Table of Contents

Chapter 1: Introduction

1.1 Historical perspective

The birth and early evolution of metazoans is thought to have occurred some 500 million year ago, following the rise of atmospheric oxygen levels on Earth as caused by the expansion of oxygen-producing photosynthetic cyanobacteria [1]. As they evolved from mitochondria-containing eukaryotes, metazoans developed the capability to utilise atmospheric oxygen for energy production from the breakdown of glucose by oxidative phosphorylation, as opposed to the less efficient anaerobic glycolysis [1]. Energy produced from oxidative phosphorylation in the form of adenosine triphosphate (ATP) fuels most of the key processes required for cellular maintenance and survival, and therefore forms the fundamental basis of the dependency on oxygen for all metazoans, including humans.

Given the importance of oxygen to all metazoans, the presence of mechanisms to sense and respond to fluctuations in oxygen concentrations, both at the cellular and whole organism levels, is crucial. Early efforts to understand the molecular basis of the regulation of physiological response to hypoxia focused on erythropoietin (EPO). The production of EPO, a glycoprotein hormone involved in erythropoiesis (the formation of red blood cells), was observed to be induced at low oxygen levels [2, 3]. Further detailed studies on the *EPO* gene locus revealed a short sequence of DNA (located at the 3′ end of the gene locus) that controls the transcription of *EPO* in an oxygen-dependent manner [4-6]. The discovery of this DNA element subsequently led to the characterisation of the transcription factor that binds to this sequence, i.e. the hypoxia-inducible factor (HIF) [4, 7]. HIF was subsequently found to bind similar sequences of DNA (termed the hypoxia responsive elements, HREs) to control the

expression of a myriad of genes induced in response to limiting oxygen. HIF is now regarded as a master regulator of the cellular transcriptional response to hypoxia [8].

1.2 The hypoxia-inducible factor (HIF) oxygen sensing pathway

HIF is a heterodimeric transcription factor complex consisting of two subunits, namely the HIFα and HIFβ subunits [7]. Both HIF subunits are part of the basic helix-loop-helix (bHLH)-Per-Arnt-Sim (PAS) protein family [7]. HIFα is constitutively synthesised in cells but is rapidly degraded under normoxic conditions (normoxia). In the presence of sufficient oxygen, the hydroxylation of conserved prolyl-residues located within the oxygen dependent degradation domains (ODDs) of HIFα is catalysed by the prolyl hydroxylase domain (PHD) enzymes (**Figure 1.1**) [9-13]. This oxygen-dependent prolyl hydroxylation occurs within the conserved LXXLAP motifs of HIFα, and forms a recognition site for the binding of the von Hippel-Lindau tumour suppressor protein (pVHL). pVHL is a targeting component of the VCB (pVHL-Elongin C-Elongin B) complex, which causes polyubiquitination and subsequent degradation of HIFα via the 26S proteasomal pathway [9-13]. Under low oxygen concentrations, when oxygen is limiting, the activity of the PHDs are inhibited, leading to reduced HIFα prolyl-hydroxylation, thereby hindering HIFα degradation and resulting in the stabilisation of HIFα. The stabilised HIFα subsequently translocates to the nucleus, forms a complex with HIFβ, and binds to the HRE sequences (RCGTG) in the DNA for the activation of its target genes [7, 14]. A further level of transcriptional regulation is established through the activity of factor inhibiting HIF (FIH), which hydroxylates an asparagine (Asn) residue located in the HIFα *C*-terminal transactivation domain (CTAD) [15-17]. Hydroxylation of this Asn residue prevents the binding of HIFα to the CH1 domain of co-activators CBP/p300, leading to a decrease in HIFα transcriptional activity [15-20]. Of note, it has been proposed that CBP/p300 also binds HIFα at the *N*-terminal transactivation domain (NTAD) and is thus

able to form a transcriptionally active HIF complex, albeit via a different domain (CH3) [21]. The PHDs and FIH, collectively termed the HIF hydroxylases, are assigned as cellular oxygen sensors due to their kinetic properties in isolation and in cells, which link their use of oxygen to HIFα degradation. The HIF hydroxylases thereby connects the availability of oxygen directly to the transcriptional control of the hypoxic response.

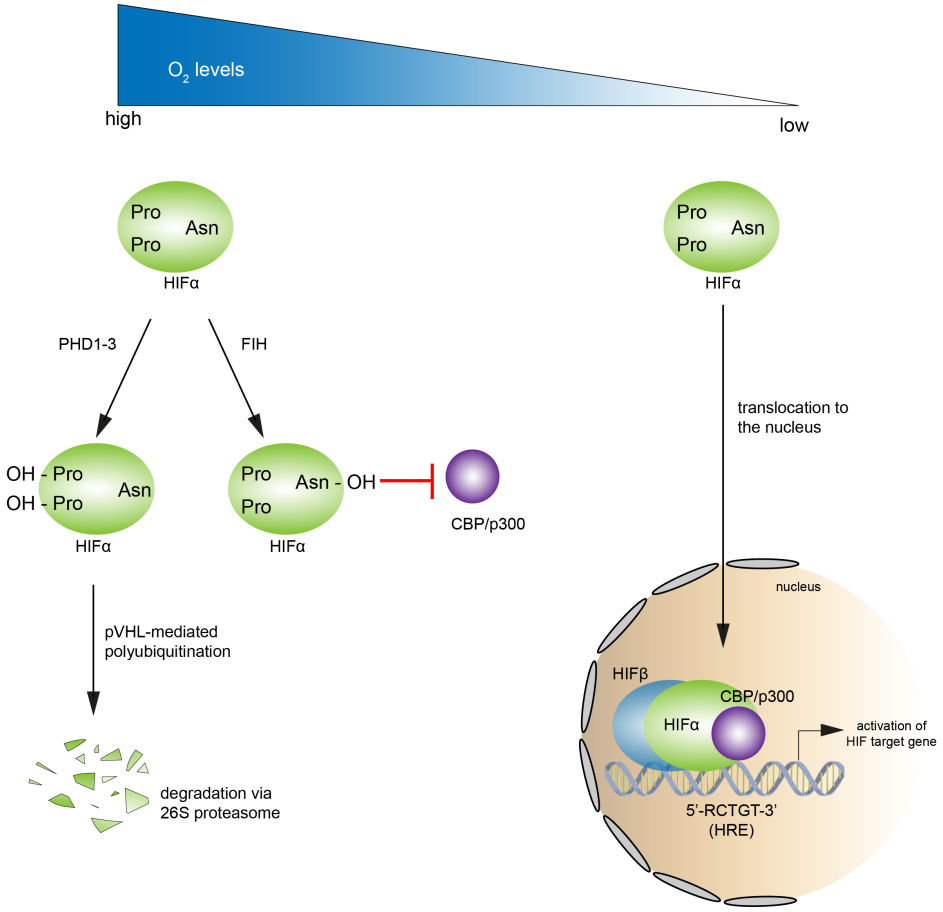

Figure 1.1 Schematic diagram illustrating the regulation of HIFα by the PHDs and FIH. When oxygen is not limiting, the PHDs hydroxylate conserved proline residues in the oxygen degradation domains of HIFα (Pro402 and Pro564 in human HIF1α), leading to pVHL-mediated polyubiquitination and proteolytic degradation. FIH hydroxylates an asparagine residue in the *C*-terminal transactivation domain of HIFα (Asn803 in human HIF1α), which blocks the binding of HIFα to co-activators CBP/p300. When oxygen levels become limiting, the HIFα prolyl and asparaginyl hydroxylations are suppressed, leading to the stabilisation and activation of HIF transcriptional activity. PHD: prolyl hydroxylase domain enzyme, FIH: factor inhibiting HIF, Pro: Proline, OH-Pro: Hydroxyproline, Asn: Asparagine, Asn-OH: Hydroxyasparagine, pVHL: von Hippel-Lindau tumour suppressor protein, CBP: CREB-binding protein, p300: E1A binding protein p300, HRE: hypoxia-responsive element.

1.3 The hypoxia-inducible factors (HIFs)

In humans, there are three isoforms of the HIFα subunit, with HIF1α being the first to be discovered [7], followed by HIF2α [22], and then HIF3α [23]. HIF1α is ubiquitously expressed across different tissues and cells. HIF2α expression was initially thought to be restricted to endothelial cells [22], but was later found to be widely expressed in various human cell lines [24] and in multiple organs in rats [25]. The HIF1α and HIF2α proteins share a high degree of similarity; they both contain a bHLH domain, two PAS domains, *N*- and *C*-terminal oxygen dependent degradation domains (ODDs), and *N*- and *C*-terminal transactivation domains (TADs) (**Figure 1.2**). The bHLH and PAS domains are important for DNA binding and dimerisation with the HIF1β subunit [26]. HIF3α is less well studied and its role is still not well understood. Studies have shown that HIF3α mRNA is subjected to numerous alternative splicing events, with each variant expressed variably across human tissues [27, 28]. In contrast to HIF1α and HIF2α, none of the human HIF3α splice variants contain the CTAD domain, and they only possess one conserved proline residue in the ODD domain corresponding to the proline residue 564 of the HIF1α CODD (except one variant, HIF3α-4 which does not have an ODD domain) [27, 28]. In a similar manner to HIF1α and HIF2α, the conserved proline in HIF3α splice variants can be hydroxylated by the PHDs and the hydroxylated form is a target for pVHL binding, polyubiquitination and subsequently, proteasomal degradation [28, 29]. HIF3α splice variants have been proposed to act either as dominant negative regulators, or as transcriptional activators in a context-dependent manner [28-31].

The other subunit of the HIF heterodimer is HIF1β, also known as the aryl hydrocarbon receptor nuclear translocator (ARNT) [7]. There are two homologues of HIF1β, namely ARNT2 [32] and ARNT3 (also known as MOP3, BMAL1) [33]. HIF1β is thought to be the

primary binding partner of the HIFα subunits, although later studies suggest that ARNT2 can also form a heterodimer with HIF1α and participate in the HIF-mediated transcriptional response [34, 35]. On the other hand, ARNT3 is not thought to be involved in the hypoxic response *in vivo* [36] but dimerises with another member of the bHLH-PAS protein family, CLOCK as part of the regulation of the mammalian circadian rhythm [37]. HIF1β is expressed ubiquitously [32, 38], whereas ARNT2 expression is restricted to the central nervous system and kidney [32, 39]. Interestingly, hypoxic upregulation of HIF1β was initially observed at the protein and mRNA levels in human hepatoma Hep3B cells exposed to 1% O_2 [7], in contrast to the generalised view that it is not subjected to oxygen regulation. Recent studies show that the hypoxic regulation of HIF1β is observed in some cell lines (such as Hep3B, human breast cancer MCF-7 cells, human melanoma 518A2 and A375 cells), but not others (such as human neuroblastoma Kelly cells and human hepatocellular carcinoma HepG2 cells) [40-42]. This hypoxic regulation of HIF1β protein was also shown to be dependent on the length and severity of the hypoxic exposure [40-42]. It has been proposed that this may be a cell-type specific regulatory mechanism to prevent HIF1β from becoming limiting [40], and could be involved in the proposed role of long HIF3α splice variants acting either as dominant negative regulators or activators of HIF transcriptional response depending on the cellular HIF1β availability [28].

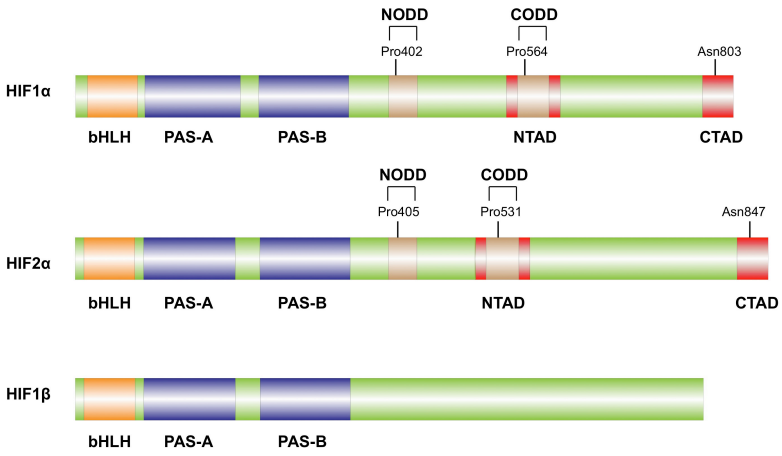

Figure 1.2 Domain structures of the human HIF1α, HIF2α and HIF1β. Figure adapted from [8].

1.4 The HIF prolyl and asparaginyl hydroxylases

The HIF hydroxylases are part of the Fe(II)/2OG dependent dioxygenase enzyme family, which consists of more than 60 human enzymes involved in a variety of biological roles (including collagen biosynthesis, fatty acid metabolism, histone demethylation and nucleic acid demethylation) [43]. There are three HIF prolyl hydroxylase isoforms, PHD1, PHD2 and PHD3 [12, 13]. All three PHDs share a high degree of sequence conservation within their *C*-terminal catalytic domains [44], although they have different substrate preferences. PHD1 and 2 have been shown to catalyse the hydroxylation of both CODD and NODD, whereas PHD3 only hydroxylates CODD efficiently both *in vitro* and in cells [12, 45, 46]. A flexible loop (between β-strands 2 and 3 of PHD2 [47, 48], **Figure 1.3**) involved in substrate binding has been demonstrated to play a role in this apparent substrate selectivity [44]. Studies across multiple human cell lines under normoxia have revealed a more abundant and widespread expression of PHD2 protein, whereas the protein levels of PHD1 and PHD3 are more restricted and generally lower [49]. There were also differences in the sub-cellular localisations for each of the PHD isoforms, with PHD1 detected exclusively in the nucleus, PHD2 mainly in the cytoplasm and PHD3 distributed homogenously in the cytoplasm and the nucleus (based on localisation of overexpressed FLAG-tagged proteins in human osteosarcoma U2OS cells as observed by confocal microscopy) [50]. Another similar study by confocal microscopy using overexpressed FLAG-tagged PHD1, PHD2 and PHD3 in African green monkey kidney cell line (COS-1) showed that PHD1 is predominantly nuclear, whereas PHD2 and PHD3 are predominantly cytoplasmic [51].

The existence of a fourth HIF prolyl hydroxylase, P4H-TM (or PH-4) has also been proposed [52, 53]. P4H-TM appears to be more similar to the collagen prolyl hydroxylases (CPHs) than the PHDs (based on amino acid sequence homology) and it is localised in the endoplasmic

reticulum (ER) membrane [52, 53]. Although *in vitro* studies show that P4H-TM is able to hydroxylate HIF1α NODD and CODD peptide substrates, HIF hydroxylation by this isoform in cells or *in vivo* has not been demonstrated and its effect on HIF may be indirect [53]. Thus, its proposed role as a HIF hydroxylase requires further investigation.

Like the PHDs, the HIF asparaginyl hydroxylase FIH is also a 2OG-dependent dioxygenase, although it is more closely related to the 2OG-dependent dioxygenase subfamily of JmjC-domain containing proteins than the PHDs [17, 54]. Like PHD2, FIH is also found mainly in the cytoplasm (based on overexpression of FLAG-tagged FIH in U2OS cells) [50]. Studies on human cell lines reveal that FIH protein is broadly expressed across multiple cell lines [55].

Crystal structures of the catalytic domains of PHD2 (tPHD2) [47, 48] and FIH [54, 56] reveal the presence of a double-stranded β-helix (DSBH) core fold (also known as the jelly-roll fold) conserved in all 2OG-dependent dioxygenases (**Figure 1.3**). Within this motif, the Fe(II) iron is coordinated in an octahedral manner by the highly conserved HXD…H triad found in most 2OG-dependent dioxygenases [8]. Based on crystallographic studies, the Fe(II) ion is coordinated in the FIH active site by the side chains of His199, Asp201 and His279, whereas the Fe(II) ion is coordinated in the PHD2 active site by His313, Asp315 and His374 (**Figure 1.3**). Structural studies also reveal FIH as a dimer, with the *C*-terminal helices from each monomer forming an interlocking arrangement [54, 56].

Both the PHDs and FIH catalyse the hydroxylation of HIF using 2OG and oxygen as co-substrates and releasing succinate and carbon dioxide as products (**Figure 1.4**) [12, 13, 16, 17]. The reaction mechanism for hydroxylation by the PHDs and FIH follows that of the consensus mechanism for all 2OG-dependent dioxygenases (**Figure 1.5**) [57, 58]: 2OG binds

directly to the active site Fe(II) followed by prime substrate binding in close proximity. This induces a conformational change, which enables displacement of the final Fe(II)-coordinated H_2O molecule by O_2. Subsequent oxidative decarboxylation of 2OG leads to formation of succinate, carbon dioxide and a reactive Fe(IV)-oxo intermediate. This intermediate performs the hydroxylation step, likely via hydrogen abstraction and radical rebound. This proposed mechanism is supported by spectroscopic, kinetic and structural evidence [59].

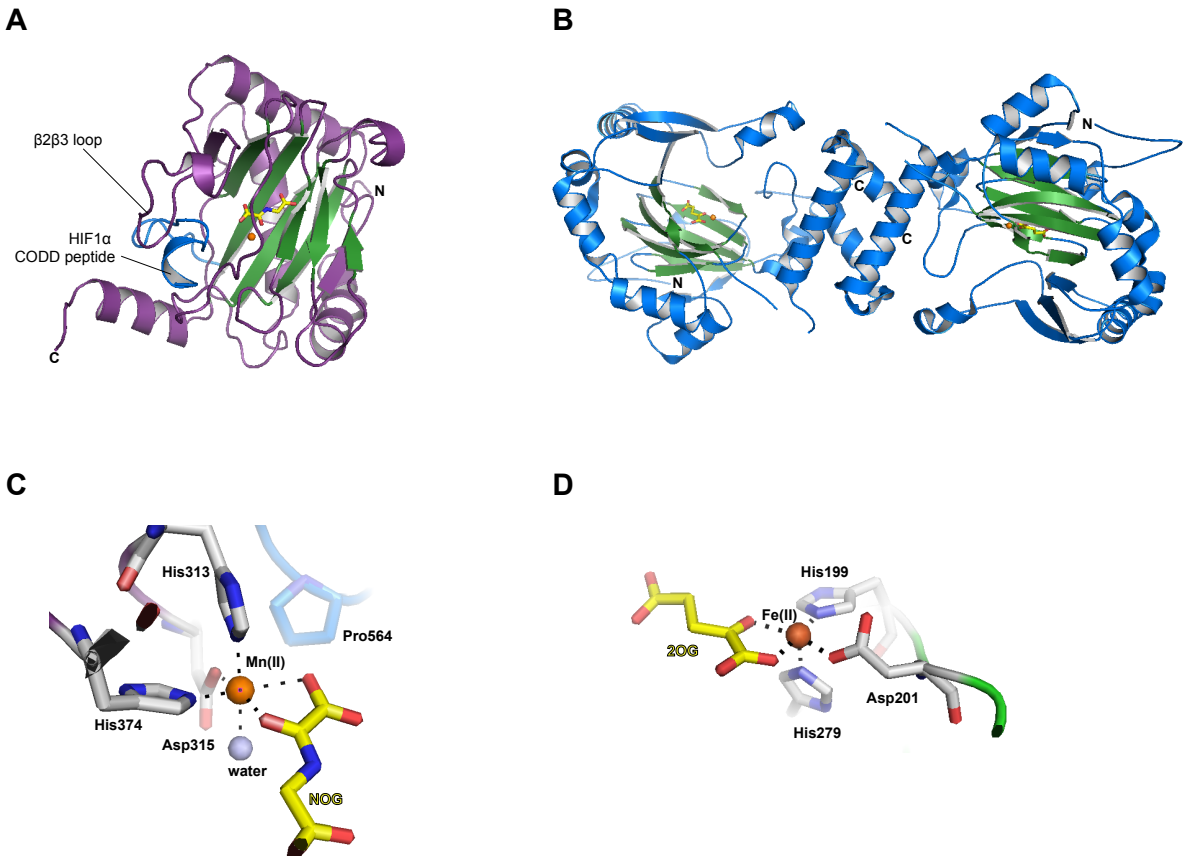

Figure 1.3 Views from crystal structures of the catalytic domains of PHD2 (tPHD2) (PDB ID: 3HQR) [47] and FIH (PDB ID: 1H2N) [54]. (**A**) Cartoon representation of tPHD2 in complex with NOG (yellow), Mn(II) (orange) and HIF1α CODD peptide (blue). (**B**) Cartoon representation of the dimeric FIH in complex with 2OG (yellow) and Fe(II) (orange). (**C**) Active site of PHD2 highlighting the metal coordination by His313, Asp315 and His374. (**D**) Active site of FIH highlighting metal coordination by His199, Asp201 and His279.

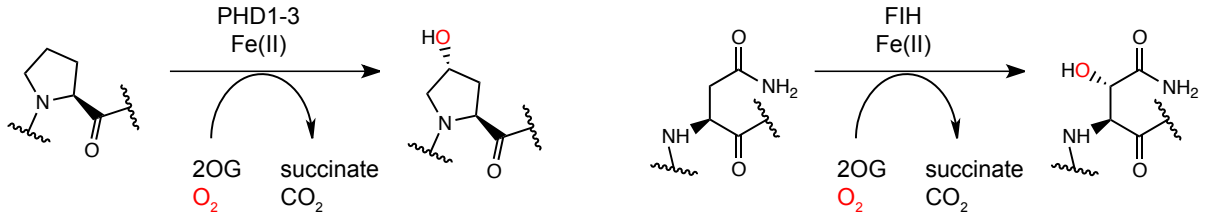

Figure 1.4 HIFα prolyl hydroxylation reaction as catalysed by the PHDs (left). HIFα asparaginyl hydroxylation reaction as catalysed by FIH (right). Figure adapted from [60].

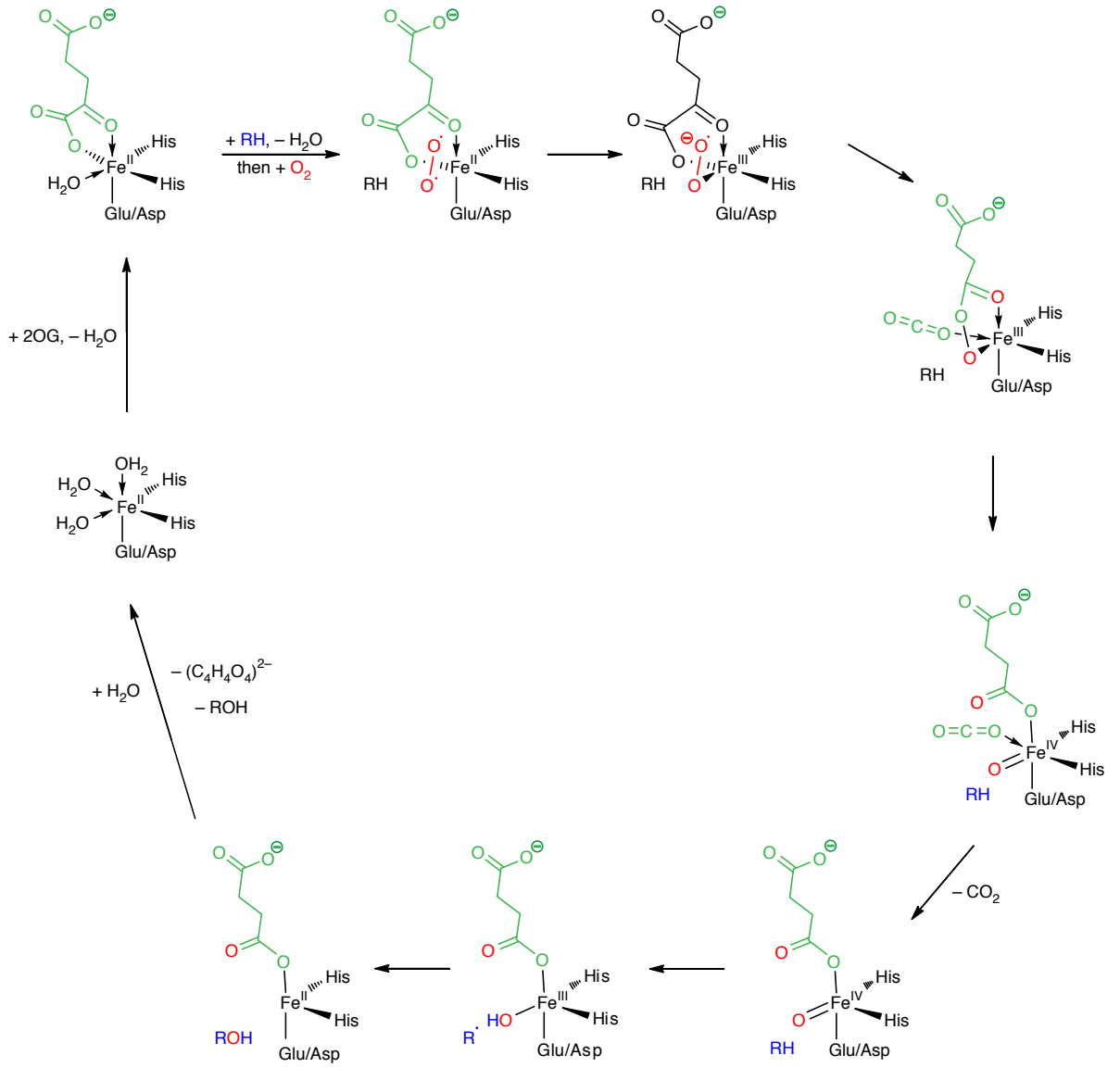

Figure 1.5 Outline of the consensus reaction mechanism of 2OG-dependent dioxygenases (refer to main text for details). Figure adapted from [61].

1.5 HIF hydroxylases as oxygen sensors

The oxygen-dependent nature of HIF hydroxylation led to the proposal that the HIF hydroxylases act as cellular oxygen sensors. For an enzyme to be considered an oxygen sensor, its activity in cells must be sensitive to changes in oxygen concentration over a biologically relevant range. It is proposed that from a kinetic perspective, this might be characterised by a high $K_M(O_2)$; the $K_M(O_2)$ of FIH has been reported to be in the range of 90-150 μM, whereas the $K_M(O_2)$ values of the PHDs have been reported to be 200-250 μM, depending on the lengths and sequence of HIF1α peptides used as substrates [46, 62]. The particularly high values reported for the PHDs indicate that these enzymes may be highly sensitive to changes in O_2 concentration (under non-limiting concentrations of all other factors). The observations that PHD2 reacts slowly with oxygen *in vitro* suggests that the reaction with oxygen is rate limiting, consistent with its role as oxygen sensor [63]. Overall, the kinetic data indicate that the activities of the PHDs and, to a lesser degree FIH, may be limited by the levels of oxygen in cells (which is expected to be lower than the apparent K_M values for oxygen determined for the HIF hydroxylases), thereby allowing them to function as cellular oxygen sensors [64]. Cellular studies have indeed revealed that FIH remains active in a greater degree of hypoxia than the PHDs [55, 65].

PHD2 has been regarded as the dominant oxygen sensor in cells in normoxia, based on the abundance of PHD2 in multiple cell types and the greater stabilisation of HIF1α by PHD2 silencing alone [49, 66]. Additionally, systemic homozygous PHD2 deletion in mice leads to embryonic lethality, whereas mice with homozygous deletion of PHD1 and PHD3 are viable [67]. However, all three PHDs are proposed to play non-redundant roles and contribute to the regulation of HIF1α and HIF2α, as shown by the greater stabilisation of HIF1α when all three PHD isoforms were downregulated [49]. Haematological defects were also observed in mice

with the genetic deletion of both the PHD1 and PHD3 [68]. Interestingly, silencing of PHD3 in cells under normoxia appear to lead to greater stabilisation of HIF2α, suggesting that it may play a more important role in the regulation of HIF2α than HIF1α [49].

1.6 Alternative substrates for the HIF hydroxylases

Apart from the HIFα subunits, multiple alternative substrates have been reported for the HIF hydroxylases. Studies have reported that PHD1 and PHD2 are involved in the hydroxylation of IκB kinase-β (IκKβ), and thereby the regulation of NFκB-mediated transcriptional response [69]. PHD1 is also required for the pVHL-dependent hydroxylation and regulation of Rbp1, the large subunit of the RNA polymerase II complex [70]. PHD3 has been reported to be involved in the oxygen-dependent stability of activating transcription factor 4 (ATF4) [71]. However, no evidence of direct hydroxylation of these substrates by the PHDs *in vitro* and in cells have been reported to date.

The ubiquitination and proteasomal degradation of the β_2-adrenergic receptor (β_2AR) have also been shown to be dependent on prolyl hydroxylation proposed to be mediated by PHD3 [72]. The hydroxylation of β_2AR was shown to be dependent by PHD3 based on matrix-assisted laser-desorption/ionisation time-of-flight (MALDI-TOF) mass spectrometry analyses on GST-β_2AR (purified from *Escherichia coli*) exposed to HEK293 cell lysates with and without depletion of PHD3 by siRNA [72]. PKM2, an isoform of pyruvate kinase, the glycolytic enzyme involved in the conversion of phosphoenolpyruvate to pyruvate, is another substrate proposed to be hydroxylated by PHD3 [73]. Prolyl hydroxylation of PKM2 by PHD3 was shown by the detection of hydroxylated proline in immunoprecipitated V5-tagged-PKM2 expressed in control HeLa cells, which was reduced in PHD3-silenced HeLa cells (detection of hydroxylated proline was by immunoblotting with antibody for hydroxyproline)

[73]. TRPA1, a member of the transient receptor potential (TRP) ion channels involved in the sensory system, was also demonstrated to be mediated by the PHDs, with direct hydroxylation of TRPA1 peptide by isolated PHD2 observed by MALDI-TOF [74]. CLK2, the human homolog of the *Caenorhabditis elegans* biological clock protein clk-2 involved in DNA damage response, was proposed to be hydroxylated by PHD3, with hydroxylation of GST-tagged CLK2 by recombinant PHD3 studied using radiolabelled 2OG decarboxylation assay [75]. Hydroxylation of a centrosomal protein Cep192 was proposed to be mediated by PHD1, based on the +16 Da mass shift of Cep192 fragment peptide observed by mass spectrometry after reaction with recombinant PHD1 *in vitro* [76].

In addition to HIFα, ankryin repeat domain (ARD)-containing proteins were identified as the hydroxylation substrates of FIH, which include at least six ARD-containing proteins involved in the NFκB transcriptional response [77]. This finding led to the subsequent identification of many other ARD-containing proteins as FIH substrates (mostly involved in signalling pathways) [78-83]. Given that human ARD-containing proteins are predicted to number in the region of 300 proteins, the hydroxylation substrates of FIH may be common, although the function of such hydroxylation and their effect on HIF regulation is not yet understood [83]. It has been reported that FIH is able to distinguish HIF from the other ARD-containing proteins, which may be important in the oxygen-dependent HIF regulation by FIH [84].

The increasing evidence of alternative substrates for the HIF hydroxylases suggests that they could: 1) be involved as part of the cellular adaptation to the changes of oxygen levels, 2) act as a substrate competitor or activator of the HIF-mediated response, or 3) have unique function(s) that may not be linked to the cellular response to hypoxia. Further studies to

understand the functional consequences of non-HIF substrate hydroxylation by PHDs and FIH is therefore crucial and may give further insights into the cellular response to hypoxia.

1.7 Inhibition of the HIF prolyl hydroxylases

HIF has previously been shown to activate a wide range of transcriptional targets important for many cellular processes, including genes involved in growth, apoptosis, transport, cell migration, energy metabolism and angiogenesis (for examples, see review [8]). Recent studies based on chromatin immunoprecipitation coupled to high-throughput sequencing or tiled arrays have revealed around 500 HIF binding sites in any particular cell line studied, based on high stringency criteria (for review, see [85]). Given the involvement of the HIF signalling pathway in a variety of cellular processes, the manipulation of the HIF pathway could be beneficial for treatment of hypoxic related diseases including anaemia, cardiovascular diseases, gastrointestinal disease and wound healing [86-89]. For example, the feasibility of activating the HIF pathway to stimulate EPO production *in vivo* (as a potential therapy for anaemia) has been demonstrated in studies using conditional knockout of the PHDs and small molecule PHD inhibitors [68, 90].

The inhibition of the PHDs can be achieved by the use of iron chelators such as deferoxamine (DFO) or by transition metal ions (such as cobalt, nickel, zinc or manganese ion) to displace the active site iron. Early observations that DFO and cobalt chloride mimic hypoxia [91] were shown to be mediated at least in part, by the inhibition of the PHDs, as shown by the induction of HIF and the reduction in HIF prolyl hydroxylation by immunoblotting [65]. This strategy, however, is non-specific and is likely to affect other metal binding proteins (including other members of the 2OG-dependent dioxygenases). For a more specific inhibition of the PHDs, the 2OG/Fe(II) active site can be targeted, as shown by the identification of 2OG analogues as PHD inhibitors [92]. Selectivity can be achieved by

targeting the 2OG active site, as shown by the identification of a 2OG analogue that inhibits FIH but not PHD2 *in vitro* [93] Nevertheless, the biological selectivity of such inhibitors is dependent on whether they will also bind and inhibit other human 2OG-dependent dioxygenases. A novel class of PHD inhibitors with a specific and non-specific component (which both binds to the 2OG active site and chelate free iron) has been reported ([94], **Chapter 2**). An alternative strategy to induce HIFα has involved the disruption of HIFα-VHL binding to prevent VHL-mediated HIFα polyubiquitination and degradation [95].

A number of inhibitors targeting the HIF prolyl hydroxylases have been reported in the academic and patent literature (for review, see [88, 96]), including some currently in the late stages of clinical trials. Compounds currently in clinical and pre-clinical trials (mostly for the treatment of anaemia of chronic kidney disease) include FG-4592 (developed by Fibrogen) shown in **Figure 1.6 A**, GSK-1278863 (developed by GSK) shown in **Figure 1.6 B**, BAY-85-3934 (developed by Bayer), JTZ-951 (developed by Japan Tobacco) and AKB-6548 (developed by Akebia Therapeutics) [88]. Despite the number of publications related to the identification of PHD inhibitors and the progress of PHD inhibitors in clinical trials, the selectivity of the inhibitors for the PHDs against other members of the 2OG-dependent dioxygenases has not been comprehensively studied. The roles for some 2OG-dependent dioxygenases involved in the regulation of gene expression (for example, the JmjC-domain containing subfamily of histone demethylases and nucleic acid demethylases) raises the question of whether the biological activity of PHD inhibitors could be mediated by the inhibition of these enzymes. This highlights the need for the development of suitable assays to study the selectivity of PHD inhibitors (either within the 2OG-dependent dioxygenase family or within the PHD isoforms). Further studies on the extent to which PHD inhibitors activate

the HIF transcriptional response may also provide useful insight into the possibility of selective manipulation or activation of HIF target genes.

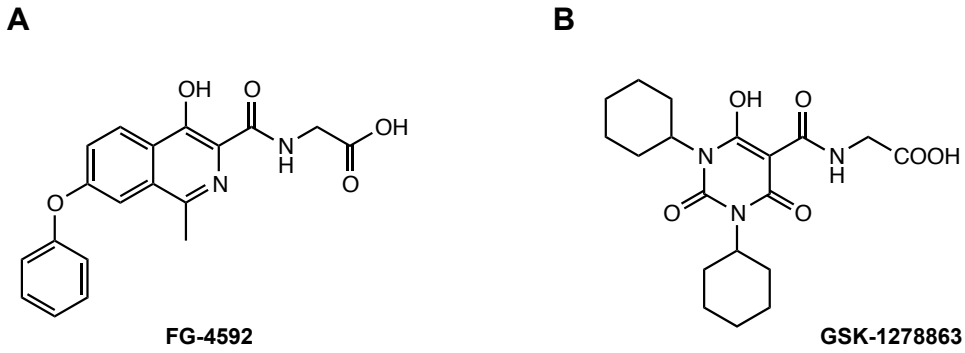

Figure 1.6 Chemical structures of two PHD inhibitors (FG-4592 [88] and GSK-1278863 [97]) currently in clinical trials.

1.8 Aims of this thesis

The overall aims for the work described in this thesis were as follows:

- To develop an *in vitro* hydroxylation assay for PHD2, which could be used for medium- to high-throughput evaluation of PHD inhibitors;
- To develop a quantitative cellular assay for HIF levels, which could be used for the determination of efficacies of PHD inhibitors in cells;
- To identify and characterise suitable PHD inhibitors for use as chemical probes for functional studies of the PHDs;
- To develop a cellular model system for the identification of PHD isoform specific inhibitors;
- To utilise the chemical probe for PHDs to study the transcriptional response to hypoxia.

1.9 References

1 Semenza, G. L. (2007) Life with oxygen. Science. **318**, 62-64

2 Franke, K., Gassmann, M. and Wielockx, B. (2013) Erythrocytosis: the HIF pathway in control. Blood. **122**, 1122-1128

3 Ratcliffe, P. J. (2013) Oxygen sensing and hypoxia signalling pathways in animals: the implications of physiology for cancer. J Physiol. **591**, 2027-2042

4 Semenza, G. L., Nejfelt, M. K., Chi, S. M. and Antonarakis, S. E. (1991) Hypoxia-inducible nuclear factors bind to an enhancer element located 3' to the human erythropoietin gene. Proc Natl Acad Sci U S A. **88**, 5680-5684

5 Beck, I., Ramirez, S., Weinmann, R. and Caro, J. (1991) Enhancer element at the 3'-flanking region controls transcriptional response to hypoxia in the human erythropoietin gene. J Biol Chem. **266**, 15563-15566

6 Pugh, C. W., Tan, C. C., Jones, R. W. and Ratcliffe, P. J. (1991) Functional analysis of an oxygen-regulated transcriptional enhancer lying 3' to the mouse erythropoietin gene. Proc Natl Acad Sci U S A. **88**, 10553-10557

7 Wang, G. L., Jiang, B. H., Rue, E. A. and Semenza, G. L. (1995) Hypoxia-inducible factor 1 is a basic-helix-loop-helix-PAS heterodimer regulated by cellular O2 tension. Proc Natl Acad Sci U S A. **92**, 5510-5514

8 Schofield, C. J. and Ratcliffe, P. J. (2004) Oxygen sensing by HIF hydroxylases. Nat Rev Mol Cell Biol. **5**, 343-354

9 Jaakkola, P., Mole, D. R., Tian, Y. M., Wilson, M. I., Gielbert, J., Gaskell, S. J., von Kriegsheim, A., Hebestreit, H. F., Mukherji, M., Schofield, C. J., Maxwell, P. H., Pugh, C. W. and Ratcliffe, P. J. (2001) Targeting of HIF-alpha to the von Hippel-Lindau ubiquitylation complex by O2-regulated prolyl hydroxylation. Science. **292**, 468-472

10 Maxwell, P. H., Wiesener, M. S., Chang, G. W., Clifford, S. C., Vaux, E. C., Cockman, M. E., Wykoff, C. C., Pugh, C. W., Maher, E. R. and Ratcliffe, P. J. (1999) The tumour suppressor protein VHL targets hypoxia-inducible factors for oxygen-dependent proteolysis. Nature. **399**, 271-275

11 Ivan, M., Kondo, K., Yang, H., Kim, W., Valiando, J., Ohh, M., Salic, A., Asara, J. M., Lane, W. S. and Kaelin, W. G., Jr. (2001) HIFalpha targeted for VHL-mediated destruction by proline hydroxylation: implications for O2 sensing. Science. **292**, 464-468

12 Epstein, A. C., Gleadle, J. M., McNeill, L. A., Hewitson, K. S., O'Rourke, J., Mole, D. R., Mukherji, M., Metzen, E., Wilson, M. I., Dhanda, A., Tian, Y. M., Masson, N., Hamilton, D. L., Jaakkola, P., Barstead, R., Hodgkin, J., Maxwell, P. H., Pugh, C. W., Schofield, C. J. and Ratcliffe, P. J. (2001) C. elegans EGL-9 and mammalian homologs define a family of dioxygenases that regulate HIF by prolyl hydroxylation. Cell. **107**, 43-54

13 Bruick, R. K. and McKnight, S. L. (2001) A conserved family of prolyl-4-hydroxylases that modify HIF. Science. **294**, 1337-1340

14 Wenger, R. H., Stiehl, D. P. and Camenisch, G. (2005) Integration of oxygen signaling at the consensus HRE. Sci STKE. **2005**, re12

15 Lando, D., Peet, D. J., Whelan, D. A., Gorman, J. J. and Whitelaw, M. L. (2002) Asparagine hydroxylation of the HIF transactivation domain a hypoxic switch. Science. **295**, 858-861

16 Lando, D., Peet, D. J., Gorman, J. J., Whelan, D. A., Whitelaw, M. L. and Bruick, R. K. (2002) FIH-1 is an asparaginyl hydroxylase enzyme that regulates the transcriptional activity of hypoxia-inducible factor. Genes Dev. **16**, 1466-1471

17 Hewitson, K. S., McNeill, L. A., Riordan, M. V., Tian, Y. M., Bullock, A. N., Welford, R. W., Elkins, J. M., Oldham, N. J., Bhattacharya, S., Gleadle, J. M., Ratcliffe, P. J., Pugh, C. W. and Schofield, C. J. (2002) Hypoxia-inducible factor (HIF) asparagine hydroxylase is identical to factor inhibiting HIF (FIH) and is related to the cupin structural family. J Biol Chem. **277**, 26351-26355

18 Dames, S. A., Martinez-Yamout, M., De Guzman, R. N., Dyson, H. J. and Wright, P. E. (2002) Structural basis for Hif-1 alpha /CBP recognition in the cellular hypoxic response. Proc Natl Acad Sci U S A. **99**, 5271-5276

19 Freedman, S. J., Sun, Z. Y., Poy, F., Kung, A. L., Livingston, D. M., Wagner, G. and Eck, M. J. (2002) Structural basis for recruitment of CBP/p300 by hypoxia-inducible factor-1 alpha. Proc Natl Acad Sci U S A. **99**, 5367-5372

20 McNeill, L. A., Hewitson, K. S., Claridge, T. D., Seibel, J. F., Horsfall, L. E. and Schofield, C. J. (2002) Hypoxia-inducible factor asparaginyl hydroxylase (FIH-1) catalyses hydroxylation at the beta-carbon of asparagine-803. Biochem J. **367**, 571-575

21 Ruas, J. L., Berchner-Pfannschmidt, U., Malik, S., Gradin, K., Fandrey, J., Roeder, R. G., Pereira, T. and Poellinger, L. (2010) Complex regulation of the transactivation function of hypoxia-inducible factor-1 alpha by direct interaction with two distinct domains of the CREB-binding protein/p300. J Biol Chem. **285**, 2601-2609

22 Tian, H., McKnight, S. L. and Russell, D. W. (1997) Endothelial PAS domain protein 1 (EPAS1), a transcription factor selectively expressed in endothelial cells. Genes Dev. **11**, 72-82

23 Gu, Y. Z., Moran, S. M., Hogenesch, J. B., Wartman, L. and Bradfield, C. A. (1998) Molecular characterization and chromosomal localization of a third alpha-class hypoxia inducible factor subunit, HIF3alpha. Gene Expr. **7**, 205-213

24 Wiesener, M. S., Turley, H., Allen, W. E., Willam, C., Eckardt, K. U., Talks, K. L., Wood, S. M., Gatter, K. C., Harris, A. L., Pugh, C. W., Ratcliffe, P. J. and Maxwell, P. H. (1998) Induction of endothelial PAS domain protein-1 by hypoxia: characterization and comparison with hypoxia-inducible factor-1alpha. Blood. **92**, 2260-2268

25 Wiesener, M. S., Jurgensen, J. S., Rosenberger, C., Scholze, C. K., Horstrup, J. H., Warnecke, C., Mandriota, S., Bechmann, I., Frei, U. A., Pugh, C. W., Ratcliffe, P. J., Bachmann, S., Maxwell, P. H. and Eckardt, K. U. (2003) Widespread hypoxia-inducible expression of HIF-2alpha in distinct cell populations of different organs. FASEB J. **17**, 271-273

26 Lisy, K. and Peet, D. J. (2008) Turn me on: regulating HIF transcriptional activity. Cell Death Differ. **15**, 642-649

27 Pasanen, A., Heikkila, M., Rautavuoma, K., Hirsila, M., Kivirikko, K. I. and Myllyharju, J. (2010) Hypoxia-inducible factor (HIF)-3alpha is subject to extensive alternative splicing in human tissues and cancer cells and is regulated by HIF-1 but not HIF-2. Int J Biochem Cell Biol. **42**, 1189-1200

28 Heikkila, M., Pasanen, A., Kivirikko, K. I. and Myllyharju, J. (2011) Roles of the human hypoxia-inducible factor (HIF)-3alpha variants in the hypoxia response. Cell Mol Life Sci. **68**, 3885-3901

29 Maynard, M. A., Qi, H., Chung, J., Lee, E. H., Kondo, Y., Hara, S., Conaway, R. C., Conaway, J. W. and Ohh, M. (2003) Multiple splice variants of the human HIF-3 alpha locus are targets of the von Hippel-Lindau E3 ubiquitin ligase complex. J Biol Chem. **278**, 11032-11040

30 Zhang, P., Yao, Q., Lu, L., Li, Y., Chen, P. J. and Duan, C. (2014) Hypoxia-inducible factor 3 is an oxygen-dependent transcription activator and regulates a distinct transcriptional response to hypoxia. Cell Rep. **6**, 1110-1121

31 Tanaka, T., Wiesener, M., Bernhardt, W., Eckardt, K. U. and Warnecke, C. (2009) The human HIF (hypoxia-inducible factor)-3alpha gene is a HIF-1 target gene and may modulate hypoxic gene induction. Biochem J. **424**, 143-151

32 Hirose, K., Morita, M., Ema, M., Mimura, J., Hamada, H., Fujii, H., Saijo, Y., Gotoh, O., Sogawa, K. and Fujii-Kuriyama, Y. (1996) cDNA cloning and tissue-specific expression of a novel basic helix-loop-helix/PAS factor (Arnt2) with close sequence similarity to the aryl hydrocarbon receptor nuclear translocator (Arnt). Mol Cell Biol. **16**, 1706-1713

33 Hogenesch, J. B., Gu, Y. Z., Jain, S. and Bradfield, C. A. (1998) The basic-helix-loop-helix-PAS orphan MOP3 forms transcriptionally active complexes with circadian and hypoxia factors. Proc Natl Acad Sci U S A. **95**, 5474-5479

34 Maltepe, E., Keith, B., Arsham, A. M., Brorson, J. R. and Simon, M. C. (2000) The role of ARNT2 in tumor angiogenesis and the neural response to hypoxia. Biochem Biophys Res Commun. **273**, 231-238

35 Sekine, H., Mimura, J., Yamamoto, M. and Fujii-Kuriyama, Y. (2006) Unique and overlapping transcriptional roles of arylhydrocarbon receptor nuclear translocator (Arnt) and Arnt2 in xenobiotic and hypoxic responses. J Biol Chem. **281**, 37507-37516

36 Cowden, K. D. and Simon, M. C. (2002) The bHLH/PAS factor MOP3 does not participate in hypoxia responses. Biochem Biophys Res Commun. **290**, 1228-1236

37 Gekakis, N., Staknis, D., Nguyen, H. B., Davis, F. C., Wilsbacher, L. D., King, D. P., Takahashi, J. S. and Weitz, C. J. (1998) Role of the CLOCK protein in the mammalian circadian mechanism. Science. **280**, 1564-1569

38 Carver, L. A., Hogenesch, J. B. and Bradfield, C. A. (1994) Tissue specific expression of the rat Ah-receptor and ARNT mRNAs. Nucleic Acids Res. **22**, 3038-3044

39 Drutel, G., Kathmann, M., Heron, A., Schwartz, J. C. and Arrang, J. M. (1996) Cloning and selective expression in brain and kidney of ARNT2 homologous to the Ah receptor nuclear translocator (ARNT). Biochem Biophys Res Commun. **225**, 333-339

40 Mandl, M., Kapeller, B., Lieber, R. and Macfelda, K. (2013) Hypoxia-inducible factor-1beta (HIF-1beta) is upregulated in a HIF-1alpha-dependent manner in 518A2 human melanoma cells under hypoxic conditions. Biochem Biophys Res Commun. **434**, 166-172

41 Mandl, M. and Depping, R. (2014) Hypoxia-inducible ARNT (HIF-1beta): a rare exception? Mol Med

42 Wolff, M., Jelkmann, W., Dunst, J. and Depping, R. (2013) The Aryl Hydrocarbon Receptor Nuclear Translocator (ARNT/HIF-1beta) is influenced by hypoxia and hypoxia-mimetics. Cell Physiol Biochem. **32**, 849-858

43 Loenarz, C. and Schofield, C. J. (2008) Expanding chemical biology of 2-oxoglutarate oxygenases. Nat Chem Biol. **4**, 152-156

44 Flashman, E., Bagg, E. A., Chowdhury, R., Mecinovic, J., Loenarz, C., McDonough, M. A., Hewitson, K. S. and Schofield, C. J. (2008) Kinetic rationale for selectivity toward N- and C-terminal oxygen-dependent degradation domain substrates mediated by a loop region of hypoxia-inducible factor prolyl hydroxylases. J Biol Chem. **283**, 3808-3815

45 Landazuri, M. O., Vara-Vega, A., Viton, M., Cuevas, Y. and del Peso, L. (2006) Analysis of HIF-prolyl hydroxylases binding to substrates. Biochem Biophys Res Commun. **351**, 313-320

46 Hirsila, M., Koivunen, P., Gunzler, V., Kivirikko, K. I. and Myllyharju, J. (2003) Characterization of the human prolyl 4-hydroxylases that modify the hypoxia-inducible factor. J Biol Chem. **278**, 30772-30780

47 Chowdhury, R., McDonough, M. A., Mecinovic, J., Loenarz, C., Flashman, E., Hewitson, K. S., Domene, C. and Schofield, C. J. (2009) Structural basis for binding of hypoxia-inducible factor to the oxygen-sensing prolyl hydroxylases. Structure. **17**, 981-989

48 McDonough, M. A., Li, V., Flashman, E., Chowdhury, R., Mohr, C., Lienard, B. M., Zondlo, J., Oldham, N. J., Clifton, I. J., Lewis, J., McNeill, L. A., Kurzeja, R. J., Hewitson, K. S., Yang, E., Jordan, S., Syed, R. S. and Schofield, C. J. (2006) Cellular oxygen sensing: Crystal structure of

hypoxia-inducible factor prolyl hydroxylase (PHD2). Proc Natl Acad Sci U S A. **103**, 9814-9819

49 Appelhoff, R. J., Tian, Y. M., Raval, R. R., Turley, H., Harris, A. L., Pugh, C. W., Ratcliffe, P. J. and Gleadle, J. M. (2004) Differential function of the prolyl hydroxylases PHD1, PHD2, and PHD3 in the regulation of hypoxia-inducible factor. J Biol Chem. **279**, 38458-38465

50 Metzen, E., Berchner-Pfannschmidt, U., Stengel, P., Marxsen, J. H., Stolze, I., Klinger, M., Huang, W. Q., Wotzlaw, C., Hellwig-Burgel, T., Jelkmann, W., Acker, H. and Fandrey, J. (2003) Intracellular localisation of human HIF-1 alpha hydroxylases: implications for oxygen sensing. J Cell Sci. **116**, 1319-1326

51 Huang, J., Zhao, Q., Mooney, S. M. and Lee, F. S. (2002) Sequence determinants in hypoxia-inducible factor-1alpha for hydroxylation by the prolyl hydroxylases PHD1, PHD2, and PHD3. J Biol Chem. **277**, 39792-39800

52 Oehme, F., Ellinghaus, P., Kolkhof, P., Smith, T. J., Ramakrishnan, S., Hutter, J., Schramm, M. and Flamme, I. (2002) Overexpression of PH-4, a novel putative proline 4-hydroxylase, modulates activity of hypoxia-inducible transcription factors. Biochem Biophys Res Commun. **296**, 343-349

53 Koivunen, P., Tiainen, P., Hyvarinen, J., Williams, K. E., Sormunen, R., Klaus, S. J., Kivirikko, K. I. and Myllyharju, J. (2007) An endoplasmic reticulum transmembrane prolyl 4-hydroxylase is induced by hypoxia and acts on hypoxia-inducible factor alpha. J Biol Chem. **282**, 30544-30552

54 Elkins, J. M., Hewitson, K. S., McNeill, L. A., Seibel, J. F., Schlemminger, I., Pugh, C. W., Ratcliffe, P. J. and Schofield, C. J. (2003) Structure of factor-inhibiting hypoxia-inducible factor (HIF) reveals mechanism of oxidative modification of HIF-1 alpha. J Biol Chem. **278**, 1802-1806

55 Stolze, I. P., Tian, Y. M., Appelhoff, R. J., Turley, H., Wykoff, C. C., Gleadle, J. M. and Ratcliffe, P. J. (2004) Genetic analysis of the role of the asparaginyl hydroxylase factor inhibiting hypoxia-inducible factor (FIH) in regulating hypoxia-inducible factor (HIF) transcriptional target genes [corrected]. J Biol Chem. **279**, 42719-42725

56 Dann, C. E., 3rd, Bruick, R. K. and Deisenhofer, J. (2002) Structure of factor-inhibiting hypoxia-inducible factor 1: An asparaginyl hydroxylase involved in the hypoxic response pathway. Proc Natl Acad Sci U S A. **99**, 15351-15356

57 Price, J. C., Barr, E. W., Tirupati, B., Bollinger, J. M., Jr. and Krebs, C. (2003) The first direct characterization of a high-valent iron intermediate in the reaction of an alpha-ketoglutarate-dependent dioxygenase: a high-spin FeIV complex in taurine/alpha-ketoglutarate dioxygenase (TauD) from Escherichia coli. Biochemistry. **42**, 7497-7508

58 Clifton, I. J., McDonough, M. A., Ehrismann, D., Kershaw, N. J., Granatino, N. and Schofield, C. J. (2006) Structural studies on 2-oxoglutarate oxygenases and related double-stranded beta-helix fold proteins. J Inorg Biochem. **100**, 644-669

59 Hausinger, R. P. (2004) FeII/alpha-ketoglutarate-dependent hydroxylases and related enzymes. Crit Rev Biochem Mol Biol. **39**, 21-68

60 Chowdhury, R., Candela-Lena, J. I., Chan, M. C., Greenald, D. J., Yeoh, K. K., Tian, Y. M., McDonough, M. A., Tumber, A., Rose, N. R., Conejo-Garcia, A., Demetriades, M., Mathavan, S., Kawamura, A., Lee, M. K., van Eeden, F., Pugh, C. W., Ratcliffe, P. J. and Schofield, C. J. (2013) Selective Small Molecule Probes for the Hypoxia Inducible Factor (HIF) Prolyl Hydroxylases. ACS Chem Biol. **8**, 1488-1496

61 Tarhonskaya, H., Rydzik, A. M., Leung, I. K., Loik, N. D., Chan, M. C., Kawamura, A., McCullagh, J. S., Claridge, T. D., Flashman, E. and Schofield, C. J. (2014) Non-enzymatic chemistry enables 2-hydroxyglutarate-mediated activation of 2-oxoglutarate oxygenases. Nat Commun. **5**, 3423

62 Koivunen, P., Hirsila, M., Kivirikko, K. I. and Myllyharju, J. (2006) The length of peptide substrates has a marked effect on hydroxylation by the hypoxia-inducible factor prolyl 4-hydroxylases. J Biol Chem. **281**, 28712-28720

63 Flashman, E., Hoffart, L. M., Hamed, R. B., Bollinger, J. M., Jr., Krebs, C. and Schofield, C. J. (2010) Evidence for the slow reaction of hypoxia-inducible factor prolyl hydroxylase 2 with oxygen. FEBS J. **277**, 4089-4099

64 Ehrismann, D., Flashman, E., Genn, D. N., Mathioudakis, N., Hewitson, K. S., Ratcliffe, P. J. and Schofield, C. J. (2007) Studies on the activity of the hypoxia-inducible-factor hydroxylases using an oxygen consumption assay. Biochem J. **401**, 227-234

65 Tian, Y. M., Yeoh, K. K., Lee, M. K., Eriksson, T., Kessler, B. M., Kramer, H. B., Edelmann, M. J., Willam, C., Pugh, C. W., Schofield, C. J. and Ratcliffe, P. J. (2011) Differential sensitivity of hypoxia inducible factor hydroxylation sites to hypoxia and hydroxylase inhibitors. J Biol Chem. **286**, 13041-13051

66 Berra, E., Benizri, E., Ginouves, A., Volmat, V., Roux, D. and Pouyssegur, J. (2003) HIF prolyl-hydroxylase 2 is the key oxygen sensor setting low steady-state levels of HIF-1alpha in normoxia. EMBO J. **22**, 4082-4090

67 Takeda, K., Ho, V. C., Takeda, H., Duan, L. J., Nagy, A. and Fong, G. H. (2006) Placental but not heart defects are associated with elevated hypoxia-inducible factor alpha levels in mice lacking prolyl hydroxylase domain protein 2. Mol Cell Biol. **26**, 8336-8346

68 Takeda, K., Aguila, H. L., Parikh, N. S., Li, X., Lamothe, K., Duan, L. J., Takeda, H., Lee, F. S. and Fong, G. H. (2008) Regulation of adult erythropoiesis by prolyl hydroxylase domain proteins. Blood. **111**, 3229-3235

69 Cummins, E. P., Berra, E., Comerford, K. M., Ginouves, A., Fitzgerald, K. T., Seeballuck, F., Godson, C., Nielsen, J. E., Moynagh, P., Pouyssegur, J. and Taylor, C. T. (2006) Prolyl hydroxylase-1 negatively regulates IkappaB kinase-beta, giving insight into hypoxia-induced NFkappaB activity. Proc Natl Acad Sci U S A. **103**, 18154-18159

70 Mikhaylova, O., Ignacak, M. L., Barankiewicz, T. J., Harbaugh, S. V., Yi, Y., Maxwell, P. H., Schneider, M., Van Geyte, K., Carmeliet, P., Revelo, M. P., Wyder, M., Greis, K. D., Meller, J. and Czyzyk-Krzeska, M. F. (2008) The von Hippel-Lindau tumor suppressor protein and Egl-9-Type proline hydroxylases regulate the large subunit of RNA polymerase II in response to oxidative stress. Mol Cell Biol. **28**, 2701-2717

71 Koditz, J., Nesper, J., Wottawa, M., Stiehl, D. P., Camenisch, G., Franke, C., Myllyharju, J., Wenger, R. H. and Katschinski, D. M. (2007) Oxygen-dependent ATF-4 stability is mediated by the PHD3 oxygen sensor. Blood. **110**, 3610-3617

72 Xie, L., Xiao, K., Whalen, E. J., Forrester, M. T., Freeman, R. S., Fong, G., Gygi, S. P., Lefkowitz, R. J. and Stamler, J. S. (2009) Oxygen-regulated beta(2)-adrenergic receptor hydroxylation by EGLN3 and ubiquitylation by pVHL. Sci Signal. **2**, ra33

73 Luo, W., Hu, H., Chang, R., Zhong, J., Knabel, M., O'Meally, R., Cole, R. N., Pandey, A. and Semenza, G. L. (2011) Pyruvate kinase M2 is a PHD3-stimulated coactivator for hypoxia-inducible factor 1. Cell. **145**, 732-744

74 Takahashi, N., Kuwaki, T., Kiyonaka, S., Numata, T., Kozai, D., Mizuno, Y., Yamamoto, S., Naito, S., Knevels, E., Carmeliet, P., Oga, T., Kaneko, S., Suga, S., Nokami, T., Yoshida, J. and Mori, Y. (2011) TRPA1 underlies a sensing mechanism for O2. Nat Chem Biol. **7**, 701-711

75 Xie, L., Pi, X., Mishra, A., Fong, G., Peng, J. and Patterson, C. (2012) PHD3-dependent hydroxylation of HCLK2 promotes the DNA damage response. J Clin Invest. **122**, 2827-2836

76 Moser, S. C., Bensaddek, D., Ortmann, B., Maure, J. F., Mudie, S., Blow, J. J., Lamond, A. I., Swedlow, J. R. and Rocha, S. (2013) PHD1 links cell-cycle progression to oxygen sensing through hydroxylation of the centrosomal protein Cep192. Dev Cell. **26**, 381-392

77 Cockman, M. E., Lancaster, D. E., Stolze, I. P., Hewitson, K. S., McDonough, M. A., Coleman, M. L., Coles, C. H., Yu, X., Hay, R. T., Ley, S. C., Pugh, C. W., Oldham, N. J., Masson, N., Schofield, C. J. and Ratcliffe, P. J. (2006) Posttranslational hydroxylation of ankyrin repeats in IkappaB proteins by the hypoxia-inducible factor (HIF) asparaginyl hydroxylase, factor inhibiting HIF (FIH). Proc Natl Acad Sci U S A. **103**, 14767-14772

78 Coleman, M. L., McDonough, M. A., Hewitson, K. S., Coles, C., Mecinovic, J., Edelmann, M., Cook, K. M., Cockman, M. E., Lancaster, D. E., Kessler, B. M., Oldham, N. J., Ratcliffe, P. J. and Schofield, C. J. (2007) Asparaginyl hydroxylation of the Notch ankyrin repeat domain by factor inhibiting hypoxia-inducible factor. J Biol Chem. **282**, 24027-24038

79 Ferguson, J. E., 3rd, Wu, Y., Smith, K., Charles, P., Powers, K., Wang, H. and Patterson, C. (2007) ASB4 is a hydroxylation substrate of FIH and promotes vascular differentiation via an oxygen-dependent mechanism. Mol Cell Biol. **27**, 6407-6419

80 Cockman, M. E., Webb, J. D., Kramer, H. B., Kessler, B. M. and Ratcliffe, P. J. (2009) Proteomics-based identification of novel factor inhibiting hypoxia-inducible factor (FIH) substrates indicates widespread asparaginyl hydroxylation of ankyrin repeat domain-containing proteins. Mol Cell Proteomics. **8**, 535-546

81 Webb, J. D., Muranyi, A., Pugh, C. W., Ratcliffe, P. J. and Coleman, M. L. (2009) MYPT1, the targeting subunit of smooth-muscle myosin phosphatase, is a substrate for the asparaginyl hydroxylase factor inhibiting hypoxia-inducible factor (FIH). Biochem J. **420**, 327-333

82 Zheng, X., Linke, S., Dias, J. M., Gradin, K., Wallis, T. P., Hamilton, B. R., Gustafsson, M., Ruas, J. L., Wilkins, S., Bilton, R. L., Brismar, K., Whitelaw, M. L., Pereira, T., Gorman, J. J., Ericson, J., Peet, D. J., Lendahl, U. and Poellinger, L. (2008) Interaction with factor inhibiting HIF-1 defines an additional mode of cross-coupling between the Notch and hypoxia signaling pathways. Proc Natl Acad Sci U S A. **105**, 3368-3373

83 Yang, M., Ge, W., Chowdhury, R., Claridge, T. D., Kramer, H. B., Schmierer, B., McDonough, M. A., Gong, L., Kessler, B. M., Ratcliffe, P. J., Coleman, M. L. and Schofield, C. J. (2011) Asparagine and aspartate hydroxylation of the cytoskeletal ankyrin family is catalyzed by factor-inhibiting hypoxia-inducible factor. J Biol Chem. **286**, 7648-7660

84 Wilkins, S. E., Karttunen, S., Hampton-Smith, R. J., Murchland, I., Chapman-Smith, A. and Peet, D. J. (2012) Factor inhibiting HIF (FIH) recognizes distinct molecular features within hypoxia-inducible factor-alpha (HIF-alpha) versus ankyrin repeat substrates. J Biol Chem. **287**, 8769-8781

85 Schodel, J., Mole, D. R. and Ratcliffe, P. J. (2013) Pan-genomic binding of hypoxia-inducible transcription factors. Biol Chem. **394**, 507-517

86 Botusan, I. R., Sunkari, V. G., Savu, O., Catrina, A. I., Grunler, J., Lindberg, S., Pereira, T., Yla-Herttuala, S., Poellinger, L., Brismar, K. and Catrina, S. B. (2008) Stabilization of HIF-1alpha is critical to improve wound healing in diabetic mice. Proc Natl Acad Sci U S A. **105**, 19426-19431

87 Sen Banerjee, S., Thirunavukkarasu, M., Tipu Rishi, M., Sanchez, J. A., Maulik, N. and Maulik, G. (2012) HIF-prolyl hydroxylases and cardiovascular diseases. Toxicol Mech Methods. **22**, 347-358

88 Rabinowitz, M. H. (2013) Inhibition of hypoxia-inducible factor prolyl hydroxylase domain oxygen sensors: tricking the body into mounting orchestrated survival and repair responses. J Med Chem. **56**, 9369-9402

89 Scholz, C. C. and Taylor, C. T. (2013) Targeting the HIF pathway in inflammation and immunity. Curr Opin Pharmacol. **13**, 646-653

90 Hsieh, M. M., Linde, N. S., Wynter, A., Metzger, M., Wong, C., Langsetmo, I., Lin, A., Smith, R., Rodgers, G. P., Donahue, R. E., Klaus, S. J. and Tisdale, J. F. (2007) HIF prolyl hydroxylase inhibition results in endogenous erythropoietin induction, erythrocytosis, and modest fetal hemoglobin expression in rhesus macaques. Blood. **110**, 2140-2147

91 Wang, G. L. and Semenza, G. L. (1993) Desferrioxamine induces erythropoietin gene expression and hypoxia-inducible factor 1 DNA-binding activity: implications for models of hypoxia signal transduction. Blood. **82**, 3610-3615

92 Mole, D. R., Schlemminger, I., McNeill, L. A., Hewitson, K. S., Pugh, C. W., Ratcliffe, P. J. and Schofield, C. J. (2003) 2-oxoglutarate analogue inhibitors of HIF prolyl hydroxylase. Bioorg Med Chem Lett. **13**, 2677-2680

93 McDonough, M. A., McNeill, L. A., Tilliet, M., Papamicael, C. A., Chen, Q. Y., Banerji, B., Hewitson, K. S. and Schofield, C. J. (2005) Selective inhibition of factor inhibiting hypoxia-inducible factor. J Am Chem Soc. **127**, 7680-7681

94 Yeoh, K. K., Chan, M. C., Thalhammer, A., Demetriades, M., Chowdhury, R., Tian, Y. M., Stolze, I., McNeill, L. A., Lee, M. K., Woon, E. C., Mackeen, M. M., Kawamura, A., Ratcliffe, P. J., Mecinovic, J. and Schofield, C. J. (2013) Dual-action inhibitors of HIF prolyl hydroxylases that induce binding of a second iron ion. Org Biomol Chem. **11**, 732-745

95 Buckley, D. L., Van Molle, I., Gareiss, P. C., Tae, H. S., Michel, J., Noblin, D. J., Jorgensen, W. L., Ciulli, A. and Crews, C. M. (2012) Targeting the von Hippel-Lindau E3 ubiquitin ligase using small molecules to disrupt the VHL/HIF-1alpha interaction. J Am Chem Soc. **134**, 4465-4468

96 Yan, L., Colandrea, V. J. and Hale, J. J. (2010) Prolyl hydroxylase domain-containing protein inhibitors as stabilizers of hypoxia-inducible factor: small molecule-based therapeutics for anemia. Expert Opin Ther Pat. **20**, 1219-1245

97 Johnson, B. M., Stier, B. A. and Caltabiano, S. (2014) Effect of food and gemfibrozil on the pharmacokinetics of the novel prolyl hydroxylase inhibitor GSK1278863. Clinical Pharmacology in Drug Development. **3**, 109-117

Chapter 2: The development and applications of *in vitro* luminescence assays for HIF prolyl hydroxylase PHD2

2.1 Introduction

Various types of *in vitro* assay have been used to study the HIF prolyl hydroxylases, and in particular PHD2. Initially, assays based on the production of radiolabelled CO_2 or succinate, previously used to study collagen prolyl hydroxylases (C-P4Hs), were adopted for the HIF prolyl hydroxylases [1-4]. These assays were soon followed by the development and utilisation of other methods including mass spectrometry and NMR based assays [5-7]. Although such assays have been useful for various catalytic and kinetic studies on the PHD enzymes, they are usually labour intensive, time consuming and require relatively large amount of reagents (including in some assays, the use of radioactive isotopes). While some of these assays have also been utilised for inhibition studies, they are usually limited to screening a relatively small set of compounds.

Efforts have thus been placed into developing efficient assays suitable for use in a high-throughput manner for the PHDs. One such assay is a fluorescence-based assay which relies on the derivatisation of unreacted 2OG with *o*-phenylenediamine [8]. This assay, however, is based on the measurement of 2OG turnover (which will also take into account the uncoupled turnover reaction of 2OG into succinate by PHD2 without hydroxylation of the 'prime' substrate peptide) and has also been shown to be affected by the presence of ascorbic acid [8, 9]. An alternative homogeneous time-resolved fluorescence resonance energy transfer (TR–FRET) based assay [10, 11] has also been developed, although the purification of the von Hippel-Lindau–Elongin C–Elongin B (VCB) complex, is a problem with this assay. The

shortcomings of these assays could be partly attributed to the indirect measurement of PHD activity, given the lack of hydroxyprolyl-specific antibodies for the direct detection of hydroxylated substrate (HIF1α) at the time. At the onset of the work described in this Chapter, the need for a simpler, more efficient and higher throughput assay for inhibition studies on PHD2 was thereby warranted.

The development of HIF1α hydroxyprolyl-specific antibodies, in addition to the successful adaptation of the Amplified Luminescent Proximity Homogeneous Assay (AlphaScreen) technology for studying the 2OG-dependent dioxygenase JmjC-domain containing histone demethylases suggested that this technology might be applied to the PHD enzymes [12]. The AlphaScreen technology, based on the Luminescent Oxygen Channelling Immunoassay (LOCI) [13, 14], relies on the proximity of a pair of donor and acceptor beads to produce a luminescence signal (**Figure 2.1 A-B**) [15]. The donor bead contains a photosensitiser (phthalocyanine, **I**) that converts ambient oxygen to singlet oxygen (oxygen with single excited electron) upon excitation at 680 nm wavelength [13-15]. The singlet oxygen produced, which has a half-life of 4 μsec, will only diffuse within 200 nm from the donor bead in solution before returning to its triplet ground state [13-15]. If the acceptor bead is in close enough proximity, the singlet oxygen will be captured by a thioxene (**II**) in the acceptor bead, leading to the production of a dioxetane (**III**) and an excited diester (**IV**) [13-15]. Energy is then transferred to anthracene (**V**) and subsequently rubrene (**VI**), which emits at a wavelength of 520-620 nm that is detected (**Figure 2.1 B**) [14, 15]. To appropriately study the hydroxylase activity of PHD enzymes, it was envisaged that an AlphaScreen-based assay might be developed using streptavidin-coated donor beads, Protein A-conjugated acceptor beads, commercially available anti-HIF1α hydroxylation specific antibodies (as the detection antibody) and biotinylated HIF1α peptide fragment (as the substrate) (**Figure 2.1 A**).

In humans, PHD2 catalyses the hydroxylation of HIF1α at a proline-residue 402 (Pro402) within the *N*-terminal oxygen degradation domain (NODD) and a proline-residue 564 (Pro564) within the *C*-terminal oxygen degradation domain (CODD). Thus, the human HIF1α peptides corresponding to both domains could potentially be used as substrates in the AlphaScreen assay for PHD2. The assays utilising the HIF1α NODD and CODD fragment peptides to study PHD2 activity are hereafter referred to as the PHD2 NODD AlphaScreen assay and PHD2 CODD AlphaScreen assay, respectively.

This Chapter describes the development of the PHD2 NODD and CODD AlphaScreen assays. It was envisaged that once developed and tested, these assays (particularly the PHD2 CODD AlphaScreen assay) would be a valuable screening tool for the identification of PHD2 inhibitors. Applications of these assays for the inhibition studies of PHD2 are described in this and subsequent Chapters.

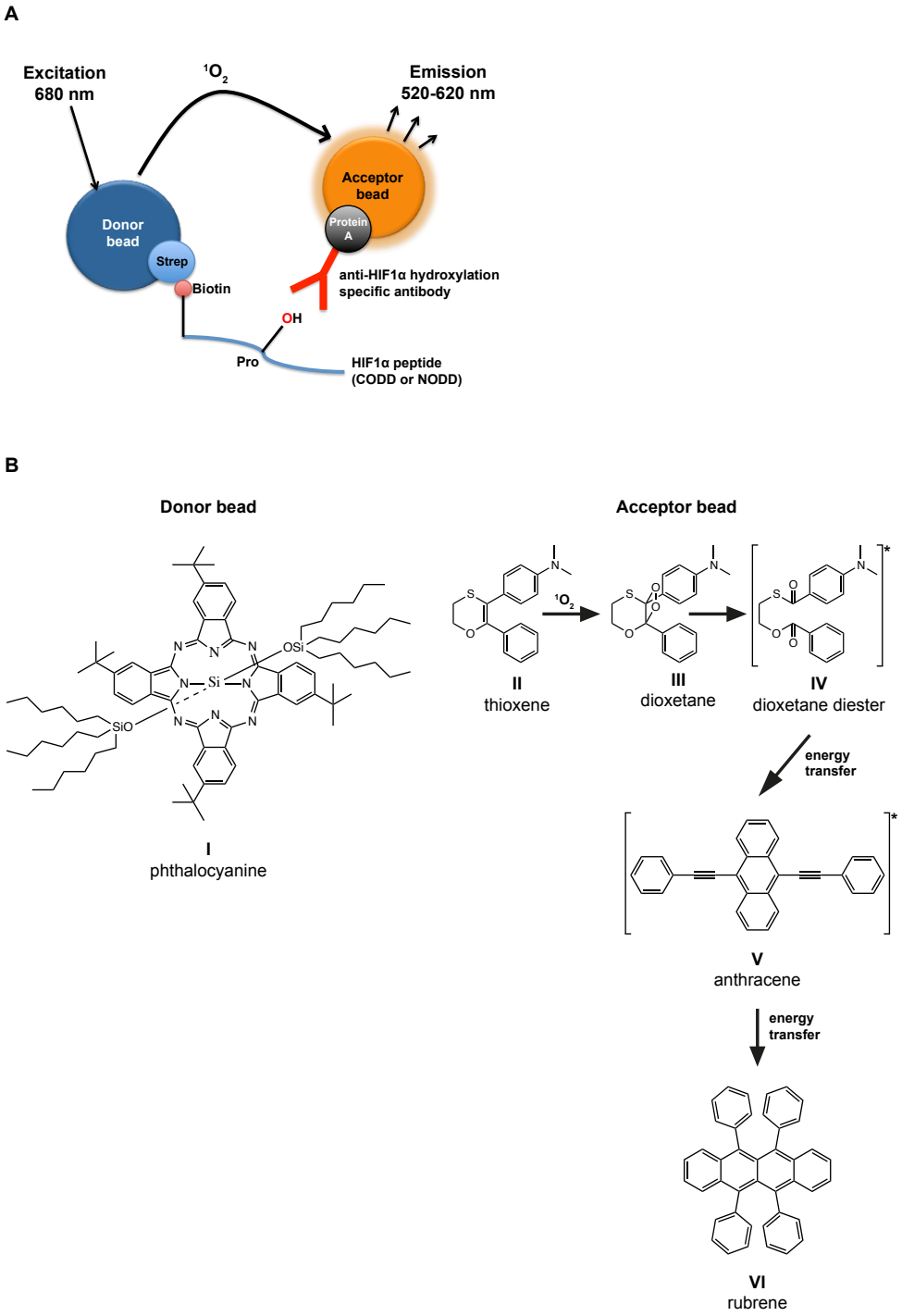

Figure 2.1 Principle of the AlphaScreen assay. (**A**) Proposed AlphaScreen assay for PHD2. A biotinylated peptide corresponding to the NODD (containing Pro402) or CODD (containing Pro564) of the human HIF1α is used as substrate. The Protein A-conjugated acceptor bead is coupled to either the anti-hydroxyPro402 antibody (for the NODD AlphaScreen assay) or the anti-hydroxyPro564 antibody (for the CODD AlphaScreen assay). A luminescence signal can be produced and detected when the donor and acceptor beads are brought into close proximity (within 200 nm) in the event of hydroxylation by PHD2. (**B**) The reaction for the generation of chemiluminescence signal in the AlphaScreen beads. Strep: Streptavidin, Pro: Proline, CODD: *C*-terminal oxygen degradation domain, NODD, *N*-terminal oxygen degradation domain. Figures adapted from [14, 15].

2.2 Development of the PHD2 AlphaScreen assay for CODD hydroxylation

A biotinylated CODD peptide (19-mer) corresponding to residues 556-574 of human HIF1α was obtained (from GL Biochem, Shanghai, China) and its potential to be used in the PHD2 AlphaScreen assay was first tested alongside the hydroxylated version of the same peptide (with *trans*-4-hydroxyproline replacing the proline residue 564). The CODD peptide in non-biotinylated form has been routinely used as substrate for PHD2 in other *in vitro* assays such as mass spectrometry and fluorescence-based assays [5-8, 16]. To investigate whether or not the AlphaScreen signal corresponds to the amount of hydroxylated HIF1α peptide, a range of concentrations of the hydroxylated and unhydroxylated biotinylated-CODD peptide substrates were detected using 1:8,000, 1:16,000, 1:32,000 and 1:64,000 dilutions of anti-hydroxy-Pro564 antibody. The assay was performed in the absence of PHD2 and co-factors (2OG, Fe(II) and L-ascorbic acid) at room temperature. The results obtained showed linearity of the luminescence signal and good selectivity for the hydroxylated over the unhydroxylated peptide (>8-fold) at up to 60 nM of CODD peptides when the assay was performed at 1:8,000 dilution of the anti-hydroxy-Pro564 antibody (**Figure 2.2**). The AlphaScreen signals at 1:16,000 and 1:32,000 dilution of the anti-hydroxy-Pro564 antibody were also proportional to the amount of hydroxylated CODD peptide, although the signals and selectivity for the hydroxylated over unhydroxylated peptide across all concentrations tested was lower than that of the 1:8,000 dilution of the antibody (**Figure 2.2**). The signal for the 1:64,000 dilution of the antibody was too low to be useful for the assay. Therefore, 60 nM of peptide and a 1:8,000 dilution of the detection antibody were used in subsequent experiments.

The enzymatic activity of the catalytic domain of human PHD2 (residues 181-426, hereafter referred to as PHD2) was then assayed at two enzyme concentrations (1 nM and 5 nM) over a time course of 25 min at room temperature with 10 μM Fe(II), 100 μM L-ascorbic acid and 2

μM 2OG (i.e. all co-factors/substrate were in excess of the enzyme concentrations). The AlphaScreen signal had been previously shown to be unaffected by the concentrations of L-ascorbic acid and Fe(II) used [12]. Assays with both concentrations of PHD2 showed detectable enzyme activity as measured by an increase in the AlphaScreen signal over time (**Figure 2.3**). A good signal-to-background ratio (S/B) of 4.2 and 8.3 were obtained after 10 min of reaction for assays using 1 nM and 5 nM of PHD2, respectively. Concentrations of PHD2 within 1 to 5 nM range were then used in subsequent experiments.

To assess the feasibility of the AlphaScreen assay for inhibition studies, the inhibitory activity of two previously reported inhibitors of PHD2, 2-(1-chloro-4-hydroxyisoquinoline-3-carboxamido) acetic acid (BIQ) and *N*-oxalylglycine (NOG) were then tested. The assays were performed at a range of inhibitor concentrations and dose response curves were fitted to determine the half-maximal inhibitory concentration (IC_{50}). The IC_{50} values of BIQ and NOG were found to be 0.33 μM and 11.2 μM, respectively (**Figure 2.4**). These values are close to the previously reported PHD2 IC_{50} values of 0.073 μM for BIQ and 18.5 μM for NOG using a TR-FRET based assay [11]. Taken together, these results indicate that the AlphaScreen methodology can be used for assaying the hydroxylation of HIF1α CODD peptide by PHD2 and that it is suitable for inhibitor studies.

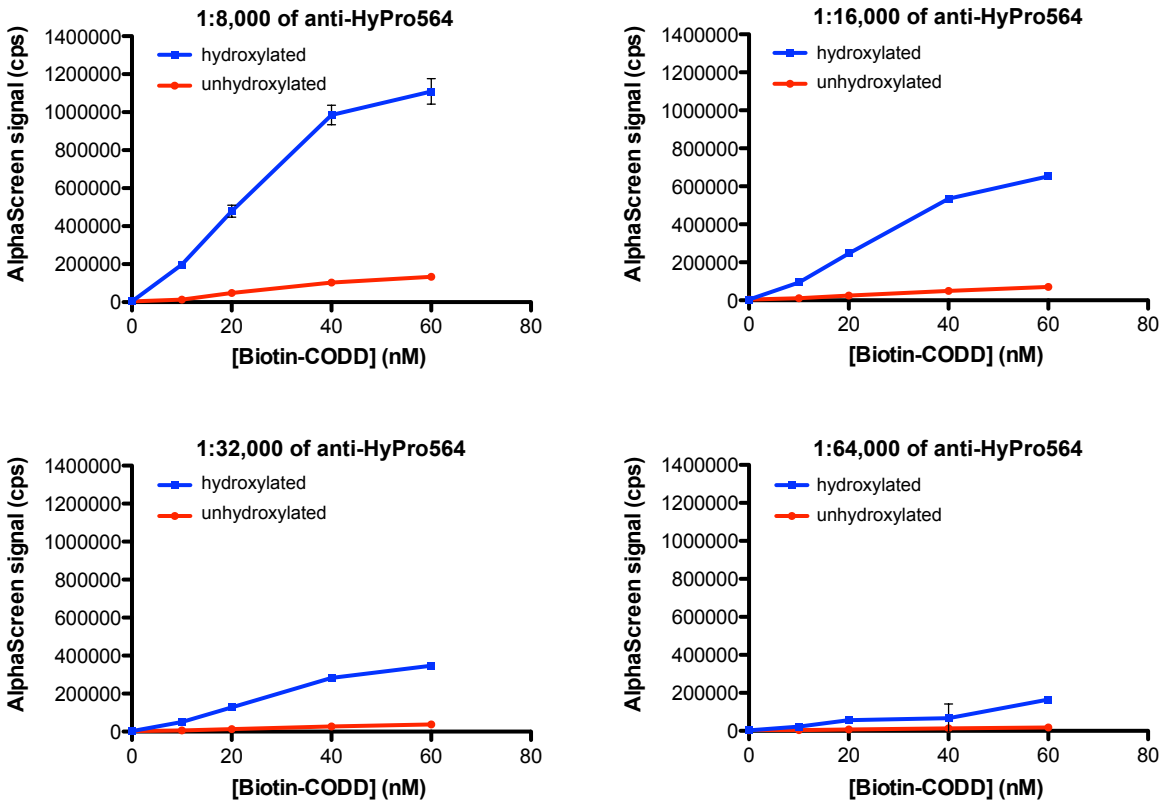

Figure 2.2 Determination of the optimal peptide and antibody concentrations for the PHD2 CODD AlphaScreen assay. Each datapoint represents the average signal ± standard deviation, n=2.

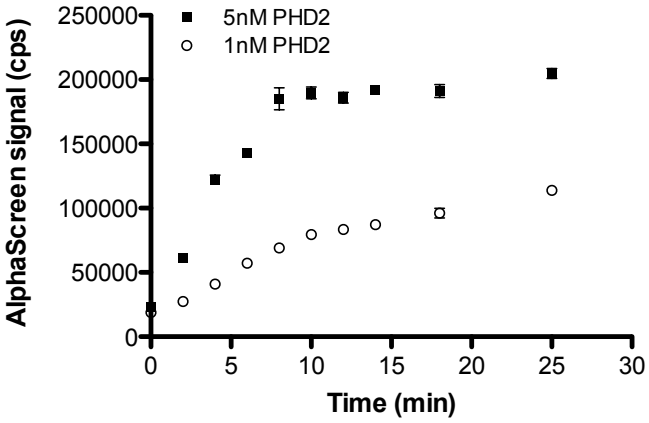

Figure 2.3 Time course experiment at two concentrations of PHD2 for CODD hydroxylation using the PHD2 CODD AlphaScreen assay. Reactions were performed at room temperature with 2 µM of 2OG, 10 µM of Fe(II), 100 µM of L-ascorbic acid and 60 nM of biotinylated CODD peptide before quenching after a specified time with 30 mM of EDTA. Each datapoint represents the average signal ± standard deviation, n=2.

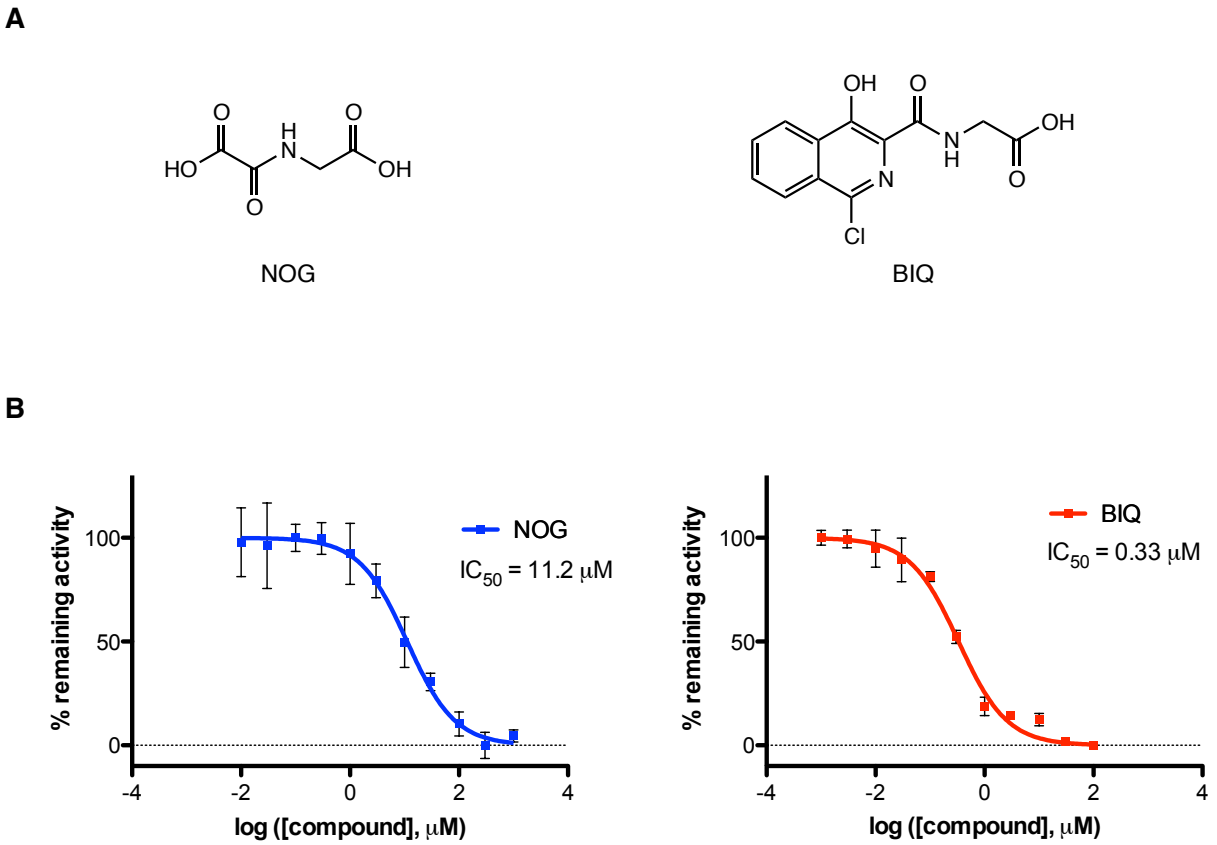

Figure 2.4 (**A**) Chemical structures of NOG and BIQ. (**B**) Inhibition curves for NOG and BIQ and their respective IC_{50} values as determined using the PHD2 CODD AlphaScreen assay. Each datapoint represents the average signal ± standard deviation, n=3. Standard assay mixtures contain 1 nM PHD2, 60 nM biotinylated CODD, 2 μM 2OG, 10 μM Fe(II) and 100 μM L-ascorbic acid. Reactions were performed at room temperature for 10 min before being quenched with 30 mM of EDTA.

2.3 Development of the PHD2 AlphaScreen assay for NODD hydroxylation

To develop the PHD2 AlphaScreen assay using the NODD peptide (19-mer; corresponding to residues 395-413 of human HIF1α) as the substrate, an analogous approach to the development of PHD2 CODD AlphaScreen assay was then taken. Firstly, the changes of AlphaScreen signal in response to different amounts of unhydroxylated and hydroxylated NODD peptides were investigated. Signal linearity and good selectivity (>5-fold) were obtained for the hydroxylated peptide over substrate peptide for concentrations up to 45 nM detected using 62.5 ng/µl and 125 ng/µl of anti-hydroxy-Pro402 antibody (**Figure 2.5**). The AlphaScreen signal became saturated for concentrations of hydroxylated peptide above 45 nM, thus 45 nM of the peptide and 62.5 ng/µl of the detection antibody was set as the initial condition for the next step in the assay development.

A time course experiment of up to 60 min was then performed with varying amounts of PHD2 (5 - 20 nM). Assay conditions such as concentrations of co-factors (2OG, Fe(II), L-ascorbic acid) and assay temperature (room temperature) were kept the same as for the PHD2 CODD AlphaScreen assay. The extent of NODD peptide hydroxylation was observed to be relatively low with less than 10 nM of PHD2 and a good signal-to-background ratio (S/B>3) was only observed at PHD2 concentrations above or equal to 10 nM (**Figure 2.6**). This observation could be due to the NODD peptide being a less efficient substrate than the CODD peptide for PHD2. CODD has previously been reported to be a better substrate than NODD for PHD2, as shown by the lower K_M values obtained for the former using other assays [1, 5, 17]. Given that the same batch of enzyme has been shown to be active for CODD hydroxylation, it is unlikely that the observed lower activity is due to enzyme degradation (although this could be further investigated by enzyme active site titration methods). 10 nM of PHD2 was selected to further optimise the assay. To ensure that that the substrate peptide

concentration is in excess of the enzyme in the assay, the effect of adding non-biotinylated NODD peptide to supplement the optimised 45 nM biotinylated NODD peptide into the assay was investigated. A time course experiment was performed using a mixture of both biotinylated (45 nM) and non-biotinylated (50 nM or 200 nM) NODD peptides over a reaction period of up to 70 min (**Figure 2.7**). To increase the detection signal, a higher concentration of the detection antibody (125 ng/µl, as tested in the earlier experiment shown in **Figure 2.5**) was used. A linear increase of signal over time and good S/B ratio (>5) was observed at up to 40 min of reaction. It was noted that the addition of increasing amounts of non-biotinylated NODD peptide did not markedly affect the amount of hydroxylated biotinylated NODD (**Figure 2.7**). This could be due to the increased hydroxylation rate of PHD2 with increasing substrates (resulting in increased hydroxylation of biotinylated NODD peptide) compensating for the opposing effects of substrate competition by the non-biotinylated NODD peptide. Taken together, the standard assay condition for the PHD2 NODD AlphaScreen assay was chosen to consist of 10 nM of PHD2, a mixture of 45 nM of biotinylated and 200 nM of non-biotinylated NODD peptides, 2 µM of 2OG, 10 µM of Fe(II) and 100 µM of L-ascorbic acid, with reaction time of 40 min at room temperature.

Finally, the inhibition of NODD hydroxylation activity of PHD2 by inhibitors (NOG and BIQ) was tested using the PHD2 NODD AlphaScreen assay under the standard assay conditions. A clear dose-response inhibition was observed and the IC_{50} values for these two compounds were successfully determined (NOG IC_{50} = 4.8 µM, BIQ IC_{50} = 8.4 µM), highlighting the feasibility of using this assay for studying the inhibition of NODD hydroxylation (**Figure 2.8**). The relative inhibitory potencies of NODD hydroxylation by NOG and BIQ were notably different than that observed for CODD hydroxylation. NOG is a better inhibitor of NODD hydroxylation than BIQ, despite the latter being a better inhibitor of

CODD hydroxylation than the former (NOG IC_{50} = 11.2 µM, BIQ IC_{50} = 0.33 µM; **Figure 2.4**). These results raise the possibility of substrate selective inhibition for PHD2.

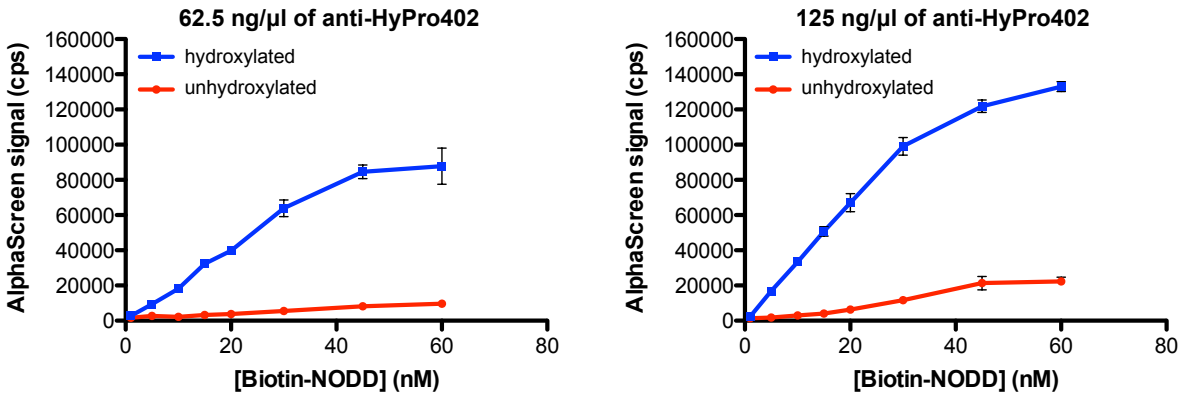

Figure 2.5 Determination of the optimal peptide and antibody concentrations for the PHD2 NODD AlphaScreen assay. Each datapoint represents the average signal ± standard deviation, n=3.

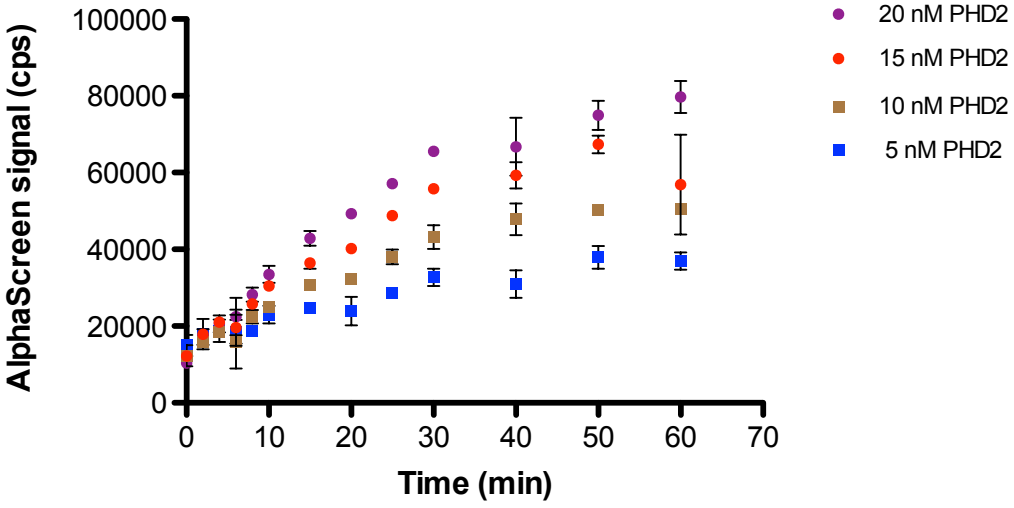

Figure 2.6 Time course experiment with varying concentrations of PHD2 for NODD hydroxylation using the PHD2 NODD AlphaScreen assay. Each datapoint represents the average signal ± standard deviation, n=3. Reactions were performed at room temperature with 2 µM of 2OG, 10 µM of Fe(II), 100 µM of L-ascorbic acid and 45 nM of biotinylated NODD peptide before quenching after the specified time with 30 mM of EDTA.

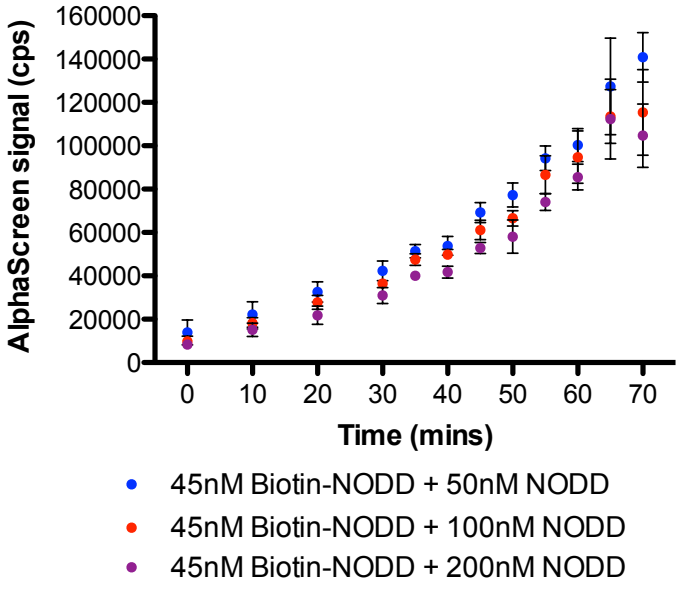

Figure 2.7 Time course experiment with 10 nM of PHD2 and varying concentrations of biotinylated NODD and non-biotinylated NODD peptide mixture using the PHD2 NODD AlphaScreen assay. Each datapoint represents the average signal ± standard deviation, n=4. Reactions were performed at room temperature with 2 μM of 2OG, 10 μM of Fe(II) and 100 μM of L-ascorbic acid before quenching after the specified time with 30 mM of EDTA.

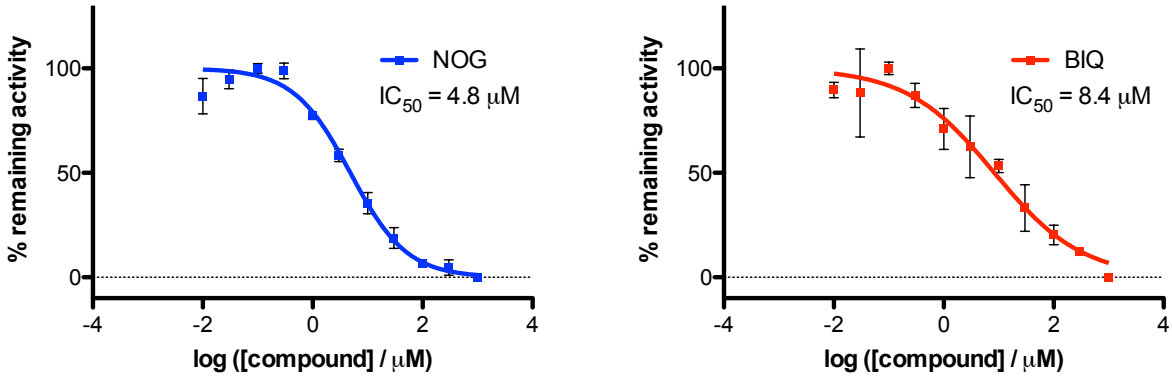

Figure 2.8 Inhibition curves for NOG and BIQ and their respective IC_{50} values using the PHD2 NODD AlphaScreen assay. Each datapoint represents the average signal ± standard deviation, n=3. Standard assay mixtures contain 1 nM PHD2, 45 nM biotinylated NODD peptide, 200 nM non-biotinylated NODD peptide, 2 μM 2OG, 10 μM Fe(II) and 100 μM L-ascorbic acid. Reactions were performed at room temperature for 40 min before being quenched with 30 mM of EDTA.

2.4 PHD2 CODD AlphaScreen assay is suitable for use in high-throughput screening

The AlphaScreen assays developed for PHD2 were carried out in a 384-well plate format, and are therefore amenable to medium or high-throughput screening. The IC_{50} values for over 100 in-house compounds (**Appendix 1**) were successfully determined using the PHD2 CODD AlphaScreen assay (**Figure 2.9, left panel**). The Z-factor, or Z′ (an indicator of assay signal dynamic range and data variation), is used to evaluate the assay quality for high-throughput screens [18]. The Z′ values were assessed for each experiment performed using the PHD2 CODD AlphaScreen assay. A Z′ value of lower than 1 but larger than or equals to 0.5 is an indication of a good assay [18]. The values of Z′ were found to be consistently above 0.5 (**Figure 2.9, right panel**), indicating that the PHD2 CODD AlphaScreen assay is suitable for use in high-throughput screening.

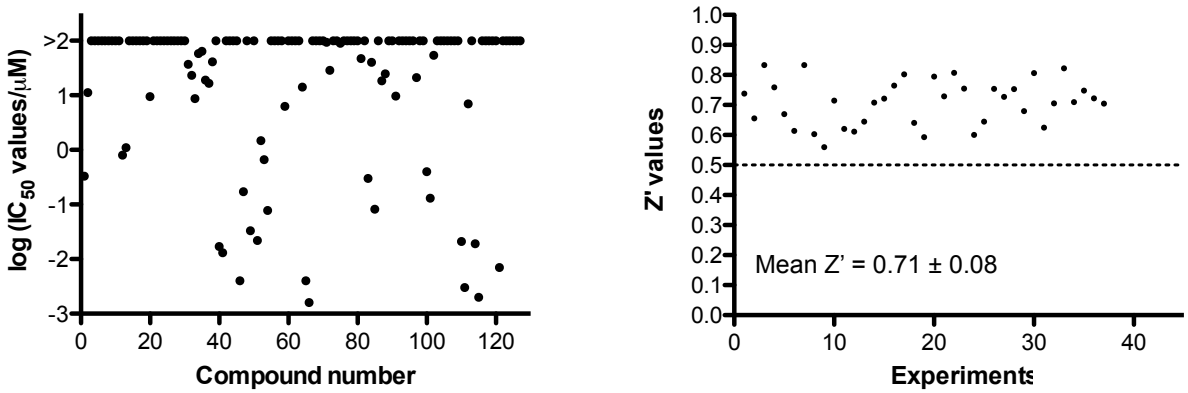

Figure 2.9 (left) Scatter plot showing the distribution of IC_{50} values (log transformed) obtained from the 127 compounds screened using the PHD2 CODD AlphaScreen assay. **(right)** Scatter plot highlighting that the distribution of Z′ values calculated from each experiment were above 0.5. Chemical structures of all compounds tested and their respective IC_{50} values as determined using the PHD2 CODD AlphaScreen assay are in **Appendix 1**.

2.5 PHD2 CODD AlphaScreen assay in the development of novel inhibitors of PHD2 using dynamic combinatorial chemistry

Note: The work in this section was done primarily in collaboration with Dr. M. Demetriades and has been reported in a modified form [19].

The dynamic-combinatorial chemistry linked to mass spectrometry (DCMS) technique is the use of protein mass spectrometry to analyse members of an interconverting mixture that bind to a target protein [20]. Attempts were initiated (by Dr. M. Demetriades [21]) to develop inhibitors of the PHDs based on the formation of boronate esters from the reversible reaction of boronic acids with a set of diols, and by monitoring their binding to PHD2 using non-denaturing electrospray ionisation mass spectrometry (ESI-MS) (**Figure 2.10**) [19]. To aid in the development of the stable analogues that mimic the structure of boronate ester hits identified by the DCMS method, the PHD2 CODD AlphaScreen assay was used to study their inhibitory potencies.

Boronate ester **1** and boronic acid **2** used in the initial DCMS experiments exhibit low inhibitory potencies against PHD2 (IC_{50} values of >1 mM and 126 μM, respectively). The subsequently prepared stable analogues designed from the boronate ester hits **3**, **4**, **5** and **6** showed an improvement in their inhibitory potencies compared to **2**, as judged by their submicromolar IC_{50} values (**Table 2.1**). These results were also consistent with their apparent affinity for PHD2 as determined by NMR spectrometry, as demonstrated by their binding constants, K_D (**Table 2.1**, data obtained from Dr. I. Leung). The methyl ester derivative of **6** was subsequently shown to be active in cells, as indicated by the upregulation HIF1α via the inhibition of PHDs but not FIH (**Figure 2.11**, work carried out with Dr. K. K. Yeoh). These results validated the DCMS approach for the identification of cell-active inhibitors of PHDs,

and demonstrate that the PHD2 CODD AlphaScreen assay can be used in determining the inhibitory potencies of novel PHD inhibitors.

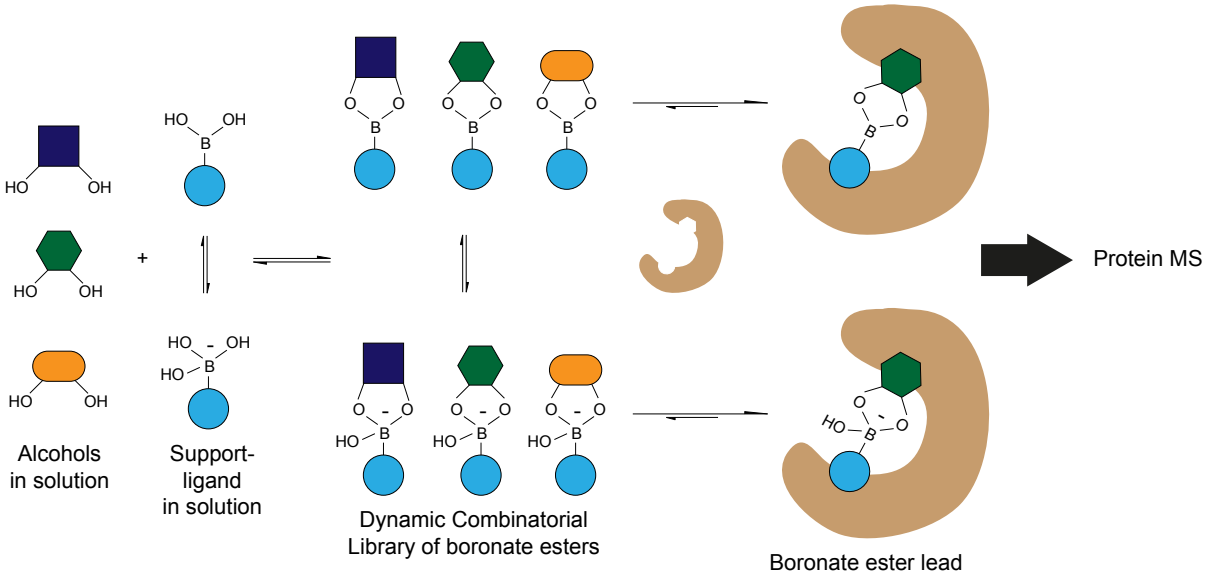

Figure 2.10 Schematic representation of the dynamic combinatorial mass spectrometry (DCMS) method used based on the formation of boronate esters from boronic acids. Figure adapted from [19].

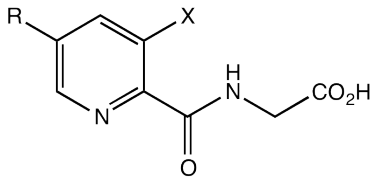

Compound	R	X	K_D (μM)	IC_{50} (μM)
1	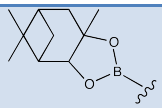	H	N/A	>1000
2	$B(OH)_2$	H	24.8	126
3	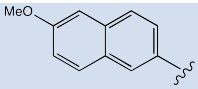	H	1.6	107
4	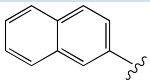	OH	0.5	0.017
5	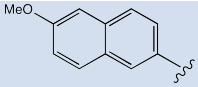	OH	0.8	0.013
6	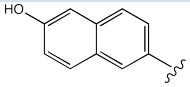	OH	0.9	0.004

Table 2.1 Binding constants (K_D) as measured by NMR spectrometry (data obtained from Dr. I. Leung) and IC_{50} values as measured by the PHD2 CODD AlphaScreen assay for selected inhibitors in the DCMS study. All compounds were synthesised by Dr. M. Demetriades [21].

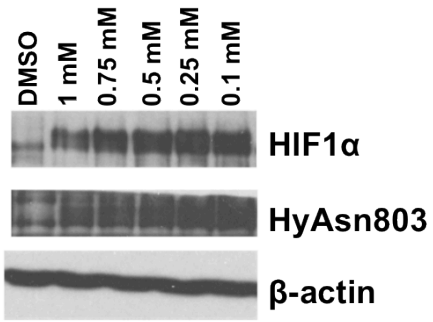

Figure 2.11 Upregulation of HIF1α in HeLa cells incubated with the methyl ester derivative of **6** for 4 h as detected by immunoblotting. The lack of inhibition of the HIF1α Asn803 hydroxylation indicates the selectivity of the compound for the PHDs over FIH. The immunoblotting analyses were carried out with Dr. K. K. Yeoh. HyAsn803: Hydroxyasparagine-803.

2.6 Inhibition studies on novel dual-action inhibitors of PHDs that induce the binding of a second iron ion

Note: The work in this section was done primarily in collaboration with Dr. K. K. Yeoh and has been reported in a modified form [22].

Most, if not all of the reported inhibitors of PHDs act by competing with 2OG for binding at the active site (see review [23]). Crystallographic studies show that PHD2 inhibitors (such as BIQ) tend to bind to the single active site metal in a bidentate manner (**Figure 2.12 A**). In cells, the PHDs can also be inhibited by reducing iron availability which leads to the induction of HIFα proteins, as demonstrated with the use of iron chelators such as deferoxamine (DFO) [24]. As a proof of principle, attempts were made to develop PHD inhibitors that can act by binding to the PHD active site and simultaneously deplete iron levels by inducing the binding of a second iron (work initiated by Dr. J. Mecinović [25]).

Initial investigations were focused on diacylhydrazine compounds, which have been proposed to form octahedral complexes with iron [27] based on molecular docking and ESI-MS studies (work carried out by Dr. J. Mecinović, Dr. A. Thalhammer and Dr. K. K. Yeoh). The docking and ESI-MS results suggests that the diacylhydrazines could induce the binding of a second iron at the PHD2 active site (proposed binding mode shown in **Figure 2.12 B**). To investigate this, 28 diacylhydrazine compounds (**Figure 2.13**) with differing potential to induce the binding of a second Fe(II) at the PHD2 active site were then shortlisted and tested for their inhibitory activities using the PHD2 CODD AlphaScreen assay. The results indicate that while most of the compounds were inactive (IC_{50} values >300 μM), there were active compounds with IC_{50} values ranging from 0.13 μM to 54 μM (**Table 2.2**). Notably, all the active single iron binding compounds (**5**, **8**, **9**, **14**, **21** and **28**) display the typical sigmoidal

inhibition curves indicative of dose-responsive inhibition, whereas the active two-iron binding compounds (**7**, **11**, **12** and **25**) exhibit atypical bimodal inhibition curves (**Figure 2.14**). This led to the hypothesis that the bimodal inhibition curves were indicative of two (or more) general mechanisms of PHD2 inhibition by these compounds – one via binding to the enzyme active site and another via chelation of free iron in solution.

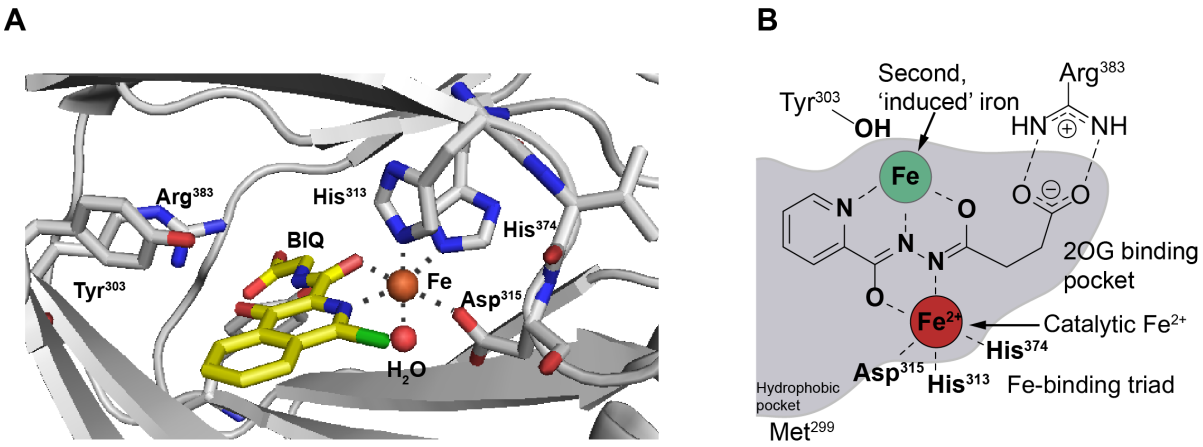

Figure 2.12 (**A**) View from a crystal structure of PHD2 active site and BIQ (PDB ID: 3HQU), a bidentate iron chelating inhibitor of PHD2 [26]. (**B**) Proposed binding of diacylhydrazines that induce binding of a second iron at the PHD2 active site. Figure B was prepared by Dr. A. Thalhammer.

It was therefore proposed that the bimodal inhibition curves are a result of the changing relative concentrations of apo-PHD2, PHD2.Fe, PHD2.Fe.inhibitor and inhibitor$_n$.Fe complexes in equilibrium. This proposal is supported by ESI-MS results (**Figure 2.15**, work carried out by Dr. M. Demetriades) for **7**, whereby the inactive PHD2.Fe$_2$.**7** complex is observed when iron is present in excess of the compound, but as the iron concentration is lowered, the active PHD2.Fe complex is observed with the inactive PHD2.Fe.**7** complex. This observation is indicative of a preferential formation of PHD2.Fe.**7** complex at lower iron concentrations, and that **7** binds more avidly to PHD2 as a two-iron complex compared to the single-iron complex. The formation of the active PHD2.Fe complex is in concordance with the slightly reduced inhibition observed at higher compound concentrations when assayed by PHD2 CODD AlphaScreen assay (phase 2 of the bimodal curve, see **Figure 2.14**). The

amount of inactive apo-PHD2 increases when **7** is further increased, most likely via chelation of free iron. The increase in inactive apo-PHD2 is indicative of increased inhibitory potency (possibly consistent with phase 3 of the bimodal inhibition curve as assayed by PHD2 CODD AlphaScreen, **Figure 2.14**). To roughly compare their inhibitory potencies, the IC_{50} values for compounds displaying the atypical inhibition curve were estimated by either removing the outliers or by analysing only the first sigmoidal phase of their respective inhibition curves (**Figure 2.14**).

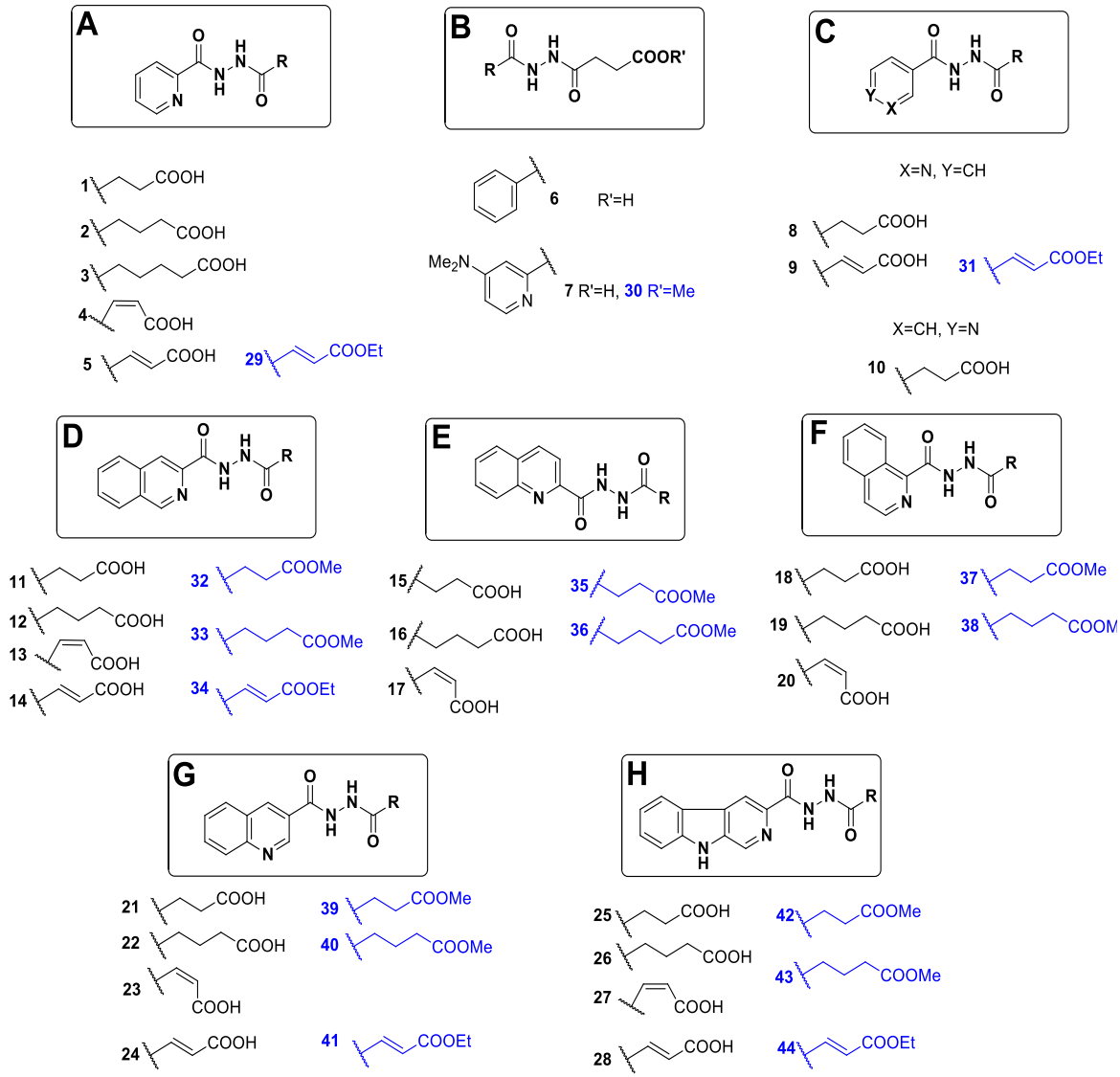

Figure 2.13 The 28 diacylhydrazine derivatives based on different scaffolds (and their methyl or ethyl ester forms, highlighted in blue) used in the dual-action PHD2 inhibitor study. Compounds were synthesised by Dr. J. Mecinović and Dr. K. K. Yeoh [25, 28].

Compound	Core	Sidechain	IC_{50}	Cell-based activity	PHD2.Fe_n.Compound Complexes in ESI-MS[a]	
					n =1	n =2
NOG (DMOG)			11.2	Active	+	
BIQ			0.33	Active	+	
1	2-Pyridyl	Succinate	>300	-		+
2	2-Pyridyl	Glutarate	>300	-		+
3	2-Pyridyl	Adipate	>300	-	No binding	
4	2-Pyridyl	Maleate	>300	-		+
5 (29)	2-Pyridyl	Fumarate	47	Active	+	
6	Phenyl	Succinate	>300	-	+	
7 (30)	4-Dimethyl-amino-pyridin-2-yl	Succinate	0.3[b]	Active		+
8	3-Pyridyl	Succinate	40	-	+	
9 (31)	3-Pyridyl	Fumarate	0.082	Active	+	
10	4-Pyridyl	Succinate	>300	-	+	
11 (32)	3-Isoquinolinyl	Succinate	18.4[b]	Active		+
12 (33)	3-Isoquinolinyl	Glutarate	24.6[b]	Active		+
13	3-Isoquinolinyl	Maleate	>300	-		+
14 (34)	3-Isoquinolinyl	Fumarate	9.7	Active	+	
15 (35)	2-Quinolinyl	Succinate	>300	Active		+
16 (36)	2-Quinolinyl	Glutarate	>300	Active		+
17	2-Quinolinyl	Maleate	>300	-		+
18 (37)	1-Isoquinolinyl	Succinate	>300	Active		+
19 (38)	1-Isoquinolinyl	Glutarate	>300	Active		+
20	1-Isoquinolinyl	Maleate	>300	-		+
21 (39)	3-Quinolinyl	Succinate	21	Inactive	+	
22 (40)	3-Quinolinyl	Glutarate	>300	Inactive	+	
23	3-Quinolinyl	Maleate	>300	-	+	
24 (41)	3-Quinolinyl	Fumarate	>300	Inactive	+	
25 (42)	3-9*H*-Pyrido [3,4-*b*]indolyl	Succinate	0.4[b]	ND		+
26 (43)	3-9*H*-Pyrido [3,4-*b*]indolyl	Glutarate	0.13[b]	ND		+
27	3-9*H*-Pyrido [3,4-*b*]indolyl	Maleate	ND	-		+
28 (44)	3-9*H*-Pyrido [3,4-*b*]indolyl	Fumarate	54	ND	+	

Table 2.2 Summary of the inhibitory potencies of the diacylhydrazine derivatives. IC_{50} values were obtained using the PHD2 AlphaScreen CODD assay. See **Figure 2.13** for inhibitor scaffold structures. The corresponding methyl or ethyl esters for the diacylhydrazines (ester numbers in parentheses) were tested in Hep3B cells for HIF1α induction.

[a] The number of iron ions bound in the most abundant PHD2.Fe_n.compound complex in ESI-MS experiments.

[b] Compounds that display bimodal inhibition curve and IC_{50} values were estimated as described in the main text. ND: not determined. Cell-based activity assay and ESI-MS work carried out by Dr. K. K. Yeoh and Dr. J. Mecinović as described in [25, 28].

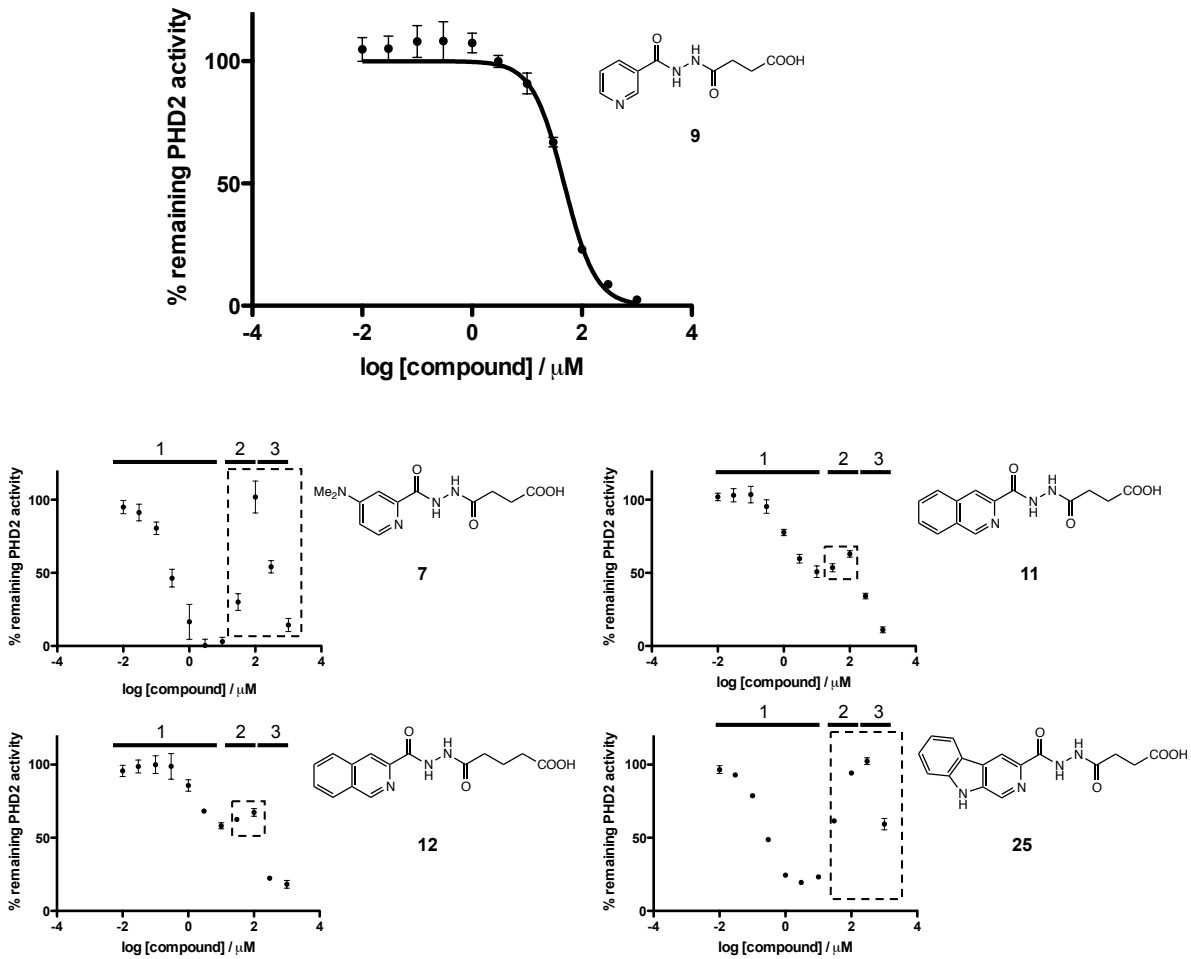

Figure 2.14 The single iron binding diacylhydrazine compounds such as **9** display typical inhibition curves, whereas the diacylhydrazines that bind two iron ions in complex with PHD2 display an atypical bimodal type of inhibition curve. The results are from the PHD2 CODD AlphaScreen assay, with each datapoint represents the average signal ± standard deviation, n≥3. For the compounds that bind two iron ions, data points highlighted in dashed boxes were removed to allow rough estimation of IC_{50} values. The black bars indicate the identified three phases of the bimodal inhibition curve (phases *1*, *2* and *3*).

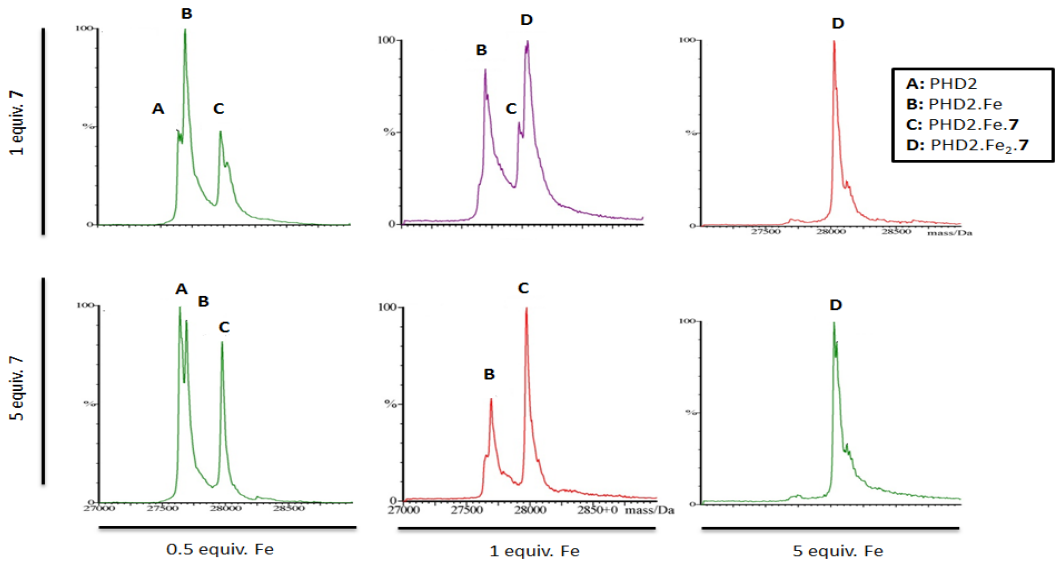

Figure 2.15 Non-denaturing ESI-MS studies with the catalytic domain of PHD2 demonstrate differential binding modes of **7** at varying iron concentrations. (**left)** When iron is limiting (0.5 equiv.), an increase in **7** led to an increase of apo-PHD2 (peak A) and PHD2.Fe.**7** (peak C) relative to PHD2.Fe (peak B), suggesting that **7** is able to chelate free iron in the solution. (**center)** When iron is equimolar to **7** (1 equiv., top spectra), **7** binds to PHD2 as either one iron (peak C) and two iron (peak D) complexes. (**right)** When iron is in excess (5 equiv.), **7** binds to PHD2 as a two iron complex (peak D). Data obtained from Dr. M. Demetriades [21]. equiv.: equivalent.

2.7 Discussion and future work

In this Chapter, the development of AlphaScreen assays for PHD2 is described. Using the AlphaScreen methodology, assays for the two substrate peptides corresponding to the two HIF1α hydroxylation sites for PHD2 were successfully developed and tested with two previously reported PHD inhibitors, NOG and BIQ. Interestingly, the relative inhibitory potencies for the two inhibitors are different in the CODD and NODD AlphaScreen assays. BIQ is approximately 33-fold more potent than NOG in inhibiting CODD hydroxylation (NOG IC_{50} = 11.2 μM, BIQ IC_{50} = 0.33 μM; **Figure 2.4**), whereas it is approximately 1.75-fold less potent than NOG in inhibiting NODD hydroxylation (NOG IC_{50} = 4.8 μM, BIQ IC_{50} = 8.4 μM; **Figure 2.8**) under the AlphaScreen assay conditions. Whilst the results from the PHD2 AlphaScreen assays may reflect true variations in the mechanisms of inhibition by the two inhibitors, the discrepancies could be due to the differences in the assay conditions (reaction time, enzyme concentrations and substrate peptide concentrations). It is possible that the binding of either BIQ or NOQ changes the structure of PHD2 in a way that differentially affects CODD or NODD binding to the PHD2.inhibitor complex. Moreover, crystallographic studies suggest that BIQ binding to the active site of PHD2 may affect HIF1α peptide binding, whereas NOG binding may not, or does not affect it to the same extent (**Figure 2.16**) [26].

The PHD2 NODD AlphaScreen assay may have utility in identifying selective inhibitor of NODD over CODD hydroxylation (or vice versa). However, the identification of such inhibitor may be practically difficult given that NODD and CODD peptides correspond to the different sites of the same protein (HIF1α) and they both bind the same site on PHD2. Mutagenesis studies suggest that a single mutation on PHD2 can affect its preference for NODD or CODD peptides. For example, the PHD2 R396A mutant preferentially

hydroxylates NODD over CODD, suggesting that this Arg396 residue is crucial for CODD (but not NODD) binding ([26] and unpublished work by Dr. R. Chowdhury). The possibility of replicating such an effect (i.e. switching the substrate peptide preference) of PHD2 by chemical intervention, which may be useful in studying the biological role of NODD and CODD, remains to be investigated.

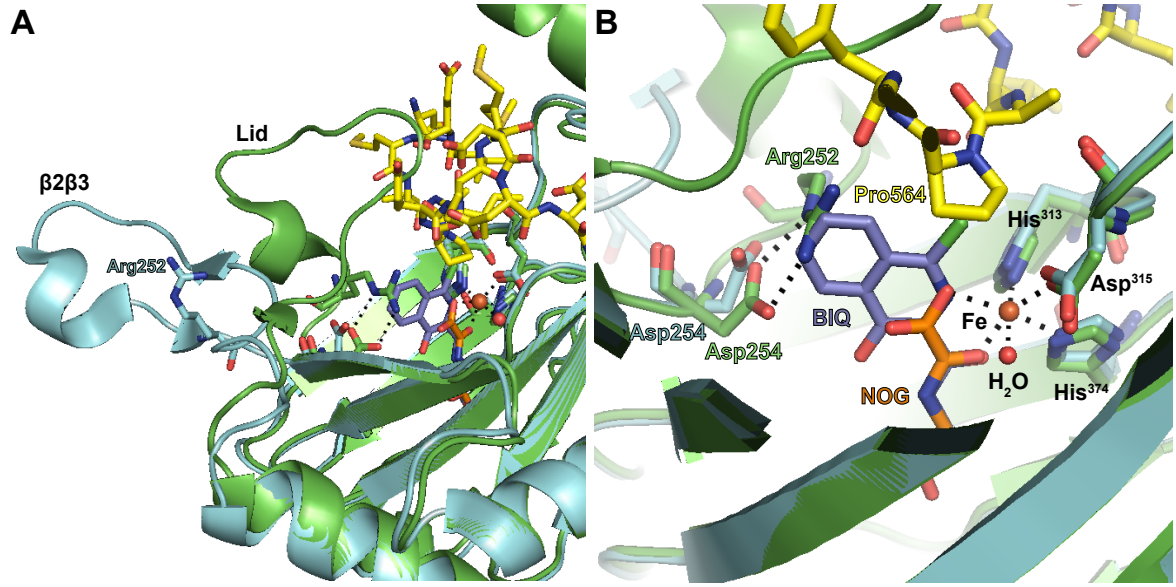

Figure 2.16 Superimposed views from crystal structures of PHD2.Fe(II).BIQ (cyan, PDB ID: 3HQU) with PHD2.Mn(II).NOG.CODD (green, PDB ID: 3HQR) [26]. HIF1α CODD peptide shown in yellow. (**A**) BIQ binding alters the conformation of the β2β3 loop, which adopts the closed (lid) conformation upon binding of CODD peptide. (**B**) BIQ binding may also affect the binding of CODD as shown by the steric clash with Pro564 of CODD peptide, which points into the active site of PHD2.

The use of the PHD2 CODD AlphaScreen assay in parallel with DCMS and NMR methods show that it can enable the identification of novel inhibitors for PHD2. Stable analogues designed from the boronate ester identified from our DCMS studies and optimised using the AlphaScreen assay subsequently led to the development of potent and cell-permeable PHD inhibitors. It is, however, important to note that inhibitor binding to PHD2 as revealed by ESI-MS may not necessarily correspond to good inhibitory potency when assayed using activity assays such as the PHD2 CODD AlphaScreen assay (as observed in the dual-action inhibitor study). This may be due to the different conditions in both assays, for example the

ESI-MS studies were conducted in gaseous phase as opposed to in solution for the AlphaScreen assay. Additionally, the binding kinetics of the inhibitor (such as weak/tight binders) may also be a factor.

As in many other *in vitro* assays, the unphysiological reaction conditions used (such as high concentrations of iron) can also lead to difficulties in the interpretation of results. This is evident in the dual action inhibitor study, where atypical inhibition curves were obtained for the two iron binding inhibitors, as opposed to a typical sigmoidal inhibition curve for the single iron binding inhibitors. It may be of interest to investigate how other known iron chelating inhibitors or iron chelators, including those in clinical use [29], affect the *in vitro* activities of PHD2 using the PHD2 CODD AlphaScreen assay.

Overall, the AlphaScreen methodology has been shown to be useful for the inhibition studies on PHD2. The PHD2 AlphaScreen assay is quick, non-radioactive, uses relatively low amount of enzyme and is amenable for high-throughput screening. There are, however, certain disadvantages of this assay – such as the inability to use this assay for detailed/initial rate kinetic studies due to the saturation of signal at high peptide substrate concentrations. Further efforts should also be put into developing the AlphaScreen technology for the other isoforms of PHD (i.e. PHD1 and PHD3) and FIH. PHD1 and PHD3 proteins have been difficult to purify in large amount, so the relatively low concentrations of enzymes required for the AlphaScreen assay may be particularly useful for these proteins. The development of these assays could be valuable in aiding the development of isoform specific inhibitors of PHDs and/or for the selectivity studies on inhibitors targeting other members of the 2OG-dependent dioxygenases.

2.8 Materials and methods

2.8.1 Reagents

Reagents were obtained from Sigma Aldrich (St. Louis, USA) or Alfa Aesar (Ward Hill, USA) unless otherwise stated. AlphaScreen General IgG (Protein A) detection kit was obtained from PerkinElmer Life and Analytical Sciences (Waltham, USA). The rabbit polyclonal anti-hydroxy-Pro402 (07-1585) was obtained from Millipore (Billerica, USA). The rabbit monoclonal antibody anti-hydroxy-Pro564 clone D43B5 (3434S) was obtained from Cell Signaling (Danvers, USA).

2.8.2 Protein and peptides

Purified PHD2$^{181-426}$ proteins were prepared by Dr. O. King as previously reported [16]. Biotinylated 19-mer HIF1α peptides (CODD, CODD-OH and NODD peptides) and non-biotinylated 19-mer HIF1α NODD peptide were purchased from GL Biochem (Shanghai, China). Biotinylated 19-mer HIF1α NODD-OH peptide was prepared by Dr. C. Loenarz. The sequences of the peptides are as follows:

Peptide	**Sequences**
CODD	DLDLEMLAPYIPMDDDFQL
CODD-OH	DLDLEMLAHypYIPMDDDFQL
NODD	DALTLLAPAAGDTIISLDF
NODD-OH	DALTLLAHypAAGDTIISLDF

Hyp = *trans*-4-hydroxyproline

Biotinylated peptides are biotin-labeled at the *N*-terminus of the peptide.

2.8.3 PHD2 CODD AlphaScreen assay

AlphaScreen inhibition assays for CODD hydroxylation were carried out in 384-well white ProxiPlates (PerkinElmer, Waltham, USA) in 10 μl reaction volumes in the AlphaScreen buffer (50mM HEPES pH 7.5 buffer, 0.01% Tween-20 and 0.1% BSA) at room temperature. The final concentration of DMSO in each reaction was 0.2%. Standard reaction mixtures consisted of the following final concentrations of reagents:

Enzyme mixture	PHD2	1 - 5 nM
	L-ascorbic acid	100 μM
	$FeSO_4.7H_2O$	10 μM
Peptide mixture	2OG	2 μM
	Biotin-CODD	60 nM

Compounds (of various concentrations in DMSO) were pre-incubated with the enzyme mixture for 15 minutes before the reaction was initiated by the addition of the peptide mixture. Reactions were allowed to proceed for 10 minutes at room temperature. Each reaction was then quenched with 5 μl of 30 mM EDTA. 5 μl of CODD bead mix[a] were then added to the reaction mixture and incubated for 1 hour at room temperature. The plates were analysed using an EnVision Multilabel plate reader (Perkin Elmer, Waltham, USA) with laser excitation at 680 nm wavelength and 570 nm wavelength emission filter. IC_{50} values were calculated using GraphPad Prism 5.0 (GraphPad Software Inc., La Jolla, USA).

[a] CODD bead mix contained AlphaScreen beads (AlphaScreen streptavidin-conjugated donor and Protein A-conjugated acceptor beads; PerkinElmer, Waltham, USA) pre-incubated with 1:8,000 rabbit monoclonal anti-hydroxy-Pro564 antibody for at least 30 min at room temperature prior to use.

2.8.4 PHD2 NODD AlphaScreen assay

AlphaScreen inhibition assays for NODD hydroxylation were carried out in 384-well white ProxiPlates (PerkinElmer, Waltham, USA) in 10 μl reaction volumes in the AlphaScreen buffer (50mM HEPES pH 7.5 buffer, 0.01% Tween-20 and 0.1% BSA) at room temperature. The final concentration of DMSO in each reaction was 0.2%. Standard reaction mixtures consisted of the following final concentrations of reagents:

Enzyme mixture	PHD2	10 nM
	L-ascorbic acid	100 μM
	$FeSO_4.7H_2O$	10 μM
Peptide mixture	2OG	2 μM
	NODD	200 nM
	Biotin-NODD	45 nM

Compounds (of various concentrations in DMSO) were pre-incubated with the enzyme mixture for 15 minutes before the reaction was initiated by the addition of the peptide mixture. Reactions were allowed to proceed for 40 minutes at room temperature. Each reaction was quenched with 5 μl of 30 mM EDTA. 5 μl of NODD bead mixture[b] were then added to the reaction mixture and incubated for 1 hour at room temperature. The plates were analysed using an EnVision Multilabel plate reader (Perkin Elmer, Waltham, USA) with laser excitation at 680 nm wavelength and 570 nm wavelength emission filter. IC_{50} values were calculated using GraphPad Prism 5.0 (GraphPad Software Inc., La Jolla, USA).

[b] NODD bead mix contained AlphaScreen beads (AlphaScreen streptavidin-conjugated donor and Protein A-conjugated acceptor beads; PerkinElmer, Waltham, USA) pre-incubated with 125 ng/µl of rabbit polyclonal anti-hydroxy-Pro402 antibody for at least 30 min at room temperature prior to use.

2.8.5 Determination of Z′ values

Z′ values were calculated as described [18] using the control data from each experiment.

$$\boldsymbol{Z'} = 1 - \frac{3\sigma_{c+} + 3\sigma_{c-}}{|\mu_{c+} - \mu_{c-}|}$$

The above formula was used for **Z′** value calculations, where*:*

σ_{c+} = standard deviation of positive control signal

σ_{c-} = standard deviation of negative control signal

μ_{c+} = mean signal for positive control

μ_{c-} = mean signal for negative control

The positive control signal is the signal obtained for the assay done without the presence of inhibitor. The negative control signal is the signal obtained for the pre-quenched assay reaction without the presence of inhibitor (with EDTA pre-added to the assay mixture prior to initiation of reaction).

2.9 References

1 Hirsila, M., Koivunen, P., Gunzler, V., Kivirikko, K. I. and Myllyharju, J. (2003) Characterization of the human prolyl 4-hydroxylases that modify the hypoxia-inducible factor. J Biol Chem. **278**, 30772-30780

2 Li, D., Hirsila, M., Koivunen, P., Brenner, M. C., Xu, L., Yang, C., Kivirikko, K. I. and Myllyharju, J. (2004) Many amino acid substitutions in a hypoxia-inducible transcription factor (HIF)-1alpha-like peptide cause only minor changes in its hydroxylation by the HIF prolyl 4-hydroxylases: substitution of 3,4-dehydroproline or azetidine-2-carboxylic acid for the proline leads to a high rate of uncoupled 2-oxoglutarate decarboxylation. J Biol Chem. **279**, 55051-55059

3 Wirthner, R., Balamurugan, K., Stiehl, D. P., Barth, S., Spielmann, P., Oehme, F., Flamme, I., Katschinski, D. M., Wenger, R. H. and Camenisch, G. (2007) Determination and modulation of prolyl-4-hydroxylase domain oxygen sensor activity. Methods Enzymol. **435**, 43-60

4 Kanelakis, K. C., Palomino, H. L., Li, L., Wu, J., Yan, W., Rosen, M. D., Rizzolio, M. C., Trivedi, M., Morton, M. F., Yang, Y., Venkatesan, H., Rabinowitz, M. H., Shankley, N. P. and Barrett, T. D. (2009) Characterization of a robust enzymatic assay for inhibitors of 2-oxoglutarate-dependent hydroxylases. J Biomol Screen. **14**, 627-635

5 Flashman, E., Bagg, E. A., Chowdhury, R., Mecinovic, J., Loenarz, C., McDonough, M. A., Hewitson, K. S. and Schofield, C. J. (2008) Kinetic rationale for selectivity toward N- and C-terminal oxygen-dependent degradation domain substrates mediated by a loop region of hypoxia-inducible factor prolyl hydroxylases. J Biol Chem. **283**, 3808-3815

6 Flashman, E., Davies, S. L., Yeoh, K. K. and Schofield, C. J. (2010) Investigating the dependence of the hypoxia-inducible factor hydroxylases (factor inhibiting HIF and prolyl hydroxylase domain 2) on ascorbate and other reducing agents. Biochem J. **427**, 135-142

7 Flashman, E., Hoffart, L. M., Hamed, R. B., Bollinger, J. M., Jr., Krebs, C. and Schofield, C. J. (2010) Evidence for the slow reaction of hypoxia-inducible factor prolyl hydroxylase 2 with oxygen. FEBS J. **277**, 4089-4099

8 McNeill, L. A., Bethge, L., Hewitson, K. S. and Schofield, C. J. (2005) A fluorescence-based assay for 2-oxoglutarate-dependent oxygenases. Anal Biochem. **336**, 125-131

9 Rose, N. R., McDonough, M. A., King, O. N., Kawamura, A. and Schofield, C. J. (2011) Inhibition of 2-oxoglutarate dependent oxygenases. Chem Soc Rev. **40**, 4364-4397

10 Dao, J. H., Kurzeja, R. J., Morachis, J. M., Veith, H., Lewis, J., Yu, V., Tegley, C. M. and Tagari, P. (2009) Kinetic characterization and identification of a novel inhibitor of hypoxia-inducible factor prolyl hydroxylase 2 using a time-resolved fluorescence resonance energy transfer-based assay technology. Anal Biochem. **384**, 213-223

11 Stubbs, C. J., Loenarz, C., Mecinovic, J., Yeoh, K. K., Hindley, N., Lienard, B. M., Sobott, F., Schofield, C. J. and Flashman, E. (2009) Application of a proteolysis/mass spectrometry method for investigating the effects of inhibitors on hydroxylase structure. J Med Chem. **52**, 2799-2805

12 Kawamura, A., Tumber, A., Rose, N. R., King, O. N., Daniel, M., Oppermann, U., Heightman, T. D. and Schofield, C. (2010) Development of homogeneous luminescence assays for histone demethylase catalysis and binding. Anal Biochem. **404**, 86-93

13 Ullman, E. F., Kirakossian, H., Singh, S., Wu, Z. P., Irvin, B. R., Pease, J. S., Switchenko, A. C., Irvine, J. D., Dafforn, A., Skold, C. N. and et al. (1994) Luminescent oxygen channeling immunoassay: measurement of particle binding kinetics by chemiluminescence. Proc Natl Acad Sci U S A. **91**, 5426-5430

14 Ullman, E. F., Kirakossian, H., Switchenko, A. C., Ishkanian, J., Ericson, M., Wartchow, C. A., Pirio, M., Pease, J., Irvin, B. R., Singh, S., Singh, R., Patel, R., Dafforn, A., Davalian, D., Skold, C., Kurn, N. and Wagner, D. B. (1996) Luminescent oxygen channeling assay (LOCI): sensitive, broadly applicable homogeneous immunoassay method. Clin Chem. **42**, 1518-1526

15 http://www.perkinelmer.com/CMSResources/Images/APP_AlphaScreen_Principles.pdf

16 McNeill, L. A., Flashman, E., Buck, M. R., Hewitson, K. S., Clifton, I. J., Jeschke, G., Claridge, T. D., Ehrismann, D., Oldham, N. J. and Schofield, C. J. (2005) Hypoxia-inducible factor prolyl hydroxylase 2 has a high affinity for ferrous iron and 2-oxoglutarate. Mol Biosyst. **1**, 321-324

17 Ehrismann, D., Flashman, E., Genn, D. N., Mathioudakis, N., Hewitson, K. S., Ratcliffe, P. J. and Schofield, C. J. (2007) Studies on the activity of the hypoxia-inducible-factor hydroxylases using an oxygen consumption assay. Biochem J. **401**, 227-234

18 Zhang, J. H., Chung, T. D. and Oldenburg, K. R. (1999) A Simple Statistical Parameter for Use in Evaluation and Validation of High Throughput Screening Assays. J Biomol Screen. **4**, 67-73

19 Demetriades, M., Leung, I. K., Chowdhury, R., Chan, M. C., McDonough, M. A., Yeoh, K. K., Tian, Y. M., Claridge, T. D., Ratcliffe, P. J., Woon, E. C. and Schofield, C. J. (2012) Dynamic combinatorial chemistry employing boronic acids/boronate esters leads to potent oxygenase inhibitors. Angew Chem Int Ed Engl. **51**, 6672-6675

20 Ramstrom, O. and Lehn, J. M. (2002) Drug discovery by dynamic combinatorial libraries. Nat Rev Drug Discov. **1**, 26-36

21 Demetriades, M. (2013) Dynamic combinatorial mass spectrometry for 2-oxoglutarate oxygenase inhibition. University of Oxford (D.Phil thesis)

22 Yeoh, K. K., Chan, M. C., Thalhammer, A., Demetriades, M., Chowdhury, R., Tian, Y. M., Stolze, I., McNeill, L. A., Lee, M. K., Woon, E. C., Mackeen, M. M., Kawamura, A., Ratcliffe, P. J., Mecinovic, J. and Schofield, C. J. (2013) Dual-action inhibitors of HIF prolyl hydroxylases that induce binding of a second iron ion. Org Biomol Chem. **11**, 732-745

23 Yan, L., Colandrea, V. J. and Hale, J. J. (2010) Prolyl hydroxylase domain-containing protein inhibitors as stabilizers of hypoxia-inducible factor: small molecule-based therapeutics for anemia. Expert Opin Ther Pat. **20**, 1219-1245

24 Wang, G. L. and Semenza, G. L. (1993) Desferrioxamine induces erythropoietin gene expression and hypoxia-inducible factor 1 DNA-binding activity: implications for models of hypoxia signal transduction. Blood. **82**, 3610-3615

25 Mecinović, J. (2009) Enzymatic and Non-Enzymatic Iron Catalysis: Mechanistic and Inhibition Studies. University of Oxford (D.Phil thesis)

26 Chowdhury, R., McDonough, M. A., Mecinovic, J., Loenarz, C., Flashman, E., Hewitson, K. S., Domene, C. and Schofield, C. J. (2009) Structural basis for binding of hypoxia-inducible factor to the oxygen-sensing prolyl hydroxylases. Structure. **17**, 981-989

27 Bernhardt, P. V., Chin, P. and Richardson, D. R. (2001) Unprecedented oxidation of a biologically active aroylhydrazone chelator catalysed by iron(III): serendipitous identification of diacylhydrazine ligands with high iron chelation efficacy. J Biol Inorg Chem. **6**, 801-809

28 Yeoh, K. K. (2012) Studies on the inhibition of human hypoxia inducible factor (HIF) hydroxylases. University of Oxford (D.Phil thesis)

29 Heli, H., Mirtorabi, S. and Karimian, K. (2011) Advances in iron chelation: an update. Expert Opin Ther Pat. **21**, 819-856

Chapter 3: The development of quantitative cellular assays for HIF levels

3.1 Introduction

As described in **Chapter 1**, the inhibition of PHDs in cells leads to the stabilisation of HIFα proteins, and subsequently the activation of the HIF transcriptional pathway. Quantification of HIFα levels by immunoblotting is widely used to measure the extent of PHD inhibition in cells (for example, see [1]). Cell lines of interest are usually treated with or without the candidate PHD inhibitor, before being harvested and analysed for the changes in the HIFα protein level and HIFα hydroxylation status by immunoblotting. However, this method is laborious, time consuming and semi-quantitative. Studying the inhibition of endogenous PHDs by this method becomes a challenging task when it involves a large number of inhibitors, especially when comparison of the relative activity for each inhibitor is required.

Another method to indirectly monitor the inhibition of endogenous PHDs in cells is by indirectly measuring the transcriptional activity of the HIF protein using a cellular reporter assay, such as firefly luciferase-based reporter assays (for examples, see [2, 3]). Typically, a construct containing the luciferase gene under the control of a minimal promoter and hypoxia responsive elements (HREs) is expressed either stably or transiently in a cell line of interest. This cell line is then treated with or without the candidate PHD inhibitors and the activation of the transcriptional activity of HIF is inferred by the measured increase in the production of light from the luciferase expressed. While this technique is quantitative, the transcriptional activity of HIF is not a direct indicator for PHD inhibition, for reasons including the possibility of FIH inhibition leading to the activation of HIF transcriptional activity [4-6]. A

cellular luciferase assay based on the HIF oxygen-dependent degradation domain (ODD) fused to the luciferase reporter gene [7] is a better assay to distinguish the inhibition of the PHDs from that of FIH, although like the HRE-luciferase reporter assay, cell lines of interest would still have to be individually transfected (stably or transiently) with the reporter plasmid before the assay can be performed. Therefore, comparison of the inhibitor activity on endogenous PHDs in different cell lines may be difficult.

Thus, directly monitoring the levels of HIFα and the levels of HIF1α hydroxylation within the ODD, is arguably the best method to measure the extent of endogenous PHD inhibition in cells. To do this, the development of a quantitative assay, particularly one that is suitable for medium- to high-throughput screening, is required. Although the traditional enzyme-linked immunosorbent assay (ELISA) was first taken into consideration, the broader dynamic range and the multiplexing capability of an electrochemiluminescence assay platform with carbon electrode plates developed by Meso Scale Discovery (MSD) [8] made it a potentially useful assay for development as a medium- to high-throughput assay for HIF levels. This assay is hereafter referred to as the MSD assay.

The work in this Chapter describes the development of the MSD assays for HIF1α and HIF2α proteins as quantitative assays for measuring endogenous PHD inhibition. The feasibility of this assay in detecting the changes to the hydroxylation status of HIF1α and in measuring the activity of PHD inhibitors *in vivo* were also explored. The applications of these assays in the cellular and animal studies of PHD inhibitors are described in **Chapter 4**.

3.2 Principle of MSD electrochemiluminescence assay

In principle, the MSD assay is similar to that of a traditional sandwich ELISA (**Figure 3.1**), with the exception that the former is based on electrochemiluminescence instead of colorimetric detection [9]. The antigen of interest in a lysate mixture is first captured by a capture antibody immobilised on a carbon electrode surface of the MSD 96-well Multi Array plate. The captured antigen can then be detected either by a labelled primary antibody, or an unlabelled primary antibody used with a labelled secondary antibody that recognises the primary antibody. The primary or secondary antibody must be labelled with a sulfonated derivative of ruthenium (II) tris-bipyridine, *N*-hydroxysuccinimide (hereafter referred to as $Ru(bpy)_3$ or MSD SULFO-TAG™ NHS) (**Figure 3.2**, left panel) [10]. When the antigen of interest is captured, the labelled antibody would be brought to close proximity to the carbon electrode surface of the plate, which can be induced to generate an electrochemiluminescence signal in the presence of tripropylamine (TPA) as a co-reactant (**Figure 3.2**, right panel) [11, 12]. The signal generation is based on the high-energy electron transfer reaction between the oxidised ruthenium-complex and a neutral radical of TPA, leading to the formation of an excited-state ruthenium-complex. This excited state ruthenium-complex returns to the ground state with the emission of a photon at 620 nm wavelength, which is detected using the MSD Sector S600 instrument that converts the light intensity to a numerical value. The electrochemiluminescence signal is proportional to the amount of the ruthenium-complex present at the electrode [11, 12].

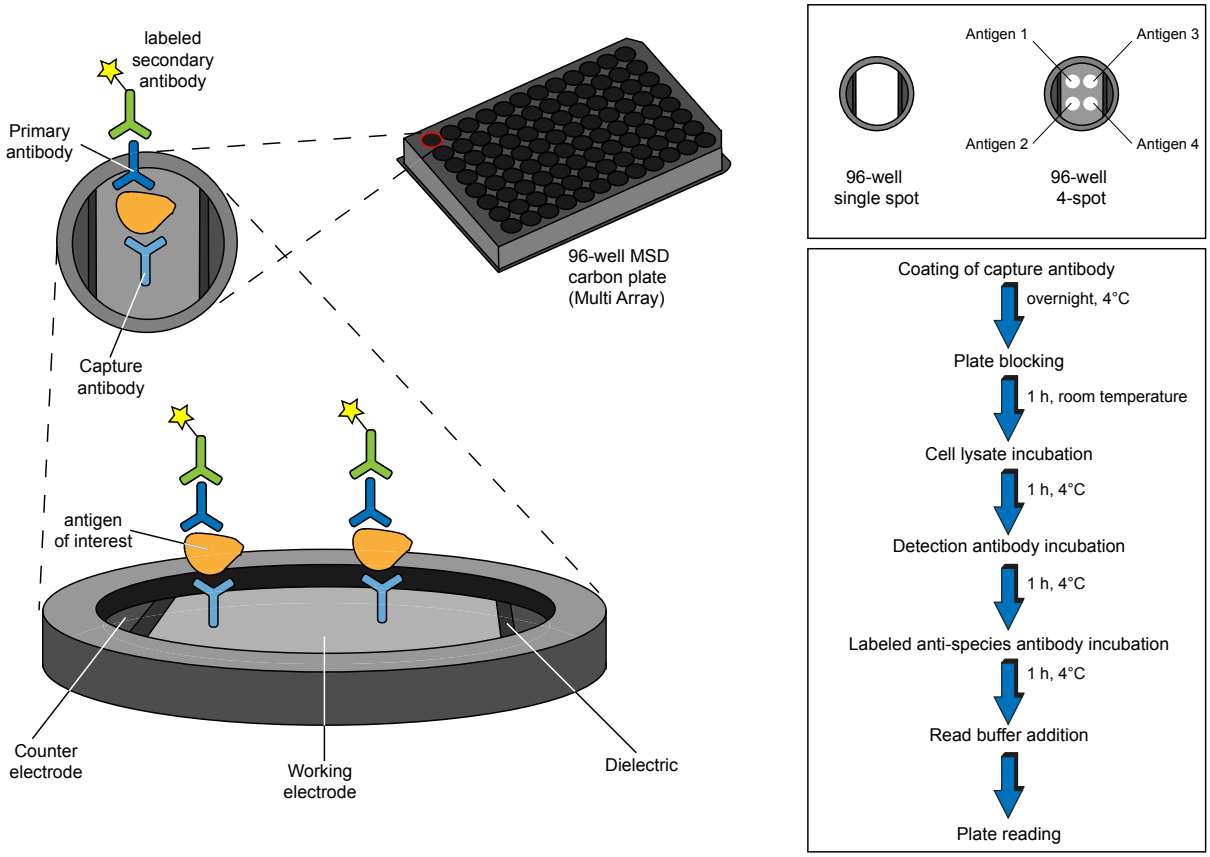

Figure 3.1 The principle of the MSD assay. (**left**) The capture antibody is immobilised on the carbon electrode surface of the 96-well MSD Multi-Array plate to capture the antigen of interest. The captured antigen can be detected either with a labelled primary antibody, or an unlabelled primary antibody used in combination with a labelled secondary antibody. (**top right**) The MSD assay can be designed to detect single or multiple antigens within the same well, such as the detection of up to 4 antigens with the 96-well 4-spot plates. (**bottom right**) A schematic diagram of the protocol for a standard MSD assay. Figure adapted from [9].

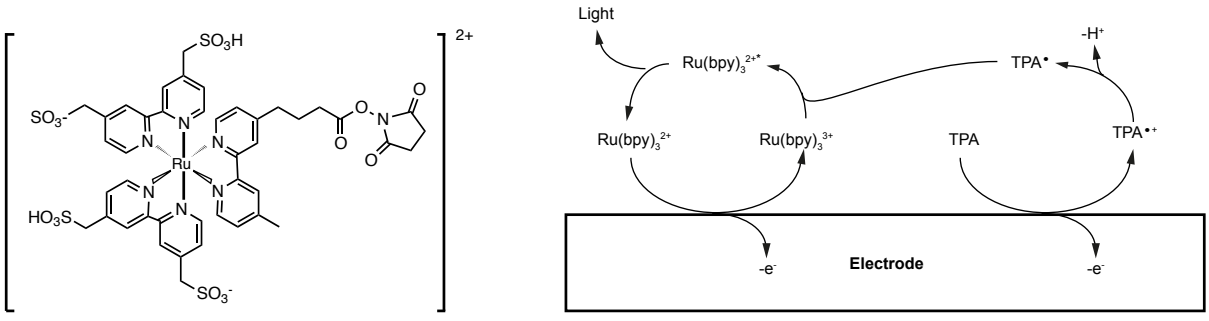

Figure 3.2 (**left**) The MSD SULFO-TAG™ NHS or $Ru(bpy)_3$ label used for the generation of electrochemiluminescence signal. (**right**) The mechanism of electrochemiluminescence signal generation. TPA: tripropylamine. Figure adapted from [9, 12].

3.3 Selection of HIF1α and HIF2α antibodies

In MSD assays, the capture antibody has to be purified and be free of carrier proteins (such as bovine serum albumin or gelatin). Unpurified antibodies such as serum/antiserum from an immunised host, tissue culture supernatant or ascites fluid are not suitable as capture antibodies due to the presence of other proteins that would bind to the surface of the plate and thereby compete with the antibody of interest [13].

The primary antibody can be used in purified or unpurified form, but only if it is used with an MSD SULFO-TAG™ NHS labelled secondary antibody. If there is no secondary antibody, the primary antibody has to be purified before it can be directly labelled with the MSD SULFO-TAG™ NHS ester (which forms an amide bond in reaction with the primary amine groups within the antibody) [10]. This labelling reaction can be hindered by reagents containing primary amines and strong nucleophiles (such as Tris buffer, glycine, azide and glycerol), thus any commercial antibodies supplied in the presence of these would have to be purified or buffer-exchanged before they can be labelled [10]. For simplicity, the HIF1α and HIF2α MSD assays would be developed with unlabelled primary antibodies used in combination with labelled secondary antibodies.

To identify suitable capture and primary antibodies for the HIF1α and HIF2α MSD assay, a selection of commercially-sourced and in-house antibodies recognising different epitopes of HIF1α and HIF2α were shortlisted (**Table 3.1** and **Table 3.2**). These antibodies were also selected based on their potential to detect native proteins, according to the applications that they have been tested in. A total of five HIF1α antibodies and three HIF2α antibodies were chosen for the assay development.

Antibody name	Application tested	Recognition epitope/ immunogen	Host species/ clonality	Species reactivity	Sources
1) Y-15 (supplied without BSA)	WB, IF, ELISA	A peptide mapping near the *N*-terminus of the human HIF1α	Goat (polyclonal)	Human, Mouse, Rat	Santa Cruz Biotechnology (Cat. No.: sc-12542)
2) NB100-479 (supplied without BSA)	WB, IF, ICC, IHC	A fusion protein containing mouse HIF1α residues 530-825	Rabbit (polyclonal)	Human, Mouse, Rat, Primate	Novus Biologicals (Cat. No.: NB100-479)
3) TL-54 (supplied with BSA)	WB, IF	Human HIF1α peptide residues 610-727	Mouse (monoclonal)	Human	BD Transduction Laboratories (Cat. No.: 610958)
4) H1alpha67 (supplied without BSA)	WB, IF, ICC, IHC, IP, ChIP	A fusion protein containing human HIF1α residues 432-528	Mouse (monoclonal)	Human, Mouse, Rat, Primate	Novus Biologicals (Cat. No.: NB100-105)
5) PM14 (unpurified serum from immunised host)	WB, ChIP	A fusion protein containing mouse HIF1α residues 445-553	Rabbit serum (polyclonal)	Human, Mouse	Ratcliffe/Pugh laboratory [14]

WB: Western Blot, IF: Immunofluorescence, ICC: Immunocytochemistry, IHC: Immunohistochemistry, ELISA: Enzyme-linked immunosorbent assay, IP: Immunoprecipitation, ChIP: Chromatin immunoprecipitation, Cat. No.: Catalogue number.

Table 3.1 HIF1α antibodies shortlisted for the development of the HIF1α MSD assay.

Antibody name	Application tested	Recognition epitope/ immunogen	Host species/ clonality	Species reactivity	Sources
1) 190b (supplied without BSA)	WB, ELISA, Flow cytometry, IHC	Human HIF2α residues 535-631	Mouse (monoclonal)	Human, Mouse, Rat	Novus Biologicals (Cat. No.: NB100-132)
2) NB100-122 (supplied without BSA)	WB, IF, ICC, IHC, ELISA, ChIP, IP	A peptide derived from the *C*-terminus of mouse/human HIF2α	Rabbit (polyclonal)	Human, Mouse, Rat, Fish	Novus Biologicals (Cat. No.: NB100-122)
3) PM9 (unpurified serum from immunised host)	WB, ChIP	A fusion protein containing mouse HIF2α residues 357-439	Rabbit (polyclonal)		Ratcliffe/Pugh laboratory [14]

WB: Western Blot, IF: Immunofluorescence, ICC: Immunocytochemistry, IHC: Immunohistochemistry, ELISA: Enzyme-linked immunosorbent assay, IP: Immunoprecipitation, ChIP: Chromatin immunoprecipitation, Cat. No.: Catalogue number.

Table 3.2 HIF2α antibodies shortlisted for the development of the HIF2α MSD assay.

3.4 Development of the HIF1α MSD assay

For HIF1α, only the Y15, NB100-479 and H1alpha67 antibodies could be tested as the capture antibody for the MSD assay, as they are supplied without carrier proteins. The potential of the Y-15 antibody as a capture antibody was first tested with either TL-54 or NB100-479 as the primary antibody. HeLa cells were treated with deferoxamine (DFO) for 4 h to induce HIF and lysed using the standard MSD lysis buffer (refer to **Section 3.10 Materials and methods** for buffer components) to be used as the positive control lysate. The lysates from untreated HeLa cells were used as the negative control. Protein assay was used to quantify the total protein in the cell lysate. The MSD assay was performed and the ratio of mean positive signal over mean negative signal (P/N) was calculated as a measure of the assay performance. The positive signal was the signal produced with the HIF1α stabilised DFO-treated lysate, whereas the negative signal was the signal produced with the untreated cells containing normoxic HIF1α. The Y-15 (capture) and TL-54 (primary) antibody pair consistently produced signal with P/N ratio of above 8.5 with total cell lysate of 2.5 µg to 20 µg (**Figure 3.3**). The Y-15 (capture) and NB100-479 (primary) antibody pair produced a higher signal in the positive control lysate than the earlier antibody pair tested, but the P/N ratio was lower (below 4).

The H1alpha67 antibody was then tested as the capture antibody, in combination with either the NB100-479, Y-15 or PM14 antibodies as the primary antibody. In this experiment, a positive control lysate (i.e. one with HIF1α present) was prepared from HepG2 cells treated with the proteasome inhibitor MG132 for 4 h before being harvested with the standard MSD lysis buffer. MG132 has been shown to cause cellular HIF1α stabilisation under normoxia [15]. Negative control lysate was similarly prepared from untreated HepG2 cells. When tested using the MSD assay, the H1alpha67 antibody (as capture antibody) in combination with

either NB100-479 or PM14 (as primary antibody) produced a good detection signal with P/N ratio of >15.1 and >8.1, respectively (**Figure 3.4**). Although a direct comparison cannot be made against the previous experiments on the Y-15 antibody (**Figure 3.3**) due to the different cell lysates used, the working antibody pairs with H1alpha67 as the capture antibody produced higher signal and P/N ratio compared to the antibody pairs with Y-15 as the capture antibody, at equivalent total cell lysate. With this observation in mind and taking into consideration that NB100-479 can be commercially-sourced whereas PM14 is a limited in-house antibody, the H1alpha67-NB100-470 (capture antibody – detection antibody) combination was chosen for further assay optimisation.

To investigate the lower limit of detection using the H1alpha67-NB100-479 antibody combination, the total HepG2 cell lysates were serially diluted (to concentrations below 5 μg) and tested in the MSD assay. As shown in **Figure 3.5**, the HIF1α signal could still be detected when using as little as 0.625 μg of the positive cell lysate (mean signal of 21 763), with P/N ratio of >15.8 in all concentrations of total cell lysate tested. Taken together, the H1alpha67 (as the capture antibody) and NB100-479 (as the primary antibody) pair is suitable for the detection of HIF1α using the MSD assay, with a broad dynamic range and high sensitivity.

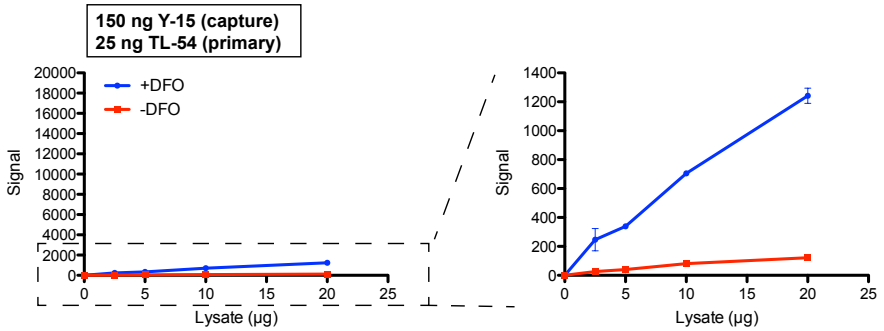

Lysate (µg)	Mean positive signal	P/N
20.0	1 242	10.2
10.0	705	8.7
5.0	339	8.5
2.5	247	9.5

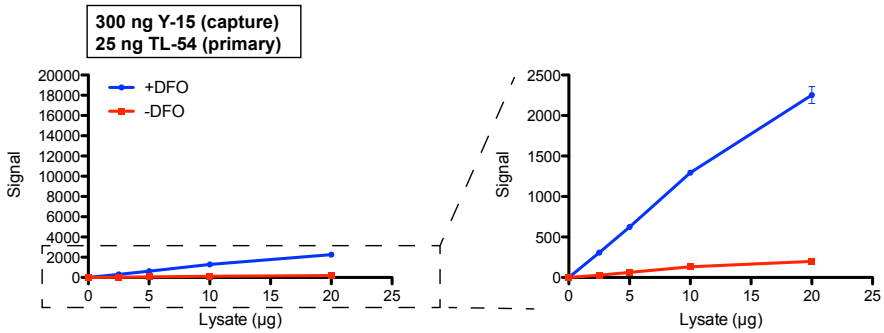

Lysate (µg)	Mean positive signal	P/N
20.0	2 253	11.4
10.0	1 295	9.7
5.0	624	9.9
2.5	308	11.2

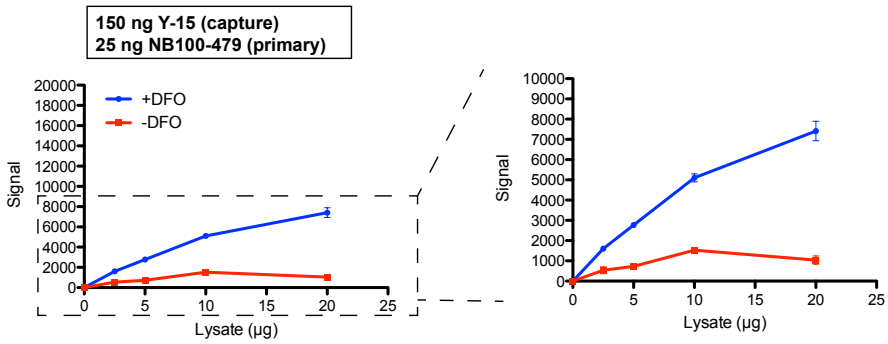

Lysate (µg)	Mean positive signal	P/N
20.0	7 415	7.1
10.0	5 100	3.3
5.0	2 771	3.8
2.5	1 608	3.0

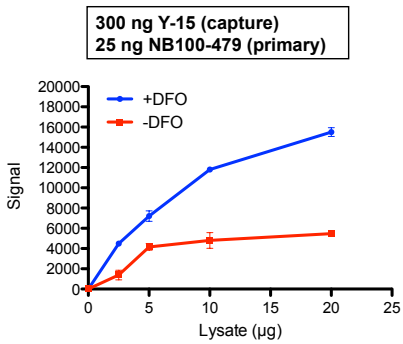

Lysate (µg)	Mean positive signal	P/N
20.0	15 508	2.8
10.0	11 812	2.5
5.0	7 210	1.7
2.5	4 494	3.2

Figure 3.3 Y-15 HIF1α antibody was tested as the capture antibody in combination with either TL-54 or NB100-479 antibodies as the primary antibody in the MSD assay for HIF1α. Lysates from HeLa cells ± DFO were used as controls. Each data point represents the average signal ± standard deviation, n=2.

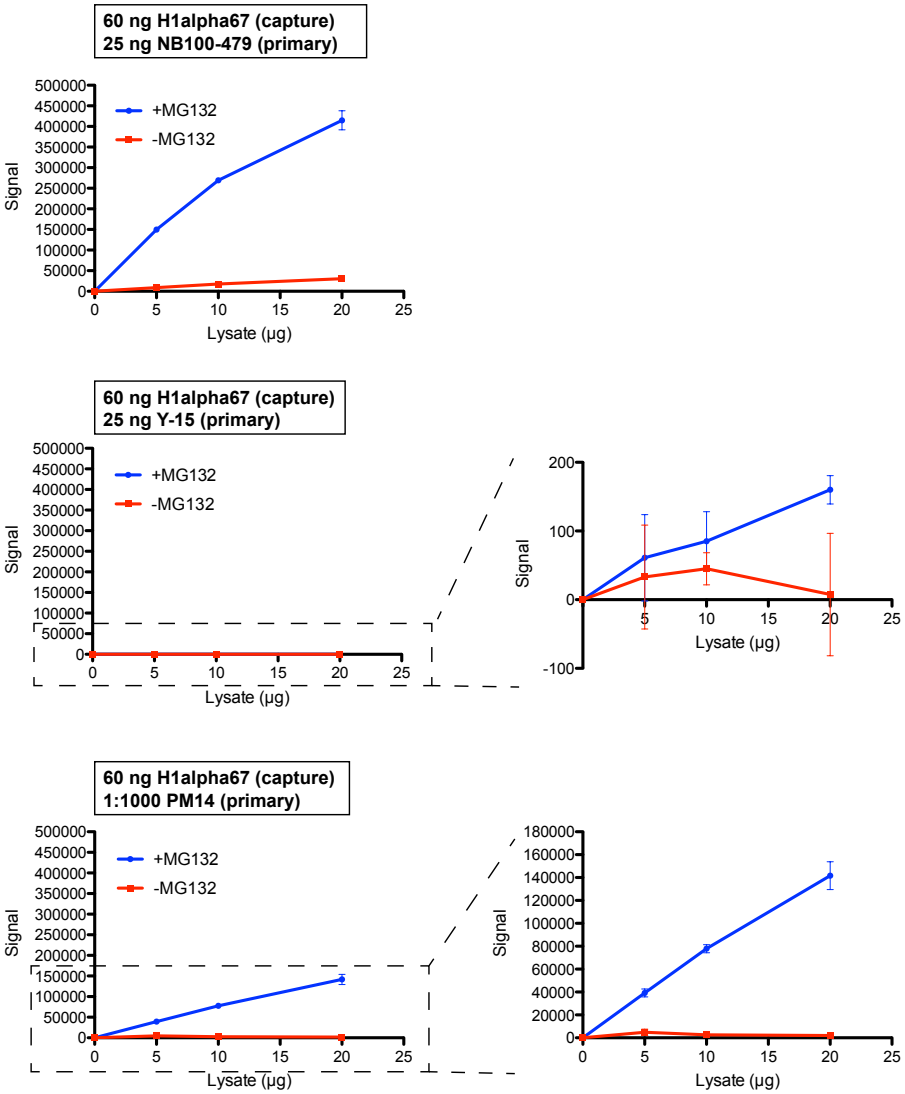

Lysate (µg)	Mean positive signal	P/N
20.0	414 860	13.6
10.0	269 338	15.1
5.0	149 978	16.6

Lysate (µg)	Mean positive signal	P/N
20.0	160	21.3
10.0	85	1.9
5.0	61	1.8

Lysate (µg)	Mean positive signal	P/N
20.0	141 690	69.0
10.0	77 917	29.3
5.0	39 196	8.1

Figure 3.4 H1alpha67 HIF1α antibody was tested as the capture antibody in combination with either NB100-479, Y-15 or PM14 HIF1α antibodies as the primary antibody in the MSD assay for HIF1α. Lysates from HepG2 cells ± MG132 were used as controls. Each data point represents the average signal ± standard deviation, n=2.

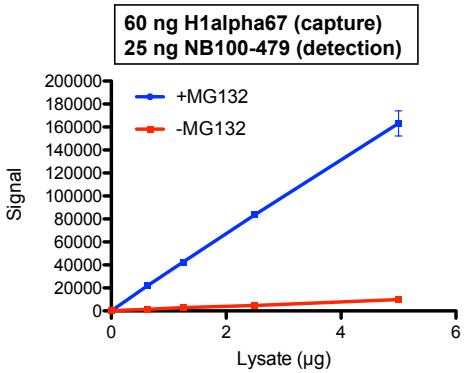

Lysate (µg)	Mean positive signal	P/N
5	163 229	16.7
2.5	83 784	18.2
1.25	42 518	15.8
0.625	21 763	16.9

Figure 3.5 The chosen antibody pair for HIF1α MSD assay, H1alpha67 (as capture antibody) and NB100-479 (as primary antibody) was tested at total cell lysate of lower than 5 µg. Lysates from HepG2 cells ± MG132 were used as controls. Each data point represents the average signal ± standard deviation, n=2.

3.5 Development of the HIF2α MSD assay

An analogous approach to that used for HIF1α was undertaken to develop an MSD-based assay for HIF2α. A positive control lysate was prepared from HepG2 cells treated with proteasome inhibitor MG132 for 4 h before being harvested with MSD lysis buffer. Untreated HepG2 cell lysate was prepared as the negative control. The 190b (as the capture antibody) and PM9 (as the primary antibody) pair was the first to be tested. This antibody pair produced a mean positive signal of 6038 at 5 µg lysate and P/N ratio of >9.8 in all concentrations (5 - 20 µg) of total cell lysate tested (**Figure 3.6**). In a separate experiment using the same cell lysates, two more antibody pairs were tested (190b as capture antibody with NB100-122 as primary antibody, and NB100-122 as capture antibody with 190b as primary antibody). The results reveal that the 190b (capture antibody) with NB100-122 (primary antibody) pair produced the highest mean positive signal (in comparison to all tested antibody pairs at equivalent total cell lysate), with P/N ratio of above 20.7 for all concentrations (0.625 – 5 µg) of total cell lysate tested. Hence, this antibody pair was chosen as the preferred combination for further optimisation of the HIF2α MSD assay.

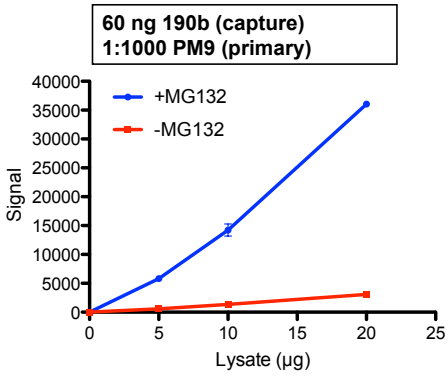

Lysate (µg)	Mean positive signal	P/N
20	36 062	11.6
10	14 969	10.4
5	6 038	9.8

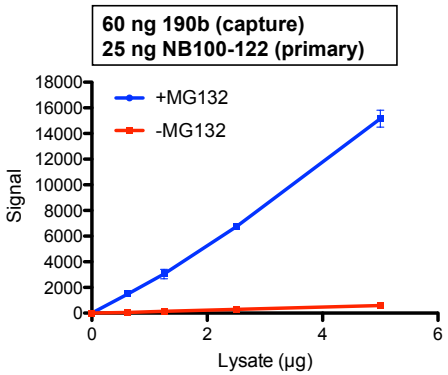

Lysate (µg)	Mean positive signal	P/N
5	15 152	25.5
2.5	6 725	22.8
1.25	3 046	20.7
0.625	1 489	32.4

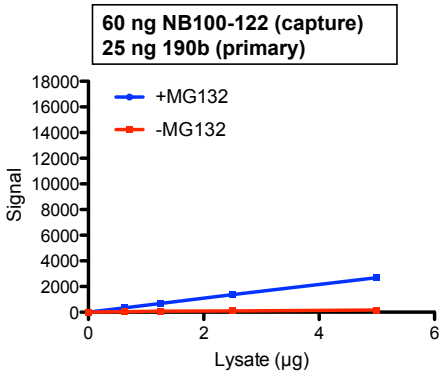

Lysate (µg)	Mean positive signal	P/N
5	2 695	15.7
2.5	1 371	13.8
1.25	676	8.5
0.625	330	10.5

Figure 3.6 Three combinations of HIF2α antibodies were tested in the MSD assay for the detection of HIF2α. Lysates from HepG2 cells ± MG132 were used as controls. Each data point represents the average signal ± standard deviation, n=2.

3.6 Detection of HIF1α NODD, CODD and CAD hydroxylation using the MSD assay

Following the successful detection of HIF1α and HIF2α using the MSD assays, the feasibility of assaying for HIF1α NODD, CODD and CAD hydroxylation using the MSD assay was investigated. For the detection of HIF1α NODD and CODD hydroxylation, hydroxylation-specific HyPro402 and HyPro564 antibodies (previously used in the PHD2 CODD and NODD AlphaScreen assays, as described in **Chapter 2**) were each used as primary antibody in combination with capture antibody H1alpha67 (i.e. the same capture antibody selected for the HIF1α MSD assay). In this experiment, lysate from HepG2 cells treated with MG132 was used as the positive control, whereas two negative control lysates were prepared (one from untreated HepG2 cells, and another from DFO-treated HepG2 cells). Results show that only the MG132-treated HepG2 cells produced positive signal in both the HIF1α CODD and NODD MSD assay, whereas DFO-treated and untreated HepG2 cells produced minimal signal (**Figure 3.7**). While both DFO and MG132 treatment can lead to the stabilisation of HIF1α, HIF1α hydroxylation at both the CODD and NODD are expected to occur with the MG132 treatment but not with DFO treatment, due to the inhibition of the PHDs by the latter via sequestration of iron. These results are consistent with the results obtained with the MSD assay, with HIF1α NODD and CODD hydroxylation detected in the MG132-treated cell lysate but not in the DFO-treated cell lysate and untreated cell lysate. Good P/N ratio (>17.9 and >33 for HIF1α CODD and NODD hydroxylation at lysate concentration as low as 0.625 μg, respectively) were also obtained for both HIF1α CODD and NODD hydroxylation detection.

For the detection of HIF1α CAD hydroxylation, the NB100-479 antibody was used as the capture antibody with HIF1α CAD hydroxylation specific HyAsn803 antibody as the primary antibody. The capture antibody chosen for the HIF1α MSD assay, H1alpha67 was not used as

the capture antibody in this case in combination with HyAsn803 antibody. This is because both the H1alpha67 and HyAsn803 antibodies are mouse antibodies and would cross-react with the labelled anti-mouse IgG antibody used to complete the antibody "sandwich" (i.e. the secondary antibody). The H1alpha67 antibody can only be used as the capture antibody in combination with HyAsn803 antibody if the latter is purified and labelled with the ruthenium-complex directly. Similar to the experiment conducted for the detection of HIF1α CODD and NODD hydroxylation, cell lysates prepared from the MG132-treated, DFO-treated and untreated HepG2 cells were used as controls. The results show HIF1α CAD hydroxylation could be detected in both the MG132-treated and DFO-treated HepG2 cell lysate, with minimal signal detected for the untreated HepG2 cell lysate. This is consistent with the previous observation in renal cell carcinoma cells with reconstituted VHL (RCC4/VHL cells), whereby DFO-induced HIF1α stabilisation show detectable CAD hydroxylation by immunoblotting [1]. Taken together, the results suggest that the extent of HIF1α NODD, CODD and CAD hydroxylation can be assayed using the MSD methodology.

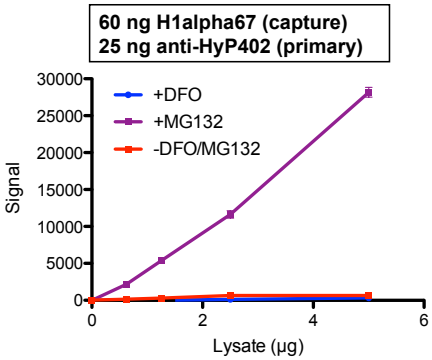

Lysate (µg)	Mean signal (+MG132)	P/N
5	28 170	44.5
2.5	11 636	18.9
1.25	5 345	19.4
0.625	2 174	17.9

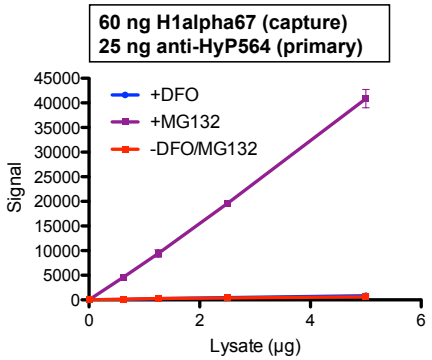

Lysate (µg)	Mean positive signal	P/N
5	40 870	65.9
2.5	19 587	49.2
1.25	9 425	33.0
0.625	4 650	38.3

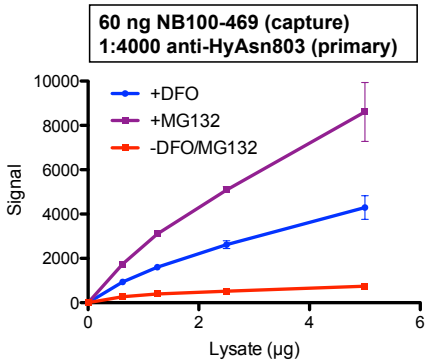

Lysate (µg)	Mean signal (+MG132)	Mean signal (+DFO)	P/N
5	8 610	4 927	11.6
2.5	5 091	2 624	9.7
1.25	3 104	1 603	7.8
0.625	1 747	937	6.5

Figure 3.7 The detection of HIF1α NODD, CODD and CAD hydroxylation using hydroxylation specific antibodies in the MSD assay. Lysates from HepG2 cells ± MG132 or DFO were used as controls. Each data point represents the average signal ± standard deviation, n=2.

3.7 Optimisation of the HIF1α and HIF2α MSD assays

In the feasibility studies described previously, all cell lysates were prepared using the recommended standard MSD lysis buffer (see section **3.10 Materials and methods** for buffer composition). The standard MSD lysis buffer is a non-denaturing lysis buffer (containing 1% Triton X-100, a non-ionic detergent for cell membrane permeabilisation) to minimise denaturation of the capture antibody during the lysate incubation step. It was not known whether HIF1α could be maximally extracted using this lysis buffer. To investigate this, immunoblotting analysis was carried out to study the efficiency of HIF1α extraction using MSD lysis buffer with different compositions of Triton X-100 in comparison to a denaturing Urea-SDS (USD) buffer (**Figure 3.8**). Unexpectedly, it was observed that increasing concentrations of Triton X-100 resulted in lower HIF1α extraction (also observed in **Figure 3.9**), which could be due to the increased formation of detergent micelles. It was noted that although the level of HIF1α is higher with lower concentrations of Triton X-100 (an indication of better extraction efficiency), the amount of HIF1α detected is still lower than that observed using USD buffer.

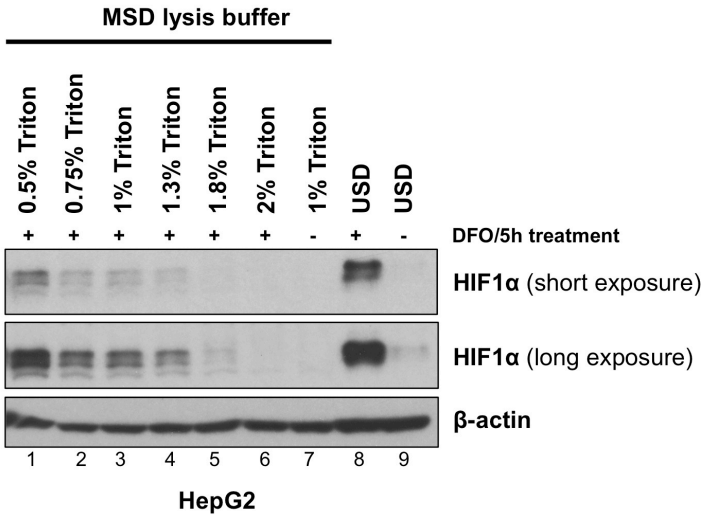

Figure 3.8 The MSD lysis buffer with various concentrations of Triton X-100 were tested for their efficiency in extracting DFO-induced HIF1α in HepG2 cells by immunoblotting. (HIF1α antibody: mouse monoclonal antibody TL-54).

The lower levels of HIF1α detected in cells lysed with the non-denaturing MSD lysis buffer could be due to either partial degradation of HIF1α or inefficient extraction of HIF1α (HIF1α may remain associated with the genomic DNA in the cell lysate pellet). To explore these possibilities, the levels of HIF1α in HeLa cells induced by DFO were investigated by varying the lysis buffer condition, such as by increasing the salt concentration, exploring the use of another detergent (NP40) or by adding benzonase (a type of nuclease to remove DNA/RNA). Immunoblot analysis in **Figure 3.9** indicates that there was no marked improvement with the addition of benzonase with high levels of HIF1α still detectable in the pellet. When lysis buffer with higher salt concentration (450 mM instead of 150 mM) was used, HIF1α was no longer detected in the pellet, suggesting that it was fully dissociated from genomic DNA and was released into the supernatant of the cell lysate. There was no marked difference in the levels of HIF1α when either NP40 or Triton X-100 were used (at the same concentration, i.e. 0.5%), indicating that both detergents were equally effective. In conclusion, efficient HIF1α extraction can be achieved with the use of the standard MSD lysis buffer at 0.5% Triton and 450 mM NaCl.

Although high salt lysis buffer leads to better HIF1α extraction, it was not known whether the high salt condition would also affect the binding of HIF1α to the capture antibody in the MSD assay. To test this, the same total cell lysates previously prepared using the standard MSD lysis buffer with different salt and Triton X-100 concentrations were compared using the MSD assay (**Figure 3.10**). Lower signals were detected from the lysates prepared using lysis buffers with higher salt concentration compared to ones with lower salt concentration, despite a higher amount of HIF1α detected earlier by immunoblotting in the former (compare levels of HIF1α in **Figure 3.10** to levels of HIF1α in **Figure 3.9**). Thus, the results suggest that although the high salt buffer is optimum for the maximum extraction of HIF1α, the

signals detected by MSD assay could be affected, possibly due to the effect of high salt on the antibody-antigen binding.

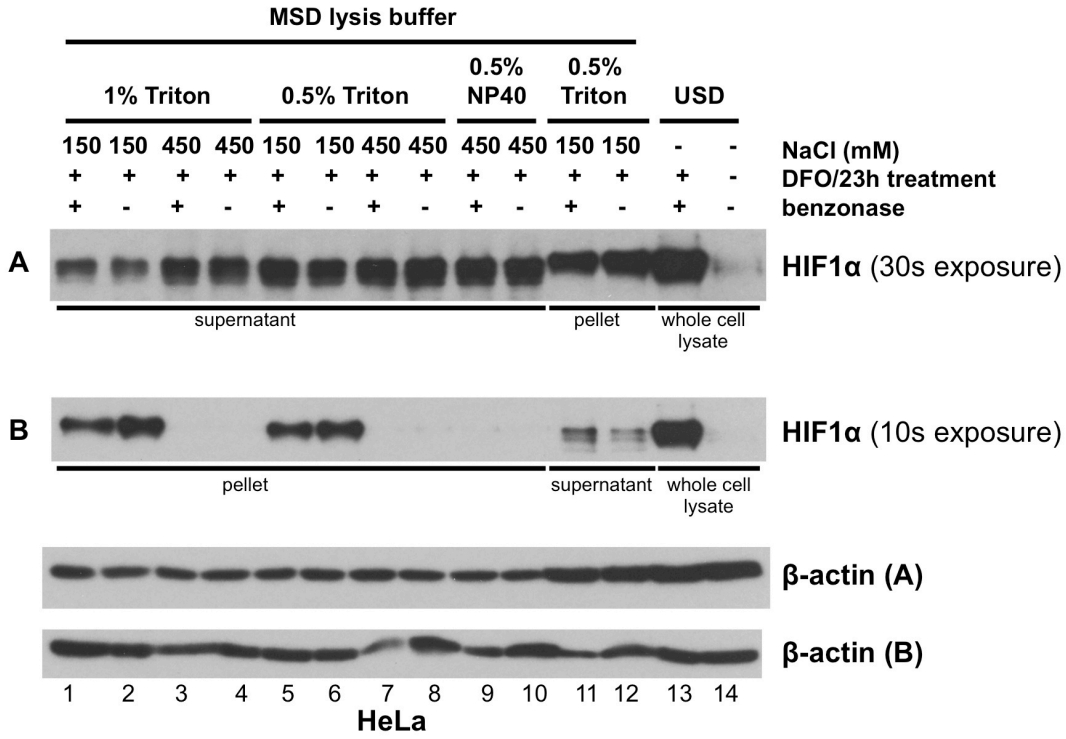

Figure 3.9 Immunoblots showing the HIF1α extraction efficiencies of MSD lysis buffers with different constituents of detergent, salt and benzonase in comparison to USD buffer. HeLa cells were treated with DFO for 23 h to induce HIF1α. (HIF1α antibody: mouse monoclonal antibody TL-54).

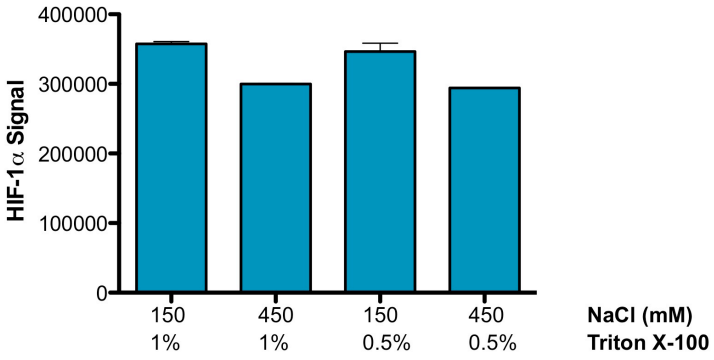

Figure 3.10 The MSD assay detection of HIF1α extracted with the MSD lysis buffer with different Triton X-100 and NaCl concentrations. Each data point represents the average signal ± standard deviation, n=2.

To investigate whether or not the HIF1α detection signal is still linear when a high salt lysis buffer is used, further experiments were carried out using the HIF1α MSD assay. A HIF1α positive control lysate was prepared from Hep3B treated with DFO for 4 h using the high salt lysis buffer, with the untreated cells as the negative control lysate. The assays were also carried out at higher concentrations of the capture and primary antibodies to see if the drop in detection signal when the high salt lysis buffer is used could be improved. The results show that a linear increase in the signal with increasing positive control lysate concentrations could still be observed under the high salt lysis condition across all antibody concentrations tested (**Figure 3.11**). The mean positive signal remained high (>23 k at 5 µg of lysate) and a good P/N ratio (16.7 at 5 µg of lysate) could still be obtained even at the lowest concentrations of capture and detection antibody used. Therefore, 60 ng of H1alpha67 (capture antibody) and 25 ng of NB100-479 (primary antibody) were chosen as the standard conditions for the HIF1α MSD assay.

An equivalent experiment was carried out using the HIF2α MSD assay using the same control cell lysates and resulted in similar observations to that observed with the HIF1α MSD assay (**Figure 3.12**). Although the P/N ratio remained above 14, the mean positive signal for HIF2α detection at 5 µg dropped to below 1.5 k at the lowest antibody concentrations used under the high salt lysis buffer condition (**Figure 3.12**). Thus, to maximise the dynamic range of detection, the highest concentration of capture and primary antibody tested (120 ng of capture antibody 190b and 50 ng of primary antibody NB100-122) was chosen as the standard condition for the HIF2α MSD assay.

3.8 Detection of HIF1α and HIF2α in mouse liver tissue using the HIF MSD assays

To investigate whether the MSD assays could be used for the detection of HIF1α and HIF2α in mouse tissues, liver lysates were prepared from mice treated with either the PHD inhibitor

BIQ (positive control) or vehicle (negative control) for 1 h (work carried out in collaboration with Dr T. Bishop and L. Nicholls). The mouse liver tissues were harvested 1 h after intraperitonial injections of either BIQ or vehicle, snap frozen with liquid nitrogen and kept at -80°C before being homogenised in either RIPA buffer, high salt MSD lysis buffer or USD buffer. The levels of HIF1α and HIF2α in the mouse liver tissues were then examined by immunoblotting and the corresponding MSD assays (**Figure 3.13**). As expected, both HIF1α and HIF2α were induced in the liver tissues of BIQ-treated mice compared to vehicle-treated control mice (**Figure 3.13, top left panel**). The efficiency of HIF1α extraction varies according to the different homogenisation buffers used, as indicated by the different levels of HIF1α induction by immunoblotting (**Figure 3.13, bottom left panel**). The best extraction efficiency (according to the levels of HIF1α) was obtained using USD buffer, followed closely by RIPA buffer. The high salt MSD lysis buffer is the poorest homogenisation buffer with the least amount of HIF1α extracted.

When tested using the MSD assays for HIF1α and HIF2α, clear inductions of both HIF1α and HIF2α levels were observed in the positive control liver lysate for both the RIPA and high salt MSD homogenisation buffers used (**Figure 3.13, right panel**). However, it is worth noting that although a higher amount of HIF1α was detected in the positive control liver extracted with RIPA buffer compared to that extracted with high salt MSD buffer, the signal generated in the MSD assays were actually lower in the RIPA extracted lysate. This could be due to the presence of sodium dodecyl sulfate (SDS) in the RIPA buffer, which is mildly denaturing and may affect the capture antibody in the MSD assay. Taken together, the results indicate the MSD assays can also be used for the detection of HIF1α and HIF2α in mouse tissues, although further optimisation of the homogenisation condition is required to improve the assay for such use.

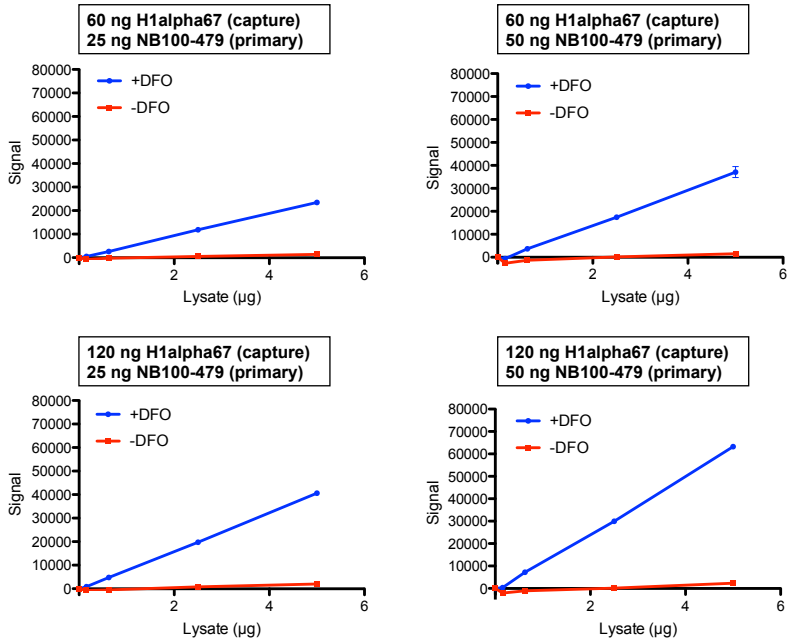

Capture antibody (ng)	Primary antibody (ng)	Mean positive signal at 5 µg lysate	P/N at 5 µg lysate
60	25	23 467	16.7
60	50	37 105	24.5
120	25	40 610	20.3
120	50	63 279	26.8

Figure 3.11 The MSD assay detection of HIF1α extracted from cells using the high salt MSD lysis buffer. Different concentrations of capture and primary antibody were tested. Lysates from Hep3B cells ± DFO were used as controls. Each data point represents the average signal ± standard deviation, n=2.

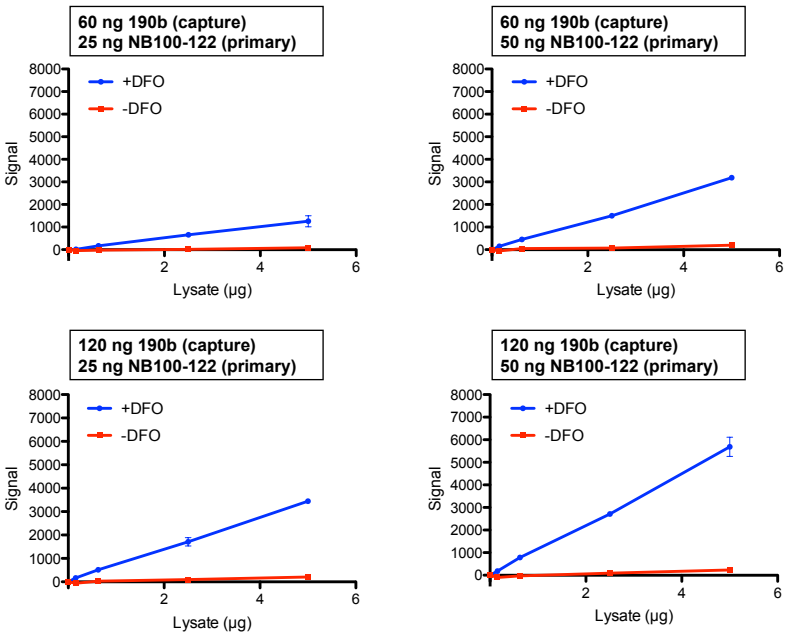

Capture antibody (ng)	Primary antibody (ng)	Mean positive signal at 5 µg lysate	P/N
60	25	1 257	14.7
60	50	3 187	16.4
120	25	3 447	16.5
120	50	5 687	24.4

Figure 3.12 The MSD assay detection of HIF2α extracted from cells using the high salt MSD lysis buffer. Different concentrations of capture and primary antibody were tested. Lysates from Hep3B cells ± DFO were used as controls. Each data point represents the average signal ± standard deviation, n=2.

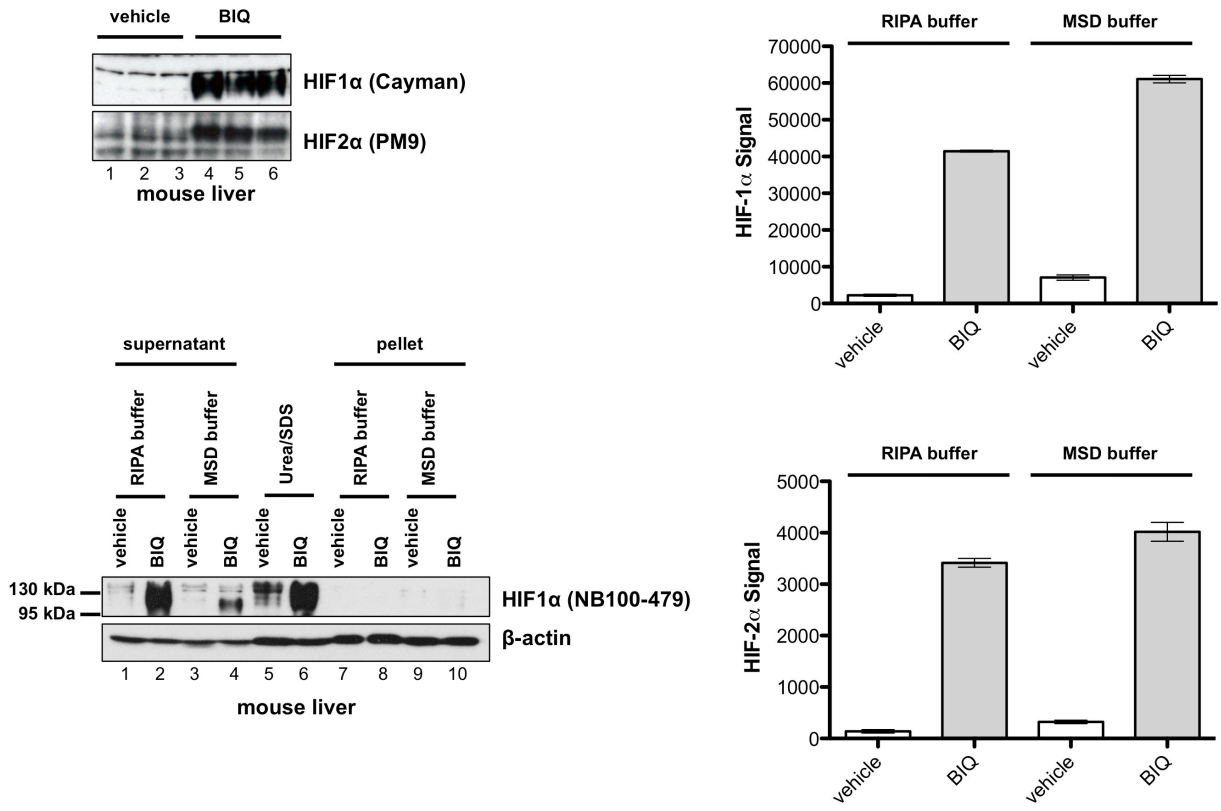

Figure 3.13 The detection of the HIF1α and HIF2α in mouse liver tissues. (**top left**) HIF1α and HIF2α immunoblots of the mouse liver tissues extracted from three mice treated with PHD inhibitor BIQ and three mice treated with vehicle control. Mouse liver tissues were homogenised in USD buffer. (Work carried out by Dr T. Bishop and L. Nicholls.) (**bottom left**) Immunoblot showing the amount of HIF1α detected from mouse liver tissues homogenised using RIPA buffer, high salt MSD buffer or USD buffer. (**top right**) The detection of HIF1α in the mouse liver tissues using the HIF1α MSD assay. (**bottom right**) The detection of HIF2α in the mouse liver tissues using the HIF2α MSD assay. Each bar in the MSD assay results represents the average signal ± standard deviation, n=3.

3.9 Discussion and future work

The work described in this Chapter relates to the development of MSD-based assays for the detection of HIF1α and HIF2α in cell lysates. Both assays were successfully developed and tested for the detection of HIF1α and HIF2α in human cell lysates as well as in mouse liver tissue lysates. The assay is easy to perform, relatively quick and is amenable to medium- or high-throughput screening. Other advantages include the broad dynamic range and the high sensitivity of the electrochemiluminescence technology behind the assay. The multiplexing capability of the MSD assay (e.g. the detection of HIF1α and HIF2α in the same lysate in the same well of the 96-well plate) is one of the main advantages of the assay that has yet to be explored in this preliminary study.

For HIF1α detection, three out of the five antibody pairs tested worked in the MSD assay, with one pair (H1alpha67 as capture antibody, NB100-479 as primary antibody) subsequently being chosen for the standard HIF1α MSD assay. Three antibody pairs were tested for the detection of HIF2α using the MSD assay with varying degrees of detection sensitivity. The antibody pair consisting of 190b as the capture antibody and NB100-122 as the primary antibody was the best out of the three pairs tested and was therefore chosen for the standard HIF2α MSD assay. It was noted that one of the antibodies in each of the chosen pairs for both MSD assays is polyclonal (NB100-479 for HIF1α, NB100-122 for HIF2α), and that the performance of such antibody may vary from batch to batch. Thus, a sufficient amount of the same antibody batch should be stocked and/or the performance of a new batch of antibody should be tested alongside a previously approved batch. Alternatively, the feasibility of using two monoclonal antibodies as a pair for HIF1α and HIF2α detection using the MSD assay should also be investigated.

During the development of the HIF1α and HIF2α MSD assays, DFO- or MG132-treated cell lysates were used as positive controls for HIFα proteins. Although the detection of a non-specific factor (for example, a factor that may be induced under these conditions) in these lysates were unlikely due to the use of two independently-produced antibodies in both assays, studies in cells with targeted knockout or knockdown of HIFα isoforms may provide further validation for the detection specificity of the HIF1α and HIF2α MSD assays. In the present study, all samples were prepared from cell lysates treated under normoxic conditions. Given the important role of HIF in hypoxia (for review, see [16]), the capability of the MSD assays in detecting HIFα isoforms stabilised under hypoxic conditions should also be investigated.

The feasibility of using MSD assay technology to detect the CODD, NODD and CAD hydroxylation levels of HIF1α was also explored. The results reveal that all three hydroxylation levels of HIF1α can be detected using the MSD assay utilising hydroxylation specific antibodies, although further validation and optimisation of the antibody concentration could be carried out. Such assays could be useful for studying the role of PHD isoforms given the difference in their preferences for the hydroxylation of HIF1α NODD and HIF1α CODD [17, 18] and may aid the development of PHD isoform specific inhibitors. The HIF1α CAD hydroxylation MSD assay would also be useful for the identification of inhibitors selective for PHDs over FIH.

In the studies using mouse liver tissues, both HIF1α and HIF2α MSD assays were found to be capable of detecting mouse HIF1α and HIF2α. The use of different homogenisation buffers, however, should be investigated and optimised further, as the initial study indicate that the extraction efficiency of HIF1α is poor using the non-denaturing MSD lysis buffer (even at high salt concentration). On the other hand, the use of the mildly denaturing RIPA buffer

(containing 0.1% SDS, full list of ingredients in section **3.10 Materials and methods**) has been shown to affect the detection signal to a certain extent, possibly via denaturation of the capture antibody during the lysate incubation. This could possibly be resolved by diluting the tissue lysates in the similar buffer without SDS after homogenisation prior to detection by the MSD assay. Given the promising results of the MSD assays in mouse liver tissue, the possibility of detecting HIF1α and HIF2α in other mouse tissues as well as in human tissues should also be investigated.

Overall, the results demonstrate that the MSD assay technology is a promising method for the quantitative detection of HIF1α and HIF2α in cells and in tissues. The costs of the proprietary carbon electrode 96-well plates and plate readers required for the MSD assay, however, is substantial. Nevertheless, the HIF1α and HIF2α MSD assays should be complementary to immunoblotting, particularly in the cellular studies of PHD inhibitors.

3.10 Materials and methods

Buffers and reagents

Reagents

All the following reagents were from Sigma Aldrich (St. Louis, USA) with their corresponding catalogue numbers, unless stated otherwise: Deferoxamine mesylate salt (DFO) (D9533), Triton X-100 (X100), NP-40 (IGEPAL CA-630) (I8896), Tween-20 (P1379), skimmed milk powder (70166), EGTA (E3889), EDTA (E9884), NaCl (S5886), sodium dodecyl sulphate (SDS) (L4390), sodium deoxycholate (D6750), MG132 (BML-PI102-0025; Enzo Life Sciences, Exeter, UK), complete protease inhibitor cocktail (11 873 580 001, Roche Applied Science, Mannheim, Germany), Benzonase (70746-3; Millipore, Billerica, USA), 2-Mercaptoethanol (M3148).

Standard MSD Lysis buffer

Reagent	**Final concentration**
NaCl	150 mM
Tris, pH 7.4	20 mM
EDTA, pH 8	1 mM
EGTA pH 8	1 mM
Triton X-100	1%

Complete protease inhibitor cocktail (1x final concentration) and DFO (100 µM final concentration) were added before use. For High Salt MSD lysis buffer, the final concentration of NaCl is 450 mM (instead of 150 mM) and the final concentration of Triton X-100 is 0.5% (instead of 1%).

RIPA buffer

Reagent	**Final concentration**
NaCl	150 mM
Tris, pH 7.4	50 mM
EDTA pH 8	1 mM
EGTA pH 8	1 mM
Sodium deoxycholate	0.5%
SDS	0.1%
Triton X-100	1%

Urea-SDS (USD) buffer

Reagent	**Volume**
8M urea (in water)	10 ml
Glycerol	1 ml
20% SDS	0.5 ml
1M Tris-HCl pH 7.5	0.1 ml
Total volume	**11.6 ml**

*1 mM final DTT and 1X final complete protease inhibitor cocktail to be added before use.

4X Sample Buffer

Reagent	**Volume**
SDS	1.6 g
2-Mercaptoethanol	0.8 ml
Glycerol	8 ml
Bromophenol blue	0.08 g
1M Tris-HCl pH 6.8	0.1 ml
Water	up to 19.2 ml
Total volume	**19.2 ml**

Cell culture

HeLa and Hep3B cells were cultured in DMEM (D6546-500ML; Sigma Aldrich, St. Louis, USA). HepG2 cells were cultured in RPMI-1640 (R0883; Sigma Aldrich, St. Louis, USA). All cell culture media was supplemented with 10% fetal bovine serum (F7524-500ML; Sigma Aldrich, St. Louis, USA), 2 mM L-glutamine (G7513-100ML; Sigma Aldrich, St. Louis, USA), 50 units/ml of penicillin, and 50 μg/ml of streptomycin (P0781-100ML; Sigma Aldrich, St. Louis, USA). Cells were treated with either 100 μM of DFO or 25 μM of MG132 before being harvested with lysis buffer.

Antibodies for MSD assay

Antibodies for HIF1α: goat polyclonal antibody Y-15 (sc-12542; Santa Cruz Biotechnology, Dallas, USA), mouse monoclonal antibody TL-54 (610958; BD Transduction Laboratories, San Jose, USA), rabbit polyclonal antibody NB100-479 (Novus Biologicals, Littleton, USA),

mouse monoclonal antibody H1alpha67 (NB100-105; Novus Biologicals, Littleton, USA), rabbit polyclonal antibody PM14 (Ratcliffe/Pugh laboratory, University of Oxford, UK [14]),

Antibodies for HIF2α: mouse monoclonal antibody 190b (NB100-132; Novus Biologicals, Littleton, USA), rabbit polyclonal antibody NB100-122 (Novus Biologicals, Littleton, USA), rabbit polyclonal PM9 (Ratcliffe/Pugh laboratory, University of Oxford, UK [14]).

Other antibodies: rabbit polyclonal anti-HyPro402 (07-1585; Millipore, Billerica, USA), rabbit monoclonal anti-HyPro564 clone D43B5 (3434S; Cell Signalling, Danvers, USA), mouse monoclonal anti-HyAsn803 (kind gift from Dr. M. K. Lee, KRIBB, Republic of Korea [19])

MSD SULFO-TAG™ labelled secondary antibodies for MSD assay (all from Meso Scale Discovery, Rockville, USA): goat polyclonal anti-mouse antibody (R32AC-1), goat polyclonal anti-rabbit antibody (R32AB-1), donkey polyclonal anti-goat antibody (R32AG-5).

Antibodies for immunoblotting

Antibodies for human HIF1α: mouse monoclonal antibody TL-54 (610958; BD Transduction Laboratories, San Jose, USA).

Antibodies for mouse HIF1α: rabbit polyclonal antibody (10006421; Cayman Chemical, Michigan, USA), rabbit polyclonal antibody NB100-479 (Novus Biologicals, Littleton, USA).

Antibodies for mouse HIF2α: rabbit polyclonal PM9 (Ratcliffe/Pugh laboratory, University of Oxford, UK [14]).

HRP-conjugated mouse monoclonal anti-beta-actin antibody clone AC-15 (ab49900; Abcam, Cambridge, UK).

Secondary antibodies for immunoblotting (all from Dako, Glostrup, Denmark, unless stated otherwise): HRP-conjugated swine polyclonal anti-rabbit IgG (P0399), HRP-conjugated goat anti-mouse IgG (P0447).

Standard MSD assay protocol

1. Bare Standard Bind 96-well MSD Multi Array plates (Meso Scale Discovery, Rockville, USA) were coated with capture antibody in phosphate buffered saline (PBS) buffer for at least 16 h at 4°C.
2. The coating antibody was removed from the plates, then blocked with 5% skimmed milk (in PBS) for at least 45 min with shaking at room temperature.
3. The plates were then washed three times with Tris Wash Buffer (50 mM Tris buffer with 0.5% Tween-20 and 150 mM NaCl, pH 7.6) before cell or tissue lysates were added and incubated at room temperature with shaking.
4. After 1 h, the plates were washed three times with Tris Wash Buffer, then the unlabelled primary antibody was added into each well and incubated for 1 h at room temperature with shaking.
5. The plates were washed three times with Tris Wash Buffer before the MSD SULFO-TAG™ labelled secondary antibody (25 ng/well) was added and incubated for 1 h at room temperature with shaking.

6. The plates were washed three times with Tris Wash Buffer, then 150 µl/well of 2X Read Buffer (R92TC-1; Meso Scale Discovery, Rockville, USA) were added.
7. Finally, the plates were read with an MSD Sector S600 reader (Meso Scale Discovery, Rockville, USA). Signals generated were normalised to "buffer-only" control.

Standard HIF1α MSD assay

The HIF1α MSD assay was carried out according to the standard MSD assay protocol as above, using the following antibodies:

Capture antibody: H1alpha67

Primary antibody: NB100-479

Secondary antibody: MSD SULFO-TAG™ labelled goat anti-rabbit antibody

Standard HIF2α MSD assay

The HIF2α MSD assay was carried out according to the standard MSD assay protocol as above, using the following antibodies:

Capture antibody: 190b

Primary antibody: NB100-122

Secondary antibody: MSD SULFO-TAG™ labelled goat anti-rabbit antibody

Cell lysate preparation - as for MSD assay

After the removal of medium, cells were washed once with ice cold PBS before the addition of lysis buffer. Cells were scraped on ice using a cell scraper, transferred promptly into an Eppendorf tube and incubated at 4°C on a tube rotator at 25 rpm. After an hour, the cell lysate was centrifuged at 13,000 rpm, 4°C. The cell supernatant was then transferred directly into the wells of the MSD Multi-Array plate to be assayed according to the Standard MS

assay protocol, or kept frozen at -80°C. Protein assay was performed on cell lysates using Bio-Rad DC Protein Assay according to manufacturer's protocol (500-0116; Bio-Rad, Hercules, USA)

Cell lysate preparation - as for immunoblotting

Unless stated otherwise, cell lysates for immunoblotting were prepared in USD buffer and 4X sample buffer (1X final), heated to 95°C for 10 minutes before being stored at -20°C or loaded into electrophoresis gel. Cell lysates were resolved by SDS-PAGE (sodium dodecyl sulphate polyacrylamide gel electrophoresis), electroblotted onto Immobilon-P PVDF membranes (IPVH00010; Millipore, Billerica, USA). Membranes were blocked with 5% skimmed milk before being probed with primary antibodies and HRP-conjugated secondary antibodies. Chemiluminescence was generated based on HRP activity after the addition of SuperSignal West Dura Chemiluminescent Substrates (34076; Thermo Fisher Scientific, Rockford, USA) to the membranes, and visualised by exposing the membranes to X-OMAT Kodak LS films (F0899; Sigma Aldrich, St. Louis, USA).

Inhibitor treatment of mice and tissue lysate preparation

Male C57BL/6 mice were treated with 30 mg/kg of inhibitor or vehicle by Dr T. Bishop and L. Nicholls as previously described [20]. The mouse liver tissues were harvested and snap frozen with liquid nitrogen before being stored at -80°C (work carried by Dr T. Bishop and L. Nicholls). A portion of the liver tissues were removed, weighed and homogenised either in RIPA buffer, high salt MSD lysis buffer or USD buffer (1 ml of buffer per 100 mg of tissue) before being analysed by immunoblotting or MSD assays.

3.11 References

1 Tian, Y. M., Yeoh, K. K., Lee, M. K., Eriksson, T., Kessler, B. M., Kramer, H. B., Edelmann, M. J., Willam, C., Pugh, C. W., Schofield, C. J. and Ratcliffe, P. J. (2011) Differential sensitivity of hypoxia inducible factor hydroxylation sites to hypoxia and hydroxylase inhibitors. J Biol Chem. **286**, 13041-13051

2 Maxwell, P. H., Wiesener, M. S., Chang, G. W., Clifford, S. C., Vaux, E. C., Cockman, M. E., Wykoff, C. C., Pugh, C. W., Maher, E. R. and Ratcliffe, P. J. (1999) The tumour suppressor protein VHL targets hypoxia-inducible factors for oxygen-dependent proteolysis. Nature. **399**, 271-275

3 Willam, C., Masson, N., Tian, Y. M., Mahmood, S. A., Wilson, M. I., Bicknell, R., Eckardt, K. U., Maxwell, P. H., Ratcliffe, P. J. and Pugh, C. W. (2002) Peptide blockade of HIFalpha degradation modulates cellular metabolism and angiogenesis. Proc Natl Acad Sci U S A. **99**, 10423-10428

4 Mahon, P. C., Hirota, K. and Semenza, G. L. (2001) FIH-1: a novel protein that interacts with HIF-1alpha and VHL to mediate repression of HIF-1 transcriptional activity. Genes Dev. **15**, 2675-2686

5 Lando, D., Peet, D. J., Gorman, J. J., Whelan, D. A., Whitelaw, M. L. and Bruick, R. K. (2002) FIH-1 is an asparaginyl hydroxylase enzyme that regulates the transcriptional activity of hypoxia-inducible factor. Genes Dev. **16**, 1466-1471

6 Stolze, I. P., Tian, Y. M., Appelhoff, R. J., Turley, H., Wykoff, C. C., Gleadle, J. M. and Ratcliffe, P. J. (2004) Genetic analysis of the role of the asparaginyl hydroxylase factor inhibiting hypoxia-inducible factor (FIH) in regulating hypoxia-inducible factor (HIF) transcriptional target genes [corrected]. J Biol Chem. **279**, 42719-42725

7 Smirnova, N. A., Rakhman, I., Moroz, N., Basso, M., Payappilly, J., Kazakov, S., Hernandez-Guzman, F., Gaisina, I. N., Kozikowski, A. P., Ratan, R. R. and Gazaryan, I. G. (2010) Utilization of an in vivo reporter for high throughput identification of branched small molecule regulators of hypoxic adaptation. Chem Biol. **17**, 380-391

8 http://www.mesoscale.com/

9 http://www.mesoscale.com/CatalogSystemWeb/WebRoot/literature/brochures/pdf/techBrochure.pdf

10 http://www.meso-scale.com/CatalogSystemWeb/Documents/MSDSulfoTag.pdf

11 Leland, J. K. and Powell, M. J. (1990) Electrogenerated chemiluminescence: An oxidative-reduction type ECL reaction sequence using tripropyl amine. J Electrochem Soc. **137**, 3127-3131

12 Schweitzer, R. H. and Abriola, L. (2002) Electrochemiluminescence. A technology evaluation and assay reformatting of the Stat6/P578 protein-peptide interaction. Methods Mol Biol. **190**, 87-106

13 http://www.mesoscale.com/CatalogSystemWeb/WebRoot/literature/notes/pdf/Multi_Array_ZF040511A.pdf

14 Lau, K. W., Tian, Y. M., Raval, R. R., Ratcliffe, P. J. and Pugh, C. W. (2007) Target gene selectivity of hypoxia-inducible factor-alpha in renal cancer cells is conveyed by post-DNA-binding mechanisms. Br J Cancer. **96**, 1284-1292

15 Jaakkola, P., Mole, D. R., Tian, Y. M., Wilson, M. I., Gielbert, J., Gaskell, S. J., von Kriegsheim, A., Hebestreit, H. F., Mukherji, M., Schofield, C. J., Maxwell, P. H., Pugh, C. W. and Ratcliffe, P. J. (2001) Targeting of HIF-alpha to the von Hippel-Lindau ubiquitylation complex by O2-regulated prolyl hydroxylation. Science. **292**, 468-472

16 Kaelin, W. G., Jr. and Ratcliffe, P. J. (2008) Oxygen sensing by metazoans: the central role of the HIF hydroxylase pathway. Mol Cell. **30**, 393-402

17 Landazuri, M. O., Vara-Vega, A., Viton, M., Cuevas, Y. and del Peso, L. (2006) Analysis of HIF-prolyl hydroxylases binding to substrates. Biochem Biophys Res Commun. **351**, 313-320

18 Hirsila, M., Koivunen, P., Gunzler, V., Kivirikko, K. I. and Myllyharju, J. (2003) Characterization of the human prolyl 4-hydroxylases that modify the hypoxia-inducible factor. J Biol Chem. **278**, 30772-30780

19 Lee, S. H., Jeong Hee, M., Eun Ah, C., Ryu, S. E. and Myung Kyu, L. (2008) Monoclonal antibody-based screening assay for factor inhibiting hypoxia-inducible factor inhibitors. J Biomol Screen. **13**, 494-503

20 Bishop, T., Talbot, N. P., Turner, P. J., Nicholls, L. G., Pascual, A., Hodson, E. J., Douglas, G., Fielding, J. W., Smith, T. G., Demetriades, M., Schofield, C. J., Robbins, P. A., Pugh, C. W., Buckler, K. J. and Ratcliffe, P. J. (2013) Carotid body hyperplasia and enhanced ventilatory responses to hypoxia in mice with heterozygous deficiency of PHD2. J Physiol. **591**, 3565-3577

Chapter 4: Studies on selective small molecule probes for the hypoxia inducible factor (HIF) prolyl hydroxylases (PHDs)

4.1 Introduction

A chemical probe can be described as a potent, cell-permeable small molecule which selectively targets a protein and can be used to study the biological function of the target [1]. Although the development and identification of such small molecule inhibitors to be used as tool compounds is often challenging, selective and well characterised chemical probes can be very useful in studying the role of their target proteins in cells or in organisms. The rapid and transient/reversible effects of chemical probes are amongst the advantages over traditional genetic approaches (such as targeted or conditional gene deletion), allowing more control over the time and extent of the intervention. For studies in model organisms such as mouse or zebrafish, chemical probes can also be potentially applied at various developmental stages. They thus can be very valuable tools for studying the functions of crucial proteins required during development, particularly when genetic ablation of these proteins cause embryonic lethality in animal models. The use of chemical probes, however, can be misleading if the selectivity of the probe used is poorly characterised [1].

Since the discovery of the PHDs and the identification of their roles in regulating HIF as part of the key cellular response to hypoxia [2, 3], various PHD inhibitors have been developed and reported in the academic and patent literature (for examples, see [4] and references therein). As described in **Chapter 1**, the PHDs are part of the large 2OG-dependent dioxygenase protein family consisting of more than 60 human proteins. All members within

the 2OG-dependent dioxygenase protein family require oxygen and 2OG for their catalytic activities, and they share structural similarities [5]. While the importance of other 2OG-dependent dioxygenases in cellular response to changes in oxygen concentrations (if any) is still not well understood, their biological roles (for example, in regulating gene expression via histone or nucleic acid modifications) raises the question of whether the biological effects observed with PHD inhibitors could be partly mediated by the off-target inhibition of these proteins. FIH, another human 2OG-dependent dioxygenase, is also involved in the regulation of HIF in response to hypoxia [6, 7]. Given that several PHD inhibitors are already in the late stages of clinical trials for treatment of anaemia [4, 8], the selectivity of PHD inhibitors, often omitted in published studies, is thus an important issue. Poorly characterised non-selective PHD inhibitors may lead to invalid conclusions if used as chemical probes by academic researchers, in addition to causing undesirable side effects if they are being used in clinics [1].

In the work described in this Chapter, selected PHD inhibitors were studied and investigated for their potentials to be used as tool compounds for probing the biological roles of the PHDs. The work included studies using the *in vitro* assay for PHD2 (described in **Chapter 2**) and selectivity profiling using biochemical assays for representative members of the human 2OG-dependent dioxygenase family. The mechanism of action for candidate PHD probes was explored using crystallographic and NMR-based studies, followed by cellular and *in vivo* studies in model organisms. Further studies using the identified chemical probes for PHDs are described in subsequent Chapters. Part of the work described in this Chapter has been reported in a modified form [9].

4.2 Determination of inhibitory potencies using the PHD2 CODD AlphaScreen assay and selectivity profiling of chemical probe candidates for the PHDs

As reported in **Chapter 2** based on studies using the PHD2 CODD AlphaScreen assay, PHD2 can be inhibited *in vitro* by the generic 2OG-dependent dioxygenases inhibitor NOG (**1a**, PHD2 IC_{50} **=** 11.2 μM) and the PHD inhibitor BIQ (**2**, PHD2 IC_{50} **=** 0.33 μM). Apart from inhibiting PHD2, **1a** has been shown to inhibit other members of the human 2OG-dependent dioxygenase family (including FIH) and thus, cannot be used to effectively probe the function of the PHDs [10]. As a starting point towards the identification of a suitable chemical probes for the PHDs, compound **2**, as well as two other previously reported potent PHD2 inhibitors, quinolone **3** [11] and dihydropyrazole **10** [4] were shortlisted for further characterisation.

To investigate the potentials of developing these inhibitors as chemical probes for the PHDs, analogues of **3** and **10** were synthesised (**Figure 4.1**). Compound **3** and its derivatives were synthesised by Dr. J.I. Candela-Lena, whereas compound **10** and its derivatives were synthesised by V.G. Pérez and Dr. O. Atasoylu. These inhibitors developed were then tested for their ability to inhibit PHD2 activity using the PHD2 CODD AlphaScreen assay. The results validated both **3** and **10** as potent inhibitors of PHD2 as previously reported, with IC_{50} values of 33 nM and 1.6 nM, respectively (**Figure 4.1**). Compound **9**, the carboxylic acid derivative of **10** also potently inhibits PHD2 (IC_{50} = 4 nM). Most of the quinolone derivatives tested are active as submicromolar inhibitors of PHD2 except for **4** (IC_{50} > 300 μM), with **5** being the most potent in the series (IC_{50} = 22 nM). Notably **3**, **5**, **9** and **10** are more potent than BIQ (IC_{50} = 0.3 μM, see **Chapter 2**).

To investigate the selectivity for the PHDs, selected inhibitors were screened against a panel of other human 2OG-dependent dioxygenases, including the human JumonjiC (JmjC)-

domain-containing histone demethylases (HDMs; work carried out by Dr. A. Tumber), γ-butyrobetaine hydroxylase (BBOX; work carried out by A. Rydzik) and fat mass and obesity associated protein (FTO; work carried out by Dr. M. Demetriades and W. S. Aik). The HDMs assays utilised the same AlphaScreen methodology as the PHD2 CODD AlphaScreen assay (with enzyme concentrations within the range of 0.2 to 25 nM) [10], the BBOX assay employed a fluoride-detection-based fluorescence assay [12] and FTO assay is based on liquid chromatography coupled to mass spectrometry (LC-MS) [13]. The results reveal that **5**, **9** and **10** were at least 430-fold more selective for PHD2 over the other human 2OG-dependent dioxygenases tested, as judged by their IC_{50} values (**Table 4.1**). In comparison, BIQ (**2**) is only 10-fold more selective for PHD2 over FTO. Given their good inhibitory potencies and selectivity for PHD2 over the panel of human 2OG-dependent dioxygenases tested, **5**, **9** and **10** are suitable candidates for further investigations as chemical probes for the PHDs.

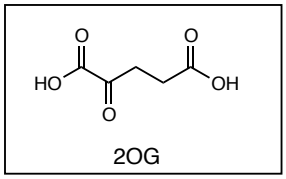

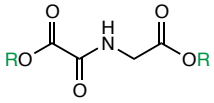

R = H, **1a** (NOG)
R = CH_3, **1b** (DMOG)

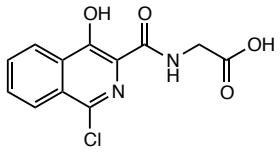

BIQ, **2**

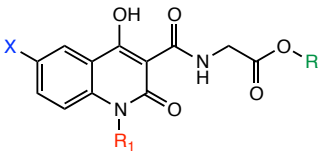

	X	R_1	R	PHD2 IC_{50} (μM)
3	H	CH_3	H	0.033
4	H	CH_3		>300
5	H		H	0.022
6	H		H	1.47
7	H	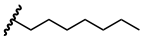	H	0.66
8	Br		H	0.078

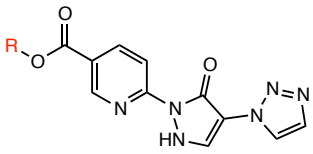

	R	PHD2 IC_{50} (μM)
9	H	0.004
10		0.0016

Figure 4.1 Chemical structures of the quinolones (**3**-**8**) and dihydropyrazoles (**9** and **10**) with their inhibitory potencies as determined by the PHD2 CODD AlphaScreen assay. Chemical structures of NOG (a catalytically inactive analogue of 2OG, **1a**) and its cell-permeable ester derivative (**1b**, DMOG) were shown alongside 2OG and BIQ (**2**) for comparison.

	2	3	5	9	10
JMJD1A	>20	>100	>100	>20	>20
JMJD2A	>20	>100	100	n.d.	n.d.
JMJD2C	>20	>100	100	n.d.	n.d.
JMJD2E	>20	>100	>100	>20	>20
JMJD3	>20	>100	>100	>20	>20
FBLX11	>20	100	52	20	20
JARID1C	549.6	443.2	159	>100	>100
BBOX1	18	n.d.	9.5	>50	73
FTO	3	4	11	37	49
PHD2	0.3	0.033	0.022	0.0048	0.0016
	10-fold	121-fold	431-fold	4,166-fold	12,500-fold

Table 4.1 Selectivity profiling of selected compounds against a panel of human 2OG-dependent dioxygenases. IC_{50} values are in μM. The second lowest IC_{50} value for each compound (highlighted in green), was used to calculate the degree of selectivity of each compound for PHD2 at the bottom of the table. n.d. = not determined.

4.3 Investigation of the binding mode of candidate PHD chemical probes using crystallography and NMR-based assay

Note: The crystallographic studies in this section were carried out by Dr. R. Chowdhury. NMR studies were carried out by Dr. I. Leung.

To obtain mechanistic insights into PHD inhibition mediated by the candidate PHD probes, crystallographic studies were conducted using the PHD2 catalytic domain (residues 181 – 426). For the quinolone series, a crystal structure of PHD2 in complex with **3** and Mn(II) (as a non reactive substitute for Fe(II) ion) was successfully obtained (**Figure 4.2**) [9]. However, attempts to crystallise PHD2 with **5** were unsuccessful. Analyses of the PHD2.Mn(II).**3** complex reveal that the bicyclic heteroatomic ring of **3** is positioned towards the entrance of the active site opening, between the hydrophobic residues Tyr310, Met299 and Trp389 of PHD2. At the active site, **3** coordinates Mn(II) in a bidentate manner with its carboxylate

side-chain forming hydrogen bonds with Arg383 and Tyr329 within the 2OG binding pocket, similar to that seen in the PHD2.Mn(II)NOG complex (PDB ID: 3HQR [14]).

To predict the binding mode of **5**, a model of the inhibitor in complex with PHD2 and Mn(II) was generated using the crystal structure of PHD2.Mn(II).**3** as the template (**Figure 4.2 B-C**). The model predicts similar bidentate coordination to the Mn(II) and interaction of the carboxylate with Arg383 within the 2OG binding pocket as in the PHD2.Mn(II).**3** complex. The benzyl group of **5** is predicted to project towards the hydrophobic region located at opening of the active site (**Figure 4.2 B**).

The positioning of the aromatic rings of **3** towards the active site opening is also likely to make a steric clash with, at least, Pro564 of the HIF1α *C*-terminal oxygen dependent degradation domain (CODD), as judged by the superimposition of PHD2.Mn(II).**3** with the structure of PHD2.Mn(II).**1a**.CODD complex (**Figure 4.2 D**). Similarly, the predicted projection of the benzyl group of **5** towards the opening of the active site is also expected to result in the steric clash with the Pro564 residue of the CODD. Thus, the combined structural/modelling analyses suggest that the CODD substrate peptide will not be able to form a productive complex with PHD2 in the presence of **3** and **5**, indicating that these inhibitors may prevent both 2OG and CODD binding.

For the dihydropyrazoles inhibitors, a crystal structure of PHD2 in complex with **9** and Mn(II) was successfully obtained. Attempts to crystallise PHD2 with **10**, however, were unsuccessful. In the PHD2.Mn(II).**9** complex, **9** coordinates to Mn(II) in a bidentate manner via the nitrogen atom of the pyridine ring and the oxygen atom of the pyrazolone ring (**Figure 4.3**). The triazole ring of **9** is positioned into the active site of PHD2, whereas the carboxylate

side-chain is positioned towards the entrance of the active site opening. Compound **10** is likely to bind in a similar manner to that observed with **9**, with the tertiary butyl group expected to be accommodated into the space at the entrance of the active site opening.

In addition to crystallographic and modelling studies, the mechanism of action of the inhibitors was studied by competition-based nuclear magnetic resonance (NMR) methods using [^{13}C]-2OG or [^{13}C]-CODD as reporter ligands [15]. The displacement of these labelled ligands from PHD2 can be monitored in the presence of the candidate PHD probes to investigate their mode of actions. Using single inhibitor concentration, the results show that **5** displaces 2OG from PHD2, consistent with its binding to the 2OG active site of PHD2 based on the model predicted from the crystallographic studies (**Figure 4.4**). However, [^{13}C]-CODD was not displaced by **5**, suggesting that CODD can still bind to PHD2 in the presence of **5**, possibly with PHD2 adopting a different orientation to prevent the steric clash between the benzyl group of **5** with CODD (as predicted from the model structure) or that the projection of the groups into the peptide binding area is insufficient to block CODD from binding. Studies with **10** show similar results to that observed with **5**, with 2OG (but not CODD) displaced from PHD2, suggesting that **10** competes with 2OG at the active site of PHD2. Interestingly, another reported PHD2 inhibitor, BNS [16] (used as a control in this experiment) can displace both 2OG and CODD from PHD2, suggesting that this inhibitor binds overlapping regions of the 2OG and CODD substrate binding site (**Figure 4.4**).

Taken together, the crystallographic and NMR-based studies suggest that the candidate PHD probes (**3**, **5**, **9** and **10**) inhibit PHD2 via binding to its 2OG active site. However, it remains unclear to what extent the binding of these inhibitors can prevent the productive binding of CODD substrate to PHD2.

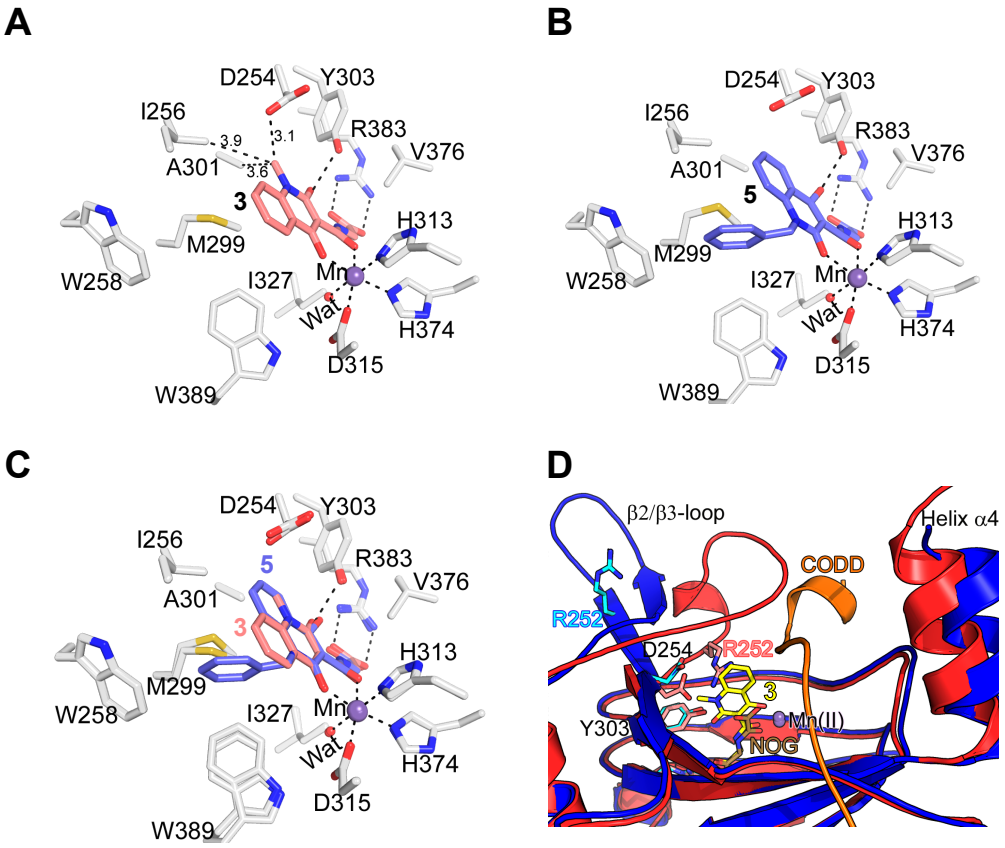

Figure 4.2 (**A**) A crystal structure of PHD2.Mn(II).**3** complex (PDB ID: 4BQW). (**B**) A model of PHD2.Mn(II).**5** based on PHD2.Mn(II).**3** crystal structure as the template. (**C**) Superimposition of the PHD2.Mn(II).**3** structure and a PHD2.Mn(II).**5** model. (**D**) Superimposition of PHD2.Mn(II).**3** (blue ribbon) and PHD2.Mn(II).**1a**.CODD (red ribbons, PDB ID: 3HQR), illustrating the proposed blockage of CODD binding to PHD2 by **3**. Figures prepared by Dr. R. Chowdhury [9].

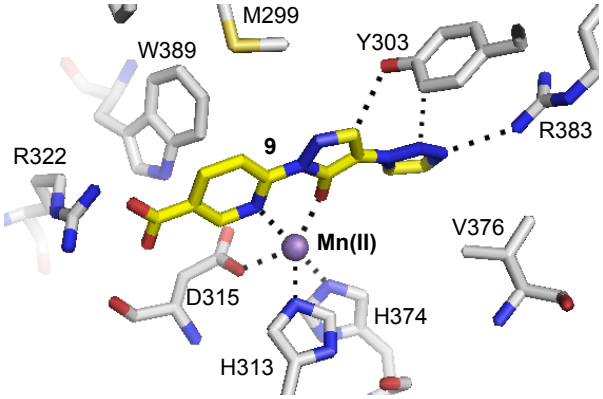

Figure 4.3 View from the crystal structure PHD2 in complex with **9** and Mn(II).

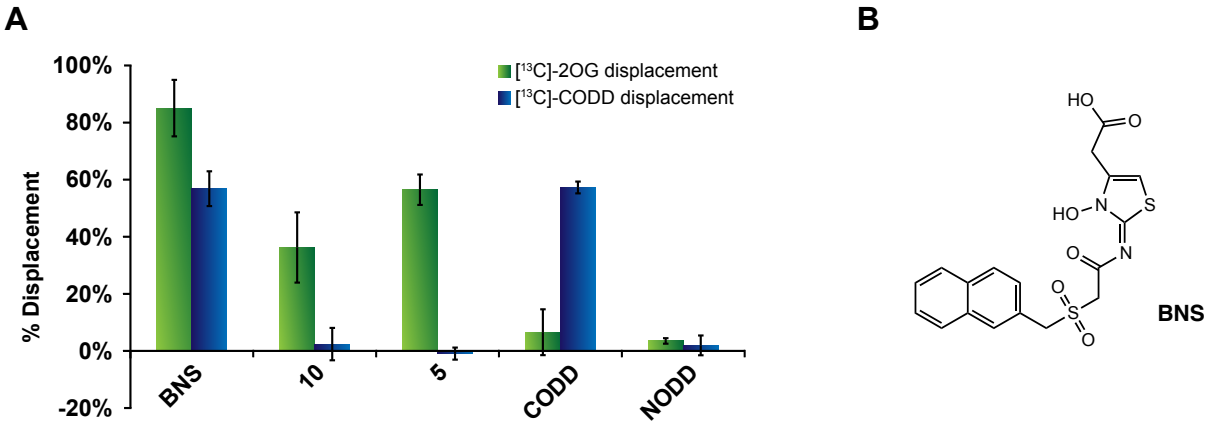

Figure 4.4 (**A**) Single concentration inhibitor displacement of [^{13}C]-2OG and [^{13}C]-CODD obtained using the NMR method. The assay mixture contained 50 μM apo-PHD2, 400 μM Zn(II), 50 μM [^{13}C]-2OG, 40 μM [^{13}C]-CODD and 800 μM inhibitor. Unlabelled CODD peptide was used as control. Errors shown represent the standard deviation from the means in three separate measurements. Data obtained from Dr. I. Leung. (**B**) Chemical structure of BNS.

4.4 Investigation of the cellular efficacies of the candidate chemical probes for the PHDs

To test the efficacy of the inhibitors in cells, the effect of the quinolone inhibitors (**3**-**8**) on the hydroxylation states of HIF1α were initially investigated in a HIF1α-stabilised human renal cell carcinoma (RCC4) cell line. The extent of the differential HIF1α hydroxylation were analysed by immunoblotting using hydroxylation specific antibodies (as described in **Chapter 2** and **Chapter 3**) [17, 18]. DMOG (**1b**, the cell-permeable ester of the generic 2OG-dependent dioxygenase inhibitor, NOG) was used as a control. As shown in **Figure 4.5 A-B**, CODD hydroxylation (HyPro564) was inhibited by **3** and **5**, highlighting their inhibitory activity against the PHDs. In line with the PHD2 CODD AlphaScreen results, **4** (IC_{50} > 300 μM) did not inhibit HIF1α hydroxylation in cells (**Figure 4.5 A**, *lanes 6-7*). HIF1α CAD hydroxylation (HyAsn803) was largely unaffected by the inhibitors tested. There were also no detectable changes to the levels of PHD2, supporting the hypothesis that these inhibitors block PHD activity via binding to the 2OG active site and not by altering the levels of PHD2 in cells.

The quinolone inhibitors were then tested in the VHL-competent cell lines HEK293T, U2OS and RCC4/VHL. Inhibition of the PHDs leads to normoxic stabilisation of HIF1α, and thus can be used as indicator of the extent of PHD inhibition. In **Figure 4.5 C-E**, the stabilisation of HIF1α in HEK293T, U2OS and RCC4/VHL by the quinolones **3**, **5**, **6**, **7** and **8** is observed. The changes to the HIF1α CAD hydroxylation levels were consistent with the levels of HIF1α, indicating that FIH was not inhibited by these compounds at the concentrations tested. As a rough comparison of cellular efficacies, the induction of HIF1α in RCC4/VHL cells was analysed across various concentrations of the **5** and **8** in comparison to BIQ. The results indicate that **5** was approximately 5-fold more potent than BIQ and about 2-fold more potent than **8** in RCC4/VHL cells (**Figure 4.5 E**). In general, the cellular efficacies of the inhibitors in the various VHL-competent cell lines tested were consistent with the IC_{50} values of the inhibitors as measured by the PHD2 CODD AlphaScreen assay, with **5** being the most potent in cells (IC_{50} = 22 nM), followed by **3** (IC_{50} = 33 nM) and **8** (IC_{50} = 78 nM).

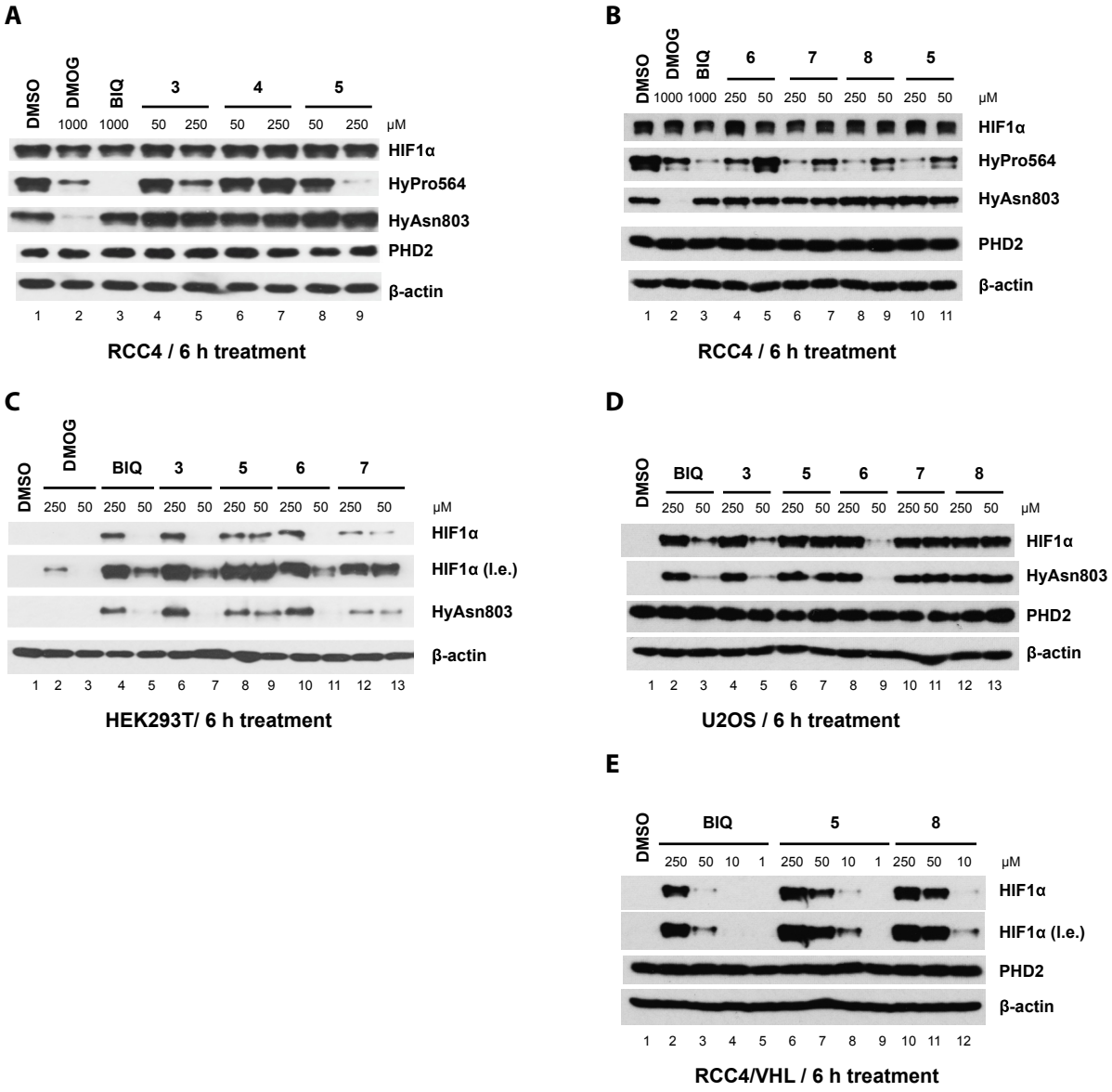

Figure 4.5 Cellular inhibition studies of the quinolone series in human cell lines. (**A-B**) Immunoblot showing the selective inhibition of the HIF1α prolyl- over asparaginyl-hydroxylation (HyPro564 over HyAsn803) in RCC4 cells. **4** is shown to be inactive. (**C-E**) Immunoblots showing the dose-dependent upregulation of HIF1α in VHL-competent human cell lines (HEK239T, U2OS and RCC4/VHL) by the quinolone series. Note the lack of inhibition of HIF1α asparaginyl-hydroxylation (HyAsn803). Results from (**A**) and (**C**) work were carried out by Dr. K. K. Yeoh. HyPro564: HIF1α CODD hydroxylation; HyAsn803: HIF1α CAD hydroxylation; l.e.: long exposure.

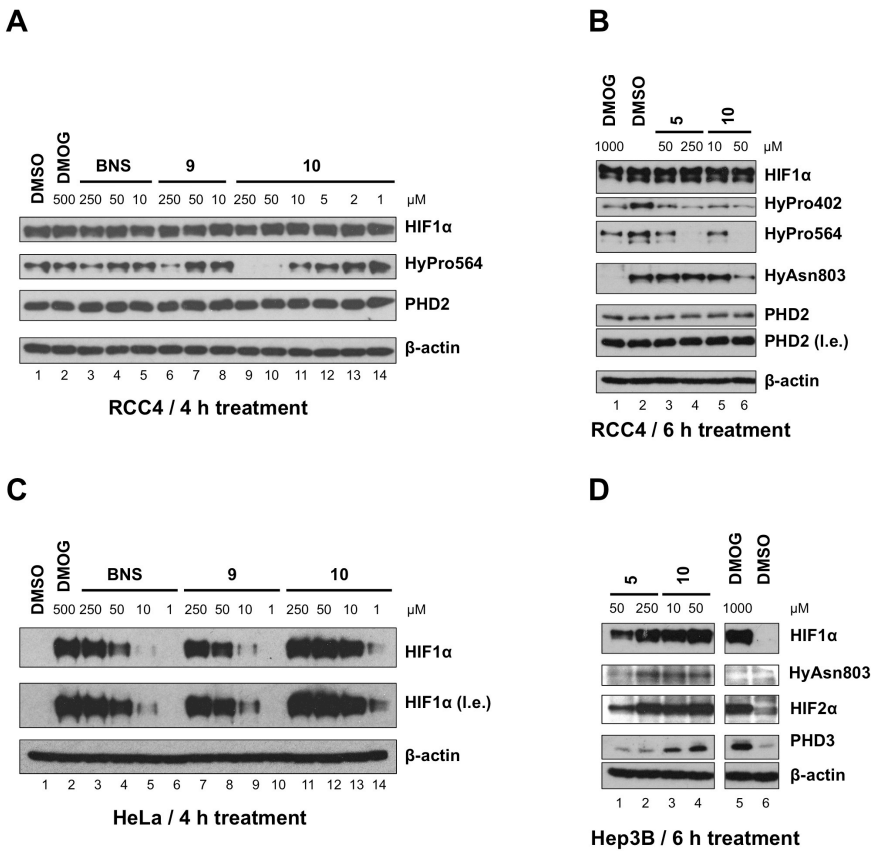

Figure 4.6 Cellular inhibition studies of the dihydropyrazole compounds in human cell lines. (**A-B**) Immunoblot showing the selective inhibition of the HIF1α prolyl- over asparaginyl-hydroxylation in RCC4. (**C-D**) Immunoblots showing the dose-dependent upregulation of HIF1α in VHL-competent human cell lines (HeLa and Hep3B) by the PHD inhibitors. Note the lack of inhibition of HIF1α asparaginyl-hydroxylation. HyPro402: HIF1α NODD hydroxylation; HyPro564: HIF1α CODD hydroxylation; HyAsn803: HIF1α CAD hydroxylation; l.e.: long exposure.

In the inhibition studies of the dihydropyrazoles (**9** and **10**) in RCC4 cells, both were able to block the prolyl-hydroxylation of HIF1α without affecting the levels of PHD2, consistent with their proposed mode of action (**Figure 4.6 A**). Notably, **10** was shown to be more potent in inhibiting HIF1α prolyl-hydroxylation than quinolone **5** (**Figure 4.6 B**, compare *lanes 3-4* to *5-6*), although the inhibition of the HIF1α asparaginyl-hydroxylation can be observed at 50 µM of **10**. This is likely due to the concentration used being above that sufficient for **10** to fully inhibit the PHDs in RCC4 cells. In VHL-competent HeLa cells, both **9** and **10** were able to induce HIF1α, with **10** displaying a higher inhibitory potency as judged by the higher

levels of HIF1α induction at lower doses (**Figure 4.6 C**). Induction of both HIF1α and HIF2α levels were observed in Hep3B cells treated with **5** and **10** (**Figure 4.6 D**), with **10** markedly more potent than **5**. Overall, these results suggest that the candidate PHD chemical probes tested are generally selective for PHDs over FIH (when used at a suitable concentration in cells), with **5** and **10** being the preferred candidates for use as chemical probes for PHDs based on their selectivity and potencies in cells.

Using the HIF1α MSD assay (as described in **Chapter 3**), the relative potencies of **5** and **10** were compared in three human cell lines (MCF-7, U2OS and Hep3B). The results show that the HIF1α EC_{50} (half maximal effective concentration) values are consistent with the observations from immunoblotting, with **10** displaying better inhibitory potency (lower HIF1α EC_{50} values) than **5** in the cell lines tested (**Figure 4.7**). Notably, there are differences in the HIF1α EC_{50} values across different cell lines for the same inhibitor, which could (at least in part) be due to the variable levels of endogenous PHDs in these cell lines [19].

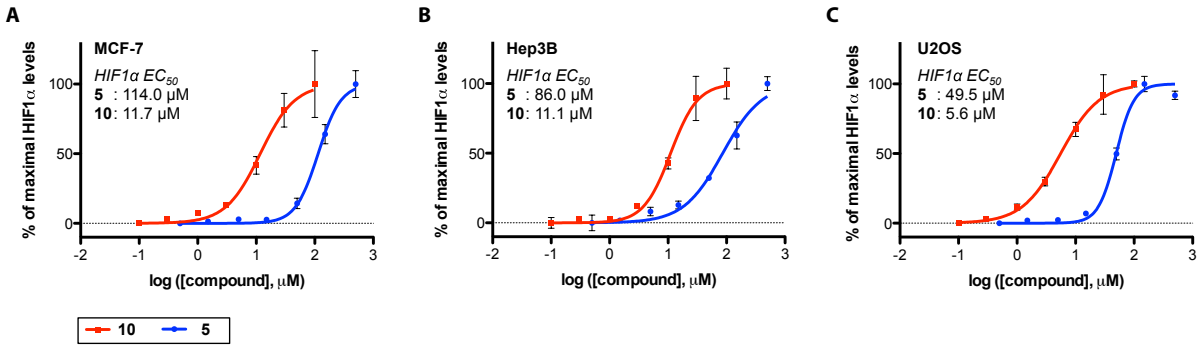

Figure 4.7 The dose-dependent upregulation of HIF1α in (**A**) MCF-7, (**B**) Hep3B and (**C**) U2OS cells measured using the HIF1α MSD assay. Each data point represents the average signal ± standard deviation, n=2.

The inhibition kinetics of **5** and **10** in cells were also investigated by monitoring their ability to induce HIF1α and HIF2α in cells over time by immunoblotting. Time course experiments were carried out in MCF-7 cells over a treatment period of 1 to 16 h, in comparison to hypoxia (0.5% O_2) or DMOG (**1b**) treatment over a similar period. The results reveal that

both **5** and **10** are able to induce HIF1α and HIF2α in MCF-7 cells as early as 1 h after treatment (**Figure 4.8**). Both HIFα isoforms were maximally induced between 3-5 h of inhibitor treatment, before gradually decreasing after 8-16 h. Under hypoxia, both HIFα isoforms were induced at a slower rate compared to inhibitor treatment (**Figure 4.8 A-B**, compare *lanes 2-4* with *lanes 7-9*), before reaching peak levels at 5-8 h. On the other hand, DMOG induced HIF1α maximally after 3 h but this induction gradually decreases after 5 h (**Figure 4.8 C**). For both **5** and **10**, the HIF1α CAD hydroxylation levels over time were, in general, consistent with the levels of HIF1α induction, suggesting that FIH activity was not inhibited. Under hypoxia, HIF1α CAD hydroxylation can still be detected albeit at a lower level than that observed with **5** or **10** treatment, suggesting that FIH activity was partially inhibited (consistent with known ability of FIH to remain active in hypoxia to a greater degree than the PHDs [18]). As expected, HIF1α CAD hydroxylation was not observed with DMOG (indicating that both the PHDs and FIH were inhibited).

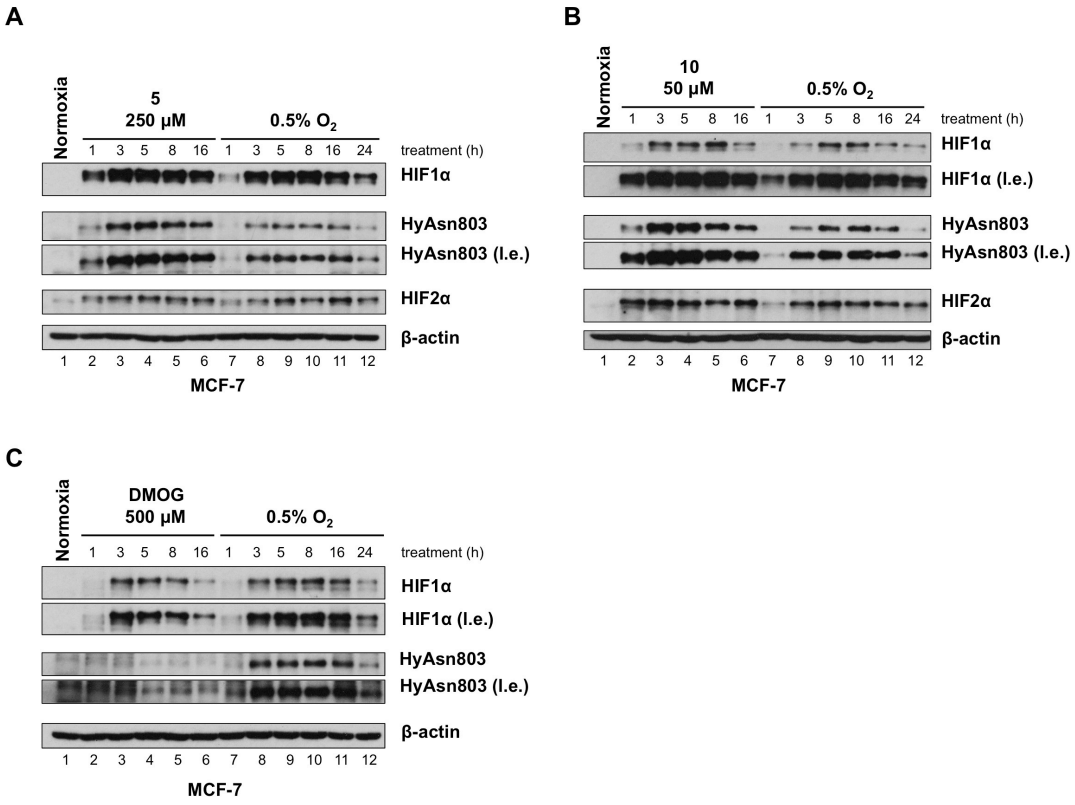

Figure 4.8 Time course experiments in MCF-7 cells with (**A**) **5** (**B**) **10** and (**C**) DMOG in comparison to hypoxia (0.5% O_2) by immunoblotting. HyAsn803: HIF1α CAD hydroxylation; l.e.: long exposure.

4.5 Investigation of the utility of the candidate PHD chemical probes in animal studies

Note: The zebrafish studies in this section were carried out by D. Greenald in the laboratory of Dr. F. van Eeden (University of Sheffield). Studies in mice were carried out by Dr. T. Bishop and Dr. E. Hodson (Ratcliffe/Pugh laboratory, University of Oxford).

To investigate the utility of the quinolone compounds as *in vivo* probes, quinolones **3** and **5** were tested alongside DMOG and BIQ in a *phd3::gfp* transgenic zebrafish model expressing GFP under the control of *phd3* promoter elements [20]. The activation of HIF pathway in this zebrafish model can be monitored spatially based on the site of GFP expression. In this study, 3 days post fertilisation transgenic zebrafish embryos were treated with the compounds (10 μM) or controls (no treatment or DMSO) for 48 h and the expression of GFP was compared relative to controls. As shown in **Figure 4.9**, treatment with DMOG, BIQ, **3** and **5** led to an increase in GFP levels in the liver compared to untreated or DMSO controls. These results highlight the ability of the PHD inhibitors in activating the HIF pathway in an *in vivo* model.

To explore the utility of the inhibitors as chemical probes in a mammalian animal model, **5** and **10** were tested for their ability to induce HIF in mice. In this study, the inhibitors or vehicle controls were injected intraperitonially into wild type C57BL/6 mice at equivalent molar doses. After a period of time, the mice were sacrificed before harvesting their liver tissues to be analysed for HIF levels by immunoblotting and/or MSD assays (as described in **Chapter 2**). The results reveal that HIF1α was induced in the liver by **5** after 1 h of treatment, which persisted even after 2.5 h of treatment albeit at a lower level than the shorter treatment (**Figure 4.10 A** and **C**). In contrast, BIQ treatment led to a lower and shorter induction of HIF1α at equivalent molar dose. Initial experiment with a single dose of **10** for 1 h also led to induction of HIF1α in the liver (**Figure 4.10 B**). HIF2α induction in the mouse liver by **5** is

similar to that observed with HIF1α, with higher induction observed after 1 h of treatment and a lower induction after 2.5 h of treatment (**Figure 4.10 D**).

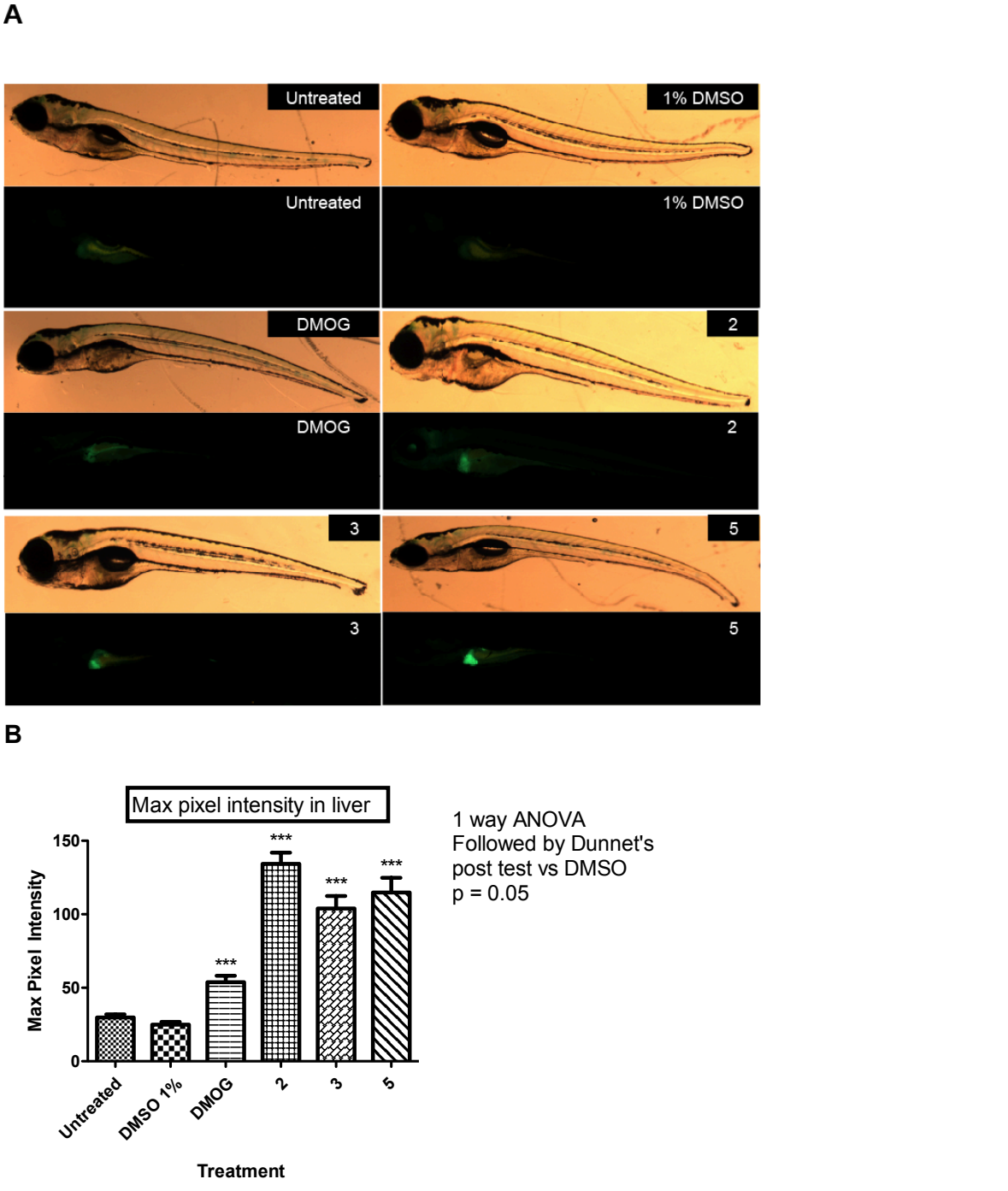

Figure 4.9 Inhibition studies in zebrafish embryos. (**A**) Brightfield and fluorescent images of the *phd3::gfp* zebrafish reporter line treated with the compounds denoted in the panels. **(B)** Maximum pixel intensity in liver of *phd3::gfp* zebrafish reporter line treated with the indicated compounds. Statistical significance against DMSO control were calculated using 1 way ANOVA followed by Dunnet's post test, *** indicates $p < 0.05$ (n=8). All figures obtained from D. Greenald [9].

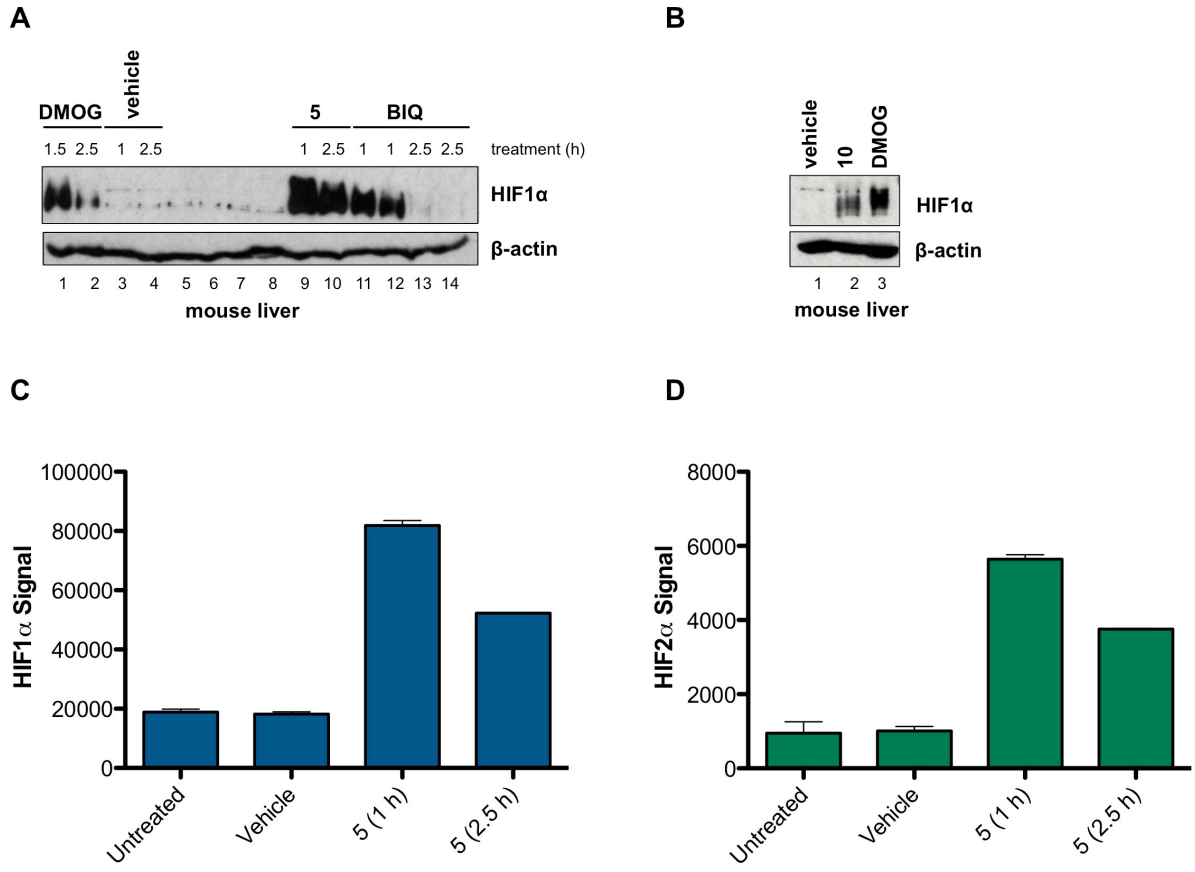

Figure 4.10 (**A**) Immunoblot showing the induction of HIF1α in the mouse liver by **5** (37.7 mg/kg) in comparison to vehicle control, DMOG (320 mg/kg) and BIQ (30 mg/kg). (**B**) Immunoblot showing induction of HIF1α in the mouse liver after 1 h treatment by **10** (35 mg/kg) in comparison to vehicle control and DMOG (160 mg/kg). Induction of (**C**) HIF1α and (**D**) HIF2α in the mouse liver by **5** as measured using the HIF MSD assays described in **Chapter 3**. Each data point represents the average signal ± standard deviation, n=3. All results obtained from Dr. E. Hodson.

4.6 Discussion and future work

Studies on selected PHD inhibitors for their potential use as chemical probes are described in this Chapter. The approach taken to identify a suitable chemical probe for PHD was to first identify the most potent PHD2 inhibitors (quinolones and dihydropyrazoles) shortlisted from the academic literature and patents using the PHD2 CODD AlphaScreen assay developed as described in **Chapter 2**. The identification of a potent inhibitor of PHD2 is a step towards identifying an inhibitor with high degree of selectivity over other human 2OG-dependent dioxygenases. As highlighted in the selectivity profiling studies on the candidate PHD chemical probes across a panel of human 2OG-dependent dioxygenases, the most potent PHD2 inhibitors (**5**, **9** and **10**) exhibit higher fold selectivity for PHD2 over the panel of 2OG-dependent dioxygenases tested (**Table 4.1**). It is noted that the IC_{50} values can only be used as an approximation of the degree of selectivity due to the different assay conditions for each of the 2OG-dependent dioxygenases assays used. Nevertheless, the utilisation of the same assay methodology (AlphaScreen) for the HDMs and PHD2 provides an estimate of the selectivity of the inhibitors tested. Given that only a subset of the large human 2OG-dependent dioxygenases family is represented in the panel of enzymes used in the selectivity studies reported in this Chapter, future work should involve testing the candidate PHD chemical probes when assays of other members of the 2OG-dependent dioxygenase family become available.

Structural studies using crystallography and NMR-based methods suggest that the active quinolones and dihydropyrazoles inhibit PHD2 via direct binding to the 2OG active site. It would be of interest to develop a PHD2 inhibitor that extends into the HIF1α substrate binding site of PHD2, to investigate whether higher selectivity or potencies can be achieved with such an inhibitor. Interestingly, BNS [16], another reported inhibitor of PHD2 was found

to displace both 2OG and CODD from PHD2 based on NMR studies. Future efforts should be put into investigating the binding mode of this inhibitor by crystallography, which has been unsuccessful so far (work carried out by Dr. R. Chowdhury) and measuring its selectivity for PHD2 over other 2OG-dependent dioxygenases.

The cellular studies on the candidate PHD probes reveal that the cellular efficacies of the inhibitors were generally consistent with the IC_{50} values as determined using the *in vitro* PHD2 CODD AlphaScreen assay. Measuring the selectivity of inhibitors across the panel of 2OG-dependent dioxygenases in a cellular context is a challenging task, given that it is likely that there will be differing endogenous levels of each 2OG-dependent dioxygenases in cells. The best candidates to be used as PHD chemical probes should ideally have the highest cellular efficacies against the PHDs with the highest degree of selectivity as determined by the *in vitro* assays on isolated proteins. High concentrations of inhibitor used will likely lead to off-target inhibition in cells, particularly if the inhibitor exhibit low degree of selectivity for the target protein over other proteins within the same family. It is also important to determine the effective concentration of the PHD inhibitors for each cell line at the desired time point of any experiment. This can be done by the monitoring the induction of HIFα levels by immunoblotting, or more quantitatively using the HIF MSD assays (as described in **Chapter 3**). Studies of candidate PHD chemical probes (**5** and **10**) in three human cell lines using the HIF1α MSD assay reveal that the effective concentrations to induce HIF1α differ across the cell lines tested, as judged by the different HIF1α EC_{50} values for each inhibitor. These results may be due to the differing levels of the PHD isoforms in each cell lines [19], although the different mechanisms of uptake/export, metabolism of the inhibitors in cells or the rates of inhibitor association/dissociation with the PHDs should not be ruled out. The induction of HIF2α and the changes of HIF1α CAD hydroxylation (to monitor the extent of FIH

inhibition) by the inhibitors should also be investigated quantitatively using the HIF2α MSD assay and HIF1α CAD MSD assay (as described in **Chapter 3**), respectively.

The time course experiment with **5** and **10** in MCF-7 cells reveal the induction of HIF1α and HIF2α (as indicators of PHD inhibition) over time in comparison to hypoxia (0.5% O_2). Notably, the induction of HIFα isoforms was quicker with the PHD inhibitors compared to hypoxia, reflecting the fast action of the inhibitors in blocking HIF-prolyl hydroxylation. Another possible explanation is that hypoxia induces the protein levels of PHD2 and PHD3 (both are downstream targets of HIF) to a higher extent than PHD inhibitors do. PHD3 could still be partially active under hypoxia [18], leading to the slower stabilisation of HIFα. The levels of PHD induction under hypoxia should be compared to that under PHD inhibitor treatment in future studies. It is unlikely that the difference was due to the rate of oxygen diffusion out of the medium given that the medium used were pre-equilibrated under the desired concentration of oxygen prior to addition into the cells.

The studies on the efficacies of the candidate PHD chemical probes in animal models provide insight into the feasibility of using these probes to explore the biology of PHDs *in vivo*. The studies using transgenic zebrafish embryos as a reporter for HIF activation show that quinolones **3** and **5** were active *in vivo*, highlighting their potential use as chemical probes for the PHDs. Both **5** and **10** were also shown to induce HIF1α in the mouse liver. Pharmacokinetic and pharmacodynamic analyses of the PHD inhibitors would be useful in aiding the effectiveness of using them as chemical probes for the PHDs. Work is currently in progress (unpublished work by Dr. T. Bishop and Dr. E. Hudson) to investigate whether the chemical probes for PHD can also mimic the ventilatory phenotype observed in $PHD2^{+/-}$ mice, which was not observed with pharmacological intervention using BIQ [21].

Overall, the work described in this Chapter has revealed potential selective and potent small molecule inhibitors of PHDs that can be used as chemical probes in biological studies. A similar approach should be employed in the future for characterisation of PHD inhibitors (including compound **6** described in **Chapter 2**, which was not included in this initial study). Taken together, **5** (hereafter referred to as IOX2) and **10** (hereafter referred to as IOX4) were identified as preferred chemical probes for the PHDs.

4.7 Materials and methods

The following were as described in previous Chapters:

- *PHD2 CODD AlphaScreen assay* **(Chapter 2)**
- *Buffers and reagents* **(Chapter 3)**
- *Cell lysate preparation - as for immunoblotting* (**Chapter 3**)
- *Cell lysate preparation - as for MDS asssay* (**Chapter 3**)
- *Immunoblotting* **(Chapter 3)**
- *Standard HIF1α and HIF2α MSD assay* **(Chapter 3)**
- *Inhibitor treatment of mice and tissue lysate preparation* **(Chapter 3)**

In vitro selectivity profiling studies

In vitro demethylation assays for the HDMs (AlphaScreen) were carried out by Dr. A. Tumber as previously described [10]. *In vitro* fluoride-detection-based fluorescence assays for BBOX were carried out by A. Rydzik as previously described [12]. *In vitro* assays for FTO were carried out by Dr. M. Demetriades and W. S. Aik as previously described [13].

Crystallographic studies

Crystallographic and modelling studies on PHD2 were carried out Dr. R. Chowdhury as described [9].

[^{13}C]-2OG and [^{13}C]-CODD NMR studies

[^{13}C]-2OG and [^{13}C]-CODD NMR studies were carried out by Dr. I. Leung as previously described [15]. Standard assay mixture contained 50 μM apo-PHD2, 400 μM Zn(II), 50 μM [^{13}C]-2OG, 40 μM [^{13}C]-CODD and 800 μM inhibitor.

Cell culture

Human cell lines (Hep3B, HeLa, MCF-7, U2OS, RCC4, RCC4/VHL) were cultured in DMEM (D6546-500ML; Sigma Aldrich, St. Louis, USA) each supplemented with 10% fetal bovine serum (F7524-500ML; Sigma Aldrich, St. Louis, USA), 2 mM L-glutamine (G7513-100ML; Sigma Aldrich, St. Louis, USA), 50 units/ml of penicillin, and 50 μg/ml of streptomycin (P0781-100ML; Sigma Aldrich, St. Louis, USA).

Antibodies for immunoblotting

Antibody for human HIF1α was as described in **Chapter 3**, mouse monoclonal HIF2α antibody 190b (NB100-132; Novus Biologicals, Littleton, USA), rabbit polyclonal anti-HyPro402 (07-1585; Millipore, Billerica, USA), rabbit monoclonal anti-HyPro564 clone D43B5 (3434S; Cell Signalling, Danvers, USA), mouse monoclonal anti-HyAsn803 (kind gift from Dr. M. K. Lee, KRIBB, Republic of Korea). Secondary antibodies were as described in **Chapter 3**.

Hypoxia experiments

Hypoxia incubations of cells were performed in *In vivo*$_2$ 400 hypoxic workstations (Ruskin Technologies, Bridgend, United Kingdom). Cell culture medium and PBS were pre-equilibrate at the desired oxygen concentration in the hypoxic workstations for at least overnight (16 h) prior to addition to the cells for the desired period of time. Medium were removed and cells were washed with PBS before being harvested with USD lysis buffer and processed for immunoblotting.

Zebrafish studies

All experiments on zebrafish were carried out by D. Greenald in the laboratory of Dr. F. van Eeden (University of Sheffield) as previously described [9, 20].

4.8 References

1 Edwards, A. M., Bountra, C., Kerr, D. J. and Willson, T. M. (2009) Open access chemical and clinical probes to support drug discovery. Nat Chem Biol. **5**, 436-440

2 Bruick, R. K. and McKnight, S. L. (2001) A conserved family of prolyl-4-hydroxylases that modify HIF. Science. **294**, 1337-1340

3 Epstein, A. C., Gleadle, J. M., McNeill, L. A., Hewitson, K. S., O'Rourke, J., Mole, D. R., Mukherji, M., Metzen, E., Wilson, M. I., Dhanda, A., Tian, Y. M., Masson, N., Hamilton, D. L., Jaakkola, P., Barstead, R., Hodgkin, J., Maxwell, P. H., Pugh, C. W., Schofield, C. J. and Ratcliffe, P. J. (2001) C. elegans EGL-9 and mammalian homologs define a family of dioxygenases that regulate HIF by prolyl hydroxylation. Cell. **107**, 43-54

4 Yan, L., Colandrea, V. J. and Hale, J. J. (2010) Prolyl hydroxylase domain-containing protein inhibitors as stabilizers of hypoxia-inducible factor: small molecule-based therapeutics for anemia. Expert Opin Ther Pat. **20**, 1219-1245

5 Aik, W., McDonough, M. A., Thalhammer, A., Chowdhury, R. and Schofield, C. J. (2012) Role of the jelly-roll fold in substrate binding by 2-oxoglutarate oxygenases. Curr Opin Struct Biol. **22**, 691-700

6 Hewitson, K. S., McNeill, L. A., Riordan, M. V., Tian, Y. M., Bullock, A. N., Welford, R. W., Elkins, J. M., Oldham, N. J., Bhattacharya, S., Gleadle, J. M., Ratcliffe, P. J., Pugh, C. W. and Schofield, C. J. (2002) Hypoxia-inducible factor (HIF) asparagine hydroxylase is identical to factor inhibiting HIF (FIH) and is related to the cupin structural family. J Biol Chem. **277**, 26351-26355

7 Lando, D., Peet, D. J., Gorman, J. J., Whelan, D. A., Whitelaw, M. L. and Bruick, R. K. (2002) FIH-1 is an asparaginyl hydroxylase enzyme that regulates the transcriptional activity of hypoxia-inducible factor. Genes Dev. **16**, 1466-1471

8 Rabinowitz, M. H. (2013) Inhibition of hypoxia-inducible factor prolyl hydroxylase domain oxygen sensors: tricking the body into mounting orchestrated survival and repair responses. J Med Chem. **56**, 9369-9402

9 Chowdhury, R., Candela-Lena, J. I., Chan, M. C., Greenald, D. J., Yeoh, K. K., Tian, Y. M., McDonough, M. A., Tumber, A., Rose, N. R., Conejo-Garcia, A., Demetriades, M., Mathavan, S., Kawamura, A., Lee, M. K., van Eeden, F., Pugh, C. W., Ratcliffe, P. J. and Schofield, C. J. (2013) Selective Small Molecule Probes for the Hypoxia Inducible Factor (HIF) Prolyl Hydroxylases. ACS Chem Biol. **8**, 1488-1496

10 Rose, N. R., Woon, E. C., Tumber, A., Walport, L. J., Chowdhury, R., Li, X. S., King, O. N., Lejeune, C., Ng, S. S., Krojer, T., Chan, M. C., Rydzik, A. M., Hopkinson, R. J., Che, K. H., Daniel, M., Strain-Damerell, C., Gileadi, C., Kochan, G., Leung, I. K., Dunford, J., Yeoh, K. K., Ratcliffe, P. J., Burgess-Brown, N., von Delft, F., Muller, S., Marsden, B., Brennan, P. E.,

McDonough, M. A., Oppermann, U., Klose, R. J., Schofield, C. J. and Kawamura, A. (2012) Plant growth regulator daminozide is a selective inhibitor of human KDM2/7 histone demethylases. J Med Chem. **55**, 6639-6643

11 Murray, J. K., Balan, C., Allgeier, A. M., Kasparian, A., Viswanadhan, V., Wilde, C., Allen, J. R., Yoder, S. C., Biddlecome, G., Hungate, R. W. and Miranda, L. P. (2010) Dipeptidyl-quinolone derivatives inhibit hypoxia inducible factor-1alpha prolyl hydroxylases-1, -2, and -3 with altered selectivity. J Comb Chem. **12**, 676-686

12 Rydzik, A. M., Leung, I. K., Kochan, G. T., Thalhammer, A., Oppermann, U., Claridge, T. D. and Schofield, C. J. (2012) Development and application of a fluoride-detection-based fluorescence assay for gamma-butyrobetaine hydroxylase. Chembiochem. **13**, 1559-1563

13 Aik, W., Demetriades, M., Hamdan, M. K., Bagg, E. A., Yeoh, K. K., Lejeune, C., Zhang, Z., McDonough, M. A. and Schofield, C. J. (2013) Structural basis for inhibition of the fat mass and obesity associated protein (FTO). J Med Chem. **56**, 3680-3688

14 Chowdhury, R., McDonough, M. A., Mecinovic, J., Loenarz, C., Flashman, E., Hewitson, K. S., Domene, C. and Schofield, C. J. (2009) Structural basis for binding of hypoxia-inducible factor to the oxygen-sensing prolyl hydroxylases. Structure. **17**, 981-989

15 Leung, I. K., Demetriades, M., Hardy, A. P., Lejeune, C., Smart, T. J., Szollossi, A., Kawamura, A., Schofield, C. J. and Claridge, T. D. (2013) Reporter ligand NMR screening method for 2-oxoglutarate oxygenase inhibitors. J Med Chem. **56**, 547-555

16 Tegley, C. M., Viswanadhan, V. N., Biswas, K., Frohn, M. J., Peterkin, T. A., Chang, C., Burli, R. W., Dao, J. H., Veith, H., Rogers, N., Yoder, S. C., Biddlecome, G., Tagari, P., Allen, J. R. and Hungate, R. W. (2008) Discovery of novel hydroxy-thiazoles as HIF-alpha prolyl hydroxylase inhibitors: SAR, synthesis, and modeling evaluation. Bioorg Med Chem Lett. **18**, 3925-3928

17 Lee, S. H., Jeong Hee, M., Eun Ah, C., Ryu, S. E. and Myung Kyu, L. (2008) Monoclonal antibody-based screening assay for factor inhibiting hypoxia-inducible factor inhibitors. J Biomol Screen. **13**, 494-503

18 Tian, Y. M., Yeoh, K. K., Lee, M. K., Eriksson, T., Kessler, B. M., Kramer, H. B., Edelmann, M. J., Willam, C., Pugh, C. W., Schofield, C. J. and Ratcliffe, P. J. (2011) Differential sensitivity of hypoxia inducible factor hydroxylation sites to hypoxia and hydroxylase inhibitors. J Biol Chem. **286**, 13041-13051

19 Appelhoff, R. J., Tian, Y. M., Raval, R. R., Turley, H., Harris, A. L., Pugh, C. W., Ratcliffe, P. J. and Gleadle, J. M. (2004) Differential function of the prolyl hydroxylases PHD1, PHD2, and PHD3 in the regulation of hypoxia-inducible factor. J Biol Chem. **279**, 38458-38465

20 Santhakumar, K., Judson, E. C., Elks, P. M., McKee, S., Elworthy, S., van Rooijen, E., Walmsley, S. S., Renshaw, S. A., Cross, S. S. and van Eeden, F. J. (2012) A zebrafish model to

study and therapeutically manipulate hypoxia signaling in tumorigenesis. Cancer Res. **72**, 4017-4027

21 Bishop, T., Talbot, N. P., Turner, P. J., Nicholls, L. G., Pascual, A., Hodson, E. J., Douglas, G., Fielding, J. W., Smith, T. G., Demetriades, M., Schofield, C. J., Robbins, P. A., Pugh, C. W., Buckler, K. J. and Ratcliffe, P. J. (2013) Carotid body hyperplasia and enhanced ventilatory responses to hypoxia in mice with heterozygous deficiency of PHD2. J Physiol. **591**, 3565-3577

Chapter 5: Towards the identification of PHD isoform specific inhibitor using cellular based model systems

5.1 Introduction

As described in **Chapter 1**, there are three human isoforms of the PHDs (PHD1, PHD2 and PHD3), with PHD2 being regarded as the most important isoform, in part due to its abundance and more widespread tissue distribution [1, 2]. Evolutionary studies on the HIF oxygen sensing pathway reveal that the gene encoding for PHD2 may have arisen before gene duplication events giving rise to genes encoding for the other PHD isoforms [3]. PHD isoforms other than PHD2 have been found to be prevalent in vertebrates (and in a few invertebrates), suggesting that they may play a role in the oxygen sensing of higher organisms [3]. Although the roles of PHD1 and PHD3 have been studied, their biological roles remain less well understood. It remains unclear why the HIF oxygen sensing pathway in humans requires more than one PHD isoform. The differential tissue distribution and expression levels of the PHDs suggest that the different PHD isoforms play a cell-type specific role [2]. Additionally, changes in the expression levels of PHD2 and PHD3 (both of which are HIF target genes) in response to changes in oxygen concentrations provide an indication that they may be involved in a feedback loop that fine-tunes the levels of HIF and/or in cellular adaptation to reoxygenation. Although PHD2 has been the focus of many studies due to its apparent dominant role in the human oxygen sensing pathway, PHD1 and PHD3 should not be neglected as they are likely to have important biological roles.

To enable *in vitro* investigations on the PHD isoforms, attempts have been made to isolate and purify large quantities of catalytically active recombinant PHD1 and PHD3. However,

these attempts have been problematic (due to low protein yield and/or instability of the isolated protein), despite previous reports on the purification of these proteins [4-6]. An alternative approach has involved substituting cysteine residues within PHD3 to increase its stability; the isolated PHD3 protein has been shown to be catalytically active (unpublished work by Dr. R. Chowdhury). A caveat for this approach is that the cysteine-mutated PHD3 may not have the same properties as the wild-type PHD3 and therefore, interpretation of the results of any studies with this mutant may be misleading. Another approach taken was to isolate the proteins using a baculovirus expression system in insect cells ([7] and work carried by Dr. G. Kochan).

To complement the attempts to study the PHD isoforms *in vitro*, it was proposed that re-expression of individual PHDs in a PHD-null cell model would allow for the investigation of each PHD isoform in a more biological setting. It was also envisaged that the development of such a system would enable selectivity studies on small molecule PHD inhibitors, which may lead to the identification of PHD-isoform specific small molecule inhibitors. These small molecules can then be used as chemical probes to study the biological roles of the PHD isoforms in cells or in animals, in addition to aiding *in vitro* investigations (such as serving as ligands or protein stablisers in crystallographic studies).

Previously, an immortalised mouse embryonic fibroblast (MEF) cell line lacking all three PHD isoforms (hereafter referred to as the TKO or triple-knockout cells) had been generated and characterised [8]. HIF1α protein is constitutively stabilised in this cell line due to the lack of PHDs, and individual re-expression of PHD1-3 in this cell line is expected to downregulate HIF1α levels. A pan-PHD inhibitor which inhibits all three PHDs should induce HIF1α levels in the TKO cells re-expressing either PHD1, PHD2 or PHD3, whereas an isoform specific

PHD inhibitor is expected to only induce HIF1α in the TKO cells re-expressing the PHD isoform that is targeted by the specific inhibitor. HIF2α protein was undetected in the TKO cell line under normoxia or hypoxia by immunoblotting (unpublished work by Dr. Y-M. Tian).

This Chapter describes work aimed at developing a cellular model by engineering the TKO cells to re-express individual PHD isoforms. Initial work was carried out on the constitutive expression of the PHD isoform genes; this was followed by the development of an inducible expression system. Preliminary inhibitor studies are also described, with some degree of selectivity within the PHD isoforms observed with the PHD inhibitors tested. The work described in this Chapter was carried out in collaboration with Dr. Y-M. Tian and Dr. T-L. Yeh.

5.2 PHD-null MEF cells with individual re-expression of PHD isoforms as a cellular model system for studying PHD isoform specific inhibition

To investigate whether PHD inhibitors exhibit any effect on the TKO cells (without PHD re-expression), the TKO cell line was treated with the PHD inhibitors IOX2 and IOX4 (the development of which is described in **Chapter 4**,) as well as the generic 2OG-dependent dioxygenase inhibitor DMOG and the proteasome inhibitor MG132 (**Figure 5.1**). HIF1α levels with and without inhibitor treatment were analysed by immunoblotting. The results show that neither DMOG nor any of the PHD inhibitors have an effect on the HIF1α levels in TKO cells (**Figure 5.1 A**). These results provide an indication that the inhibitors do not (at least substantially) upregulate HIF1α levels via PHD-independent processes, such as by increasing the rate of HIF1α transcription or translation. The results also support the absence of the proposed fourth HIF prolyl hydroxylase (P4H-TM) [9] in this cell line, which was

undetected at the mRNA level (unpublished work, Dr. Y-M. Tian). Notably, proteasome inhibition by MG132 was observed to increase HIF1α levels in the TKO cells, in line with previous reports on oxygen-independent and prolyl hydroxylation-independent degradation of HIF1α via the proteasome pathway [10, 11].

5.2.1 Constitutive re-expression of PHD isoforms in PHD-null MEF cells

To develop a cellular system for exploring the selectivity of PHD inhibitors, the initial strategy employed was to reintroduce each PHD isoform individually into the TKO cells using lentiviral transduction, followed by analyses on the effects of PHD inhibitors, either on unsorted pools of cells after transduction or on fluorescence-activated cell sorting (FACS)-sorted transduced cells (**Figure 5.1 C**). Viral vectors for the expression of either FLAG-tagged full-length human PHD1, PHD2 or PHD3 were introduced individually by lentiviral transduction in the TKO cells (work carried out by Dr. Y-M. Tian). Each vector also encodes for a GFP expression cassette for co-expression via an internal ribosome entry site (IRES), allowing for cell sorting of positively transduced cells.

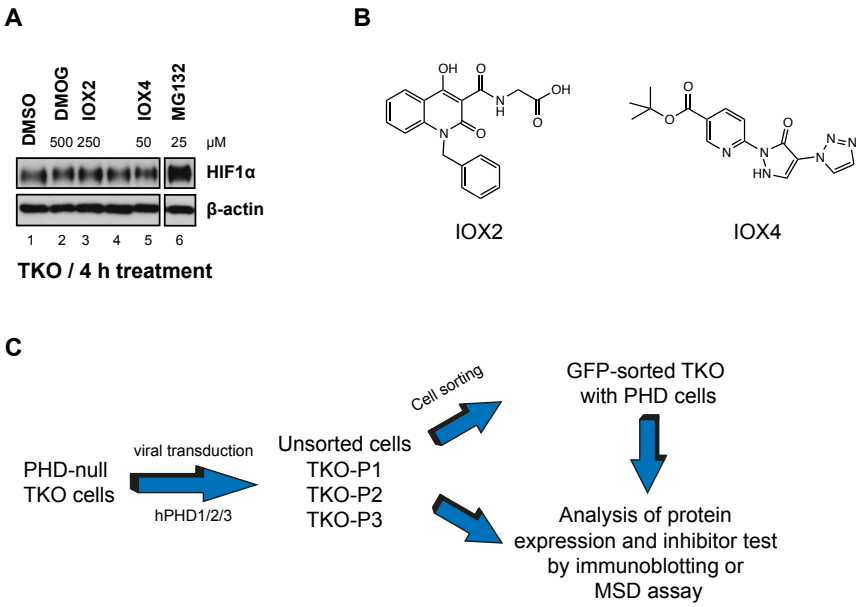

Figure 5.1 (**A**) Effect of PHD inhibitors in the TKO cells after 4 h of treatment. (**B**) Chemical structures of IOX2 and IOX2. (**C**) Schematic diagram of the strategy for developing a cellular model to investigate PHD isoform selectivity of inhibitors. hPHD1/2/3: human PHD1/PHD2/PHD3.

Following lentiviral transduction, the unsorted TKO cells were analysed by immunoblotting under various conditions, including under the treatment of PHD inhibitors (work carried out by Dr. Y-M. Tian). The TKO cells transduced with PHD1, PHD2 and PHD3 vectors are hereafter referred to as the TKO-P1, TKO-P2 and TKO-P3 cells, respectively. The expression of each PHD isoform was confirmed by the immunodetection of FLAG-tagged protein in each cell line. Under normoxia, HIF1α in all three TKO cell lines was not detected, indicating that each PHD isoform was catalytically active at a sufficient level to supress endogenous HIF1α levels in the TKO cells (**Figure 5.2 A-C**, *lane 1*). The cells were also responsive to proteasomal blockage and hypoxia (0.1% O_2), with HIF1α levels being upregulated in all three TKO cell lines under these conditions (**Figure 5.2 A-C**, *lanes 2* and *7*). Interestingly, treatment with various PHD inhibitors produced differential responses in each of the TKO cell lines. BNS was able to induce HIF1α in the TKO-P2 to a higher extent than the TKO-P1 cells, whereas in the TKO-P3 cells, the HIF1α levels remained undetected (**Figure 5.2 A-C**, *lane 6*). These results suggest that BNS is more selective for PHD2 than PHD1 or PHD3. On the other hand, BIQ and BIQ-B induced HIF1α levels in the TKO-P2 and TKO-P3 cells to a higher extent than the TKO-P1 cells, suggesting that they inhibit PHD2 and PHD3, but were less active against PHD1 (**Figure 5.2 A-C**, *lanes 4* and *5*).

The apparently selective effects on HIF1α by the inhibitors could be due to the differential ability of each PHD isoform to hydroxylate HIF1α. Based on *in vitro* and cellular studies, both PHD1 and PHD2 are reported to hydroxylate both NODD (Pro402 for both human and mouse HIF1α) and CODD (Pro564 for human HIF1α, Pro577 for mouse HIF1α), whereas PHD3 only hydroxylates CODD efficiently [12, 13]. To investigate the ability of each PHD isoform re-expressed in the TKO cells to hydroxylate HIF1α, the HIF1α hydroxylation status in the TKO re-expressing PHD cell lines (in the presence of proteasome inhibitor MG132)

was analysed by immunoblotting (work carried out by Dr. Y-M. Tian). As shown in **Figure 5.3** and in agreement with previous reports, both NODD and CODD hydroxylations were detected in the TKO-P1 and TKO-P2 cells, whereas only CODD hydroxylation was detected in the TKO-P3 cells. As expected, there was also no detectable hydroxylation at CODD or NODD sites in the control TKO cells (**Figure 5.3 B**, *lane 1*). These results show that the hydroxylation of CODD alone is sufficient to degrade HIF1α (as shown in the TKO-P3 cells), consistent with previous studies [12, 14].

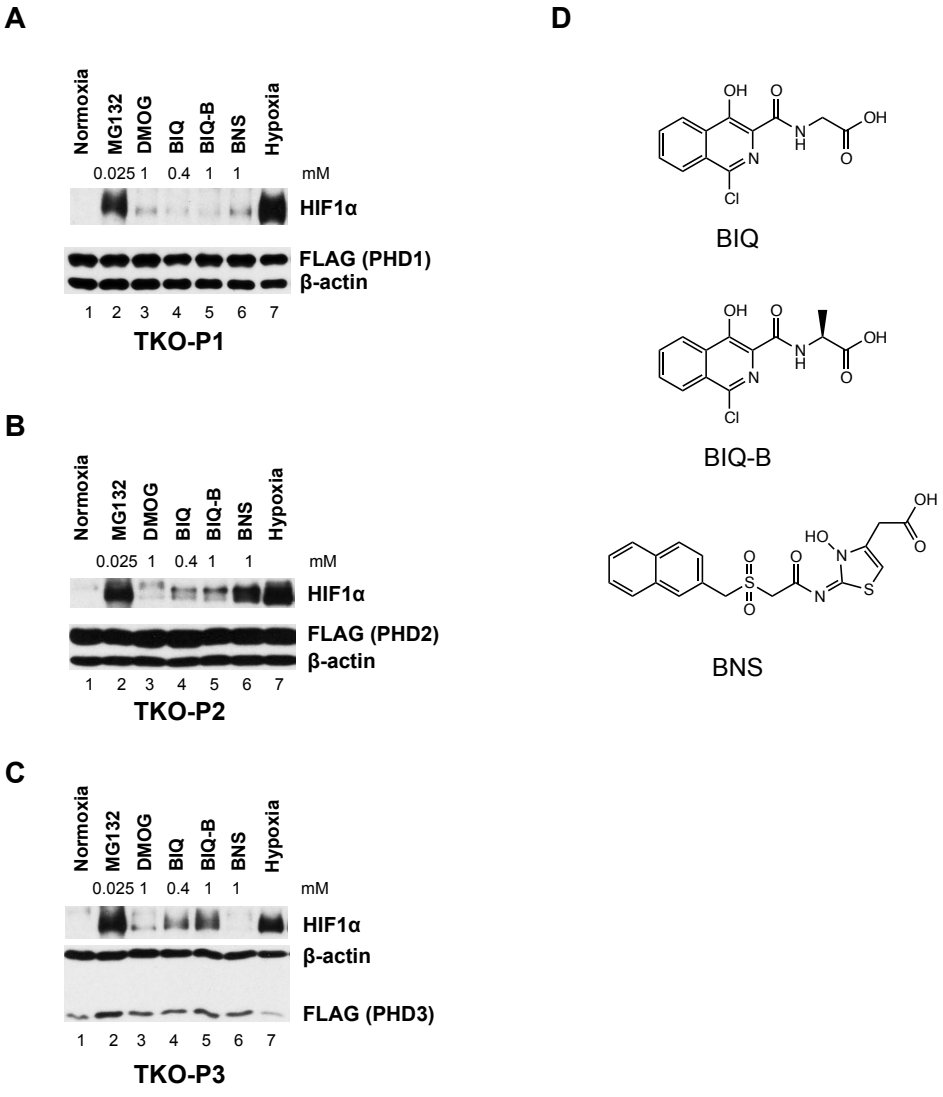

Figure 5.2 Effect of PHD inhibitors in the unsorted TKO cells transduced with the expression vector for the production of (**A**) hPHD1, (**B**) hPHD2 or (**C**) hPHD3. 44 h after lentiviral transduction, cells were treated with inhibitors for 4 h or under hypoxia (0.1% O_2) for 6 h. Immunoblots obtained from Dr. Y-M. Tian. (**D**) Chemical structures of the PHD inhibitors used in this study.

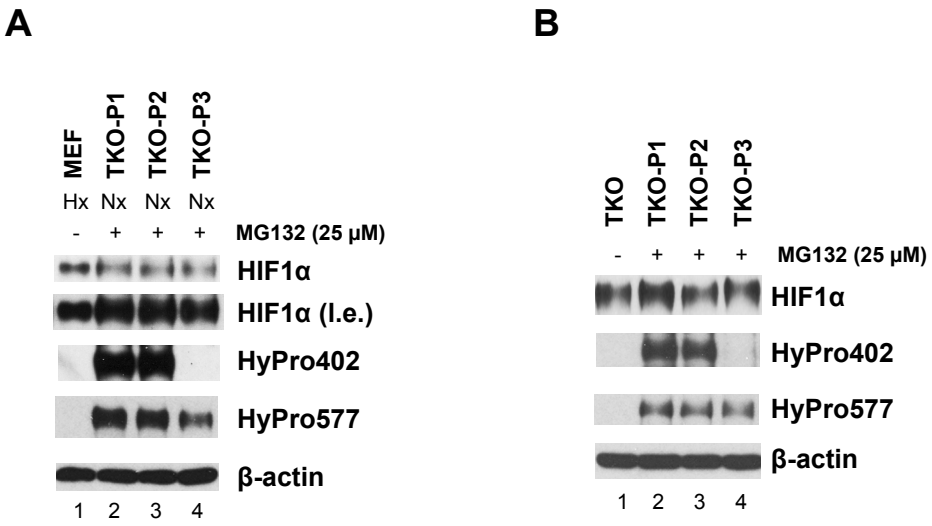

Figure 5.3 HIF1α hydroxylation by human PHD isoforms produced in the TKO cells. Comparison of HIF1α hydroxylation status of the unsorted TKO cells transduced with human PHD isoforms in the presence of MG132 with (**A**) hypoxic-treated wildtype mouse embryonic fibroblast (MEF) cells and (**B**) untreated TKO cells. Immunoblots obtained from Dr. Y-M. Tian. MEF: wild-type mouse embryonic fibroblast, TKO: PHD-null cells, Nx: normoxia, Hx, hypoxia (0.1% O_2, 16 h), l.e.: long exposure.

To eliminate possible interference from non-transduced cells within the unsorted pool following transduction, the TKO-P1, TKO-P2 and TKO-P3 cells were then sorted by FACS based on GFP expression (work carried out by Dr. Y-M. Tian). The expression levels of PHD isoforms in the GFP-sorted cells were analysed by immunoblotting using PHD2 or PHD3 antibodies and were compared to the endogenous PHD levels in the human neuroblastoma Kelly cell line. The PHD2 levels in the GFP-sorted TKO-P2 cells (TKO-P2R3) were markedly higher than the levels of PHD2 detected in Kelly cells (**Figure 5.4 A**). Similarly, the PHD3 levels in the GFP-sorted TKO-P3 cells (TKO-P3R7) were also markedly higher than in the Kelly cells (**Figure 5.4 B**). The comparison of PHD1 levels in the transduced TKO cell lines and the endogenous PHD levels in Kelly cells were not made due to the lack of a sufficiently good PHD1 antibody for immunoblotting. Nevertheless, comparisons of the FLAG-tagged protein levels in the GFP-sorted TKO-P1 cells (TKO-P1R7) to that of the TKO-P2R3, TKO-P3R7 and TKO-P3R3 (the GFP-sorted TKO-P3 cells with lower GFP

expression) cells by immunoblotting suggest that the PHD1 levels in the transduced cells were likely to be overexpressed compared to the endogenous levels (**Figure 5.4 C**). The PHD2 immunoblot also shows a higher amount of PHD2 produced in the unsorted TKO-P2 cells compared to the endogenous levels in the Kelly cells (**Figure 5.4 D**). Overall, the results demonstrate that each PHD isoform were expressed at a markedly higher level in the transduced TKO cells compared to the endogenous PHD levels in Kelly cells.

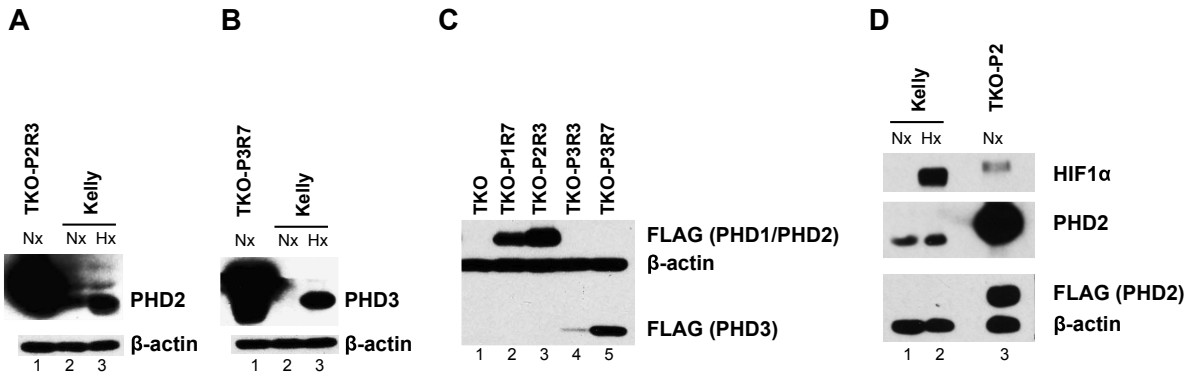

Figure 5.4 The TKO cells transduced with human PHD1-3 in comparison with the human neuroblastoma Kelly cells by immunoblotting. (**A**) The PHD2 levels in the TKO-P2R3 cells in comparison to that in Kelly cells. (**B**) The PHD3 levels in the TKO-P3R7 cells in comparison to that in the Kelly cells. (**C**) The comparison of FLAG-tagged protein levels in the GFP-sorted TKO cells transduced with PHD1-3. (**D**) The levels of FLAG-tagged protein and PHD2 in the unsorted TKO-P2 cells in comparison to that in Kelly cells. Immunoblots obtained from Dr. Y-M. Tian. Nx: normoxia, Hx, hypoxia (0.1% O_2, 14 h).

Despite the unphysiologically high levels of PHD isoforms in the transduced TKO cells, the effects of PHD inhibitors (BNS and BIQ, as in **Figure 5.2**) on each of the GFP-sorted TKO cell lines re-expressing PHD1, PHD2 and PHD3 were investigated. To enable better quantification of HIF1α levels, the HIF1α MSD assay, as described in **Chapter 3**, was used. The results reveal that BNS is better at inducing HIF1α in the TKO-P2R3 cells than in the TKO-P1R7, TKO-P3R3 and TKO-P3R7 cells, suggesting a preference of this inhibitor for PHD2 over PHD1 and PHD3 (**Figure 5.5**). As for BIQ, the highest HIF1α induction was observed in the TKO-P3R7 cells, followed by the TKO-P2R3, TKO-P3R3 and TKO-P1R7

cells, suggesting that BIQ preferentially inhibits PHD2 and PHD3 in cells. This proposal is consistent with the previous observation by immunoblotting with the unsorted TKO cells re-expressing each of the PHD isoform, as shown in **Figure 5.2**.

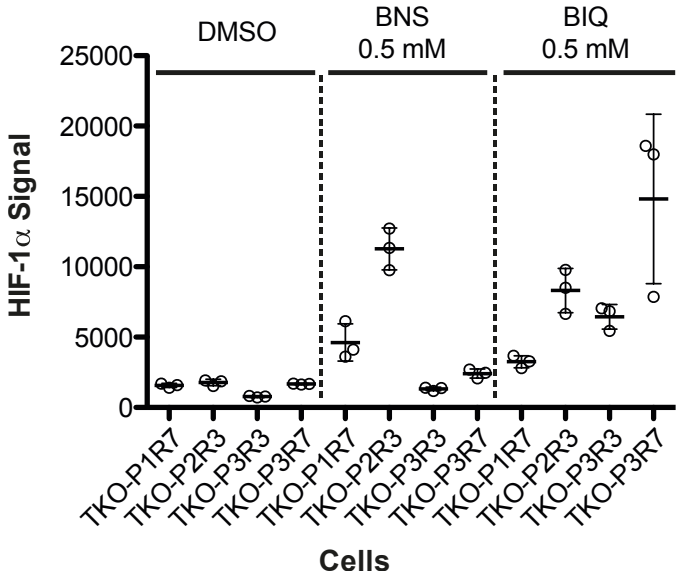

Figure 5.5 HIF1α induction in the GFP-sorted TKO cells transduced with either the PHD1, PHD2 or PHD3 expression vectors, after 4 h treatment with PHD inhibitors BIQ (**3**) or BNS (**5**). HIF1α levels were detected using the HIF1α MSD assay. Each datapoint represents the value from each of the 3 biological replicates with mean and standard deviation highlighted.

Overall, the results from the PHD-null TKO cells engineered to re-express PHD1, PHD2 and PHD3 separately demonstrate that selective inhibition within the PHD isoforms may be achieved. However, the constitutive expression levels of each PHD isoform in this cellular model is not ideal, given that the differential relative expression of each isoform may affect the apparent selectivity of the tested PHD inhibitors. Furthermore, the unphysiologically high expression levels of each PHD isoform in this cellular model may result in the need for high inhibitor concentrations to observe the inhibitory effect. Therefore, attempts were made to investigate whether or not the apparent selectivity can also be seen when each of the PHD isoforms is expressed at a comparable, lower and more physiologically-relevant levels using an inducible expression system.

5.2.2 Inducible re-expression of PHD isoforms in PHD-null MEF cells

To achieve lower levels of the PHD isoforms in the TKO cells, the approach taken was to express the PHD isoforms in an inducible-manner with a relatively weaker promoter. Analogous to the strategy used in the constitutive re-expression of PHD isoforms in the TKO cells described in the previous section of this Chapter, it was planned that the FLAG-tagged PHD isoforms would each be co-expressed with GFP but under the control of a tetracyclin-inducible promoter (Tet-on system). The vectors also contained a blasticidin resistance gene as a positive selection marker; they were introduced into the TKO cells either by lentiviral transduction or by the use of transfection reagent (cloning and transduction/transfection work was carried out by Dr. Y-M. Tian). Once the vector was introduced into the TKO cells, they were then cultured at various densities in the presence of blasticidin, followed by picking of colonies and screening by immunoblotting with and without the induction of expression using doxycycline. The TKO cells after transduction or transfection of the vector for inducible expression of PHD1, PHD2 and PHD3 are hereafter referred to as the TKO-iP1, TKO-iP2 and TKO-iP3, respectively. The overall outline of the strategy employed is shown in **Figure 5.6**.

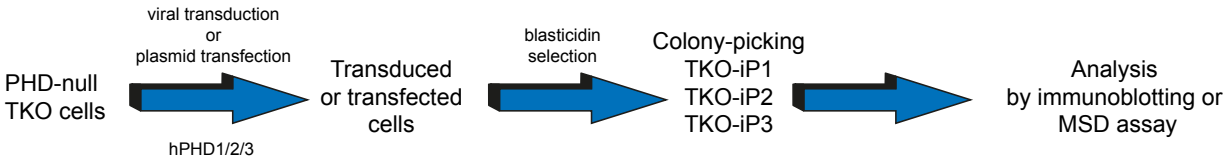

Figure 5.6 Schematic diagram of the strategy for generating a PHD-null cellular system with inducible human PHD isoform expression. hPHD1/2/3: human PHD1/2/3.

A total of 24 clones of the TKO-iP1 cells were screened by immunoblotting for the detection of FLAG-tagged protein and HIF1α, with and without the addition of doxycycline (**Figure 5.7**). Although 18 out of the 24 clones were positive for FLAG-tagged protein detection in the presence of doxycycline, only 14 were able to downregulate HIF1α. Clones 11 and 16 were

selected for subsequent experiments and are hereafter referred to as the TKO-iP1-c11 and TKO-iP1-c16, respectively.

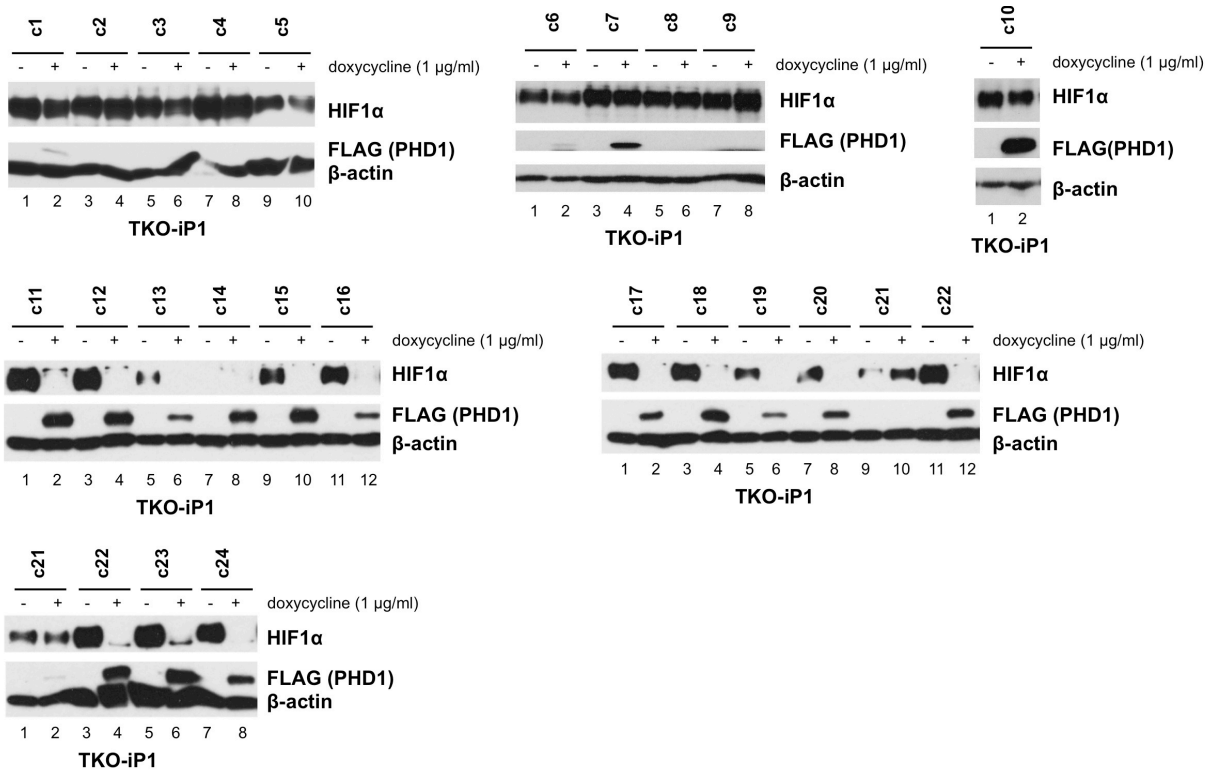

Figure 5.7 Immunoblots showing the screening of PHD1 clones cultured in the presence or absence of doxycycline (1 μg/ml) for at least 48 h. Work carried out with Dr. Y-M. Tian.

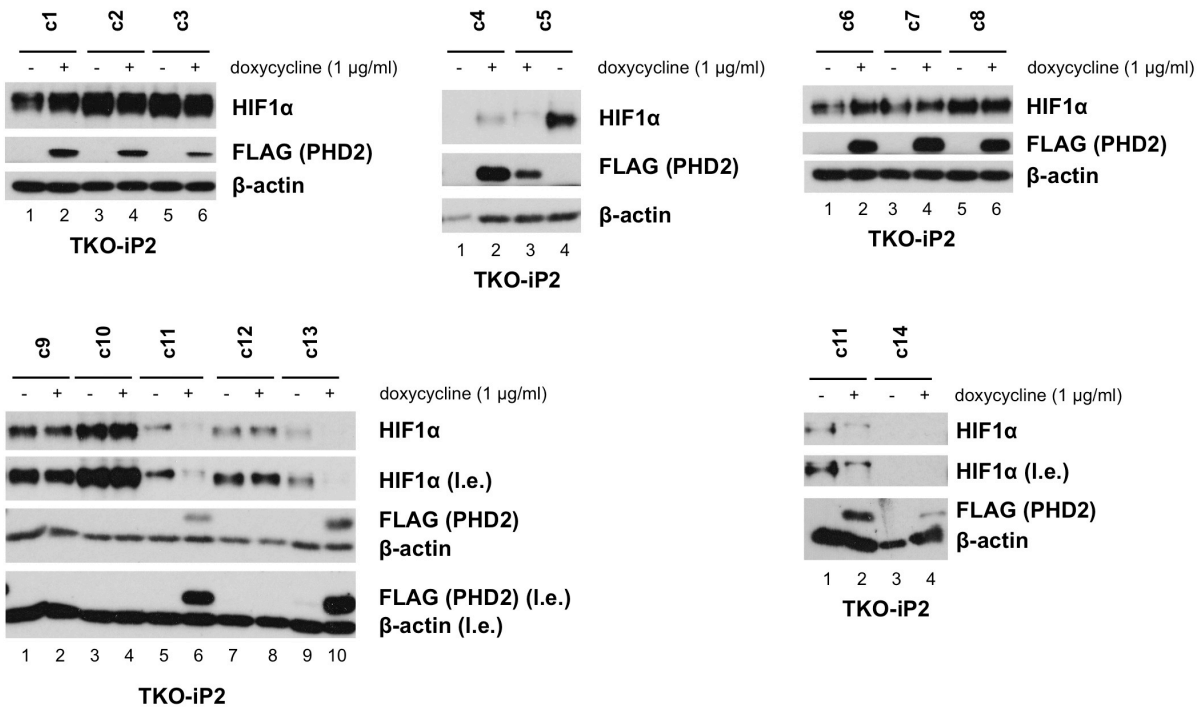

Figure 5.8 Immunoblots showing the screening of PHD2 clones cultured in the presence or absence of doxycycline (1 μg/ml) for at least 48 h. Work carried out with Dr. Y-M. Tian. l.e.: long exposure.

Similarly for the TKO-iP2 cells, a total of 14 clones were screened by immunoblotting for the changes in HIF1α and FLAG-tagged protein levels in the presence and absence of doxycycline. As shown in **Figure 5.8**, doxycycline-inducible FLAG-tagged protein was detected in the majority of the clones tested (12 out of 14), but clear downregulation of HIF1α levels in the presence of doxycycline were detected only in clones 5, 11 and 13. For cells transfected or transduced with the PHD3 vector (TKO-iP3), 11 clones were screened by immunoblotting (**Figure 5.9**). Doxycycline-mediated HIF1α downregulation was detected in the majority of the clones (clones 1, 3 – 11), although FLAG-tagged protein was only detected in a small proportion of the clones. Nevertheless, the levels of PHD2 and PHD3 in the TKO-iP2 and TKO-iP3 clones were also tested by immunoblotting using PHD2 and PHD3 antibodies, alongside endogenous control lysates from normoxic- or hypoxic-treated Kelly cells (**Figure 5.10**). The results reveal that the levels of PHD2 in the TKO-iP2 clones (with the exception of TKO-iP2-c4) were higher but comparable to the endogenous levels in

Kelly cells under normoxia (**Figure 5.10 A**). The levels of PHD3 in the TKO-iP3 clones were also within the same order of magnitude as the endogenous levels in Kelly cells under hypoxia (**Figure 5.10 B-C**) (PHD3 was not detected under normoxia in Kelly cells). Based on this comparison, the TKO-iP2-c5, TKO-iP2-c13 and TKO-iP3-c11 cells were subcloned before further experiments to ensure that each clone was pure and originated from a single clone.

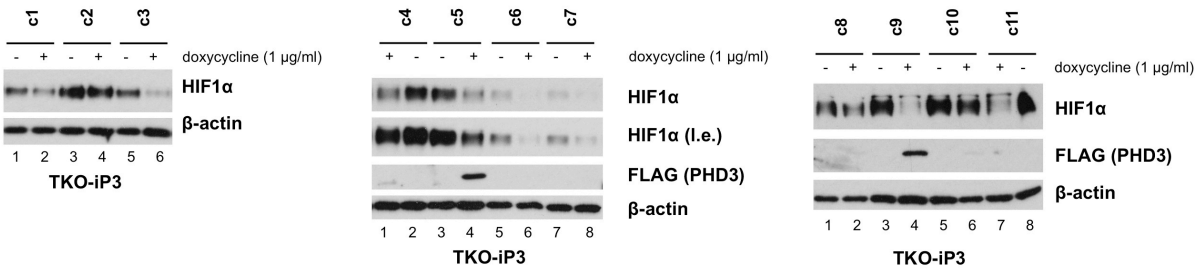

Figure 5.9 Immunoblots showing the screening of PHD3 clones cultured in the presence or absence of doxycycline (1 µg/ml) for at least 48 h. Work carried out with Dr. Y-M. Tian.

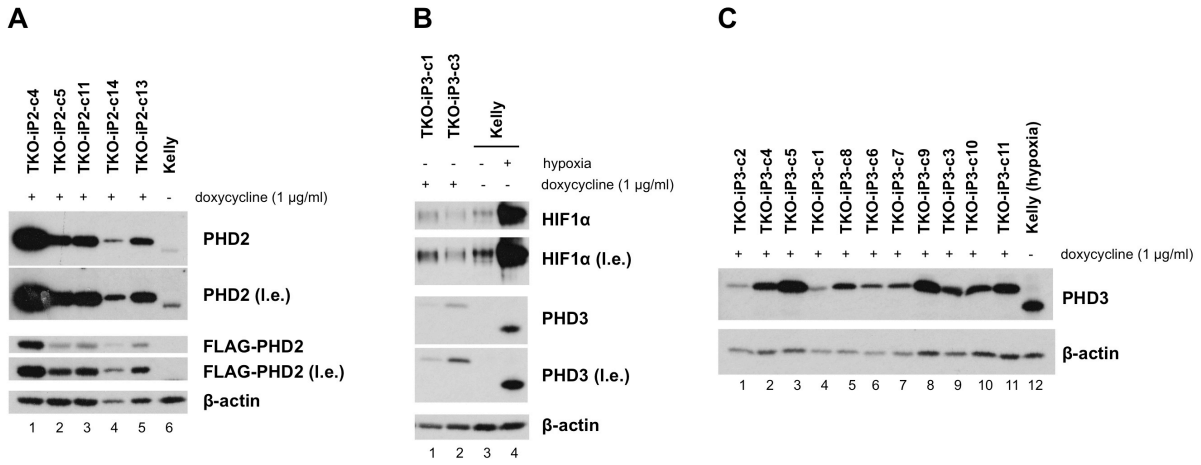

Figure 5.10 PHD levels in selected PHD2 and PHD3 clones cultured in the presence of doxycycline (1 µg/ml) for at least 48 h compared with endogenous PHD2 in Kelly cells by immunoblotting. Work carried out with Dr. Y-M. Tian. l.e.: long exposure, Hx: hypoxia (0.1% O_2, 14 h).

To tune the PHD production to a level closer to the endogenously observed levels in Kelly cells, the selected TKO-iP1, TKO-iP2 and TKO-iP3 cells were treated with various doses of

doxycycline before being analysed for HIF1α and FLAG-tagged protein levels by immunoblotting (work carried out by Dr. Y-M. Tian and Dr. T-L. Yeh). All the TKO-iP1, TKO-iP2 and TKO-iP3 clones were shown to be responsive to doxycycline in a dose-dependent manner, as shown by the decreasing HIF1α levels and the increasing FLAG-tagged protein levels when higher amounts of doxycycline were added (**Figure 5.11**). Following this work, the appropriate doses of doxycycline were used for each clone in an attempt to mimic the endogenous levels in Kelly cells before being tested by immunoblotting. The levels of FLAG-tagged protein in the TKO-iP1-c11 cells treated with 50 ng/ml of doxycycline was comparable to that of the TKO-iP2-c13 cells treated with 35 ng/ml of doxycycline (**Figure 5.12 A**). Under this concentration of doxycycline, the TKO-iP2-c13 cells were shown to be roughly equal to that in Kelly cells under the treatment of hypoxia (**Figure 5.12 B**). As for the TKO-iP3-c11a cells (a subclone of the TKO-iP3-c11 cells), the levels of PHD3 in the presence of 250 ng/ml of doxycycline were roughly equal to those in hypoxic-treated Kelly cells (**Figure 5.12 C**). Overall, these results show that endogenous levels of PHD isoforms can be selectively achieved in the PHD-null TKO cells using the Tet-inducible expression system.

Before proceeding to test the effect of PHD inhibitors in these cells, the induction of PHD isoforms at various durations of doxycycline treatment was investigated. The immunoblotting results demonstrate that 17 h of doxycycline treatment was sufficient to induce the FLAG-tagged protein levels in a dose-dependent manner, and the protein production was sustained up to 41 h of doxycycline treatment in the TKO-iP1-c11, TKO-iP2-13 and TKO-iP3-c11a cells (**Figure 5.13 A-C**, work carried out by Dr. Y-M. Tian and Dr. T-L. Yeh). To investigate whether the cells remained responsive to doxycycline after multiple passages, HIF1α levels in these cells were analysed using the MSD HIF1α assay under varying doses of doxycycline

(17 h treatment) after approximately one month in culture (work done in collaboration with Dr. T-L. Yeh). The results shown in **Figure 5.13 D** indicate that while both the TKO-iP2-13 and TKO-iP3-11a cells remained responsive to doxycycline as previously observed, the TKO-iP1-c11 cells had lost their sensitivity to doxycycline.

Nonetheless, the effects of PHD inhibitors (BNS, BIQ and IOX2) and DMOG were tested in the TKO-iP2-c13 and TKO-iP3-c11a cells by immunoblotting (this work was carried out by Dr. Y-M. Tian and Dr. T-L. Yeh). BNS was found to efficiently induce HIF1α in the TKO-iP2-c13 cells (**Figure 5.14,** *lane 4*) but was less effective doing so in the TKO-iP3-c11a cells (**Figure 5.14,** *lane 11*), suggesting some selectivity of BNS for PHD2 over PHD3. On the other hand, IOX2 and BIQ induced HIF1α to similar levels in both the TKO-iP2-c13 and TKO-iP3-c11a cells, indicating that they inhibit both PHD2 and PHD3 with similar efficiency (**Figure 5.14**). These results are in agreement with the results obtained with the constitutive overexpression of PHD isoforms in the TKO cells, with BNS preferring PHD2 over PHD1 and PHD3, while BIQ preferring PHD2 and PHD3 over PHD1 (as shown previously on **Figures 5.2** and **5.5**).

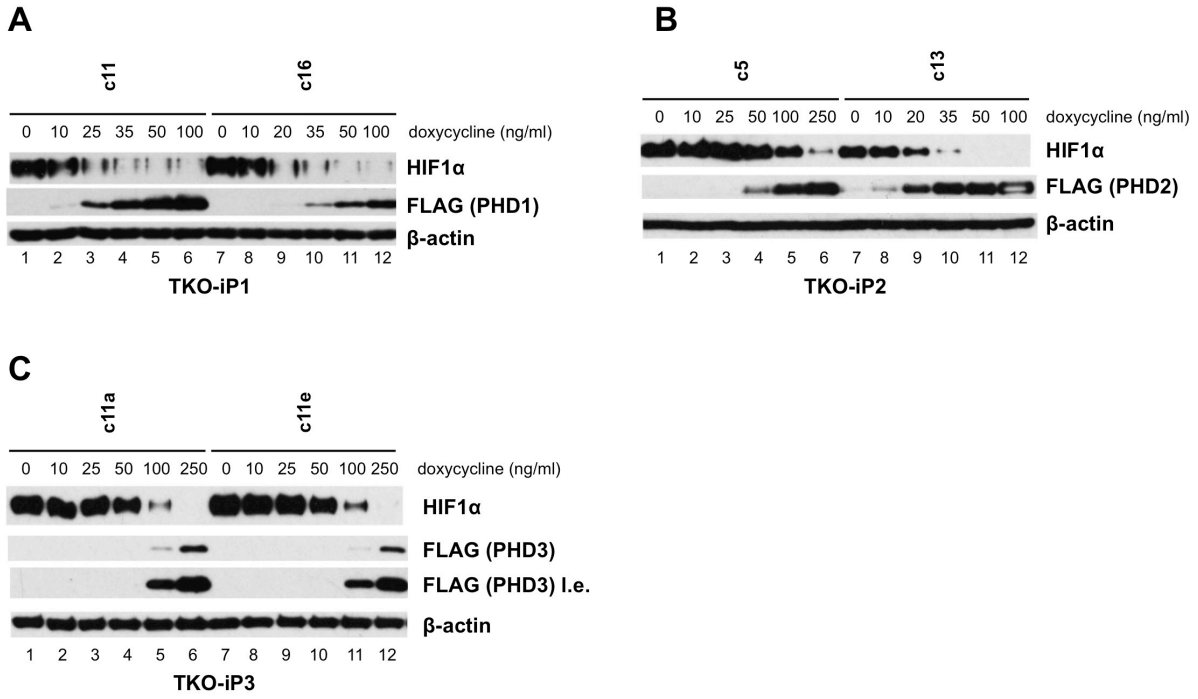

Figure 5.11 Immunoblots showing the changes to HIF1α and FLAG-tagged protein levels after 17 h treatment of doxycycline at the indicated concentrations in the (**A**) TKO-iP1 clones, (**B**) TKO-iP2 clones and (**C**) TKO-iP3 clones. Immunoblot obtained from Dr. Y-M. Tian and Dr. T-L. Yeh. l.e.: long exposure.

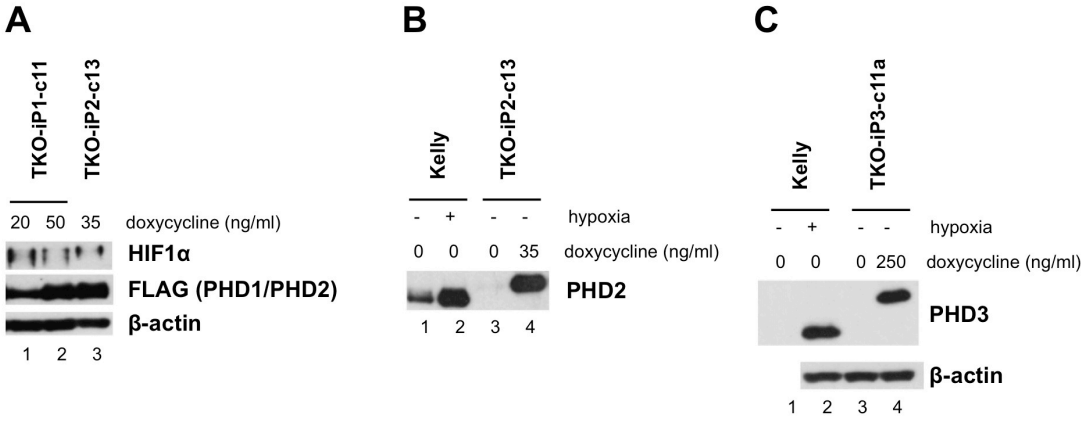

Figure 5.12 Detection of PHD levels by immunoblotting on selected PHD1, PHD2 and PHD3 clones cultured in the presence of doxycycline at the indicated concentrations. (**A**) Comparison of PHD levels in the TKO-iP1-c11 cells with the TKO-iP2-c13 cells by immunoblotting based on FLAG-tagged protein levels. (**B**) Comparison of PHD2 levels in the TKO-iP2-c13 cells (normoxia) and Kelly cells (normoxia and hypoxia). (**C**) Comparison of PHD3 levels in the TKO-iP3-c11a cells (normoxia) and Kelly cells (normoxia and hypoxia). Immunoblots obtained from Dr. Y-M. Tian, Hx: hypoxia (0.1% O_2, 14 h).

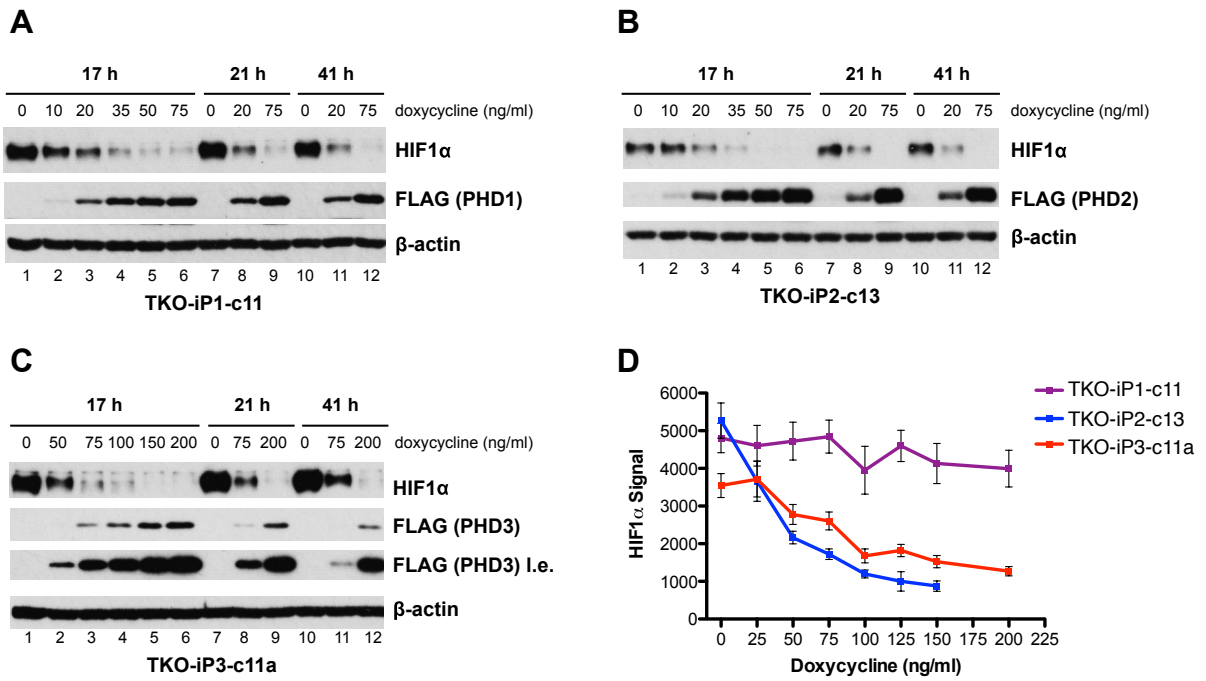

Figure 5.13 The levels of PHD isoforms 17 h, 21 h or 41 h after doxycycline treatment at the indicated concentrations as determined by immunoblotting for the (**A**) TKO-iP1-c11, (**B**) TKO-iP2-c13 and (**C**) TKO-iP3-c11a cells. Immunoblots obtained from Dr. Y-M. Tian and Dr. T-L. Yeh. (**D**) HIF1α levels in each clone as detected using the HIF1α MSD assay at various concentrations of doxycycline 17 h after doxycycline treatment. Each datapoint represents the mean signal ± standard deviation, n=4. MSD assays were carried out with Dr. T-L. Yeh. l.e.: long exposure.

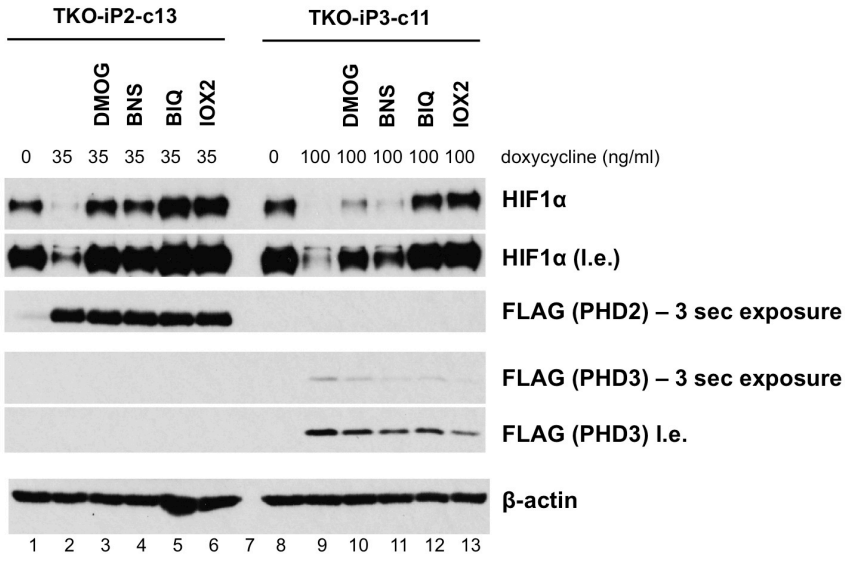

Figure 5.14 The effect of DMOG (1 mM), and PHD inhibitors BNS, BIQ and IOX2 (all 0.5 mM) on HIF1α levels in the TKO-iP2-c13 and TKO-iP3-c11a cells, as detected by immunoblotting. 13 h after treatment with doxycycline at the indicated concentrations, cells were treated with the inhibitors for 4 h. Immunoblots were obtained from Dr. Y-M. Tian. sec: seconds, l.e.: long exposure.

5.3 Discussion and future work

In this Chapter, the development of a cellular model system for studying the selective inhibition of PHD isoforms is described. Initial work on the constitutive overexpression of each PHD isoform in the PHD-null TKO cells indicated that this system may be useful, although the levels of PHD isoforms were unphysiologically high. This work paved the way to developing a similar cellular model with inducible expression of each PHD isoform. Clones of the PHD-null TKO cells expressing either human PHD1, PHD2 or PHD3 under the control of doxycycline have been successfully screened and obtained.

There were, however, several problems associated with the cellular model system. Firstly, although clones of the TKO cells with inducible expression of PHD1 were successfully obtained, the selected clone used in subsequent experiments showed that its sensitivity to doxycycline can diminish over multiple cell passages. The reason for this is unclear – it could be that the expression of the gene was silenced by subsequent epigenetic modification(s), or that the expression vector was integrated into the genome at a site that is not constitutively active for transcription. Another possible explanation is that the clone is impure or has been contaminated with another clone with less sensitivity to doxycycline. Further experiments should be conducted to examine this and investigation of whether other clones (including the clones re-expressing PHD2 and PHD3) display similar characteristic should also be carried out.

During the course of the development, it was also noted that different amounts of PHD2 and PHD3 were apparently required to downregulate HIF1α (**Figure 5.14**). The results based on FLAG-tagged protein detection suggest that a lesser amount of PHD3 (compared to PHD2) is sufficient to downregulate HIF1α stabilised in the PHD-null TKO cells. This is inconsistent

with previous observations, whereby the HIF1α hydroxylation activity of PHD2 is equal if not higher than that of PHD3 [15, 16]. However, previous studies were conducted on HIF1α peptides (but not on endogenous full length HIF1α protein) and were performed either using isolated proteins or cellular extracts. If true, the observation in the PHD-null cells suggests that the biologically relevant catalytic activity of PHD3 may be higher than that of PHD2. One possible reason is the presence of a MYND-type zinc finger domain in PHD2 not found in PHD3, which has been shown to inhibit the catalytic activity of PHD2 [17]. This may be of significance in the biological roles of PHD3, given that it is frequently expressed at low or undetectable levels during normoxia in various cell lines but is significantly induced upon hypoxia [2]. These results, however, should be interpreted with caution because the detection of the FLAG-tag epitope by the antibody used in the immunoblotting experiment may be differentially affected by the tagged protein. Another caveat is that the sub-cellular localisation of the artificially expressed human PHD isoforms in a mouse cell line may not be the same as the endogenous enzymes. Given that the changes in HIF1α levels is a readout for any indication of PHD isoform selectivity in this cellular system, the differential amount of PHD isoforms required to downregulate HIF1α became a problem by rendering the system less sensitive. For example, a compound with a 30-fold selectivity for PHD1 over PHD2 may appear to be non-selective in a cellular system wherein PHD1 is expressed a 30-fold more than PHD2. Therefore, the relative levels of PHD1, PHD2 and PHD3 in this cellular system have to be determined to avoid misinterpretation of selectivity results.

The apparent selectivity of PHD inhibitors observed in this study should also be investigated further. Additional experiments on each of the clones at various doses of the inhibitor and doxycycline have been carried out using the HIF1α MSD assay, although the results were inconclusive due to errors, in part resulting from manual operations (data not shown, work

carried out with Dr. Y-M. Tian and Dr. T-L. Yeh). Further optimisation should be conducted to minimise the error and the inhibitory potencies of each inhibitor in the PHD isoform-specific expressing cells should then be determined to allow a better understanding of their degree of selectivity for each of the PHD isoforms.

It was also observed that in some cases, the were indication of some degree of promoter leakiness (i.e. uninduced engineered cells shown to also express very small amount of PHD, for example in **Figure 5.14**, see *lane 1*). This could be due to the use of normal serum in the cell culture medium, which may contain trace amount of tetracycline. This problem could be rectified by using serum that has been tested and certified to be tetracycline-free, or by testing batches of serum for the presence of tetracycline before use.

In addition to studies on small molecule inhibitors, this cellular system could also be used to study the individual properties of each PHD isoform. The investigation on the ability of individual PHD isoforms to hydroxylate HIF1α CODD and NODD provides further support for their differential substrate preference observed in studies using isolated proteins [12, 13]. It would be of interest to investigate the differential sensitivity of each PHD isoform in these cells under variable oxygen concentrations or oxidative stress.

Overall, the cellular system developed as described in this Chapter has the potential to aid in the identification of PHD isoform-specific inhibitors, as an alternative to *in vitro* assays using HIF peptides and purified PHD proteins. This system could also be a useful tool in the investigation of the properties and roles of each of the PHD isoforms.

5.4 Materials and methods

The following were as described in previous Chapters:

- *Buffers and reagents* **(Chapter 3)**
- *Cell lysate preparation - as for immunoblotting* (**Chapter 3**)
- *Cell lysate preparation - as for MSD assay* (**Chapter 3**)
- *Immunoblotting* **(Chapter 3)**
- *Standard HIF1α MSD assay* **(Chapter 3)**
- *Hypoxia experiments* **(Chapter 4)**

Cell culture and doxycycline treatment

Mouse TKO cell line and clones derived from this cell line were cultured in DMEM (D6546-500ML; Sigma Aldrich, St. Louis, USA). Kelly cells were cultured in RPMI-1640 (R0883-500ML; Sigma Aldrich, St. Louis, USA). All cell culture media was supplemented with 10% fetal bovine serum (F7524-500ML; Sigma Aldrich, St. Louis, USA), 2 mM L-glutamine (G7513-100ML; Sigma Aldrich, St. Louis, USA), 50 units/ml of penicillin, and 50 µg/ml of streptomycin (P0781-100ML; Sigma Aldrich, St. Louis, USA). Kelly cell line was cultured by Dr. Y-M. Tian. For doxycycline treatment, cells were seeded at least 5 h prior to treated with doxycycline (D9891, Sigma Aldrich, St. Louis, USA) at the indicated concentrations and durations, followed by cell harvesting for immunoblotting or MSD assay (harvesting and lysate processing as described in **Chapter 3**).

Inhibitors

IOX2 was synthesised by Dr. J.I. Candela-Lena. IOX4 was synthesised by V.G. Pérez. BIQ and BIQ-B were synthesised by Dr. K. K. Yeoh. BNS was synthesised by Dr. C. Lejeune.

Antibodies for immunoblotting

Rabbit polyclonal antibody HIF1α NB100-479 at 1:2500 dilution (Novus Biologicals, Littleton, USA), mouse monoclonal PHD2 antibody clone-76a at 1:5 dilution [2], mouse monoclonal PHD3 antibody clone-188e at 1:10 dilution [2], mouse monoclonal anti-FLAG HRP antibody clone M2 at at 1:5000 dilution (A8592-.2MG; Sigma Aldrich, St. Louis, USA). Secondary antibodies for immunoblotting were as described in **Chapter 3**.

Cloning, viral transduction and transfection

All cloning, transfection and viral transduction work using either the pRRL viral vector (for constitutive expression of PHD isoforms) or the pTRIPz vector (for inducible expression of PHD isoforms) was carried out by Dr. Y-M. Tian.

5.5 References

1 Berra, E., Benizri, E., Ginouves, A., Volmat, V., Roux, D. and Pouyssegur, J. (2003) HIF prolyl-hydroxylase 2 is the key oxygen sensor setting low steady-state levels of HIF-1alpha in normoxia. EMBO J. **22**, 4082-4090

2 Appelhoff, R. J., Tian, Y. M., Raval, R. R., Turley, H., Harris, A. L., Pugh, C. W., Ratcliffe, P. J. and Gleadle, J. M. (2004) Differential function of the prolyl hydroxylases PHD1, PHD2, and PHD3 in the regulation of hypoxia-inducible factor. J Biol Chem. **279**, 38458-38465

3 Loenarz, C., Coleman, M. L., Boleininger, A., Schierwater, B., Holland, P. W., Ratcliffe, P. J. and Schofield, C. J. (2011) The hypoxia-inducible transcription factor pathway regulates oxygen sensing in the simplest animal, Trichoplax adhaerens. EMBO Rep. **12**, 63-70

4 Fedulova, N., Hanrieder, J., Bergquist, J. and Emren, L. O. (2007) Expression and purification of catalytically active human PHD3 in Escherichia coli. Protein Expr Purif. **54**, 1-10

5 Li, X. Y., Takasaki, C., Satoh, Y., Kimura, S., Yasumoto, K. and Sogawa, K. (2008) Expression, purification and characterization of human PHD1 in Escherichia coli. J Biochem. **144**, 555-561

6 Murray, J. K., Balan, C., Allgeier, A. M., Kasparian, A., Viswanadhan, V., Wilde, C., Allen, J. R., Yoder, S. C., Biddlecome, G., Hungate, R. W. and Miranda, L. P. (2010) Dipeptidyl-quinolone derivatives inhibit hypoxia inducible factor-1alpha prolyl hydroxylases-1, -2, and -3 with altered selectivity. J Comb Chem. **12**, 676-686

7 Koivunen, P., Hirsila, M., Kivirikko, K. I. and Myllyharju, J. (2006) The length of peptide substrates has a marked effect on hydroxylation by the hypoxia-inducible factor prolyl 4-hydroxylases. J Biol Chem. **281**, 28712-28720

8 Adam, J., Hatipoglu, E., O'Flaherty, L., Ternette, N., Sahgal, N., Lockstone, H., Baban, D., Nye, E., Stamp, G. W., Wolhuter, K., Stevens, M., Fischer, R., Carmeliet, P., Maxwell, P. H., Pugh, C. W., Frizzell, N., Soga, T., Kessler, B. M., El-Bahrawy, M., Ratcliffe, P. J. and Pollard, P. J. (2011) Renal cyst formation in Fh1-deficient mice is independent of the Hif/Phd pathway: roles for fumarate in KEAP1 succination and Nrf2 signaling. Cancer Cell. **20**, 524-537

9 Koivunen, P., Tiainen, P., Hyvarinen, J., Williams, K. E., Sormunen, R., Klaus, S. J., Kivirikko, K. I. and Myllyharju, J. (2007) An endoplasmic reticulum transmembrane prolyl 4-hydroxylase is induced by hypoxia and acts on hypoxia-inducible factor alpha. J Biol Chem. **282**, 30544-30552

10 Koh, M. Y., Darnay, B. G. and Powis, G. (2008) Hypoxia-associated factor, a novel E3-ubiquitin ligase, binds and ubiquitinates hypoxia-inducible factor 1alpha, leading to its oxygen-independent degradation. Mol Cell Biol. **28**, 7081-7095

11 Kong, X., Alvarez-Castelao, B., Lin, Z., Castano, J. G. and Caro, J. (2007) Constitutive/hypoxic degradation of HIF-alpha proteins by the proteasome is independent of von Hippel Lindau

protein ubiquitylation and the transactivation activity of the protein. J Biol Chem. **282**, 15498-15505

12 Chan, D. A., Sutphin, P. D., Yen, S. E. and Giaccia, A. J. (2005) Coordinate regulation of the oxygen-dependent degradation domains of hypoxia-inducible factor 1 alpha. Mol Cell Biol. **25**, 6415-6426

13 Hirsila, M., Koivunen, P., Gunzler, V., Kivirikko, K. I. and Myllyharju, J. (2003) Characterization of the human prolyl 4-hydroxylases that modify the hypoxia-inducible factor. J Biol Chem. **278**, 30772-30780

14 Masson, N., Willam, C., Maxwell, P. H., Pugh, C. W. and Ratcliffe, P. J. (2001) Independent function of two destruction domains in hypoxia-inducible factor-alpha chains activated by prolyl hydroxylation. EMBO J. **20**, 5197-5206

15 Huang, J., Zhao, Q., Mooney, S. M. and Lee, F. S. (2002) Sequence determinants in hypoxia-inducible factor-1alpha for hydroxylation by the prolyl hydroxylases PHD1, PHD2, and PHD3. J Biol Chem. **277**, 39792-39800

16 Tuckerman, J. R., Zhao, Y., Hewitson, K. S., Tian, Y. M., Pugh, C. W., Ratcliffe, P. J. and Mole, D. R. (2004) Determination and comparison of specific activity of the HIF-prolyl hydroxylases. FEBS Lett. **576**, 145-150

17 Choi, K. O., Lee, T., Lee, N., Kim, J. H., Yang, E. G., Yoon, J. M., Lee, T. G. and Park, H. (2005) Inhibition of the catalytic activity of hypoxia-inducible factor-1alpha-prolyl-hydroxylase 2 by a MYND-type zinc finger. Mol Pharmacol. **68**, 1803-1809

Chapter 6: Studies on the transcriptional response to hypoxia

6.1 Introduction

One of the ways cells adapt to changes in oxygen concentration is by altering the expression of hundreds of genes. The hypoxia inducible factor HIF is a key mediator in this process by regulating the transcriptional activation of an array of target genes in response to limiting oxygen concentrations [1]. HIF activation is directly linked to oxygen concentrations via the stabilisation and transactivation of the HIFα proteins in response to changes in oxygen levels [1]. As described in **Chapter 1**, the stabilisation and transcriptional activity of HIFα are regulated by the hydroxylation catalysed by the PHDs and FIH, respectively [2-5]. Whilst active in the presence of oxygen, these HIF hydroxylases lose activity in hypoxia. The selective inhibition of PHDs by small molecules is also being pursued as a potential treatment for ischaemic diseases [6, 7].

To date, however, there has been no genome wide transcriptome profiling studies carried out to investigate the extent to which PHD and/or FIH inhibition by small molecules mimics that of hypoxia. A previous microarray transcriptome profiling study using DMOG (the cell-permeable ester derivative of NOG, a pan-inhibitor of the 2OG-dependent dioxygenases), revealed a high degree of overlap between DMOG- and hypoxia upregulated genes in human breast adenocarcinoma MCF-7 cells [8]. The extent to which the effects of DMOG are mediated specifically by PHD and/or FIH inhibition is, however, unknown. This is of interest given that NOG has been shown to inhibit other members of the human 2OG-dependent dioxygenase family *in vitro* [9].

In a microarray based transcriptome profiling studies, fluorescence-labelled complementary DNA (cDNA) is typically generated from total RNA (prepared from cell lysates) and hybridised to an array containing pre-designed exon probes for the detection of transcript expression [10]. One or more probe(s) in the array can be designed to correspond to each of the known gene/transcript in the human genome, thereby allowing the pan-genomic determination of gene expression levels based on the fluorescence intensity generated for each probe. Apart from microarray based technology, transcriptome profiling studies can also be performed using RNA sequencing (RNA-seq) [10]. In this method, generally a library of cDNA fragments with attached adaptors to either one or both ends, is prepared from total RNA (or mRNA fraction). The library of cDNA fragments generated is then subjected to high-throughput sequencing, allowing the generation of reads which can then be aligned to a reference genome or transcript and can be quantified.

Given that the HIF hydroxylases require oxygen for their catalytic activity, such that oxygen levels are directly linked to the regulation of HIF stability/transactivation, it is tempting to speculate that the inhibition of PHDs and FIH is sufficient to promote the transcriptional response to hypoxia. The work described in this Chapter was therefore aimed at testing this hypothesis and expanding the understanding of the PHD- and FIH- mediated transcriptional response to hypoxia. RNA-seq was employed to profile the expression of genes in MCF-7 cells that are responsive to hypoxia in comparison with those induced by PHD inhibitors (including IOX2, one of the chemical probes developed for the PHDs as described in **Chapter 4**). The studies using MCF-7 cells reveal that subsets of hypoxia regulated genes are differentially regulated by each of the small molecule inhibitors, with the generic 2OG-dependent dioxygenase inhibitor DMOG being a better mimic of hypoxia than the more

selective PHD inhibitors. Further investigations using microarray experiments demonstrate the extent of FIH-mediated transcriptional response to hypoxia in MCF-7 cells. Based on the RNA-seq and microarray analyses, the identification of a subset of hypoxia responsive genes that are not regulated by the PHDs or FIH led to an important question of whether there is an additional "oxygen sensing" factor required to mediate the hypoxic response, which may act either independently or together with the PHDs and FIH.

6.2 DMOG is a better mimic of hypoxia than PHD inhibitors in gene expression studies on MCF-7 cells by RNA-seq

Note: The work in this Chapter was done in collaboration with Dr N. Ilott (Ponting laboratory, Department of Physiology, Anatomy and Genetics, University of Oxford), Dr J. Schödel and Dr D. Mole (Ratcliffe/Pugh laboratory, Centre for Cellular and Molecular Physiology, University of Oxford).

To investigate whether the selective inhibition of PHDs by small molecule inhibitors can invoke a similar transcriptional response to that of hypoxia (or DMOG), RNA-seq analyses were carried out on human breast cancer MCF-7 cells treated under normoxia, hypoxia (0.5% O_2), or inhibitor (either 1 mM DMOG, 250 μM IOX2, 250 μM BNS or 500 μM BIQ) for 16 h . Total RNA samples used for the RNA-seq analyses were prepared from the treated cells in biological duplicate for each condition (work carried out by Dr J. Schödel). Processing of raw sequencing data and preliminary analyses were carried out by Dr. N. Ilott. The expression levels for each protein coding genes determined from the RNA-seq analysis were expressed as fragments per kilobase of transcript per million mapped reads (FPKM). To filter out lowly expressed genes for subsequent analyses, only genes with FPKM > 2 in any of the tested conditions were considered (n=13,266). Consistent with the previous study [8], the results

reveal broad concordance in the transcriptional response to DMOG compared to that of hypoxia (**Figure 6.1**). Based on pan-genomic analysis, there are four clusters of genes that appeared to be differentially regulated genes by hypoxia, DMOG and the PHD inhibitors (IOX2, BNS and BIQ), as indicated by the expression heatmap (**Figure 6.1 A**). Cluster 1 represents genes that are upregulated by hypoxia but to a lesser degree by DMOG/PHD inhibitors; Cluster 2 represents genes that are upregulated by hypoxia and DMOG/PHD inhibitors to a similar extent; Cluster 3 represents genes that are downregulated by hypoxia, DMOG and PHD inhibitors; and Cluster 4 represents genes that are upregulated by hypoxia and DMOG but to a lesser degree by the PHD inhibitors. A total of 565 genes were significantly upregulated by hypoxia (fold change > 2, adjusted p-value < 0.05), in comparison to 418 genes upregulated by DMOG (**Figure 6.1 B**). There were fewer genes that were upregulated by the PHD inhibitors, with 248 genes induced by IOX2, 167 genes by BNS and 257 genes by BIQ (fold change > 2, adjusted p-value < 0.05). The 100 most upregulated genes in hypoxia (ranked according to fold change against normoxia) are listed in **Table 1** (all hypoxic upregulated genes listed in ***Appendix 2***). Many of the hypoxia induced genes, such as carbonic anhydrase IX (*CA9*), adrenomedullin (*ADM*), N-myc downstream regulated gene 1 (*NDRG1*) and insulin-like growth factor binding protein 3 (*IGFBP3*), have been previously reported to be induced by hypoxia in MCF-7 cells [8]. The 50 genes most upregulated by hypoxia categorised under Cluster 1, 2 and 4 are also listed in **Table 1**, **Table 2** and **Table 3**, respectively. Analyses of the 565 hypoxia upregulated genes revealed that there are 166 genes categorised in Cluster 1, 193 genes in Cluster 2 and 206 genes in Cluster 4. As shown in **Figure 6.2**, a high proportion of the hypoxia upregulated genes are also upregulated by DMOG (329 genes, 58% of hypoxia upregulated genes), whereas the overlap with genes upregulated by the PHD inhibitors was lower (<40% of hypoxia upregulated genes). Of the

PHD inhibitors tested, the selective PHD inhibitor IOX2 upregulates a higher proportion of hypoxia induced genes (40%) compared to BNS (29%) or BIQ (38%).

To investigate the functional properties of genes that were upregulated in each condition, functional enrichment analyses were carried out using the Kyoto Encyclopaedia of Genes and Genomes (KEGG) pathways analysis on DAVID website [11]. These analyses were focused on upregulated genes given that genes downregulated in hypoxia are likely to be an indirect effect of HIF or is independent of HIF [12, 13]. Genes involved in glycolysis/gluconeogenesis, fructose and mannose metabolism, starch and sucrose metabolism, and the pentose phosphate pathway were found to be upregulated in all conditions (**Figure 6.3**). Hypoxia and DMOG were also found to induce genes assigned as being involved in cancer or related pathways (as shown by the enrichment of genes involved in focal adhesion, renal cell carcinoma and bladder cancer) (**Figure 6.3** and **Table 5**). Interestingly, in contrast to DMOG and hypoxia treatment, there was no enrichment for genes in the cancer related pathways by the PHD inhibitors (**Figure 6.3**). The same functional enrichment analysis was carried out for the hypoxia upregulated gene sets (genes in Cluster 1, 2 and 4). The results reveal that the genes involved in cancer pathways, renal cell carcinoma and bladder cancer are enriched in Cluster 4 but not in Cluster 2 (**Figure 6.4**). These observations suggest that, at least under the tested conditions, the DMOG- and hypoxia-specific effects (which were not mediated by the PHD inhibitors), may play a role in cancer progression.

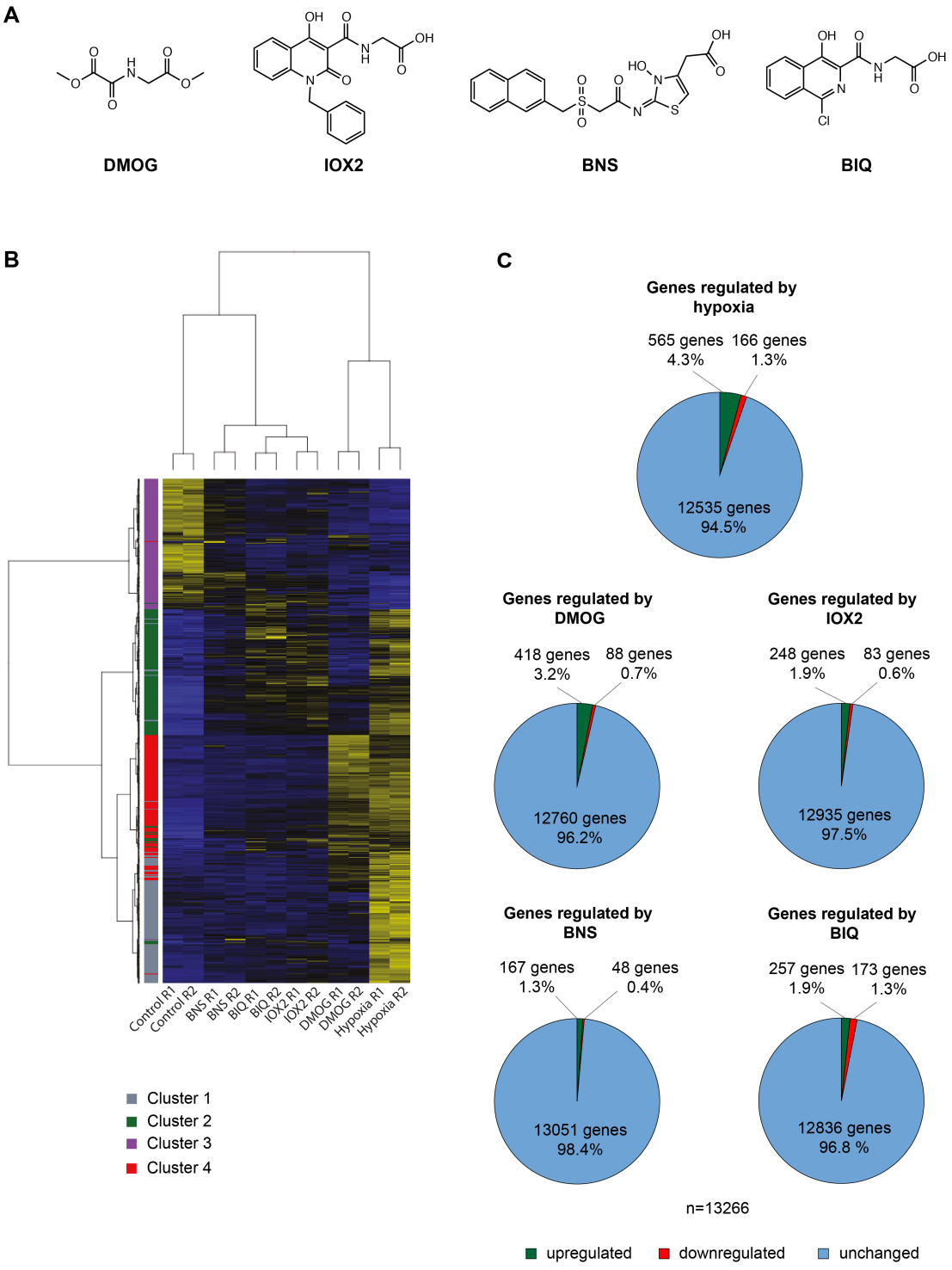

Figure 6.1 An overview of differentially regulated genes in MCF-7 cells under hypoxia (0.5% O_2), DMOG or PHD inhibitor treatment based on RNA-seq analyses. (**A**) Chemical structure of the inhibitors used (DMOG, IOX2, BNS and BIQ). (**B**) Heatmap representation of the level of gene expression for each replicate in each condition. (R1: replicate 1, R2: replicate 2). Expression levels were indicated in shades of yellow (high expression) to blue (low expression). Figure prepared by Dr N. Ilott. (**C**) The proportion of genes upregulated, downregulated or unchanged for each treatment (hypoxia, DMOG, IOX2, BNS and BIQ). n=2 per condition, fold-change > 2, adjusted p-value < 0.05, FPKM ≥ 2. FPKM: Fragments Per Kilobase of transcript per Million mapped reads.

		Fold change (adjusted p-value < 0.05)					
		Hypoxia	DMOG	IOX2	BNS	BIQ	Cluster
1	CA9	654.6	648.8	157.5	129.4	111.4	C4
2	KB-1980E6.3	110.1	20.7	39.0	28.1	26.2	C1
3	LOX	66.4	23.0	27.9	11.0	22.6	C1
4	MSLNL	52.0	10.1	5.9	5.1	5.1	C1
5	CYP1A1	50.3	4.1	3.3	3.5	5.6	C1
6	RNF183	47.4	25.3	23.0	18.7	20.1	C1
7	MAP7D2	46.9	43.8	5.6	5.0	5.1	C4
8	TMEM74B	46.2	18.7	24.0	11.8	20.9	C1
9	NDRG1	43.2	59.2	13.4	12.3	16.8	C4
10	ISM2	41.9	18.0	17.9	9.7	10.0	C1
11	CASP14	36.1	22.0	8.6	9.0	2.8	C1
12	PPFIA4	35.1	22.4	27.1	20.8	28.6	C2
13	ADM	32.6	29.4	13.1	9.3	13.0	C4
14	PPP1R3G	25.8	20.8	16.2	13.2	18.2	C2
15	PFKFB4	24.5	21.7	12.8	11.0	11.9	C4
16	SEMA5B	23.1	19.2	4.2	4.7	4.3	C4
17	SLC28A1	22.9	16.8	5.9	5.4	4.7	C4
18	FAM115C	22.4	20.0	13.3	13.2	13.9	C4
19	TLE6	20.4	9.4	9.5	5.3	6.6	C1
20	ALDOC	17.5	12.4	12.2	8.5	11.4	C2
21	SLC2A14	16.9	6.1	2.2	1.4	0.7	C1
22	PDK1	15.9	10.8	9.4	8.2	9.5	C2
23	RCN3	15.2	5.3	8.3	6.2	6.7	C1
24	LRP1	14.6	9.8	4.5	2.6	3.7	C1
25	IGFBP3	14.6	12.6	4.1	2.8	4.8	C4
26	C4orf47	14.2	5.0	14.3	8.5	13.5	C2
27	PGM1	14.0	12.8	12.3	10.7	11.3	C2
28	UPK1A	13.6	3.7	3.0	2.2	2.5	C1
29	AP000769.1	13.4	8.2	5.1	6.5	4.1	C1
30	SH3GL3	13.3	9.7	5.4	4.1	5.8	C4
31	AK4	13.1	11.3	10.4	10.2	10.6	C2
32	SCNN1B	13.1	9.9	3.0	2.2	1.7	C4
33	TMEM45A	13.1	12.3	6.3	5.0	6.4	C4
34	C2orf72	12.7	7.3	10.3	7.5	10.0	C2
35	BNIP3	12.7	11.0	9.2	8.7	9.3	C2
36	EMR2	12.2	4.4	2.3	2.3	1.6	C1
37	ANGPTL4	12.1	13.5	5.7	3.2	5.3	C4
38	SYDE1	11.9	6.9	5.2	3.9	4.0	C1
39	RP11-480I12.4	11.7	5.0	9.9	7.8	10.2	C2
40	SPAG4	11.7	6.8	8.7	6.6	7.7	C2
41	ANKRD37	11.1	13.4	5.3	4.8	5.6	C4
42	ENO2	11.0	9.9	6.0	4.3	5.7	C4
43	AMPD3	10.3	5.2	4.8	4.8	5.4	C2
44	BNIP3L	10.3	8.9	5.7	5.1	5.8	C4
45	RNF165	10.2	4.5	6.8	4.6	5.7	C2
46	C1orf51	9.8	6.7	11.6	8.5	9.9	C2
47	INHA	9.8	12.3	2.4	1.8	2.1	C4
48	LRP4	9.8	13.6	2.3	1.8	1.9	C4
49	SFXN3	9.4	6.1	4.6	3.3	4.0	C1
50	SPRY1	9.2	8.1	8.0	6.9	9.1	C2

Table 1 List of 100 genes most upregulated by hypoxia (0.5% O_2). Genes sorted according to fold induction by hypoxia compared to normoxia. Heatmap representation of the expression levels (FPKM) and fold change against normoxia by the various conditions tested are shown as determined from the RNA-seq analyses. Expression levels are indicated in shades of red (high expression) to blue/dark indigo (low expression). List of all hypoxia upregulated genes (565 genes) is provided in *Appendix 2*.

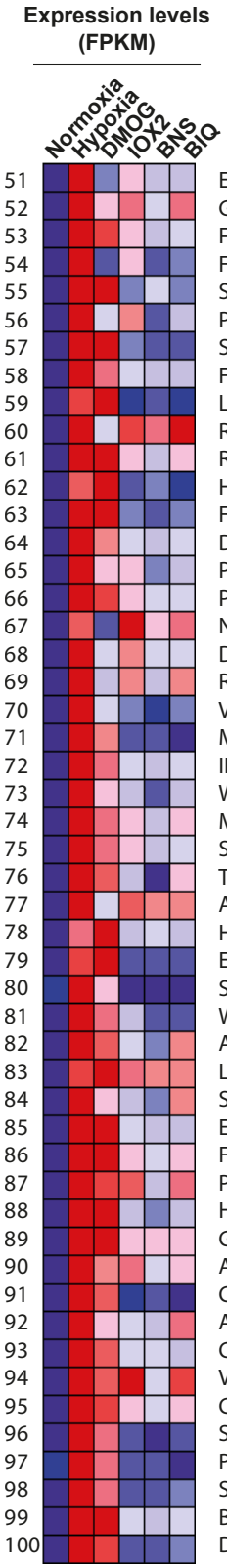

		Fold change (adjusted p-value < 0.05)					
		Hypoxia	DMOG	IOX2	BNS	BIQ	Cluster
51	EFEMP2	9.0	3.1	3.8	2.9	3.1	C1
52	GPR146	9.0	6.9	7.6	5.2	7.4	C2
53	FAM162A	8.7	8.4	5.5	4.4	5.1	C4
54	FUT3	8.6	2.4	3.2	1.9	2.4	C1
55	SERPINA9	8.6	8.4	3.1	3.6	2.7	C4
56	PLIN2	8.5	3.9	4.7	2.2	3.2	C1
57	SCNN1G	8.5	8.1	2.8	2.1	2.1	C4
58	FOS	8.5	6.5	4.3	3.4	3.5	C4
59	LOXL2	8.2	11.2	2.2	2.0	1.8	C4
60	RIMKLA	8.2	6.0	7.5	6.7	7.7	C2
61	RORA	8.0	7.6	5.0	4.0	5.2	C4
62	HEY1	7.7	10.6	2.2	2.8	1.8	C4
63	FAM13A	7.7	7.6	2.7	1.8	2.6	C4
64	DDIT4	7.6	5.4	3.5	3.3	3.4	C4
65	PDZD7	7.5	4.6	3.8	2.5	2.8	C1
66	PGK1	7.0	7.2	4.7	4.3	4.4	C4
67	NIM1	7.0	2.6	8.0	5.3	6.1	C2
68	DPYSL4	6.7	3.8	4.5	3.6	3.5	C2
69	RRAGD	6.6	3.1	4.6	3.0	4.2	C2
70	VTCN1	6.5	2.6	1.8	1.3	1.7	C1
71	MT1X	6.5	4.2	1.7	2.4	1.3	C1
72	INSIG2	6.5	5.4	3.1	2.8	3.4	C4
73	WSB1	6.4	3.6	2.5	1.9	2.3	C1
74	MXI1	6.3	5.5	4.1	3.0	4.0	C4
75	SMAD9	6.3	5.0	4.1	3.2	3.9	C4
76	THEMIS2	6.1	5.0	2.4	1.4	3.1	C4
77	ANKZF1	6.1	4.3	5.1	4.5	4.7	C2
78	HK2	6.1	8.6	3.6	3.8	3.6	C4
79	EGLN3	6.0	7.6	1.9	1.7	1.7	C4
80	S100A4	6.0	2.7	1.0	0.8	0.8	C1
81	WISP2	5.9	4.1	2.2	1.6	1.8	C1
82	ANG	5.9	6.0	3.7	2.8	4.6	C4
83	LDHA	5.8	6.8	5.1	5.1	4.8	C2
84	STYK1	5.7	3.6	2.7	2.2	3.8	C1
85	ERO1L	5.7	5.4	3.1	2.7	2.7	C4
86	FUT11	5.6	6.0	4.2	3.5	3.9	C4
87	PAM	5.5	5.5	4.8	3.5	4.6	C2
88	HILPDA	5.5	5.9	2.6	2.1	2.6	C4
89	GBE1	5.5	5.9	4.0	4.1	4.1	C4
90	AL137145.1	5.5	4.6	4.5	3.9	4.1	C2
91	C1orf116	5.5	4.7	1.4	1.5	1.1	C4
92	ACAP1	5.4	3.5	2.8	2.4	3.7	C2
93	C8orf58	5.3	5.0	3.1	2.9	2.8	C4
94	VLDLR	5.3	5.0	5.0	4.1	4.8	C2
95	C4orf3	5.3	5.1	3.7	3.5	3.7	C4
96	SLC45A1	5.2	3.9	1.5	0.9	1.5	C4
97	PADI2	5.2	3.6	1.3	1.5	0.8	C1
98	SLC2A12	5.1	3.8	1.5	1.6	1.9	C4
99	BHLHE40	5.1	5.6	3.0	2.5	2.8	C4
100	DAPK2	5.1	4.8	1.8	1.5	1.9	C4

Table 1 (continued) List of 100 genes most upregulated by hypoxia (0.5% O_2). Genes sorted according to fold induction by hypoxia compared to normoxia. Heatmap representation of the expression levels (FPKM) and fold change against normoxia by the various conditions tested are shown as determined from the RNA-seq analyses. Expression levels are indicated in shades of red (high expression) to blue/dark indigo (low expression). List of all hypoxia upregulated genes (565 genes) is provided in *Appendix 2*.

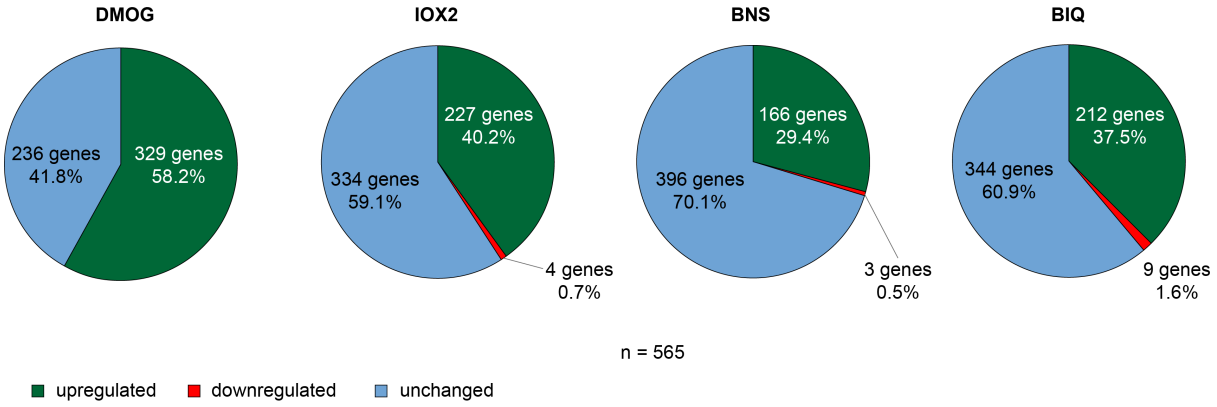

Figure 6.2 Pie charts showing the proportion of hypoxia induced genes (565 genes) that were also upregulated by either DMOG or PHD inhibitors (IOX2, BNS and BIQ) based on the RNA-seq analysis.

	Expression levels (FPKM)						Fold change (adjusted p-value < 0.05)				
	Normoxia	Hypoxia	DMOG	IOX2	BNS	BIQ	Hypoxia	DMOG	IOX2	BNS	BIQ
1							KB-1980E6.3	110.1	20.7	39.0	28.1	26.2
2							LOX	66.4	23.0	27.9	11.0	22.6
3							MSLNL	52.0	10.1	5.9	5.1	5.1
4							CYP1A1	50.3	4.1	3.3	3.5	5.6
5							RNF183	47.4	25.3	23.0	18.7	20.1
6							TMEM74B	46.2	18.7	24.0	11.8	20.9
7							ISM2	41.9	18.0	17.9	9.7	10.0
8							CASP14	36.1	22.0	8.6	9.0	2.8
9							TLE6	20.4	9.4	9.5	5.3	6.6
10							SLC2A14	16.9	6.1	2.2	1.4	0.7
11							RCN3	15.2	5.3	8.3	6.2	6.7
12							LRP1	14.6	9.8	4.5	2.6	3.7
13							UPK1A	13.6	3.7	3.0	2.2	2.5
14							AP000769.1	13.4	8.2	5.1	6.5	4.1
15							EMR2	12.2	4.4	2.3	2.3	1.6
16							SYDE1	11.9	6.9	5.2	3.9	4.0
17							SFXN3	9.4	6.1	4.6	3.3	4.0
18							EFEMP2	9.0	3.1	3.8	2.9	3.1
19							FUT3	8.6	2.4	3.2	1.9	2.4
20							PLIN2	8.5	3.9	4.7	2.2	3.2
21							PDZD7	7.5	4.6	3.8	2.5	2.8
22							VTCN1	6.5	2.6	1.8	1.3	1.7
23							MT1X	6.5	4.2	1.7	2.4	1.3
24							WSB1	6.4	3.6	2.5	1.9	2.3
25							S100A4	6.0	2.7	1.0	0.8	0.8
26							WISP2	5.9	4.1	2.2	1.6	1.8
27							STYK1	5.7	3.6	2.7	2.2	3.8
28							PADI2	5.2	3.6	1.3	1.5	0.8
29							ALOXE3	4.4	3.0	2.5	1.6	1.7
30							CYP1B1	4.4	1.2	1.5	1.5	1.4
31							KIAA1984	4.1	1.2	1.3	0.9	1.5
32							KRT15	4.1	2.6	0.9	1.3	0.9
33							LY6D	4.0	1.2	0.5	0.5	0.2
34							CKB	3.9	1.6	1.9	1.4	1.4
35							CITED2	3.9	2.8	2.0	1.7	1.9
36							EHD2	3.8	2.5	1.8	1.4	1.3
37							SYT17	3.8	1.8	2.3	1.6	1.9
38							PTAFR	3.8	2.3	1.2	0.9	0.8
39							GPR19	3.8	1.2	1.8	1.9	1.8
40							PLEKHA2	3.7	2.3	2.4	2.3	2.2
41							BIRC7	3.7	1.3	0.9	1.4	0.9
42							ARHGEF37	3.6	2.7	2.3	1.8	2.0
43							CD68	3.6	1.9	1.4	1.2	1.4
44							HSF4	3.5	2.3	2.3	1.7	2.3
45							EVPLL	3.5	1.8	1.0	0.9	1.0
46							GLRX	3.5	2.2	2.0	1.5	1.8
47							DLL1	3.4	2.2	1.6	1.5	1.8
48							PIK3IP1	3.4	2.0	1.9	2.0	2.0
49							MUC1	3.3	1.3	1.2	1.2	0.8
50							NPR3	3.3	1.2	2.2	1.3	1.6

Table 2 Cluster 1 genes. List of 50 genes most upregulated by hypoxia (0.5% O_2) categorised as Cluster 1 genes (see text for description). Heatmap representation of the expression levels (FPKM) and fold change against normoxia by the various conditions tested are shown as determined from the RNA-seq analyses. Expression levels were indicated in shades of red (high expression) to blue/dark indigo (low expression). Genes were sorted according to fold induction by hypoxia compared to normoxia.

		Fold change (adjusted p-value < 0.05)				
		Hypoxia	DMOG	IOX2	BNS	BIQ
1	PPFIA4	35.1	22.4	27.1	20.8	28.6
2	PPP1R3G	25.8	20.8	16.2	13.2	18.2
3	ALDOC	17.5	12.4	12.2	8.5	11.4
4	PDK1	15.9	10.8	9.4	8.2	9.5
5	C4orf47	14.2	5.0	14.3	8.5	13.5
6	PGM1	14.0	12.8	12.3	10.7	11.3
7	AK4	13.1	11.3	10.4	10.2	10.6
8	C2orf72	12.7	7.3	10.3	7.5	10.0
9	BNIP3	12.7	11.0	9.2	8.7	9.3
10	RP11-480I12.4	11.7	5.0	9.9	7.8	10.2
11	SPAG4	11.7	6.8	8.7	6.6	7.7
12	AMPD3	10.3	5.2	4.8	4.8	5.4
13	RNF165	10.2	4.5	6.8	4.6	5.7
14	C1orf51	9.8	6.7	11.6	8.5	9.9
15	SPRY1	9.2	8.1	8.0	6.9	9.1
16	GPR146	9.0	6.9	7.6	5.2	7.4
17	RIMKLA	8.2	6.0	7.5	6.7	7.7
18	NIM1	7.0	2.6	8.0	5.3	6.1
19	DPYSL4	6.7	3.8	4.5	3.6	3.5
20	RRAGD	6.6	3.1	4.6	3.0	4.2
21	ANKZF1	6.1	4.3	5.1	4.5	4.7
22	LDHA	5.8	6.8	5.1	5.1	4.8
23	PAM	5.5	5.5	4.8	3.5	4.6
24	AL137145.1	5.5	4.6	4.5	3.9	4.1
25	ACAP1	5.4	3.5	2.8	2.4	3.7
26	VLDLR	5.3	5.0	5.0	4.1	4.8
27	PPP1R3E	5.1	3.3	3.0	2.4	3.2
28	GYS1	5.0	3.4	4.0	3.4	3.9
29	PRELID2	5.0	3.1	3.7	3.1	3.7
30	GPR155	4.9	2.9	4.1	2.2	3.2
31	DOK3	4.9	3.2	2.4	2.9	3.0
32	DKFZP667F0711	4.8	3.1	2.8	2.4	3.6
33	RNF122	4.7	3.2	3.5	3.1	3.5
34	WDR66	4.7	3.7	3.9	3.1	3.6
35	HLA-B	4.7	2.2	3.6	3.0	3.1
36	RORC	4.6	1.1	3.0	1.7	2.8
37	FAM26F	4.5	4.2	7.5	5.6	5.7
38	RP11-268J15.5	4.4	4.1	4.4	3.4	5.5
39	PRSS53	4.4	3.6	3.5	2.9	3.4
40	CCL28	4.4	2.5	3.9	3.0	3.5
41	RNASE4	4.3	3.6	2.9	2.0	3.8
42	NOL3	4.2	2.7	2.5	2.1	2.6
43	HOXA4	4.2	2.2	3.7	2.7	3.5
44	LPIN3	4.0	2.7	2.7	2.4	2.8
45	PCP2	4.0	2.5	3.4	2.8	3.1
46	EGLN1	3.9	4.4	3.6	3.3	3.8
47	SH3D21	3.9	3.2	3.7	3.0	4.2
48	NREP	3.8	2.2	2.6	2.7	2.7
49	PTRF	3.7	2.6	3.6	2.7	3.0
50	SNTA1	3.5	2.5	3.0	2.3	2.6

Table 3 Cluster 2 genes. List of 50 genes most upregulated by hypoxia (0.5% O_2) categorised as Cluster 2 genes (see text for description). Heatmap representation of the expression levels (FPKM) and fold change against normoxia by the various conditions tested are shown as determined from the RNA-seq analyses. Expression levels were indicated in shades of red (high expression) to blue/dark indigo (low expression). Genes were sorted according to fold induction by hypoxia compared to normoxia.

		Fold change (adjusted p-value < 0.05)				
		Hypoxia	DMOG	IOX2	BNS	BIQ
1	CA9	654.6	648.8	157.5	129.4	111.4
2	MAP7D2	46.9	43.8	5.6	5.0	5.1
3	NDRG1	43.2	59.2	13.4	12.3	16.8
4	ADM	32.6	29.4	13.1	9.3	13.0
5	PFKFB4	24.5	21.7	12.8	11.0	11.9
6	SEMA5B	23.1	19.2	4.2	4.7	4.3
7	SLC28A1	22.9	16.8	5.9	5.4	4.7
8	FAM115C	22.4	20.0	13.3	13.2	13.9
9	IGFBP3	14.6	12.6	4.1	2.8	4.8
10	SH3GL3	13.3	9.7	5.4	4.1	5.8
11	SCNN1B	13.1	9.9	3.0	2.2	1.7
12	TMEM45A	13.1	12.3	6.3	5.0	6.4
13	ANGPTL4	12.1	13.5	5.7	3.2	5.3
14	ANKRD37	11.1	13.4	5.3	4.8	5.6
15	ENO2	11.0	9.9	6.0	4.3	5.7
16	BNIP3L	10.3	8.9	5.7	5.1	5.8
17	INHA	9.8	12.3	2.4	1.8	2.1
18	LRP4	9.8	13.6	2.3	1.8	1.9
19	FAM162A	8.7	8.4	5.5	4.4	5.1
20	SERPINA9	8.6	8.4	3.1	3.6	2.7
21	SCNN1G	8.5	8.1	2.8	2.1	2.1
22	FOS	8.5	6.5	4.3	3.4	3.5
23	LOXL2	8.2	11.2	2.2	2.0	1.8
24	RORA	8.0	7.6	5.0	4.0	5.2
25	HEY1	7.7	10.6	2.2	2.8	1.8
26	FAM13A	7.7	7.6	2.7	1.8	2.6
27	DDIT4	7.6	5.4	3.5	3.3	3.4
28	PGK1	7.0	7.2	4.7	4.3	4.4
29	INSIG2	6.5	5.4	3.1	2.8	3.4
30	MXI1	6.3	5.5	4.1	3.0	4.0
31	SMAD9	6.3	5.0	4.1	3.2	3.9
32	THEMIS2	6.1	5.0	2.4	1.4	3.1
33	HK2	6.1	8.6	3.6	3.8	3.6
34	EGLN3	6.0	7.6	1.9	1.7	1.7
35	ANG	5.9	6.0	3.7	2.8	4.6
36	ERO1L	5.7	5.4	3.1	2.7	2.7
37	FUT11	5.6	6.0	4.2	3.5	3.9
38	HILPDA	5.5	5.9	2.6	2.1	2.6
39	GBE1	5.5	5.9	4.0	4.1	4.1
40	C1orf116	5.5	4.7	1.4	1.5	1.1
41	C8orf58	5.3	5.0	3.1	2.9	2.8
42	C4orf3	5.3	5.1	3.7	3.5	3.7
43	SLC45A1	5.2	3.9	1.5	0.9	1.5
44	SLC2A12	5.1	3.8	1.5	1.6	1.9
45	BHLHE40	5.1	5.6	3.0	2.5	2.8
46	DAPK2	5.1	4.8	1.8	1.5	1.9
47	ZNF395	5.1	4.7	2.8	2.5	2.5
48	P4HA2	5.0	5.6	4.1	3.2	3.9
49	P4HA1	4.9	8.0	3.7	3.6	4.0
50	ERRFI1	4.8	6.5	2.1	1.4	2.0

Table 4 Cluster 4 genes. List of 50 genes most upregulated by hypoxia (0.5% O_2) categorised as Cluster 4 genes (see text for description). Heatmap representation of the expression levels (FPKM) and fold change against normoxia by the various conditions tested are shown as determined from the RNA-seq analyses. Expression levels were indicated in shades of red (high expression) to blue/dark indigo (low expression). Genes were sorted according to fold induction by hypoxia compared to normoxia.

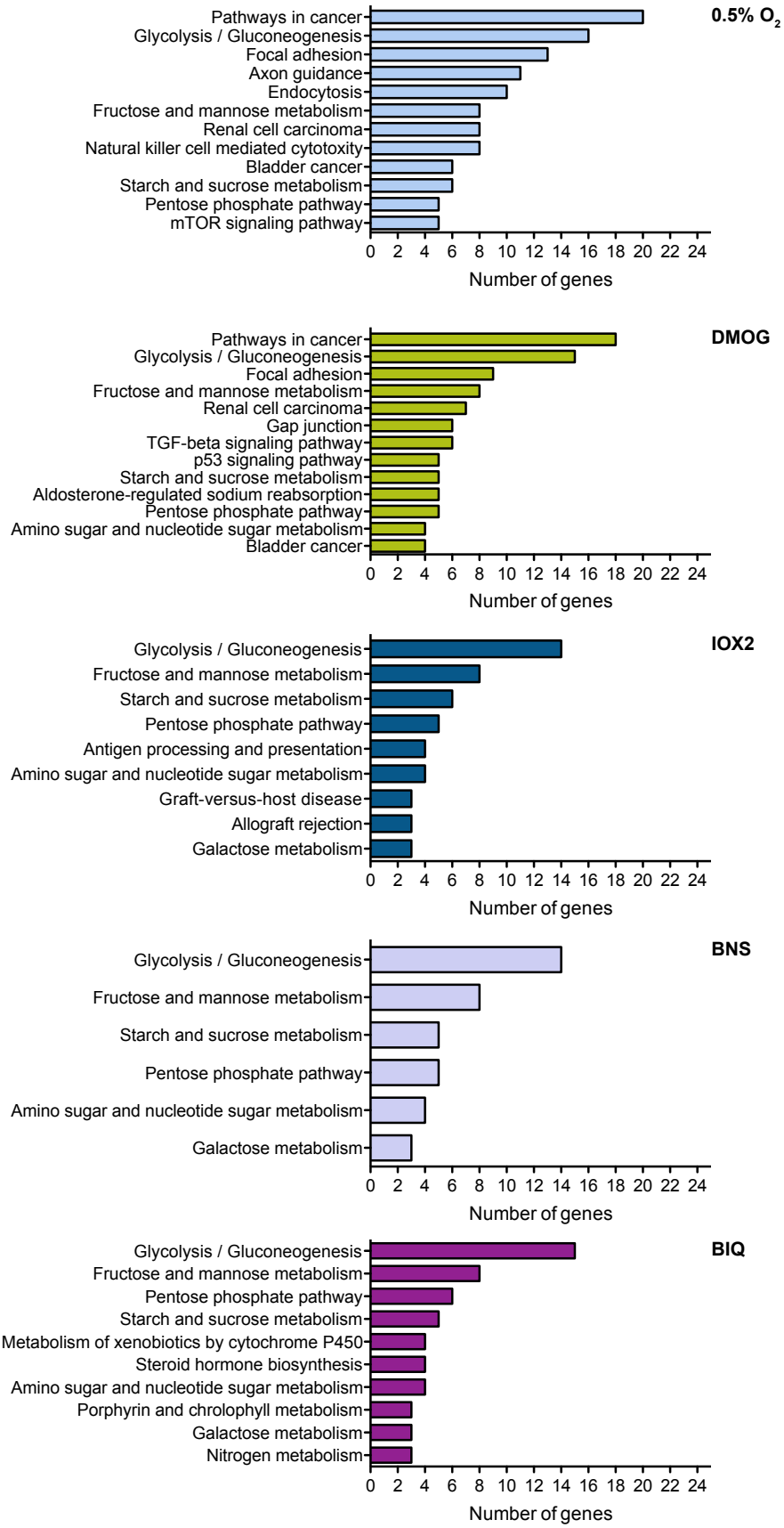

Figure 6.3 KEGG pathway functional enrichment analysis on genes upregulated by hypoxia (0.5% O_2), DMOG and PHD inhibitors (IOX2, BNS and BIQ).

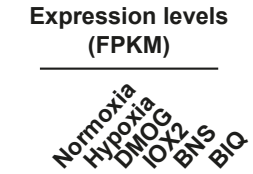

		Fold change (adjusted p-value < 0.05)				
		Hypoxia	DMOG	IOX2	BNS	BIQ
1	FOS	8.5	6.5	4.3	3.4	3.5
2	EGLN3	6.0	7.6	1.9	1.7	1.7
3	DAPK2	5.1	4.8	1.8	1.5	1.9
4	VEGFA	4.6	5.2	3.0	2.3	2.7
5	EGLN1	3.9	4.4	3.6	3.3	3.8
6	SLC2A1	3.4	3.4	2.1	2.0	2.2
7	PIAS2	3.4	2.3	3.0	2.6	2.5
8	PDGFB	3.3	3.2	1.5	1.4	1.2
9	WNT10B	3.2	1.8	1.5	1.1	1.1
10	ITGA2B	3.2	1.8	1.7	1.5	1.8
11	FGF11	3.0	3.3	2.1	2.0	2.2
12	FZD8	2.8	4.4	1.4	0.9	1.2
13	VEGFC	2.6	4.0	1.5	1.3	1.4
14	EGFR	2.6	4.5	0.9	0.9	0.7
15	VEGFB	2.2	1.8	1.7	1.6	1.7
16	JUN	2.2	2.3	1.6	1.3	1.7
17	FGFR3	2.1	1.4	0.8	0.9	0.8
18	RUNX1	2.1	2.5	1.4	1.2	1.3
19	CDKN1B	2.1	1.5	1.3	1.3	1.3
20	LAMB3	2.1	2.2	0.9	0.8	0.6

Table 5 Genes upregulated by hypoxia (0.5% O_2) associated with 'pathways in cancer' as identified from the KEGG pathway functional enrichment analysis. Genes were sorted according to fold induction by hypoxia compared to normoxia.

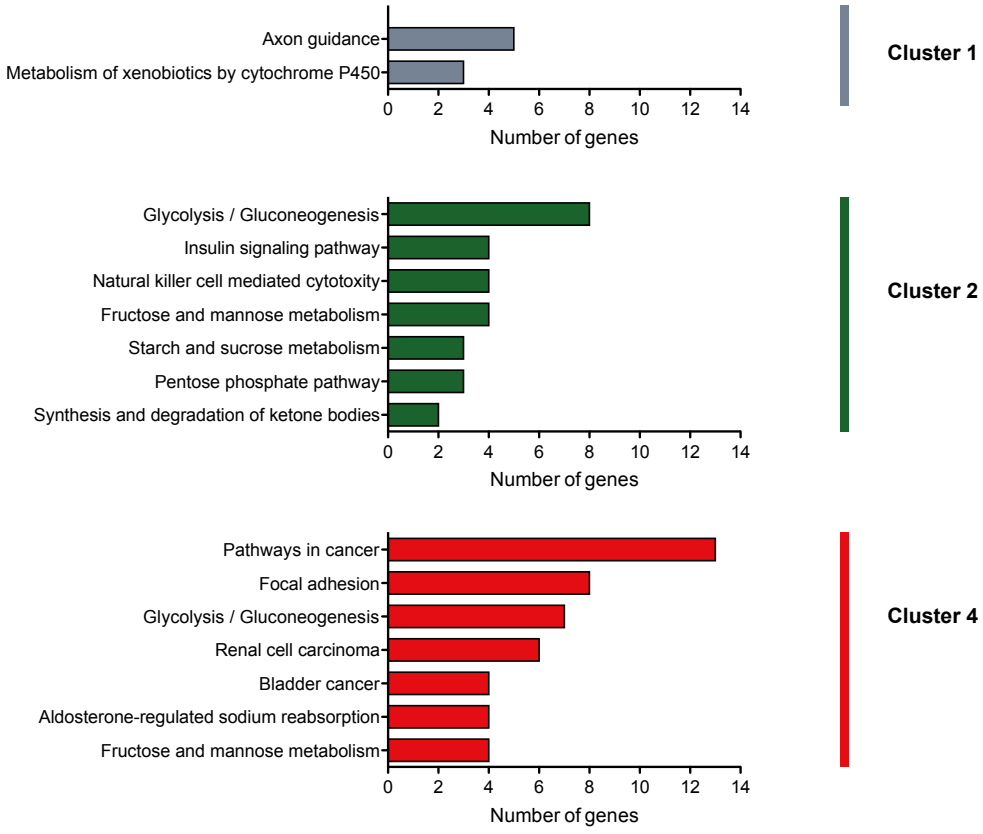

Figure 6.4 KEGG pathway functional enrichment analysis on hypoxia upregulated genes in Clusters 1, 2 and 4.

6.3 The differences between the transcriptional response to hypoxia/DMOG and PHD inhibitors are not due to HIF1α/HIF2α levels or the doses of the PHD inhibitors used

To investigate the differences between the transcriptional response to DMOG/hypoxia and PHD inhibitors, the induction of HIF1α and HIF2α were first investigated by immunoblotting at multiple concentrations of the PHD inhibitors. The results reveal that the protein levels of both HIF1α and HIF2α were maximally induced at the concentrations of PHD inhibitors used for the RNA-seq analysis and were comparable if not higher than the induction by hypoxia (**Figure 6.5 A**). Despite the similarities of the transcriptional response by DMOG and hypoxia, the extent of HIF1α induction by DMOG treatment was observed to be lower than that under hypoxia (**Figure 6.5 A**, compare *lanes 3-4* to *lane 2*). In summary, the induction of HIF1α and HIF2α by PHD inhibitors at the concentrations used in the RNA-seq analysis closely resemble that of hypoxia. Thus, the observed discrepancies in the transcriptional response between hypoxia/DMOG and PHD inhibitors is unlikely to be due to the differences in HIF1α and HIF2α levels induced by each treatment.

Interestingly, it was noted that HIF1α CODD hydroxylation (HyPro564) could be detected by immunoblotting in cells treated under hypoxia but not in cells treated with DMOG or PHD inhibitors (**Figure 6.5 B**). This is likely due to the activity of PHD3, which is induced under hypoxia and was proposed to retain significant activity even under 0.5% O_2 in MCF-7 cells [14]. It is unknown whether this could affect the HIF1α transcriptional activity. It is also unclear how the CODD-hydroxylated HIF1α manage to escape degradation by the VHL complex under hypoxic condition in MCF-7 cells. Moreover, these results support the proposal that the inhibitor dose used was sufficient.

It was proposed that the discrepancies in the transcriptional response observed with DMOG/hypoxia and PHD inhibitors were due to the effects of FIH inhibition. To investigate this proposal, the levels of HIF1α CAD hydroxylation (HyAsn803) under the treatment of DMOG, hypoxia and PHD inhibitors were compared by immunoblotting. The HIF1α CAD hydroxylation levels under the treatment of PHD inhibitors were found to be similar if not slightly higher compared to hypoxia treatment (as judged by immunoblot intensity), indicating that FIH is not inhibited under these conditions (**Figure 6.5 A**). As expected, DMOG treatment reduced HIF1α CAD hydroxylation due to its inhibitory activity against FIH (**Figure 6.5 A**). The differences in HIF1α induction, as well as the inhibitory effects on FIH by DMOG compared to hypoxia, suggest that the similarities in the transcriptional response to that of hypoxia may be, in part, due to reasons other than the inhibition of the PHDs, FIH, or both.

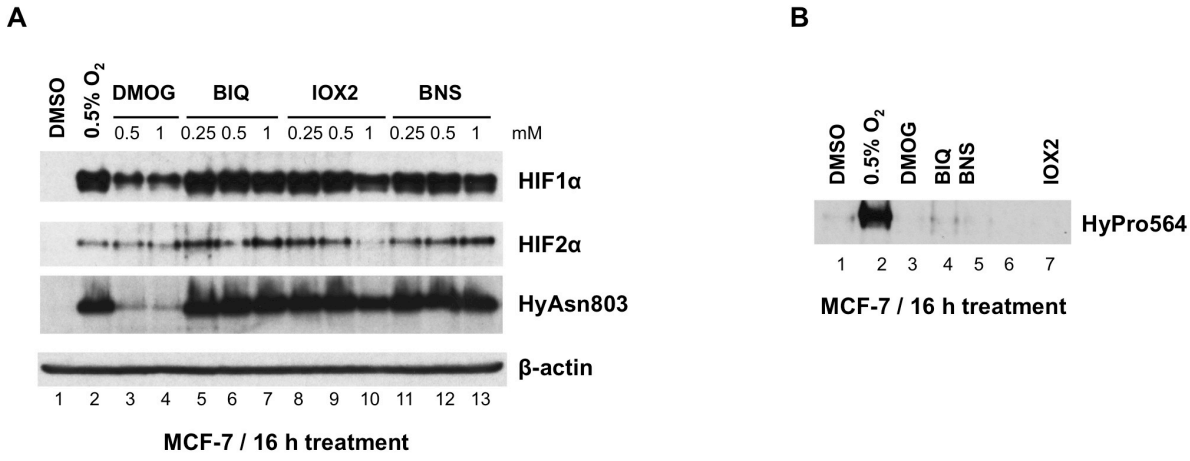

Figure 6.5 (**A**) Immunoblots for MCF-7 cells treated with either normoxia, hypoxia, DMOG, BIQ, IOX2 or BNS showing that HIF1α and HIF2α were maximally induced at the concentration of inhibitors used for the RNA-seq analysis. Note that the hydroxylation of HIF1α CAD (HyAsn803) was inhibited by DMOG but not with the PHD inhibitors and was only partially inhibited by hypoxia. (**B**) Immunoblot showing the detection of HIF1α CODD hydroxylation (HyPro564) in MCF-7 cells treated under hypoxia, which was not detected in either 1 mM DMOG, 0.5 mM BIQ, 0.25 mM BNS or 0.25 mM IOX2 treatment.

6.4 Inhibition and knockdown of FIH to study the role of FIH in mediating the transcriptional response to hypoxia

Despite the indication that non-HIF hydroxylase-related factors may contribute to altered gene expression in hypoxia, it was nevertheless of interest to investigate the effect of ablating the activity of FIH and the PHDs in comparison to DMOG and hypoxia in terms of the resulting transcriptional response. *N*-oxalyl-*D*-phenylalanine is reported to be an inhibitor of FIH which does not inhibit PHD2 *in vitro* [15]. The cell-permeable dimethyl-ester derivative of this inhibitor, hereafter referred to as DM-NOFD (**Figure 6.6 A**), was used in an attempt to inhibit cellular FIH activity. To investigate the effect of this inhibitor on HIF1α CAD hydroxylation in MCF-7 cells, the cells were treated with DM-NOFD and IOX2 (to induce HIF1α) for 16 h before being analysed by immunoblotting. The levels of HIF1α CAD hydroxylation were compared to those observed with the treatment of hypoxia for the same period. The results demonstrate that cellular treatment of DM-NOFD at 1 mM concentration in the presence of IOX2 is able to reduce the level of HIF1α CAD hydroxylation (**Figure 6.6 B**, compare *lanes 2* and *3*), although the inhibition of HIF1α CAD hydroxylation was not efficient. The extent of FIH inhibition was observed to be higher at 2 mM DM-NOFD, although there were concerns about cellular toxicity at this concentration (in addition to the slight downregulation of HIF2α, **Figure 6.6 B**, *lane 4*). When used in isolation, DM-NOFD did not upregulate HIF1α or HIF2α, indicating that it did not inhibit the PHDs, in line with the reported *in vitro* observations [15].

Given that the inhibition of FIH by DM-NOFD was incomplete, an FIH knockdown approach by RNA interference was undertaken. It was considered that the knockdown of FIH by siRNA can potentially be performed either in isolation or in combination with DM-NOFD treatment to ablate FIH activity. Three different FIH siRNAs were first tested for their ability to

downregulate FIH. As shown in **Figure 6.7 A**, all three FIH siRNAs were effective in downregulating FIH protein levels, as determined by immunoblotting. FIH siRNA 1 (hereafter referred to as FIH siRNA) was subsequently used at 5 nM concentration for all FIH knockdown experiments. Additional experiments were then carried out to investigate the effect of FIH siRNA on HIF1α CAD hydroxylation. The results show that neither DM-NOFD nor FIH siRNA treatment in the presence of IOX2 were able to markedly inhibit HIF1α CAD hydroxylation (**Figure 6.7 B**, see *lanes 6* to *10*), despite an approximately 90% knockdown of FIH at the mRNA level by the FIH siRNA (**Figure 6.7 C**). However, the combination of both treatments (DM-NOFD and FIH siRNA) successfully ablates FIH activity, as judged by the lack of detectable HIF1α CAD hydroxylation (**Figure 6.7 B**, *lane 11*). Immunoblot analysis of PHD3, one of the HIF target genes categorised as Cluster 4 in the RNA-seq analysis, shows that it can be induced to a level comparable to that of hypoxia/DMOG when both the PHDs and FIH were inhibited (**Figure 6.7 B**).

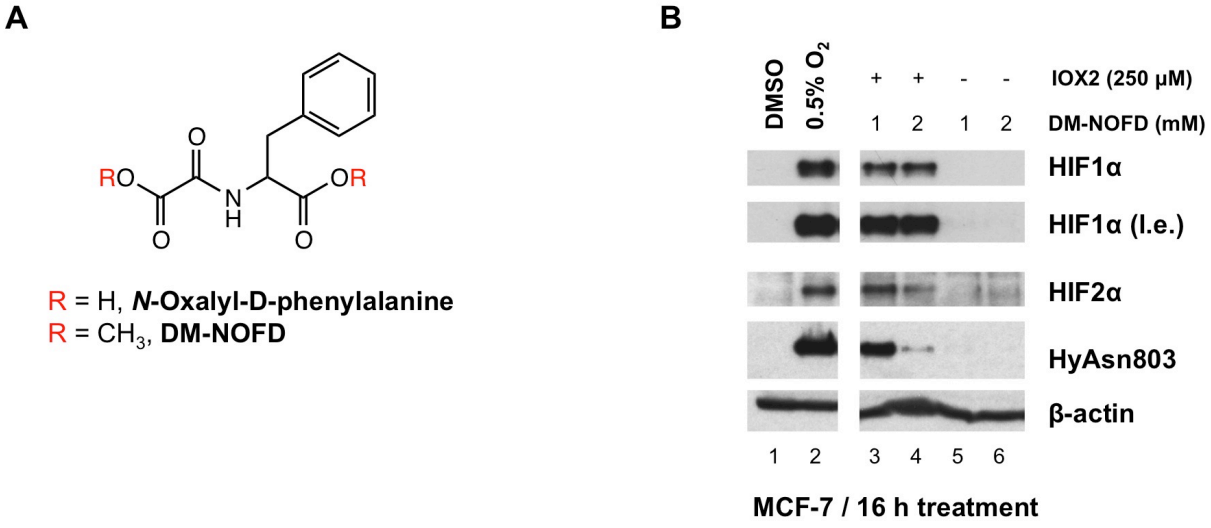

Figure 6.6 (**A**) Chemical structure of *N*-oxalyl-*D*-phenylalanine and its cell permeable ester derivative, DM-NOFD. (**B**) Immunoblotting analyses of MCF-7 cells treated with either normoxia, hypoxia, or two concentrations of DM-NOFD in the presence or absence of 250 μM of IOX2.

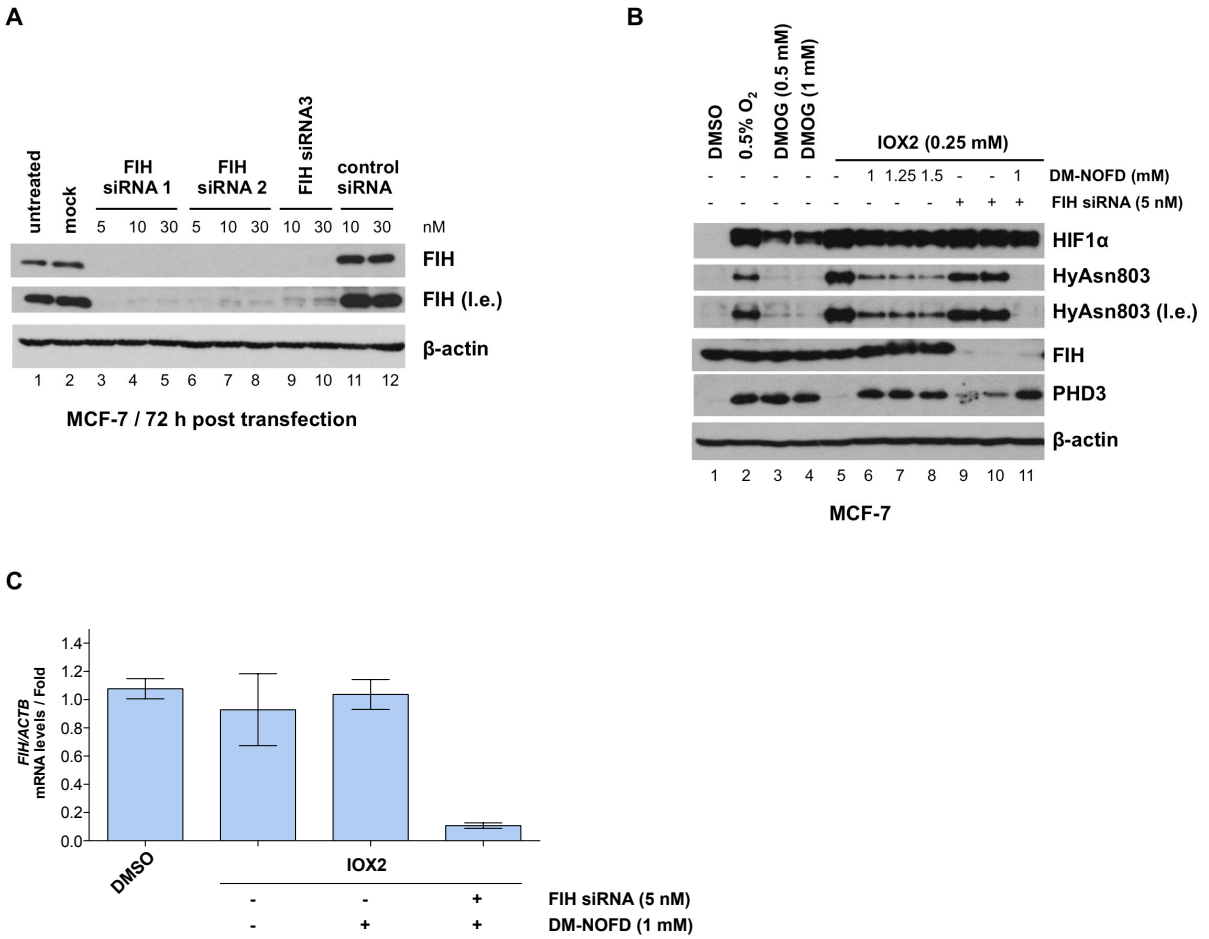

Figure 6.7 (**A**) Knockdown of FIH in MCF-7 cells using three different FIH siRNAs. FIH levels were detected by immunoblotting 72 h after transfection. Mock: transfection reagent only, control siRNA: dHIF siRNA. (**B**) Immunoblot showing the effect to HIF1α CAD hydroxylation in MCF-7 cells with the treatment of DM-NOFD alone, FIH siRNA alone, or both in combination. Cells were transfected with FIH siRNA (where indicated) or transfection reagent only for 48 h prior to a 16 h treatment of inhibitor(s) or hypoxia. (**C**) Knockdown of FIH mRNA levels by FIH siRNA as measured by qRT-PCR. Cells were transfected with FIH siRNA (where indicated) or transfection reagent only for 48 h prior to a 16 h treatment of inhibitor(s). Results are shown as mean fold change ± standard deviation, n = 3. l.e.: long exposure.

6.5 Inhibition of both the PHDs and FIH can recapitulate some but not all of the transcriptional response to hypoxia/DMOG.

To investigate whether the combined inhibition of the PHDs and FIH can promote the induction of hypoxia/DMOG upregulated genes that were partially or not induced by PHD inhibition alone, the induction of selected genes from Cluster 4 (as determined in the RNA-seq analyses) was investigated by real-time quantitative PCR (qRT-PCR). Consistent with the RNA-seq analyses, IOX2 did not upregulate the *CA9* and *EGLN3* mRNA to the level observed under hypoxia or DMOG (**Figure 6.8 A**). The combined inhibition of PHDs and FIH (i.e., treatment with IOX2, DM-NOFD and FIH siRNA), however, was able to upregulate these two genes to a similar extent as in hypoxia or DMOG. Interestingly, the combined treatment of IOX2 and DM-NOFD (without FIH siRNA) was sufficient to induce both genes to the levels observed in hypoxia/DMOG. The induction of *EGLN3* mRNA levels in **Figure 6.8 A** is also consistent with that observed for its protein PHD3 by immunoblotting (**Figure 6.7 B**). The observations, however, did not extent to *SOX9* and *CXCR4*, which are also Cluster 4 genes (genes upregulated by hypoxia/DMOG to a higher extent than the PHD inhibitors in the RNA-seq analyses). Neither partial nor complete blockade of FIH activity in the presence of IOX2 was able to upregulate the mRNA levels of *SOX9* and *CXCR4* (**Figure 6.8 A**). These results suggests that although some genes can only be upregulated to the level induced by hypoxia when both the PHDs and FIH are inhibited, the induction of a subset of hypoxia upregulated genes may require the inhibition of an additional factor(s). The transcriptional response observed with DMOG and its better concordance with the transcriptional response to hypoxia (compared to the more selective PHD inhibitors) indicate that this factor is likely to be inhibited by DMOG, thus suggesting that it may be part of the 2OG-dependent dioxygenase family.

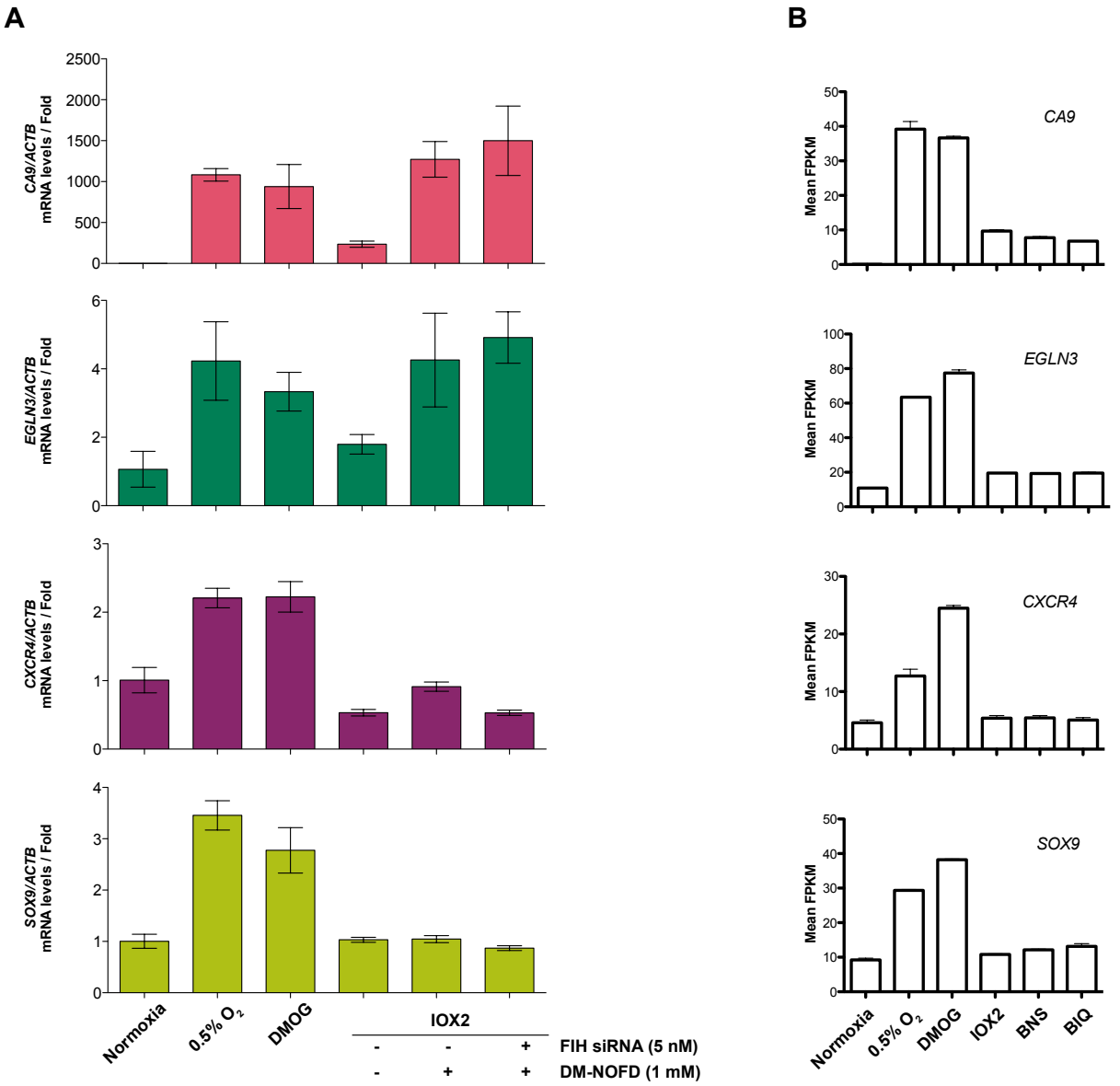

Figure 6.8 (**A**) qRT-PCR analyses for *CA9*, *EGLN3*, *CXCR4* and *SOX9* showing the differential regulation by hypoxia (0.5% O_2), DMOG, and IOX2 in the absence or presence of FIH siRNA and DM-NOFD. Cells were transfected with FIH siRNA (where indicated) or transfection reagent only for 48 h prior to a 16 h treatment of inhibitor(s). Results are shown as mean fold change ± standard deviation, n = 3. (**B**) Expression levels (FPKM) of the corresponding genes in (A) as determined by the RNA-seq analyses.

6.6 Gene expression studies by microarray to identify hypoxia regulated genes that are regulated by the PHDs, FIH, both, or neither.

Gene expression profiling by microarray was employed to study the extent to which the transcriptional response to hypoxia/DMOG is mediated by the PHDs, FIH, both (the PHDs and FIH), or by neither. It was anticipated that the expression pattern of each gene may vary according to its dependency on PHDs and/or FIH catalysis. MCF-7 cells were treated under normoxia, hypoxia (0.5% O_2), 1 mM DMOG, 250 μM IOX2, or 250 μM IOX2 with 1 mM DM-NOFD after transfection with FIH siRNA (hereafter referred to as IOX2FIHi). Total RNA samples used for the microarray were prepared from the treated cells in biological triplicate for each condition. Global gene expression analyses from the microarray results (**Figure 6.9**) reveal that 893 genes are significantly upregulated by hypoxia (fold-change > 2, adjusted p-value < 0.05). Surprisingly, there were fewer genes upregulated by DMOG (527 genes) compared to IOX2 (619 genes). These results are in contrast to that observed in the RNA-seq analyses, where higher numbers of genes were upregulated with DMOG compared to PHD inhibitors (including IOX2). The number of genes upregulated by IOX2FIHi (589 genes) were also unexpectedly lower than IOX2.

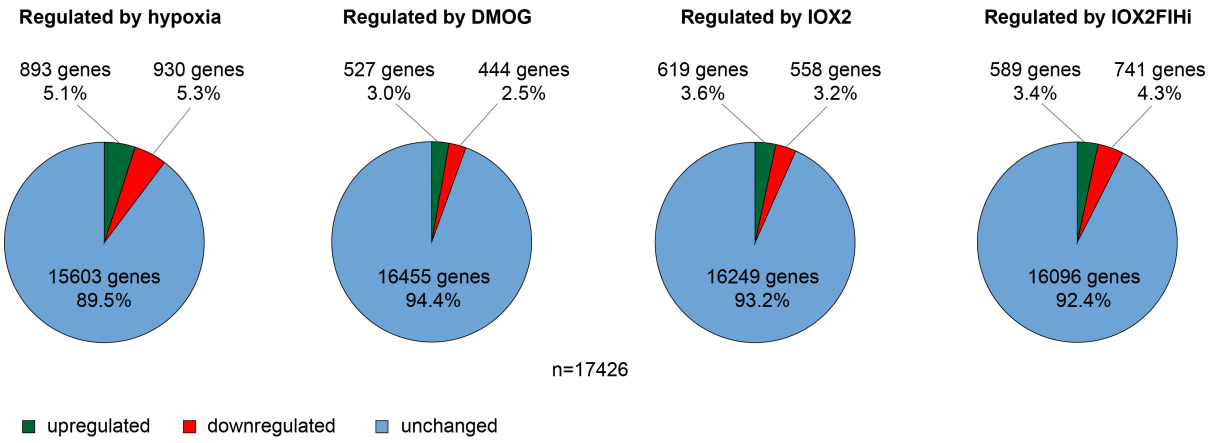

Figure 6.9 The proportion of genes upregulated, downregulated or unchanged for each treatment (hypoxia, DMOG, IOX2 and IOX2FIHi). fold-change > 2, adjusted p-value < 0.05.

Further analysis of the 893 hypoxic upregulated genes from the microarray dataset also revealed that IOX2 is a better mimic of hypoxia compared to DMOG, in contrast to the previous observation by RNA-seq under the same experimental conditions (at least with respect to the available data). 473 of the hypoxia upregulated genes (53%) were also upregulated by IOX2, whereas only 401 of the hypoxia upregulated genes (44.9%) were upregulated by DMOG (**Figure 6.10**). IOX2FIHi, induced only 429 of the 893 hypoxia upregulated genes (48%) was also a lesser mimic of hypoxia compared to IOX2, contrary to the expectation that the ablation of FIH activity will induce more hypoxia regulated genes due to increased HIF transcriptional activity. Due to the discrepancies between the RNA-seq and microarray dataset, the number of overlapping hypoxia upregulated genes in both platforms was examined. Among the 9898 genes detected by both platforms (**Figure 6.11 A**), only 173 genes were consistently upregulated by hypoxia as determined by their expression in both the RNA-seq and microarray analyses (**Figure 6.11 B** and *Appendix 3*). Box plot of gene fold-changes (log_2 transformed; hypoxia over normoxia) shows that a higher proportion of the 173 hypoxia induced genes in both platforms exhibit higher fold-changes when compared to the genes induced by hypoxia in the microarray only or RNA-seq only datasets (**Figure 6.11 C**). Notably, the median fold-change for the 173 hypoxia induced genes in both platforms was higher than that observed for genes induced either in the microarray only or the RNA-seq only datasets.

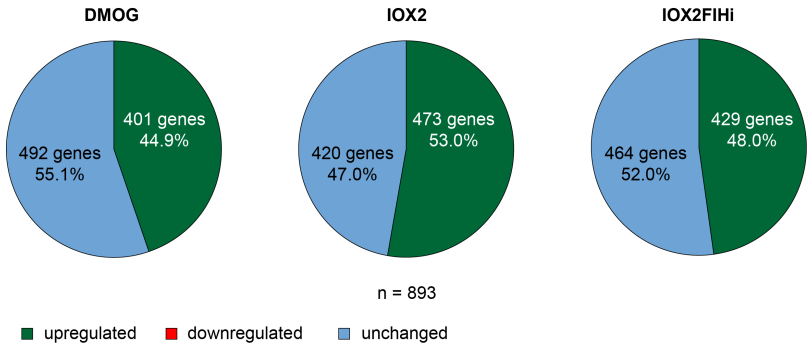

Figure 6.10 Pie charts showing the proportion of hypoxic induced genes (893 genes) that were also upregulated by either DMOG, IOX2 or IOX2FIHi based on the microarray analyses.

Despite the differences between the RNA-seq and microarray results, further analyses were carried out on the 173 overlapping hypoxia upregulated genes in both platforms. Based on the previous clustering in the RNA-seq analysis, there were 34 genes in Cluster 1, 67 genes in Cluster 2 and 72 genes in Cluster 4 out of the 173 overlapping hypoxia upregulated genes. The genes in Cluster 4 were of interest, as the fold-upregulation by hypoxia and DMOG were significantly higher than the fold-upregulation by the PHD inhibitors. The microarray gene expression profiles of the three genes from Cluster 4 (*CA9*, *EGLN3* and *SOX9*) which has been validated by qRT-PCR were analysed. All three genes were significantly upregulated by hypoxia in the microarray dataset. The expression levels of *CA9* and *EGLN3* were shown to be consistent with previous observations, whereby hypoxia and DMOG inductions were higher than that observed with IOX2 (**Figure 6.12**). The induction of these genes by IOX2 for these genes was enhanced to the level of DMOG/hypoxia induction when FIH activity was inhibited (IOX2FIHi). *SOX9*, on the other hand, was not induced by IOX2 (consistent with previous observations by RNA-seq and qRT-PCR); however, it was also not induced by DMOG in the microarray dataset. IOX2FIHi also did not induce SOX9 expression, in line with the previous observation of non-responsiveness to FIH inhibition by qRT-PCR. The expression of *CXCR4*, another gene from Cluster 4 previously validated by qRT-PCR, did not reach a signal above background in the microarray dataset and thus, could not be investigated.

The identification of genes from the microarray dataset that were upregulated by hypoxia but were not responsive to FIH inhibition may aid further investigation on the proposed novel oxygen sensing enzyme (hereafter referred to as X). If a hypoxia upregulated gene is regulated by X, the gene may either be partially or not induced by IOX2 or IOX2FIH (depending on whether the gene is regulated by X independently or collectively with PHDs and/or FIH). The upregulation of genes regulated by X may or may not be observed with

DMOG (depending on whether DMOG inhibits X). In the case of *SOX9*, upregulation by DMOG is observed in RNA-seq and qRT-PCR analysis, although this is not replicated in the microarray dataset. Ideally, the identification of more genes like *SOX9* will allow further tests to support the notion that X is likely to be a member of the 2OG-dependent dioxygenase protein family. Analysis of the 173 genes upregulated by hypoxia in both RNA-seq and microarray datasets were carried out and 8 genes that met the abovementioned criteria for genes regulated by X were shortlisted (**Table 6**). The dependency on HIF for the upregulation of these genes were investigated using the HIF1α/HIF2α knockdown microarray dataset from [8] and HIF1α/HIF2α binding by chromatin immunoprecipitation sequencing (ChIP-seq) dataset from [13], whereby both studies were also performed on MCF-7 cells. According to the criteria in the respective studies, *SCNN1B* and *SOX9* were shown to be affected by HIF1α/HIF2α knockdown, whereas *CYP1B1*, *SOX9* and *ELF3* were shown to contain a HIF binding site (**Table 7**). These findings indicate that the upregulation of these genes by hypoxia were likely to be HIF-dependent. Detailed studies on these genes should be carried out to provide an insight into the additional factor(s) that may regulate their hypoxia-mediated transcriptional response.

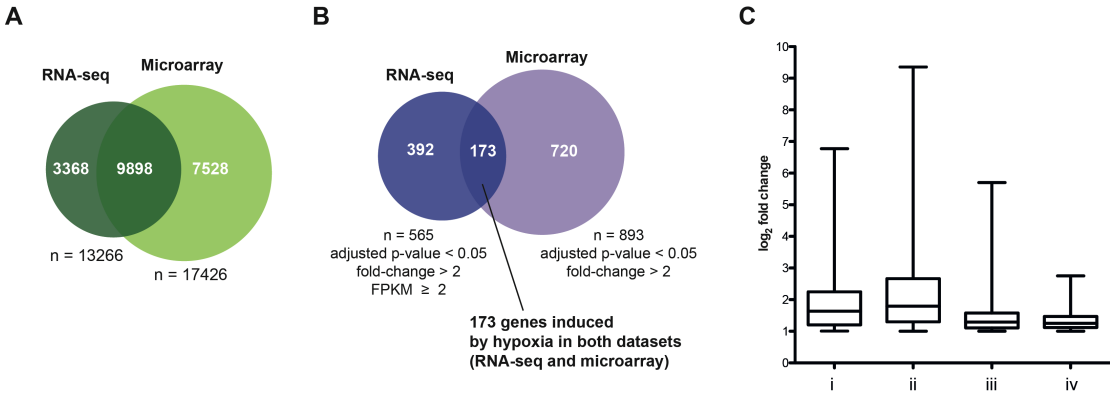

Figure 6.11 (**A**) Venn diagram showing the overlap of total expressing genes in RNA-seq and microarray. (**B**) Venn diagram showing the overlap of genes induced by hypoxia in both platforms. (**C**) Box plot illustrating the distribution of fold-change (log_2 transformed) for genes induced by hypoxia in both platforms (i and ii), in the microarray dataset only (iii) or in the RNA-seq dataset only (iv). Data from the microarray are shown in (i) and (iii), whereas data from the RNA-seq are shown in (ii) and (iv).

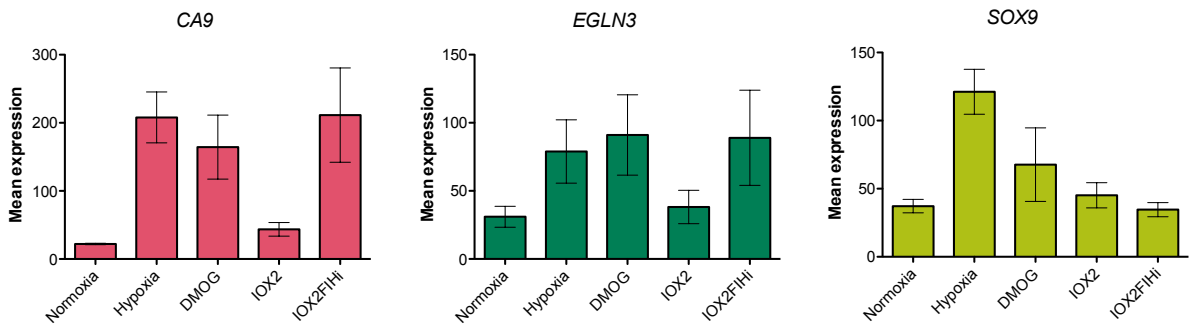

Figure 6.12 mRNA expression levels as determined from the microarray analysis of three genes (*CA9*, *EGLN3* and *SOX9*) previously studied by qRT-PCR. Note the induction of IOX2FIHi in comparison to IOX2 for *CA9* and *EGLN3*, but not *SOX9*. Each data represents the normalised mean expression ± standard deviation.

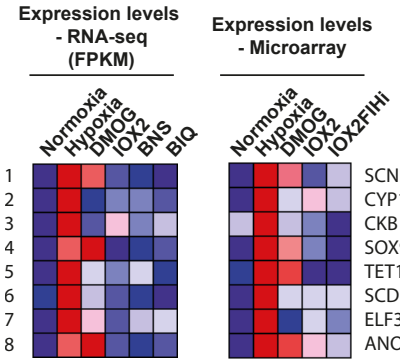

		Fold change - RNA-seq (adjusted p-value < 0.05)						Fold change - microarray (adjusted p-value < 0.05)			
		Hypoxia	DMOG	IOX2	BNS	BIQ	Cluster	Hypoxia	DMOG	IOX2	IOX2FIHi
1	SCNN1B	13.1	9.9	3.0	2.2	1.7	C4	3.6	2.2	1.3	1.5
2	CYP1B1	4.4	1.2	1.5	1.5	1.4	C1	2.2	1.4	1.5	1.3
3	CKB	3.9	1.6	1.9	1.4	1.4	C1	2.1	1.0	0.9	0.8
4	SOX9	3.5	4.7	1.2	1.4	1.5	C4	3.3	1.8	1.2	0.9
5	TET1	3.3	1.7	1.3	1.5	1.2	C1	2.1	1.8	0.9	0.9
6	SCD	2.6	1.3	1.0	1.0	0.9	C1	3.0	1.6	1.6	1.6
7	ELF3	2.3	1.6	1.2	1.3	1.4	C1	2.0	1.1	1.2	1.1
8	ANO6	2.0	2.6	1.2	1.1	1.1	C4	2.2	2.0	1.6	1.4

Table 6 The expression profile (heatmap) of the shortlisted genes that can potentially be used to study the non-PHDs/FIH factor(s) required for the hypoxia transcriptional response. Genes were sorted according to fold upregulation by hypoxia based on RNA-seq analyses. Their respective fold change compared to normoxia under the tested conditions (determined from RNA-seq and microarray analyses) were as indicated. Expression levels were indicated in shades of red (high expression) to blue/dark indigo (low expression).

SCNN1B: Amiloride-sensitive sodium channel subunit beta 1; *CYP1B1*: cytochrome P450, family 1, subfamily B, polypeptide 1; *CKB:* creatine kinase B-type; *SOX9*: SRY (sex determining region Y)-box 9; *TET1*: tet methylcytosine dioxygenase 1; *SCD*: stearoyl-CoA desaturase (delta-9-desaturase); *ELF3*: E74-like factor 3 (ets domain transcription factor, epithelial-specific); *ANO6*: anoctamin 6.

Genes affected by HIF1α siRNA and/or HIF2α siRNA [8]	Genes with HIF1α and/or HIF2α binding sites [13]
SCNN1B	*CYP1B1*
SOX9	*SOX9*
	ELF3

Table 7 List of genes shortlisted in Table 6 with their dependencies on HIF1α and/or HIF2α as determined in [8], or with HIF1α and/or HIF2α binding sites as determined in [13].

6.7 Discussion and future work

In this Chapter, pan-genomic studies aimed at investigating the transcriptional response to hypoxia in MCF-7 cells are described. Initial RNA-seq studies using DMOG and PHD inhibitors (including IOX2 which was developed as one of the chemical probes for the PHDs described in **Chapter 4**) in comparison to hypoxia (0.5% O_2) for 16 h showed that, at least under the tested conditions, DMOG is a better mimic of hypoxia compared to the PHD inhibitors in terms of changes in gene expression. Further analyses on the upregulated genes, including KEGG functional enrichment analysis, confirmed a higher degree of concordance between hypoxia and DMOG than the comparison between hypoxia and PHD inhibitors. An interesting, and potentially important observation is that genes involved in cancer pathways are enriched in both the DMOG and hypoxia upregulated gene sets, but not in PHD inhibitors upregulated gene sets. This observation may be of importance, given that PHD inhibitors are currently being developed for use in the clinic for the treatment of anemia [7]. A selective PHD inhibitor may be preferred to prevent the upregulation of genes involved in cancer. Further understanding of the pathways represented in genes upregulated by the hypoxia and PHD inhibitors will be of value in assessing the risk of compounds targeting the hypoxic pathway developed for clinical use. There were also differences between the PHD inhibitors used in terms of the different total number of genes regulated and their functional properties (based on the KEGG functional enrichment analyses), which could be due to the differences in the selectivity of each inhibitor. While IOX2 has been shown to be selective (at least *in vitro*) for the PHDs over a panel of human 2OG-dependent dioxygenases, BIQ is a less selective PHD inhibitor which also inhibits FTO (see **Chapter 4**) [16]. In the case of BIQ, future studies on genes that were regulated differentially by this inhibitor as compared to IOX2 may be of use to investigate the possible role of FTO in mediating the transcriptional response to hypoxia. The selectivity of BNS for the PHDs over other 2OG-dependent

dioxygenases, on the other hand, has not been investigated, although there is some evidence for the selectivity within the PHD isoforms (see **Chapter 5**). It is perhaps not so likely that the apparent selectivity of BNS for different PHD isoforms would have an effect on gene expression, given that HIF1α CODD hydroxylation is fully inhibited and that there were no marked differences in the levels of HIF1α and HIF2α compared to the other PHD inhibitors tested. Further investigation with the use of siRNA targeting specific PHD isoforms may be able to validate the observations seen with the PHD inhibitors used in the current study. It would also be interesting to carry out similar transcriptional studies on PHD-null cells, such as the PHD-triple-knockout mouse embryonic fibroblast cell line (TKO cells) described in **Chapter 5**. This will allow further dissection of hypoxia-regulated genes to determine whether they are dependent or independent on the PHDs. However, it should be noted that the constitutive stabilisation of HIF in the TKO cells (due to the absence of functional PHDs) may be a closer mimic of long-term hypoxia rather than short-term hypoxia. Furthermore, any effects due to the loss of PHDs in the TKO cells may be masked by unknown cellular mechanisms as part of the cellular adaptation for the loss of the PHDs after being cultured over multiple passages.

The observation that DMOG is a better hypoxia mimic compared to the PHD inhibitors supports the notion that the transcriptional responses to hypoxia are not solely mediated by the PHDs, which led to the investigation of the role of FIH. Consistent with previous studies on RCC4 cells [17], FIH activity was also not inhibited (or only partially inhibited) under 0.5% O_2 in MCF-7 cells, as judged by the immunodetection of HIF1α CAD hydroxylation (**Figure 6.5 A**). This suggests that FIH may play a less important role in the transcriptional response under this oxygen concentration, consistent with previous work on the relative importance of FIH and the PHDs at low oxygen concentrations in cells [17, 18]. Nevertheless,

given that FIH is inhibited by DMOG, the effect of ablating FIH activity (with either the combined or individual used of FIH siRNA and FIH inhibitor, DM-NOFD) in the presence of PHD inhibitor (IOX2) was investigated. The combined use of DM-NOFD with FIH siRNA was necessary in this study, given the low potency of DM-NOFD in inhibiting FIH and the persistence of HIF1α CAD hydroxylation, despite an efficient FIH knockdown (approximately 90% as determined by qRT-PCR) with the FIH siRNA. The observed persistence of HIF1α CAD hydroxylation suggests that the activity of the remaining ~10% of FIH that was present was sufficient to hydroxylate HIF1α during the 16 h period following HIF1α induction by IOX2. The low potency of DM-NOFD also highlights the need for the development of a more potent, selective and cell-permeable FIH inhibitor, which would have been useful in this study. qRT-PCR analyses on MCF-7 cells with the ablation of FIH activity show an inductive effect for two genes that were partially or not upregulated by the treatment of IOX2 alone (*CA9* and *EGLN3*). These two genes have been previously reported to be dependent on FIH [19]. However, two other hypoxia upregulated genes (*SOX9* and *CXCR4*) were not affected by PHD and FIH inhibition. This indicates that the PHDs and FIH may only play a role in inducing a subset of genes upregulated by hypoxia and DMOG, or that their inhibition alone was not sufficient for the upregulation of genes like *SOX9* and *CXCR4* .

Genome-wide expression studies using microarray on MCF-7 cells with ablated FIH activity (i.e. with the combined used of FIH siRNA and FIH inhibitor, DM-NOFD, also referred to as IOX2FIHi) in the presence of IOX2 were carried out to investigate the extent to which the transcriptional response to hypoxia is mediated by PHDs and FIH. In terms of the total number of differentially regulated genes, the results from the microarray analyses were not in line with those observed from the RNA-seq analyses – unexpectedly, fewer genes were shown to be responsive to DMOG and IOX2FIHi compared to IOX2. There were also

differences in the genes upregulated by hypoxia as determined from both the RNA-seq and microarray analyses, which could be indicative of the differences between the two platforms and/or experimental variations. One other possible explanation for the lesser effect observed by DMOG could be due to compound degradation, which should be investigated by comparing different batches of the inhibitor and/or chemical analysis to determine the purity of the compound. Genes that were upregulated by DMOG as determined from the RNA-seq analyses, which were not upregulated in the microarray study should be tested by qRT-PCR with different batches of DMOG to verify the batch issue. It is unclear whether the observation that IOX2FIHi treatment affects fewer genes than IOX2 treatment alone is indeed a biologically relevant observation – further studies or perhaps an independent experiment should be carried out to verify this observation. Additional studies with FIH-null MCF-7 cells (ongoing work by Dr Y-M. Tian) would be useful in validating the observations with IOX2FIHi and could provide further insight into the extent of FIH-mediated transcriptional response to hypoxia.

A focused analysis on the 173 hypoxia upregulated genes as determined by both microarray and RNA-seq analyses revealed a set of genes that are not responsive to PHD or FIH inhibition. This gene set includes *SOX9* (which has been validated by qRT-PCR), *SCNN1B*, *CYP1B1*, *CKB*, *TET1*, *SCD*, *ELF3* and *ANO6*. It would be of interest to investigate the additional factor(s) required to induce these genes to the same extent as in 0.5% O_2. Some of these genes were responsive to DMOG based on RNA-seq analysis (*SOX9*, *SCNN1B* and *ANO6*), indicating that the additional factor(s) may be a member of 2OG-dependent dioxygenase. The use of chemical probes and/or knockdown studies targeting members of the 2OG-dependent dioxygenase family other than the PHDs and FIH may provide an insight into the additional factor(s) that play a role in the hypoxia-mediated upregulation of these genes.

The 2OG-dependent dioxygenase enzymes all require oxygen to function, but it would be of interest to know which showed significantly reduced activity in hypoxia and were capable of eliciting a downstream effect in transcription. Notably, a recent *in vitro* study demonstrated that a human histone demethylase KDM4E (which is also a member of the 2OG-dependent dioxygenase family) reacts slowly with oxygen [20], a characteristic of an oxygen sensor previously observed with PHD2 [21]. If this observation holds true in cells and also extents to other 2OG-dependent histone demethylases, the cellular activity of the histone demethylases may respond to changes in oxygen concentrations and thereby contribute to the hypoxia-mediated transcriptional response by altering histone methylation status of target genes. It should be noted that many of the 2OG-dependent histone demethylases are also direct HIF target genes upregulated in response to hypoxia [22]. Thus, a detailed study on the histone methylation status at the loci of hypoxia induced genes which are non-responsive to PHD or FIH inhibition would be of interest.

Previous microarray studies of HIF1α/HIF2α-mediated hypoxia transcriptional response [8] and studies on HIF1α/HIF2α binding sites by ChIP-seq [13] in MCF-7 cells have enabled the classification of hypoxia upregulated genes that are likely to be dependent on HIF1α and/or HIF2α. Using information from these studies, the hypoxia upregulation of *SCNN1B*, *SOX9*, *CYP1B1* and *ELF3* are likely to be mediated, at least in part, by HIF (**Table 7**). Although *CKB*, *TET1*, *SCD* and *ANO6* were not shown to be dependent on HIF nor do they contain a HIF binding site in the studies using MCF-7 cells described, there have been reports on HIF dependency for these genes in other cell types [23-26]. It is also important to note, however, that the transcriptional regulation of genes in response to hypoxia may vary in different cell types. Previous analyses conducted on 19 gene expression datasets from 14 different cell lines revealed that only 17 genes are upregulated consistently and significantly by hypoxia or

hypoxia mimetics [27]. Nevertheless, the set of genes identified to be non-responsive to PHD or FIH inhibition in the study described in this Chapter will enable further studies on the additional factor(s) required for the hypoxia-mediated upregulation of these genes, regardless of whether they act independently or collectively with HIF.

Overall, the studies described in this Chapter suggest that at least a subset of the transcriptional response to hypoxia or DMOG may not be solely mediated by the PHDs and FIH, indicating the requirement of an alternative factor(s) to be either inhibited or activated in response to hypoxia. This additional factor(s) may work co-operatively with HIF to mediate the hypoxic response, which may require HIF stabilisation (via inhibition of the PHDs) and transactivation (via inhibition of FIH). Like the PHDs and FIH, this additional factor(s) may act as a cellular oxygen sensor if its activity is directly linked to the availability of oxygen. Further investigations are thereby warranted to provide further support and understanding of the molecular mechanism of the hypoxia-mediated transcriptional response.

6.8 Materials and methods

The following materials and methods were as described in previous Chapters:

- *Buffers and reagents* (**Chapter 3**)
- *Cell lysate preparation – as for immunoblotting* (**Chapter 3**)
- *Immunoblotting* (**Chapter 3**)

Cell culture

Human breast cancer MCF-7 cell line was cultured as described in **Chapter 4**.

Chemical compounds

DMOG, BIQ and DM-NOFD were synthesised by Dr K.K. Yeoh (Department of Chemistry). IOX2 was synthesised by Dr J.I. Candela-Lena (Department of Chemistry). BNS was synthesised by Dr. C. Lejeune (Department of Chemistry).

RNA-seq experiment

All cell culture, treatment and sample preparation for the RNA-seq experiment was performed by Dr J. Schödel (Centre for Cellular and Molecular Physiology). Subconfluent MCF-7 cells were treated either under hypoxia (0.5% O_2), 1 mM DMOG, 250 μM IOX2, 250 μM BNS or 0.5 μM BIQ for 16 h before being harvested. Total RNA was prepared using mirVana™ miRNA isolation kit (AM1560; Life Technologies, Carlsbad, USA) according to the manufacturer's protocol. RNA samples were sent to Oxford Genomics Centre, Wellcome Trust Centre for Human Genetics, Oxford for PolyA RNA library preparation and high throughput sequencing. An average of 49.66 million, 100 base pairs long, pairs of reads were obtained per sample (range 44.06M – 54.52M).

siRNA transfection experiment

Subconfluent MCF-7 cells were trypsinised and resuspended in DMEM without antibiotics. FIH or control siRNA was first diluted according to the desired concentration with Opti-MEM I Reduced Serum Medium (51985-034; Life Technologies, Carlsbad, USA) to a volume of 200 µl in the wells of 12-well cell culture plate, before 2 µl of Lipofectamine RNAiMAX (13778150; Life Technologies, Carlsbad, USA) was added. For mock control, all the reagents except siRNA was added. For untreated control, only Opti-MEM I Reduced Serum Medium was added. The plate containing the mixture was then incubated at room temperature for 10 – 20 minutes. Following that, $1x10^5$ cells (in 1 ml) were added into each well containing the siRNA, mock or control mixture (to achieve cell density of approximately 30-50% confluent 24 h after plating) and incubated for 48 h before further treatment.

The following Silencer™ Select Pre-Designed & Validated siRNA for (4392420; Life Technologies, Carlsbad, USA) were used:

FIH siRNA 1: s31197

FIH siRNA 2: s31198

siRNA for SIMA (*Drosophila melanogaster* HIF1α homolog, referred to as dHIF siRNA) and FIH siRNA 3 were obtained from Dr Y-M. Tian [18].

Microarray experiment

Following transfection with either mock or FIH siRNA 1 for 48 h, MCF-7 cells were incubated under hypoxia (0.5% O_2) in *In vivo*$_2$ 400 hypoxic workstation (Ruskin technologies, Bridgend, United Kingdom) or subjected to the indicated inhibitor treatment (250 µM IOX2 and/or 1 mM DM-NOFD) for 16 h. DMSO was added into no-inhibitor controls

(normoxia/hypoxia) to a final concentration of 1% (equivalent to the final DMSO concentration for each inhibitor treatment). Cells were subsequently harvested and total RNA was prepared using mirVana™ miRNA isolation kit (AM1560; Life Technologies, Carlsbad, USA) according to manufacturer's protocol. Genomic DNA was removed from RNA samples using TURBO DNA-free™ Kit (AM1907; Life Technologies, Carlsbad, USA) according to manufacturer's protocol. RNA samples were then sent to Oxford Genomics Centre, Wellcome Trust Centre for Human Genetics, Oxford for quality control analysis, amplification and hybridisation on HumanHT-12 v4.0 Expression BeadChip (Illumina, San Diego, USA).

RNA-seq and microarray analyses

For the RNA-seq experiment, analyses and processing of data were performed by Dr. N. Ilott as follows: Quality control analysis for RNA sequence reads was performed using Fastqc [28]. The reads were of high quality with a median quality score Q>28 at each base along the length of the reads. Reads were mapped to the human genome (Hg19) using the spliced aligner Tophat2 [29]. An average of 91.39% (range 90.55% - 92.50%) uniquely mapping reads was used for downstream analysis. Reads were counted over protein coding gene models from Ensembl (version 72) using gtf2table from the CGAT tool collection [30]. The sum of read counts over exons was used as input for differential expression analysis. DESeq [31], which uses a negative binomial distribution-based analysis was used to assess differential expression between each experimental condition and normoxia. These analyses were performed using the statistical software package R (version 2.15.2). For visualisation purposes, fragments per kilobase exon per million reads mapped (FPKM) values were calculated for each sample using Cufflinks (version 2.2.0) [32].

Microarray analysis was performed by Dr. N. Ilott using the LIMMA package [33] in R (version 2.15.2). Signal intensities generated using the BeadStudio (Illumina Inc.) software were normalised for between-array differences using quantile normalisation and $\log_2$ transformation. Differentially expressed probes between each condition and normoxia were called using an empirical bayes procedure implemented in LIMMA. A total of 21507 probes corresponding to 17426 unique genes were analysed.

KEGG functional enrichment analyses were conducted using DAVID [11].

Antibodies for immunoblotting

Antibodies for human HIF1α, human HIF2α, HyPro564 and HyAsn803 were as described in **Chapter 4**, mouse monoclonal FIH antibody clone 162c (MABE102; Millipore, Billerica, USA) [18]. Secondary antibodies were as described in **Chapter 3**.

Real-time quantitative PCR (qRT-PCR)

Total RNA preparations following genomic DNA removal were reverse-transcribed to cDNA using the High Capacity cDNA kit (4374966; Life Technologies, Carlsbad, USA) according to manufacturer's protocol. TaqMan- and SYBR Green-based qRT-PCR were then performed on the synthesised cDNA using an Applied Biosystem StepOnePlus thermocycler (Life Technologies, Carlsbad, USA). β-actin was used for normalisation and fold change was determined using the ΔΔCT method. TaqMan Fast Universal PCR Master Mix (4352042; Life Technologies, Carlsbad, USA) and Fast SYBR Green Master Mix (4385612; Life Technologies, Carlsbad, USA) were used for TaqMan- and SYBR Green-based qRT-PCR, respectively.

TaqMan probes and SYBR Green primer sequences

The following TaqMan probes were used for TaqMan-based qRT-PCR: CA9 (hs00154208_m1), FIH (h00215495_m1), β-actin (4326315E). All probes were from Life Technologies (Carlsbad, USA).

The following primers were used for SYBR Green-based qRT-PCR:

Gene	Forward primer	Reverse primer
EGLN3	CACGAAGTGCAGCCCTCTTA	TTGGCTTCTGCCCTTTCTTCA
SOX9	GGAGCTCGAAACTGACTGGA	GTTTCCGGGGTTGAAACTCG
CXCR4	GGCAGAGGAGTTAGCCAAGA	GAACAAAAGGGCACTGAGACG
β-actin	ACCATGGATGATGATATCGCC	GCCTTGCACATGCCGG

6.9 References

1 Schofield, C. J. and Ratcliffe, P. J. (2004) Oxygen sensing by HIF hydroxylases. Nat Rev Mol Cell Biol. **5**, 343-354

2 Bruick, R. K. and McKnight, S. L. (2001) A conserved family of prolyl-4-hydroxylases that modify HIF. Science. **294**, 1337-1340

3 Epstein, A. C., Gleadle, J. M., McNeill, L. A., Hewitson, K. S., O'Rourke, J., Mole, D. R., Mukherji, M., Metzen, E., Wilson, M. I., Dhanda, A., Tian, Y. M., Masson, N., Hamilton, D. L., Jaakkola, P., Barstead, R., Hodgkin, J., Maxwell, P. H., Pugh, C. W., Schofield, C. J. and Ratcliffe, P. J. (2001) C. elegans EGL-9 and mammalian homologs define a family of dioxygenases that regulate HIF by prolyl hydroxylation. Cell. **107**, 43-54

4 Hewitson, K. S., McNeill, L. A., Riordan, M. V., Tian, Y. M., Bullock, A. N., Welford, R. W., Elkins, J. M., Oldham, N. J., Bhattacharya, S., Gleadle, J. M., Ratcliffe, P. J., Pugh, C. W. and Schofield, C. J. (2002) Hypoxia-inducible factor (HIF) asparagine hydroxylase is identical to factor inhibiting HIF (FIH) and is related to the cupin structural family. J Biol Chem. **277**, 26351-26355

5 Lando, D., Peet, D. J., Gorman, J. J., Whelan, D. A., Whitelaw, M. L. and Bruick, R. K. (2002) FIH-1 is an asparaginyl hydroxylase enzyme that regulates the transcriptional activity of hypoxia-inducible factor. Genes Dev. **16**, 1466-1471

6 Rabinowitz, M. H. (2013) Inhibition of hypoxia-inducible factor prolyl hydroxylase domain oxygen sensors: tricking the body into mounting orchestrated survival and repair responses. J Med Chem. **56**, 9369-9402

7 Yan, L., Colandrea, V. J. and Hale, J. J. (2010) Prolyl hydroxylase domain-containing protein inhibitors as stabilizers of hypoxia-inducible factor: small molecule-based therapeutics for anemia. Expert Opin Ther Pat. **20**, 1219-1245

8 Elvidge, G. P., Glenny, L., Appelhoff, R. J., Ratcliffe, P. J., Ragoussis, J. and Gleadle, J. M. (2006) Concordant regulation of gene expression by hypoxia and 2-oxoglutarate-dependent dioxygenase inhibition: the role of HIF-1alpha, HIF-2alpha, and other pathways. J Biol Chem. **281**, 15215-15226

9 Rose, N. R., Woon, E. C., Tumber, A., Walport, L. J., Chowdhury, R., Li, X. S., King, O. N., Lejeune, C., Ng, S. S., Krojer, T., Chan, M. C., Rydzik, A. M., Hopkinson, R. J., Che, K. H., Daniel, M., Strain-Damerell, C., Gileadi, C., Kochan, G., Leung, I. K., Dunford, J., Yeoh, K. K., Ratcliffe, P. J., Burgess-Brown, N., von Delft, F., Muller, S., Marsden, B., Brennan, P. E., McDonough, M. A., Oppermann, U., Klose, R. J., Schofield, C. J. and Kawamura, A. (2012) Plant growth regulator daminozide is a selective inhibitor of human KDM2/7 histone demethylases. J Med Chem. **55**, 6639-6643

10 Wang, Z., Gerstein, M. and Snyder, M. (2009) RNA-Seq: a revolutionary tool for transcriptomics. Nat Rev Genet. **10**, 57-63

11 Huang da, W., Sherman, B. T. and Lempicki, R. A. (2009) Systematic and integrative analysis of large gene lists using DAVID bioinformatics resources. Nat Protoc. **4**, 44-57

12 Schodel, J., Mole, D. R. and Ratcliffe, P. J. (2013) Pan-genomic binding of hypoxia-inducible transcription factors. Biol Chem. **394**, 507-517

13 Schodel, J., Oikonomopoulos, S., Ragoussis, J., Pugh, C. W., Ratcliffe, P. J. and Mole, D. R. (2011) High-resolution genome-wide mapping of HIF-binding sites by ChIP-seq. Blood. **117**, e207-217

14 Appelhoff, R. J., Tian, Y. M., Raval, R. R., Turley, H., Harris, A. L., Pugh, C. W., Ratcliffe, P. J. and Gleadle, J. M. (2004) Differential function of the prolyl hydroxylases PHD1, PHD2, and PHD3 in the regulation of hypoxia-inducible factor. J Biol Chem. **279**, 38458-38465

15 McDonough, M. A., McNeill, L. A., Tilliet, M., Papamicael, C. A., Chen, Q. Y., Banerji, B., Hewitson, K. S. and Schofield, C. J. (2005) Selective inhibition of factor inhibiting hypoxia-inducible factor. J Am Chem Soc. **127**, 7680-7681

16 Chowdhury, R., Candela-Lena, J. I., Chan, M. C., Greenald, D. J., Yeoh, K. K., Tian, Y. M., McDonough, M. A., Tumber, A., Rose, N. R., Conejo-Garcia, A., Demetriades, M., Mathavan, S., Kawamura, A., Lee, M. K., van Eeden, F., Pugh, C. W., Ratcliffe, P. J. and Schofield, C. J. (2013) Selective Small Molecule Probes for the Hypoxia Inducible Factor (HIF) Prolyl Hydroxylases. ACS Chem Biol. **8**, 1488-1496

17 Tian, Y. M., Yeoh, K. K., Lee, M. K., Eriksson, T., Kessler, B. M., Kramer, H. B., Edelmann, M. J., Willam, C., Pugh, C. W., Schofield, C. J. and Ratcliffe, P. J. (2011) Differential sensitivity of hypoxia inducible factor hydroxylation sites to hypoxia and hydroxylase inhibitors. J Biol Chem. **286**, 13041-13051

18 Stolze, I. P., Tian, Y. M., Appelhoff, R. J., Turley, H., Wykoff, C. C., Gleadle, J. M. and Ratcliffe, P. J. (2004) Genetic analysis of the role of the asparaginyl hydroxylase factor inhibiting hypoxia-inducible factor (FIH) in regulating hypoxia-inducible factor (HIF) transcriptional target genes [corrected]. J Biol Chem. **279**, 42719-42725

19 Dayan, F., Roux, D., Brahimi-Horn, M. C., Pouyssegur, J. and Mazure, N. M. (2006) The oxygen sensor factor-inhibiting hypoxia-inducible factor-1 controls expression of distinct genes through the bifunctional transcriptional character of hypoxia-inducible factor-1alpha. Cancer Res. **66**, 3688-3698

20 Sanchez-Fernandez, E. M., Tarhonskaya, H., Al-Qahtani, K., Hopkinson, R. J., McCullagh, J. S., Schofield, C. J. and Flashman, E. (2013) Investigations on the oxygen dependence of a 2-oxoglutarate histone demethylase. Biochem J. **449**, 491-496

21 Flashman, E., Hoffart, L. M., Hamed, R. B., Bollinger, J. M., Jr., Krebs, C. and Schofield, C. J. (2010) Evidence for the slow reaction of hypoxia-inducible factor prolyl hydroxylase 2 with oxygen. FEBS J. **277**, 4089-4099

22 Pollard, P. J., Loenarz, C., Mole, D. R., McDonough, M. A., Gleadle, J. M., Schofield, C. J. and Ratcliffe, P. J. (2008) Regulation of Jumonji-domain-containing histone demethylases by hypoxia-inducible factor (HIF)-1alpha. Biochem J. **416**, 387-394

23 Glover, L. E., Bowers, B. E., Saeedi, B., Ehrentraut, S. F., Campbell, E. L., Bayless, A. J., Dobrinskikh, E., Kendrick, A. A., Kelly, C. J., Burgess, A., Miller, L., Kominsky, D. J., Jedlicka, P. and Colgan, S. P. (2013) Control of creatine metabolism by HIF is an endogenous mechanism of barrier regulation in colitis. Proc Natl Acad Sci U S A. **110**, 19820-19825

24 Mariani, C. J., Vasanthakumar, A., Madzo, J., Yesilkanal, A., Bhagat, T., Yu, Y., Bhattacharyya, S., Wenger, R. H., Cohn, S. L., Nanduri, J., Verma, A., Prabhakar, N. R. and Godley, L. A. (2014) TET1-Mediated Hydroxymethylation Facilitates Hypoxic Gene Induction in Neuroblastoma. Cell Rep

25 Zhang, Y., Wang, H., Zhang, J., Lv, J. and Huang, Y. (2013) Positive feedback loop and synergistic effects between hypoxia-inducible factor-2alpha and stearoyl-CoA desaturase-1 promote tumorigenesis in clear cell renal cell carcinoma. Cancer Sci. **104**, 416-422

26 Buchholz, B., Schley, G., Faria, D., Kroening, S., Willam, C., Schreiber, R., Klanke, B., Burzlaff, N., Jantsch, J., Kunzelmann, K. and Eckardt, K. U. (2014) Hypoxia-inducible factor-1alpha causes renal cyst expansion through calcium-activated chloride secretion. J Am Soc Nephrol. **25**, 465-474

27 Ortiz-Barahona, A., Villar, D., Pescador, N., Amigo, J. and del Peso, L. (2010) Genome-wide identification of hypoxia-inducible factor binding sites and target genes by a probabilistic model integrating transcription-profiling data and in silico binding site prediction. Nucleic Acids Res. **38**, 2332-2345

28 http://www.bioinformatics.babraham.ac.uk/projects/fastqc/.

29 Kim, D., Pertea, G., Trapnell, C., Pimentel, H., Kelley, R. and Salzberg, S. L. (2013) TopHat2: accurate alignment of transcriptomes in the presence of insertions, deletions and gene fusions. Genome Biol. **14**, R36

30 Sims, D., Ilott, N. E., Sansom, S. N., Sudbery, I. M., Johnson, J. S., Fawcett, K. A., Berlanga-Taylor, A. J., Luna-Valero, S., Ponting, C. P. and Heger, A. (2014) CGAT: computational genomics analysis toolkit. Bioinformatics. **30**, 1290-1291

31 Anders, S. and Huber, W. (2010) Differential expression analysis for sequence count data. Genome Biol. **11**, R106

32 Trapnell, C., Williams, B. A., Pertea, G., Mortazavi, A., Kwan, G., van Baren, M. J., Salzberg, S. L., Wold, B. J. and Pachter, L. (2010) Transcript assembly and quantification by RNA-Seq

reveals unannotated transcripts and isoform switching during cell differentiation. Nat Biotechnol. **28**, 511-515

33 Smyth, G. K. (2005) Limma: linear models for microarray data. Bioinformatics and Computational Biology Solutions using R and Bioconductor, R, 397-420

Chapter 7: Conclusions and future perspective

In animals, the hypoxia-inducible factor (HIF) plays a key role in mediating the cellular transcriptional response to decreased oxygen levels. The levels and activity of HIF are regulated by the PHDs and FIH, respectively. In the work described in **Chapter 2**, *in vitro* assays based on the AlphaScreen methodology (PHD2 CODD and NODD AlphaScreen assays) were developed for the inhibition studies of PHD2. These assays are suitable for use in medium- or high-throughput screens, and the PHD2 CODD AS assay has been utilised in the identification and characterisation of PHD2 inhibitors. Additionally, the PHD2 NODD AS assay could potentially be used for the identification of small molecules that selectively inhibit either the hydroxylation of NODD, CODD or both. The availability of similar AlphaScreen-based assays for the JmjC-domain containing human histone demethylases has enabled *in vitro selectivity* studies for small molecule inhibitors of PHD2.

For cellular studies of PHD inhibition, electrochemiluminescence-based assays for HIF1α and HIF2α have been developed (**Chapter 3**). These quantitative and relatively high-throughput assays can be used in complement to the immunoblotting techniques typically used to study the inhibition of the PHDs based on the induction of HIFα. The relative efficacies of small molecule inhibitors in inhibiting endogenous PHDs in various cell lines can be measured using these assays. Feasibility studies using mouse liver samples show that this assay can also be utilised for the detection of HIF1α and HIF2α in primary tissues.

The identification of PHD2 inhibitors using the *in vitro* AlphaScreen assay for PHD2 led to the characterisation of potent, selective and cell-permeable small molecule inhibitors for the PHDs (i.e. IOX2 and IOX4), as described in **Chapter 4**. These inhibitors are suitable for use as chemical probes for the functional studies on the biological roles of the PHDs, and could

serve as a complementary approach to the genetic knockout and knockdown by RNA interference methods. These chemical probes have also been shown to be active in animal models (zebrafish and mice).

In vitro studies on the selectivity of small molecule inhibitors towards different PHD isoforms have been lacking due to the difficulty in isolating PHD1 and PHD3. To circumvent this problem, a cellular model system using PHD-null mouse embryonic fibroblast cells (TKO) has been developed (**Chapter 5**). The TKO cells lack all three PHD isoforms (PHD1, PHD2 and PHD3), therefore the re-expression of individual PHD isoforms (either constitutively or in an inducible manner) in the cellular model system developed enables the determination of the isoform selectivity of PHD inhibitors based on the levels of HIF induction. Preliminary studies show some degree of selectivity within the PHD inhibitors tested, although further studies are warranted to verify the observed selectivity within the PHD isoforms.

In **Chapter 6**, pan-genomic studies to study the extent of the PHD and FIH mediated transcriptional response to hypoxia were described. Initial RNA-seq studies on the transcriptional response to DMOG and PHD inhibitors (including IOX2, the chemical probe developed for the PHDs) compared to the response to hypoxia (0.5% O_2) reveal that DMOG is a better mimic of hypoxia than the more selective PHD inhibitors. The inhibition of both the PHDs and FIH was not sufficient to explain the broad concordance between DMOG and hypoxia, suggesting that part of the transcriptional response to hypoxia is mediated by an additional factor(s). A subset of genes that were upregulated by hypoxia, but were not responsive to PHD or FIH inhibition has been identified. Some of these genes are responsive to DMOG, indicating that they may be regulated by one or more factor(s) that is part of the 2OG-dependent dioxygenase family. Further studies on these genes could potentially lead to

the identification of a novel oxygen sensor, which may work collectively or independently of the HIF pathway.

Overall, the assays and cellular model systems described in this thesis led to the identification and characterisation of PHD inhibitors *in vitro* and in cells. The identification of selective, potent and cell-permeable small molecule inhibitors for the PHDs has enabled the dissection of the role of the PHDs as cellular oxygen sensors in mediating the transcriptional response to hypoxia. Future studies utilising the assays and cellular model systems developed would facilitate the development and identification of PHD-isoform selective inhibitors, which will be beneficial in studying the roles of individual PHD isoforms in mediating the transcriptional response to hypoxia.

Appendix 1: Inhibitors tested using the PHD2 CODD AlphaScreen assay

	Compound designated name	Structure	PHD2 IC_{50} (µM)
1	BIQ	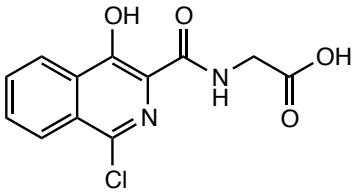	0.33
2	NOG	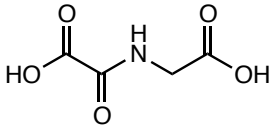	11.2
3	DE-2OG	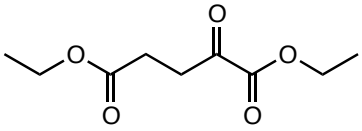	> 1000
4	DTF-2OG	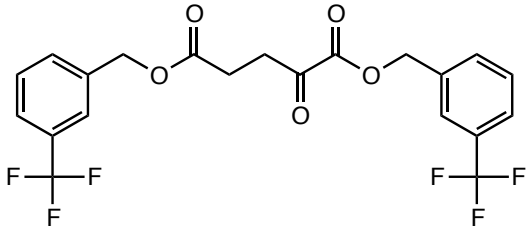	> 500
5	DM-2OG	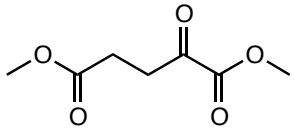	> 1000
6	MO-2OG	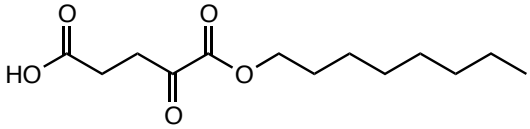	> 1000
7	DM-Fumarate	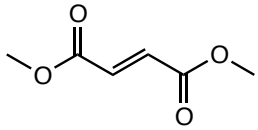	> 500
8	DM-Succinate	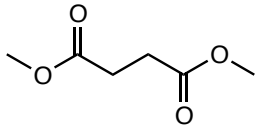	> 1000
9	ME-2OG	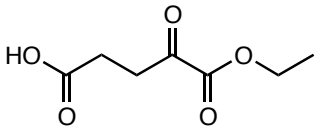	> 1000
10	MTF-2OG	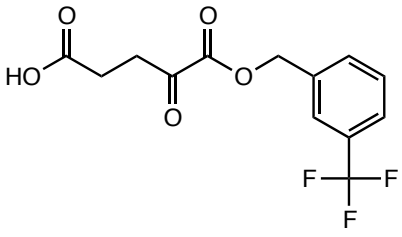	> 1000

11	MM-2OG	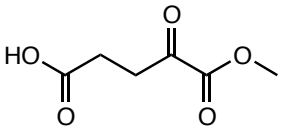	> 1000
12	Fumarate	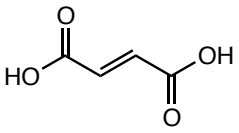	0.8
13	L-Ala-BIQ	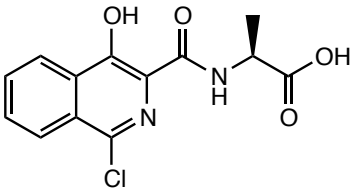	1.1
14	D-Ala-BIQ	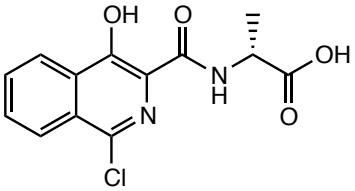	> 200
15	D-Phe-BIQ	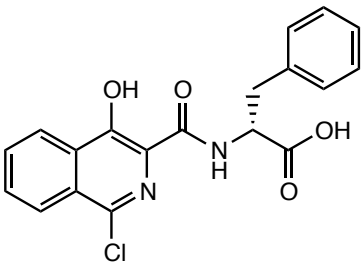	> 200
16	L-Phe-BIQ	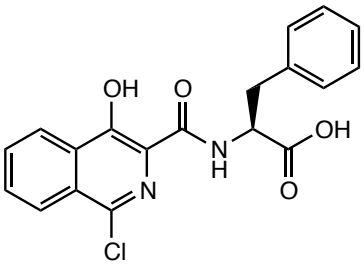	> 200
17	D-Val-BIQ	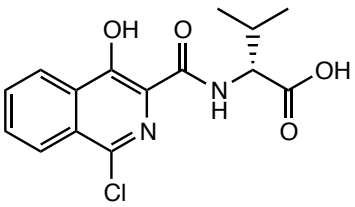	> 200
18	L-Val-BIQ	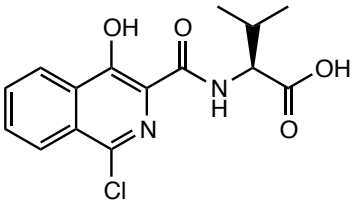	> 200
19	D-Ala-NOG	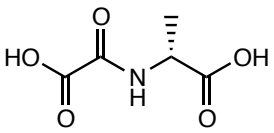	> 200

20	L-Ala-NOG	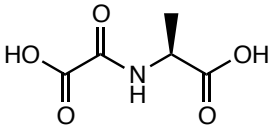	9.5
21	D-Val-NOG	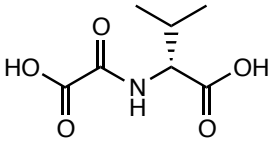	> 200
22	L-Val-NOG	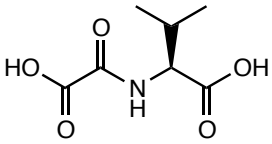	> 200
23	D-Leu-NOG	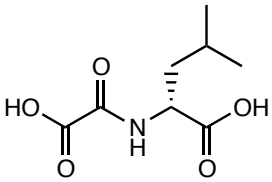	> 200
24	L-Leu-NOG	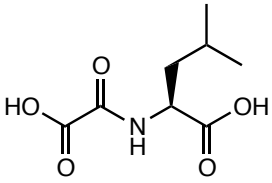	> 200
25	D-Phe-NOG	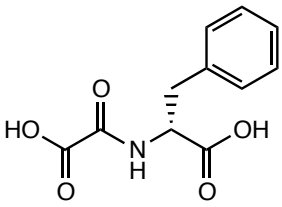	> 200
26	L-Phe-NOG	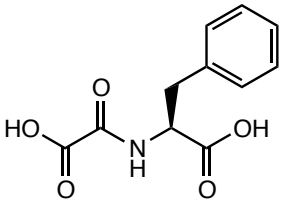	> 200
27	D-Tyr-NOG	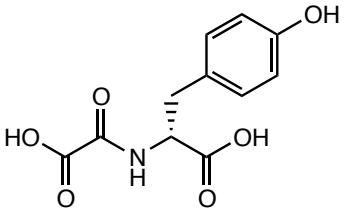	> 200
28	L-Tyr-NOG	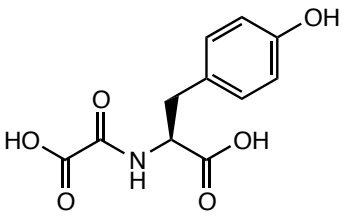	> 200

29	D-Cys-NOG	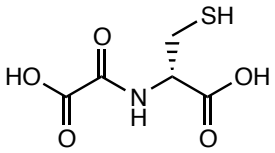	> 200
30	L-Cys-NOG	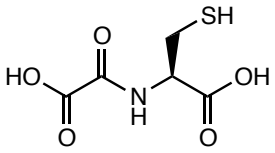	> 200
31	EW94	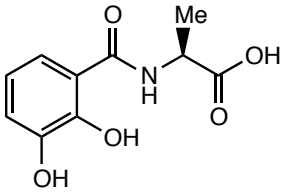	36.9
32	EW96	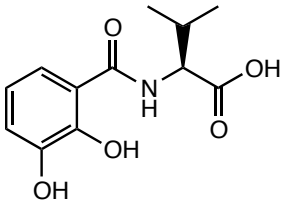	23.32
33	EW98	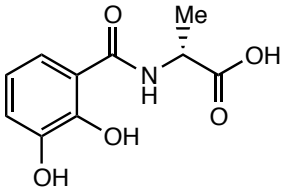	8.7
34	EW910	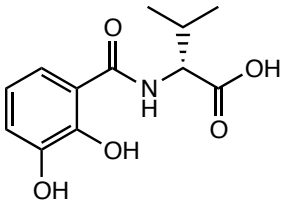	58
35	EW912	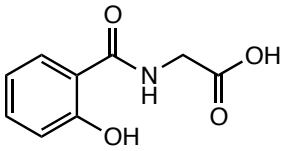	64.1
36	EW913	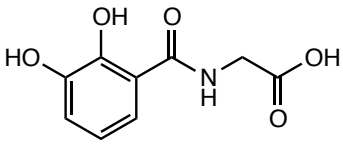	19
37	EW914	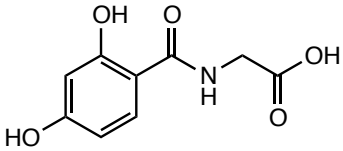	16.5
38	EW915	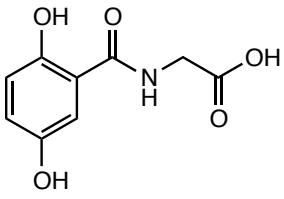	40.9

39	EW51	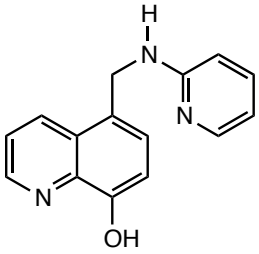	> 100
40	MD251	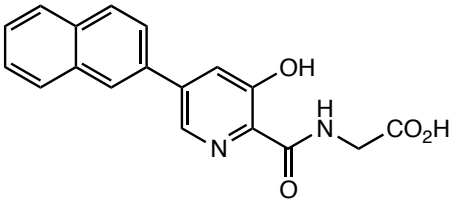	0.017
41	MD253	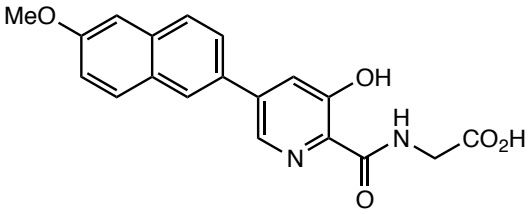	0.013
42	MD203	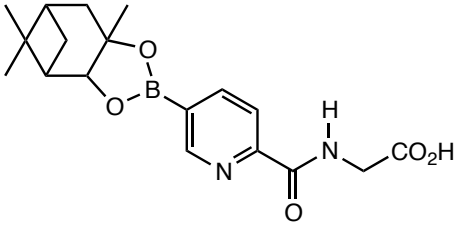	> 1000
43	MD208	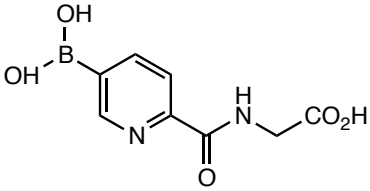	125.5
44	MD230	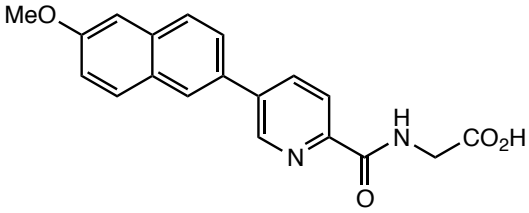	106.5
45	MD232	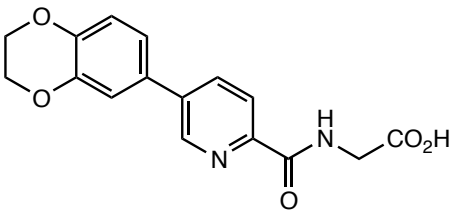	135.5
46	MD255	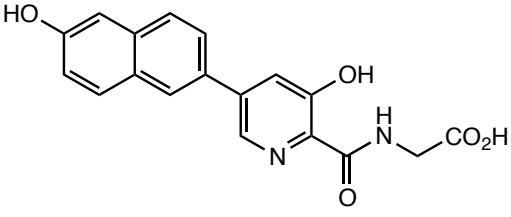	0.004

47	MD263	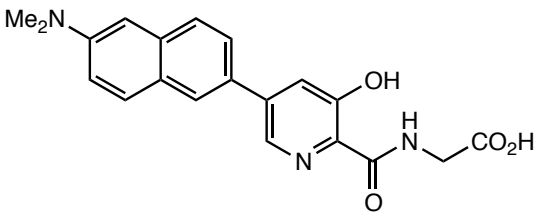	0.172
48	MD246	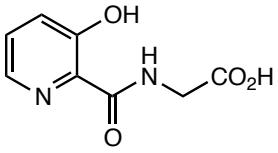	409
49	JICL25	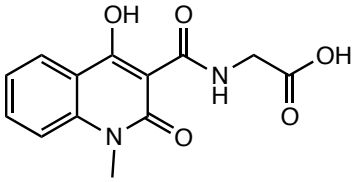	0.033
50	JICL26	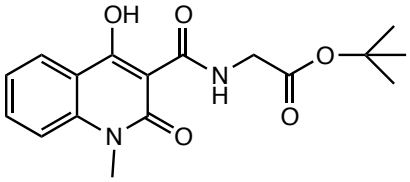	> 300
51	JICL38	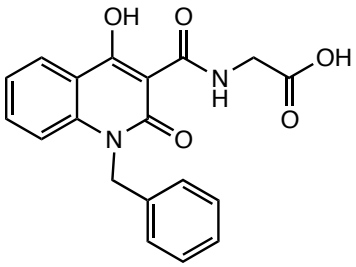	0.022
52	JICL48	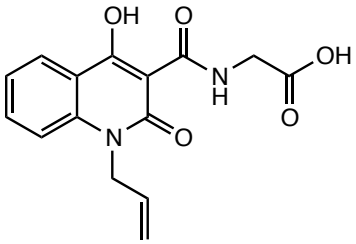	1.47
53	JICL49	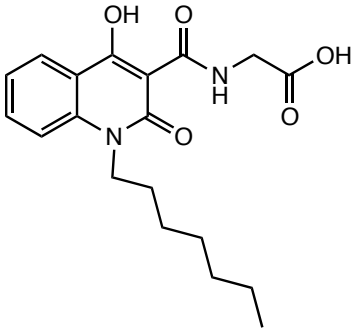	0.66

54	JICL56	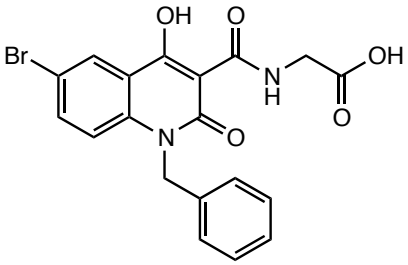	0.078
55	EW105	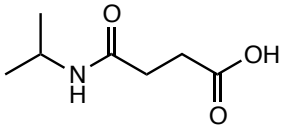	> 100
56	EW109	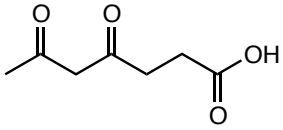	~ 100
57	EW116	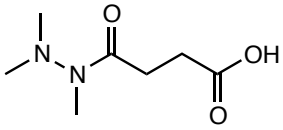	> 100
58	EW126	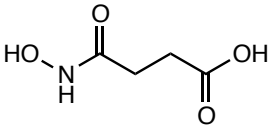	~ 100
59	CL-01-114	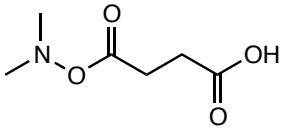	6.3
60	CL-02-058	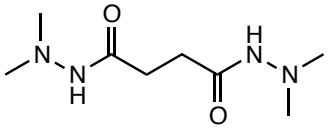	> 100
61	Daminozide	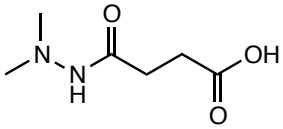	> 1000
62	EW100	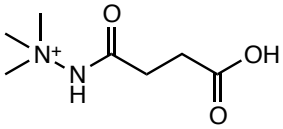	> 1000
63	EW101	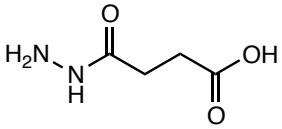	396.2
64	EW102	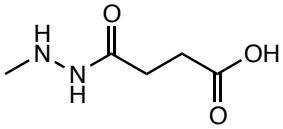	14.2
65	VGP5	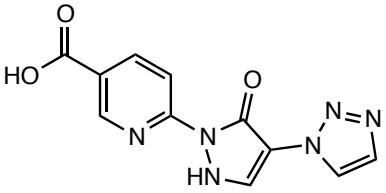	0.004

66	VFGP10B	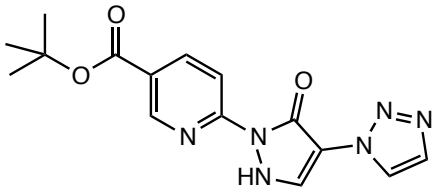	0.0016
67	VGP12B	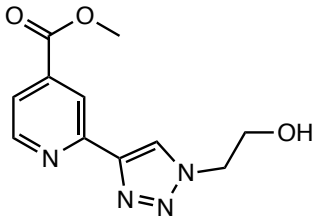	> 200
68	VGP13	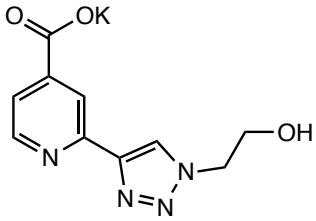	> 200
69	VGP17	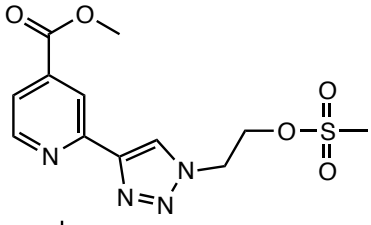	> 200
70	VGP19	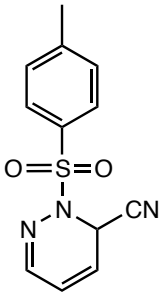	> 200
71	IOX1, 5COOH8HQ	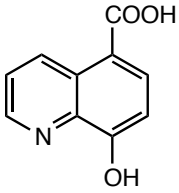	~93
72	2,4 PDCA	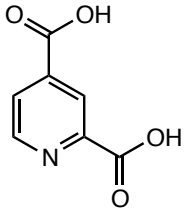	28.6
73	IS68	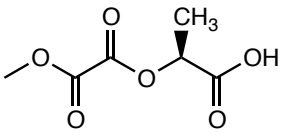	> 100

74	IS69	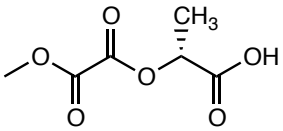	~ 100
75	8HQ	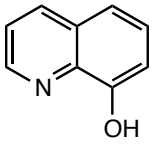	~90
76	5-NO2-8HQ	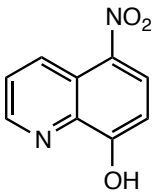	127.9
77	2Fe-6	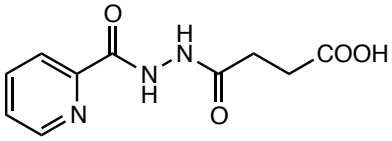	> 300
78	2Fe-7	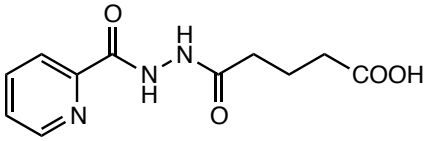	> 300
79	2Fe-8	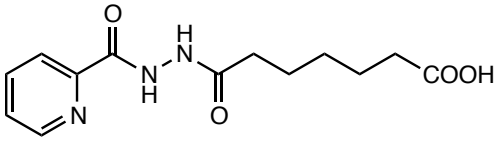	> 300
80	2Fe-9	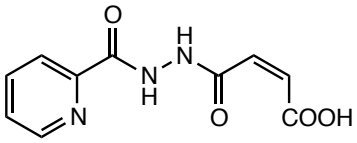	> 300
81	2Fe-10	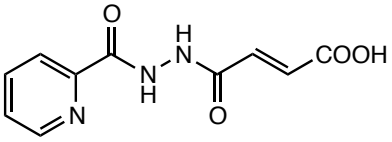	47
82	2Fe-12	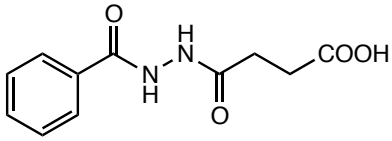	> 300
83	2Fe-18	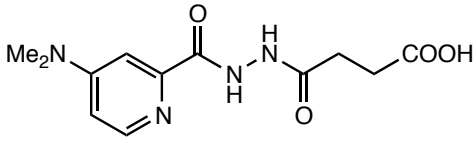	0.3
84	2Fe-19	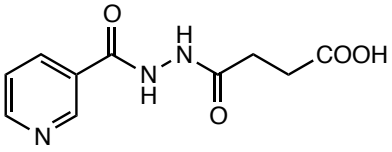	40

85	2Fe-20	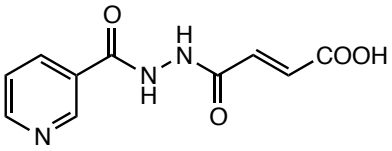	0.082
86	2Fe-21	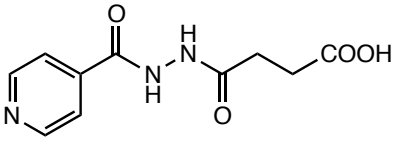	> 300
87	2Fe-22	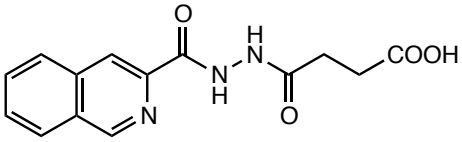	18.4
88	2Fe-23	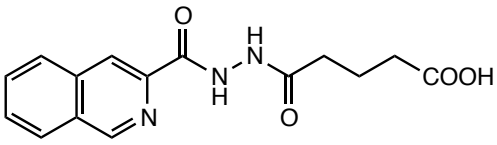	24.6
89	2Fe-24	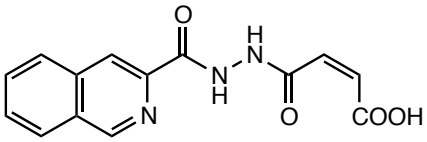	> 300
90	2Fe-25	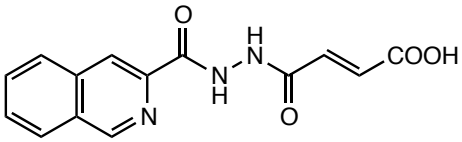	> 300
91	2Fe-26	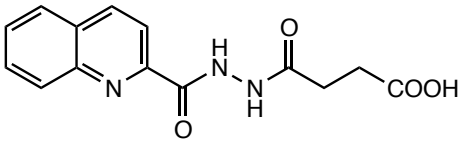	9.7
92	2Fe-27	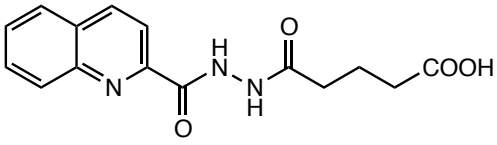	> 300
93	2Fe-28	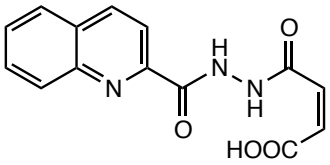	> 300
94	2Fe-29	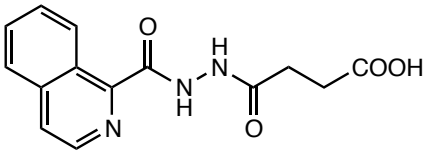	> 300
95	2Fe-30	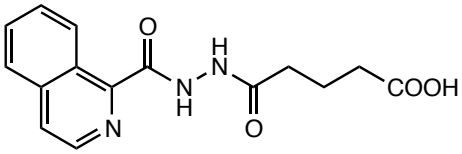	> 300

96	2Fe-31	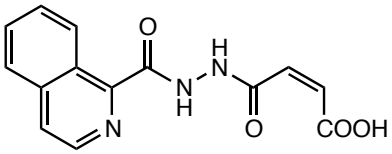	> 300
97	2Fe-32	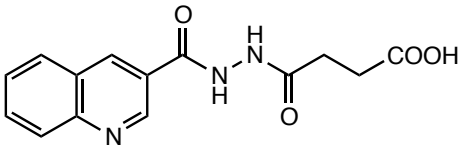	21
98	2Fe-33	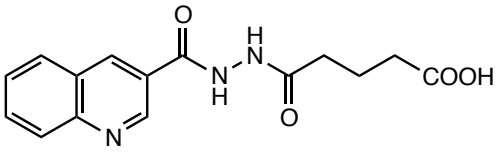	> 300
99	2Fe-34	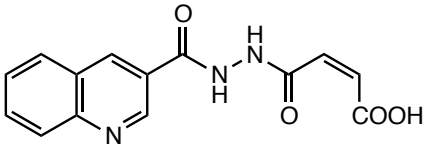	> 300
100	2Fe-39	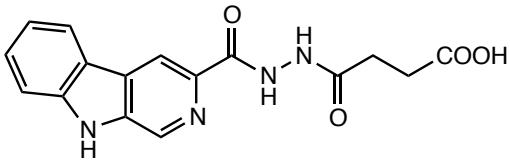	0.4
101	2Fe-40	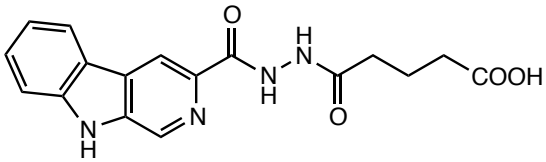	0.13
102	2Fe-42	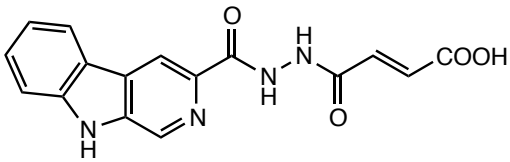	54
103	CL-03-022	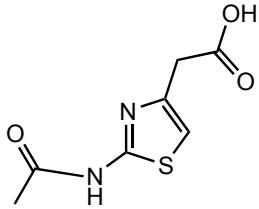	> 100
104	CL-03-024	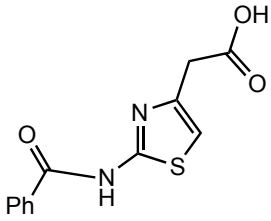	> 100
105	CL-03-026	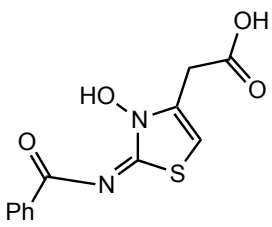	> 100

106	CL-03-028	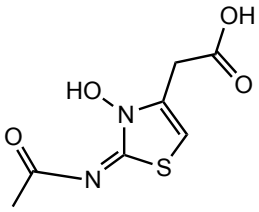	> 100
107	CL-03-080	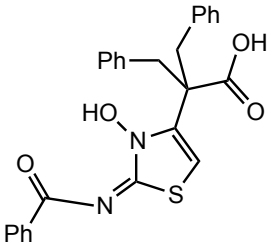	> 100
108	CL-03-092-1	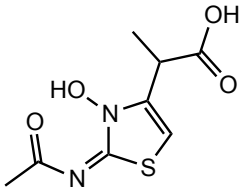	> 100
109	CL-03-130	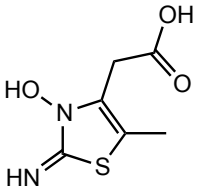	~ 100
110	CL-03-074	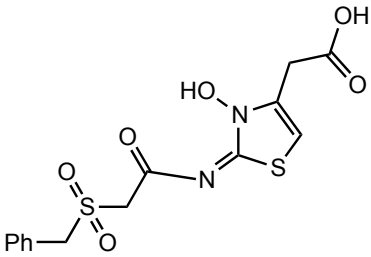	0.021
111	CL-03-154	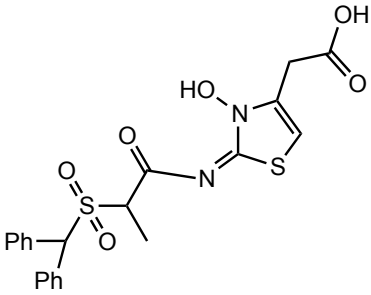	0.003
112	CL-04-058	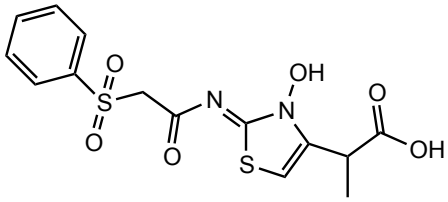	7

113	CL-04-052	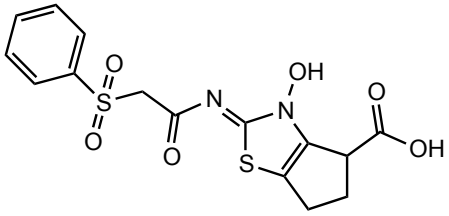	> 100
114	CL-02-176	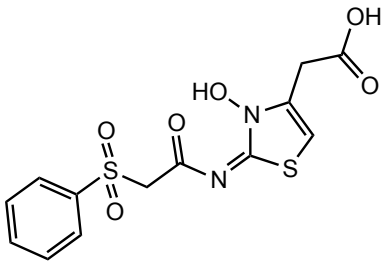	0.019
115	CL-RASHED/BNS	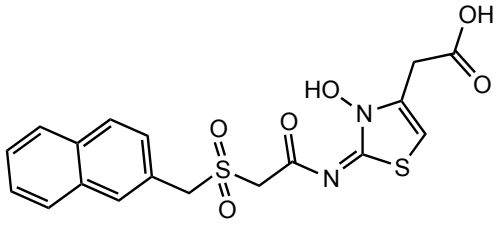	0.002
116	CL-05-156	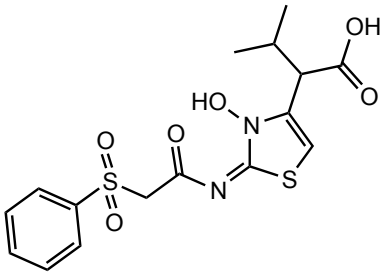	> 200
117	CL-02-180	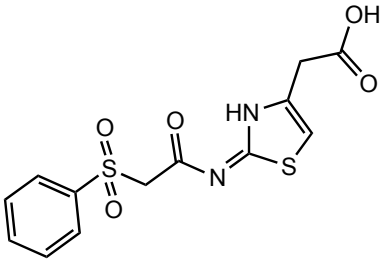	> 200
118	CL-05-158	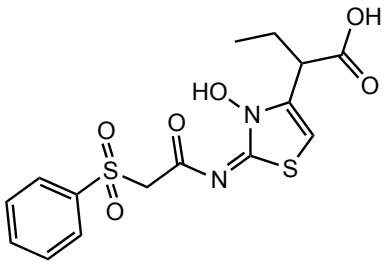	> 200
119	CL-05-142	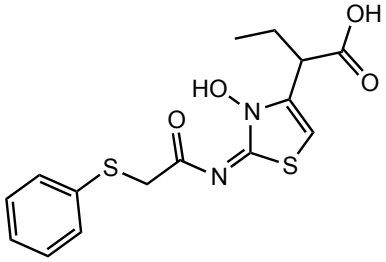	> 200

120	CL-05-186	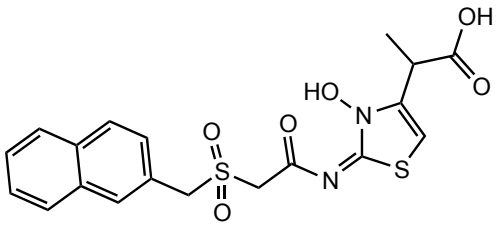	> 200
121	CL-05-190	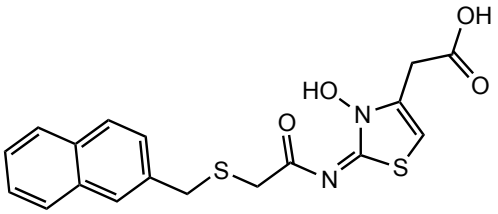	0.007
122	CL-05-212-9	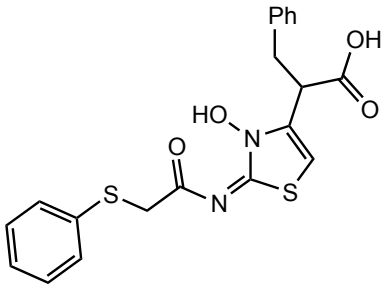	> 200
123	CL-05-212-10	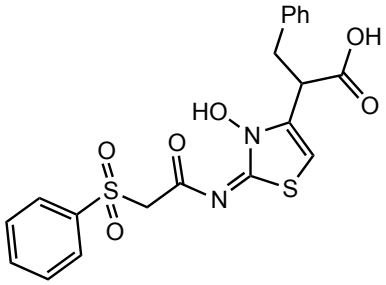	> 100
124	CL-05-212-11	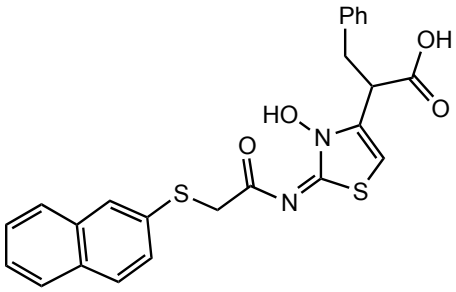	> 200
125	CL-05-212-13	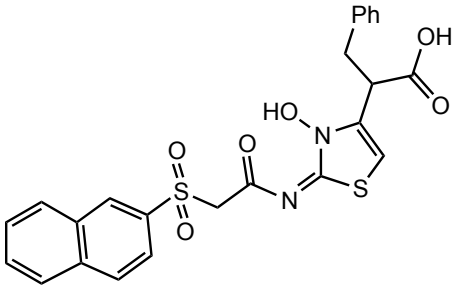	> 100

126	CL-05-219	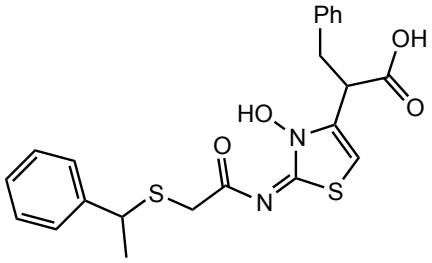	> 200
127	CL-05-221	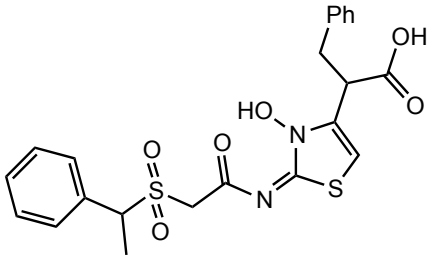	> 200

Appendix 2: Hypoxia upregulated genes (RNA-seq)

		Fold change (adjusted pvalue <0.05)					
		Hypoxia	DMOG	IOX2	BNS	BIQ	Cluster
1	CA9	654.6	648.8	157.5	129.4	111.4	C4
2	KB-1980E6.3	110.1	20.7	39.0	28.1	26.2	C1
3	LOX	66.4	23.0	27.9	11.0	22.6	C1
4	MSLNL	52.0	10.1	5.9	5.1	5.1	C1
5	CYP1A1	50.3	4.1	3.3	3.5	5.6	C1
6	RNF183	47.4	25.3	23.0	18.7	20.1	C1
7	MAP7D2	46.9	43.8	5.6	5.0	5.1	C4
8	TMEM74B	46.2	18.7	24.0	11.8	20.9	C1
9	NDRG1	43.2	59.2	13.4	12.3	16.8	C4
10	ISM2	41.9	18.0	17.9	9.7	10.0	C1
11	CASP14	36.1	22.0	8.6	9.0	2.8	C1
12	PPFIA4	35.1	22.4	27.1	20.8	28.6	C2
13	ADM	32.6	29.4	13.1	9.3	13.0	C4
14	PPP1R3G	25.8	20.8	16.2	13.2	18.2	C2
15	PFKFB4	24.5	21.7	12.8	11.0	11.9	C4
16	SEMA5B	23.1	19.2	4.2	4.7	4.3	C4
17	SLC28A1	22.9	16.8	5.9	5.4	4.7	C4
18	FAM115C	22.4	20.0	13.3	13.2	13.9	C4
19	TLE6	20.4	9.4	9.5	5.3	6.6	C1
20	ALDOC	17.5	12.4	12.2	8.5	11.4	C2
21	SLC2A14	16.9	6.1	2.2	1.4	0.7	C1
22	PDK1	15.9	10.8	9.4	8.2	9.5	C2
23	RCN3	15.2	5.3	8.3	6.2	6.7	C1
24	LRP1	14.6	9.8	4.5	2.6	3.7	C1
25	IGFBP3	14.6	12.6	4.1	2.8	4.8	C4
26	C4orf47	14.2	5.0	14.3	8.5	13.5	C2
27	PGM1	14.0	12.8	12.3	10.7	11.3	C2
28	UPK1A	13.6	3.7	3.0	2.2	2.5	C1
29	AP000769.1	13.4	8.2	5.1	6.5	4.1	C1
30	SH3GL3	13.3	9.7	5.4	4.1	5.8	C4
31	AK4	13.1	11.3	10.4	10.2	10.6	C2
32	SCNN1B	13.1	9.9	3.0	2.2	1.7	C4
33	TMEM45A	13.1	12.3	6.3	5.0	6.4	C4
34	C2orf72	12.7	7.3	10.3	7.5	10.0	C2
35	BNIP3	12.7	11.0	9.2	8.7	9.3	C2
36	EMR2	12.2	4.4	2.3	2.3	1.6	C1
37	ANGPTL4	12.1	13.5	5.7	3.2	5.3	C4
38	SYDE1	11.9	6.9	5.2	3.9	4.0	C1
39	RP11-480I12.4	11.7	5.0	9.9	7.8	10.2	C2
40	SPAG4	11.7	6.8	8.7	6.6	7.7	C2
41	ANKRD37	11.1	13.4	5.3	4.8	5.6	C4
42	ENO2	11.0	9.9	6.0	4.3	5.7	C4
43	AMPD3	10.3	5.2	4.8	4.8	5.4	C2
44	BNIP3L	10.3	8.9	5.7	5.1	5.8	C4
45	RNF165	10.2	4.5	6.8	4.6	5.7	C2
46	C1orf51	9.8	6.7	11.6	8.5	9.9	C2
47	INHA	9.8	12.3	2.4	1.8	2.1	C4
48	LRP4	9.8	13.6	2.3	1.8	1.9	C4
49	SFXN3	9.4	6.1	4.6	3.3	4.0	C1
50	SPRY1	9.2	8.1	8.0	6.9	9.1	C2
51	EFEMP2	9.0	3.1	3.8	2.9	3.1	C1
52	GPR146	9.0	6.9	7.6	5.2	7.4	C2
53	FAM162A	8.7	8.4	5.5	4.4	5.1	C4
54	FUT3	8.6	2.4	3.2	1.9	2.4	C1
55	SERPINA9	8.6	8.4	3.1	3.6	2.7	C4
56	PLIN2	8.5	3.9	4.7	2.2	3.2	C1
57	SCNN1G	8.5	8.1	2.8	2.1	2.1	C4
58	FOS	8.5	6.5	4.3	3.4	3.5	C4
59	LOXL2	8.2	11.2	2.2	2.0	1.8	C4
60	RIMKLA	8.2	6.0	7.5	6.7	7.7	C2
61	RORA	8.0	7.6	5.0	4.0	5.2	C4
62	HEY1	7.7	10.6	2.2	2.8	1.8	C4
63	FAM13A	7.7	7.6	2.7	1.8	2.6	C4
64	DDIT4	7.6	5.4	3.5	3.3	3.4	C4
65	PDZD7	7.5	4.6	3.8	2.5	2.8	C1
66	PGK1	7.0	7.2	4.7	4.3	4.4	C4
67	NIM1	7.0	2.6	8.0	5.3	6.1	C2
68	DPYSL4	6.7	3.8	4.5	3.6	3.5	C2
69	RRAGD	6.6	3.1	4.6	3.0	4.2	C2
70	VTCN1	6.5	2.6	1.8	1.3	1.7	C1
71	MT1X	6.5	4.2	1.7	2.4	1.3	C1
72	INSIG2	6.5	5.4	3.1	2.8	3.4	C4
73	WSB1	6.4	3.6	2.5	1.9	2.3	C1
74	MXI1	6.3	5.5	4.1	3.0	4.0	C4
75	SMAD9	6.3	5.0	4.1	3.2	3.9	C4
76	THEMIS2	6.1	5.0	2.4	1.4	3.1	C4
77	ANKZF1	6.1	4.3	5.1	4.5	4.7	C2
78	HK2	6.1	8.6	3.6	3.8	3.6	C4
79	EGLN3	6.0	7.6	1.9	1.7	1.7	C4
80	S100A4	6.0	2.7	1.0	0.8	0.8	C1
81	WISP2	5.9	4.1	2.2	1.6	1.8	C1
82	ANG	5.9	6.0	3.7	2.8	4.6	C4
83	LDHA	5.8	6.8	5.1	5.1	4.8	C2
84	STYK1	5.7	3.6	2.7	2.2	3.8	C1
85	ERO1L	5.7	5.4	3.1	2.7	2.7	C4
86	FUT11	5.6	6.0	4.2	3.5	3.9	C4
87	PAM	5.5	5.5	4.8	3.5	4.6	C2
88	HILPDA	5.5	5.9	2.6	2.1	2.6	C4
89	GBE1	5.5	5.9	4.0	4.1	4.1	C4
90	AL137145.1	5.5	4.6	4.5	3.9	4.1	C2
91	C1orf116	5.5	4.7	1.4	1.5	1.1	C4
92	ACAP1	5.4	3.5	2.8	2.4	3.7	C2
93	C8orf58	5.3	5.0	3.1	2.9	2.8	C4
94	VLDLR	5.3	5.0	5.0	4.1	4.8	C2
95	C4orf3	5.3	5.1	3.7	3.5	3.7	C4
96	SLC45A1	5.2	3.9	1.5	0.9	1.5	C4
97	PADI2	5.2	3.6	1.3	1.5	0.8	C1
98	SLC2A12	5.1	3.8	1.5	1.6	1.9	C4
99	BHLHE40	5.1	5.6	3.0	2.5	2.8	C4
100	DAPK2	5.1	4.8	1.8	1.5	1.9	C4
101	PPP1R3E	5.1	3.3	3.0	2.4	3.2	C2
102	ZNF395	5.1	4.7	2.8	2.5	2.5	C4
103	GYS1	5.0	3.4	4.0	3.4	3.9	C2
104	PRELID2	5.0	3.1	3.7	3.1	3.7	C2
105	P4HA2	5.0	5.6	4.1	3.2	3.9	C4
106	GPR155	4.9	2.9	4.1	2.2	3.2	C2
107	P4HA1	4.9	8.0	3.7	3.6	4.0	C4
108	DOK3	4.9	3.2	2.4	2.9	3.0	C2
109	ERRFI1	4.8	6.5	2.1	1.4	2.0	C4
110	DKFZP667F0711	4.8	3.1	2.8	2.4	3.6	C2
111	RNF122	4.7	3.2	3.5	3.1	3.5	C2
112	CCNG2	4.7	3.9	2.6	2.4	2.8	C4
113	WDR66	4.7	3.7	3.9	3.1	3.6	C2
114	HLA-B	4.7	2.2	3.6	3.0	3.1	C2
115	VEGFA	4.6	5.2	3.0	2.3	2.7	C4
116	RORC	4.6	1.1	3.0	1.7	2.8	C2
117	KCTD11	4.5	5.9	2.5	2.3	2.4	C4
118	FAM26F	4.5	4.2	7.5	5.6	5.7	C2
119	RP11-268J15.5	4.4	4.1	4.4	3.4	5.5	C2
120	PRSS53	4.4	3.6	3.5	2.9	3.4	C2
121	CCL28	4.4	2.5	3.9	3.0	3.5	C2
122	ALOXE3	4.4	3.0	2.5	1.6	1.7	C1
123	CYP1B1	4.4	1.2	1.5	1.5	1.4	C1
124	OLFML2A	4.3	3.4	1.7	1.4	1.5	C4
125	TNNI2	4.3	3.3	1.2	1.3	1.0	C4
126	EDN2	4.3	3.8	2.1	1.2	1.0	C4
127	QSOX1	4.3	5.2	2.4	2.3	2.3	C4
128	SPNS2	4.3	3.3	1.1	1.0	0.8	C4
129	RNASE4	4.3	3.6	2.9	2.0	3.8	C2
130	PAG1	4.2	4.2	1.6	1.6	1.6	C4
131	NOL3	4.2	2.7	2.5	2.1	2.6	C2
132	HOXA4	4.2	2.2	3.7	2.7	3.5	C2
133	PFKFB3	4.2	5.4	2.6	2.7	2.6	C4
134	TRIM29	4.1	4.0	1.2	0.9	0.8	C4
135	KIAA1984	4.1	1.2	1.3	0.9	1.5	C1
136	ITGA5	4.1	6.1	2.1	1.6	1.7	C4
137	KRT15	4.1	2.6	0.9	1.3	0.9	C1
138	KDM3A	4.1	5.8	2.7	2.6	2.9	C4
139	LPIN3	4.0	2.7	2.7	2.4	2.8	C2
140	BOC	4.0	3.9	3.0	2.6	2.7	C4

		Fold change (adjusted pvalue <0.05)					
		Hypoxia	DMOG	IOX2	BNS	BIQ	Cluster
141	LY6D	4.0	1.2	0.5	0.5	0.2	C1
142	PCP2	4.0	2.5	3.4	2.8	3.1	C2
143	EGLN1	3.9	4.4	3.6	3.3	3.8	C2
144	SH3D21	3.9	3.2	3.7	3.0	4.2	C2
145	CKB	3.9	1.6	1.9	1.4	1.4	C1
146	CITED2	3.9	2.8	2.0	1.7	1.9	C1
147	NREP	3.8	2.2	2.6	2.7	2.7	C2
148	EHD2	3.8	2.5	1.8	1.4	1.3	C1
149	SYT17	3.8	1.8	2.3	1.6	1.9	C1
150	PTAFR	3.8	2.3	1.2	0.9	0.8	C1
151	GPR19	3.8	1.2	1.8	1.9	1.8	C1
152	PLEKHA2	3.7	2.3	2.4	2.3	2.2	C1
153	BIRC7	3.7	1.3	0.9	1.4	0.9	C1
154	PTRF	3.7	2.6	3.6	2.7	3.0	C2
155	SCARB1	3.6	3.7	1.7	1.6	1.7	C4
156	ARHGEF37	3.6	2.7	2.3	1.8	2.0	C1
157	ISG20	3.6	3.7	1.9	1.4	1.8	C4
158	CD68	3.6	1.9	1.4	1.2	1.4	C1
159	HSF4	3.5	2.3	2.3	1.7	2.3	C1
160	SOX9	3.5	4.7	1.2	1.4	1.5	C4
161	IGFBP5	3.5	3.2	1.5	1.4	1.2	C4
162	SNTA1	3.5	2.5	3.0	2.3	2.6	C2
163	EVPLL	3.5	1.8	1.0	0.9	1.0	C1
164	GLRX	3.5	2.2	2.0	1.5	1.8	C1
165	VPS37D	3.5	2.8	2.1	2.0	1.8	C4
166	RAB3A	3.5	1.6	3.7	3.0	2.9	C2
167	PNRC1	3.4	3.9	2.1	2.2	2.5	C4
168	SLC2A1	3.4	3.4	2.1	2.0	2.2	C4
169	PLAUR	3.4	4.3	1.8	1.4	1.4	C4
170	CSRP2	3.4	2.2	3.6	2.7	2.9	C2
171	DLL1	3.4	2.2	1.6	1.5	1.8	C1
172	ZNF160	3.4	3.1	3.1	2.7	3.0	C2
173	PIAS2	3.4	2.3	3.0	2.6	2.5	C2
174	TCP11L2	3.4	3.4	2.0	1.8	2.2	C4
175	FANK1	3.4	2.8	1.6	1.4	1.5	C4
176	ARTN	3.4	3.8	1.4	1.1	0.9	C4
177	BDH2	3.4	1.5	2.0	1.5	1.8	C2
178	ILVBL	3.4	2.9	1.9	1.7	1.8	C4
179	PIK3IP1	3.4	2.0	1.9	2.0	2.0	C1
180	P2RY11	3.4	2.9	2.0	2.0	2.4	C4
181	HLA-DRB1	3.3	3.1	2.5	2.6	2.0	C4
182	ARID5A	3.3	3.0	1.9	1.8	1.6	C4
183	DSP	3.3	3.5	1.8	1.6	1.7	C4
184	MUC1	3.3	1.3	1.2	1.2	0.8	C1
185	NPR3	3.3	1.2	2.2	1.3	1.6	C1
186	MB	3.3	1.7	1.0	1.2	1.0	C1
187	METTL21B	3.3	2.1	2.0	1.7	2.0	C1
188	ALDOA	3.3	3.9	2.3	2.3	2.5	C4
189	SAMD4A	3.3	5.4	1.5	1.2	1.4	C4
190	ELF5	3.3	1.4	1.2	1.2	1.1	C1
191	PDGFB	3.3	3.2	1.5	1.4	1.2	C4
192	TET1	3.3	1.7	1.3	1.5	1.2	C1
193	PFKP	3.3	3.5	2.8	2.6	2.6	C2
194	IER3	3.3	1.6	2.0	1.6	1.6	C1
195	MPI	3.3	2.1	3.0	2.4	2.8	C2
196	PPP1R3C	3.3	3.7	2.7	2.6	2.4	C4
197	MTFP1	3.3	3.1	3.1	3.2	2.9	C2
198	LIMCH1	3.2	4.2	1.9	1.6	2.2	C4
199	NUDT13	3.2	1.5	1.9	1.9	2.3	C2
200	WNT10B	3.2	1.8	1.5	1.1	1.1	C1
201	STC1	3.2	2.8	2.8	2.6	2.3	C2
202	ATG9B	3.2	2.2	1.0	1.1	1.1	C1
203	ITGA2B	3.2	1.8	1.7	1.5	1.8	C2
204	SLC29A4	3.2	3.2	1.5	1.4	1.2	C4
205	PLCH2	3.2	1.6	1.0	0.8	0.8	C1
206	WDR54	3.2	2.0	2.7	2.3	2.6	C2
207	ZNF511	3.2	2.1	2.7	2.1	2.1	C2
208	ST8SIA6	3.2	3.7	2.1	2.0	2.0	C4
209	IL17RE	3.1	1.5	1.4	1.1	0.9	C1
210	ZNF404	3.1	2.0	2.8	2.1	2.8	C2

		Fold change (adjusted pvalue <0.05)					
		Hypoxia	DMOG	IOX2	BNS	BIQ	Cluster
211	SNCG	3.1	1.2	0.8	1.1	0.9	C1
212	MID1	3.1	2.7	2.0	1.5	1.6	C4
213	FAM211B	3.1	4.8	1.0	0.9	1.1	C4
214	FOSL2	3.1	2.2	2.2	1.9	2.0	C2
215	TXNIP	3.1	3.3	2.3	1.9	2.2	C4
216	SGPP2	3.1	1.8	2.2	1.4	1.7	C1
217	C1orf54	3.1	1.7	2.5	2.5	2.6	C2
218	GAPDH	3.1	2.7	2.6	2.3	2.7	C2
219	TNNT1	3.1	1.8	1.9	1.5	1.6	C1
220	KIAA1715	3.1	2.2	2.5	2.3	2.4	C2
221	COL4A3	3.0	3.6	1.5	1.6	1.9	C4
222	YEATS2	3.0	3.6	2.5	2.2	2.5	C4
223	MAPT	3.0	1.8	2.4	1.9	2.2	C2
224	SH2B2	3.0	2.8	2.6	1.9	2.3	C2
225	APOLD1	3.0	1.9	1.7	1.8	1.7	C1
226	BMF	3.0	1.7	1.2	1.5	1.2	C1
227	ENO1	3.0	2.8	2.0	2.1	2.1	C4
228	GPI	3.0	3.5	2.2	2.1	2.2	C4
229	SFMBT2	3.0	2.2	1.4	1.5	1.5	C1
230	FGF11	3.0	3.3	2.1	2.0	2.2	C4
231	SLC7A5	3.0	2.9	2.1	1.4	2.1	C4
232	SYT8	3.0	2.1	0.9	1.3	0.9	C1
233	FXYD6	3.0	1.9	1.4	1.3	1.2	C1
234	CNNM1	2.9	2.6	3.1	2.5	2.8	C2
235	IGFBP6	2.9	2.2	1.3	0.9	1.2	C1
236	GAD1	2.9	1.5	1.5	1.3	1.4	C1
237	LRRC3DN	2.9	2.9	1.5	1.3	1.4	C4
238	NCKIPSD	2.9	2.7	2.7	2.1	2.4	C2
239	PGAM1	2.9	3.1	2.6	2.5	2.3	C2
240	CXCR4	2.9	5.9	1.2	1.2	1.1	C4
241	RBM43	2.9	2.0	2.1	1.9	2.2	C2
242	AGO4	2.9	3.1	2.5	2.0	2.6	C2
243	STC2	2.9	2.5	1.7	1.6	1.4	C4
244	GALNT18	2.9	2.4	1.8	1.5	1.2	C4
245	ASCL2	2.9	1.0	2.8	2.5	2.2	C2
246	GPR157	2.9	2.8	1.5	1.4	1.7	C4
247	FAM216A	2.9	1.9	2.1	1.6	1.8	C2
248	ADORA2B	2.9	1.8	2.0	1.5	1.5	C1
249	FBXL8	2.9	2.0	1.9	1.6	2.0	C2
250	CLIP3	2.9	2.6	2.2	2.0	2.5	C2
251	KRT17	2.9	1.8	0.8	0.7	0.6	C1
252	GRIN3B	2.9	2.4	1.8	1.1	1.5	C4
253	ATF3	2.8	6.5	1.5	1.4	2.0	C4
254	ASPH	2.8	2.3	2.1	1.7	1.9	C2
255	ULBP1	2.8	1.6	2.7	1.2	2.0	C2
256	PLXNB3	2.8	2.0	1.7	1.4	1.6	C1
257	CREG2	2.8	1.9	1.7	1.1	1.4	C1
258	EDARADD	2.8	3.5	2.0	2.1	2.1	C4
259	FZD8	2.8	4.4	1.4	0.9	1.2	C4
260	STARD4	2.8	2.0	1.2	1.1	1.3	C1
261	DPCD	2.8	2.0	2.3	2.2	2.1	C2
262	OBSL1	2.8	3.4	1.7	1.4	1.5	C4
263	AHNAK2	2.8	1.8	1.1	1.0	0.8	C1
264	PCED1B	2.7	1.4	1.4	1.2	1.2	C1
265	FAM47E-STBD1	2.7	3.2	2.6	2.0	2.7	C2
266	ATP1B1	2.7	2.5	1.0	1.0	0.9	C4
267	HCFC1R1	2.7	1.4	1.3	1.3	1.1	C1
268	DHRS2	2.7	1.4	2.8	2.6	4.7	C2
269	FAM110C	2.7	2.4	1.6	1.5	1.7	C4
270	DEGS2	2.7	1.9	1.6	1.5	1.3	C1
271	C3orf58	2.7	2.3	2.6	2.2	2.4	C2
272	CEP250	2.7	2.2	2.1	1.7	1.8	C2
273	SORL1	2.7	2.2	1.5	1.1	1.6	C4
274	PIM1	2.7	3.0	1.4	1.2	1.3	C4
275	APAF1	2.7	2.6	2.2	2.0	2.4	C2
276	TMEM45B	2.7	2.6	1.7	1.2	1.4	C4
277	PIP5KL1	2.7	0.9	2.0	1.5	1.7	C2
278	PPME1	2.7	2.3	2.5	2.2	2.3	C2
279	FAM47E	2.7	3.2	2.6	2.0	2.7	C2
280	TENC1	2.7	1.6	1.7	1.5	1.7	C1

		Fold change (adjusted pvalue <0.05)					
		Hypoxia	DMOG	IOX2	BNS	BIQ	Cluster
281	LDHD	2.7	0.9	1.6	1.2	1.1	C1
282	APLP1	2.7	1.4	2.7	2.1	2.7	C2
283	PAQR5	2.7	1.5	1.8	1.6	1.3	C1
284	PER1	2.7	2.1	2.2	1.9	1.9	C2
285	TNFAIP8	2.7	3.1	1.4	1.5	0.9	C4
286	SLC6A3	2.7	2.5	0.9	1.7	1.6	C4
287	RPL7	2.7	0.6	0.6	0.7	0.7	C1
288	SERPINE1	2.7	4.0	1.9	1.2	1.4	C4
289	SCD	2.6	1.3	1.0	1.0	0.9	C1
290	KIAA1683	2.6	2.9	1.6	1.4	2.0	C4
291	ARID3A	2.6	2.2	1.4	1.3	1.1	C4
292	INHBA	2.6	2.6	0.9	0.8	0.5	C4
293	BTN2A2	2.6	1.4	1.6	1.1	1.7	C1
294	PROCA1	2.6	1.5	1.6	1.6	1.8	C1
295	VEGFC	2.6	4.0	1.5	1.3	1.4	C4
296	PVRL4	2.6	3.6	1.4	1.2	1.2	C4
297	ORAI3	2.6	1.9	1.7	1.6	1.9	C2
298	ALDH3B1	2.6	1.0	1.4	1.1	1.4	C1
299	KCTD12	2.6	1.9	2.4	2.1	1.8	C2
300	BCKDK	2.6	1.6	2.1	1.7	1.8	C2
301	SAPCD1	2.6	1.0	1.3	1.2	1.3	C1
302	FAM114A1	2.6	2.4	1.9	1.3	2.3	C4
303	TBC1D8B	2.6	2.0	3.1	2.5	3.2	C2
304	FAM117B	2.6	1.9	2.0	2.0	1.8	C2
305	PEX11A	2.6	1.7	2.8	2.3	2.8	C2
306	CCBP2	2.6	1.6	1.4	1.4	1.2	C1
307	TNIP1	2.6	2.6	1.8	1.7	1.8	C4
308	MMEL1	2.6	1.2	1.7	1.6	1.2	C1
309	EGFR	2.6	4.5	0.9	0.9	0.7	C4
310	ZNF292	2.6	2.6	2.1	2.0	2.1	C2
311	FOXN3	2.6	2.5	1.9	1.5	1.8	C4
312	TUBA4A	2.6	1.8	1.7	1.3	1.5	C1
313	VWA7	2.6	1.2	1.4	0.9	1.5	C1
314	STRA6	2.6	1.0	0.4	0.6	0.3	C1
315	PYGL	2.6	1.7	2.1	1.6	1.7	C2
316	MYEOV	2.6	3.1	0.6	0.7	0.3	C4
317	SLC6A6	2.6	2.7	1.0	1.1	1.1	C4
318	EVA1B	2.6	2.6	2.6	2.0	2.8	C2
319	SH3BP2	2.5	2.0	1.4	1.4	1.3	C4
320	GPR115	2.5	3.1	1.2	1.0	0.9	C4
321	DYRK4	2.5	1.8	1.9	1.5	2.0	C2
322	CNFN	2.5	1.8	1.6	1.6	1.8	C2
323	LRRC3	2.5	2.4	1.4	1.2	1.3	C4
324	EIF4EBP1	2.5	1.9	2.0	1.5	1.7	C2
325	PKM	2.5	2.9	2.2	2.2	2.1	C4
326	RAB20	2.5	1.9	1.8	1.9	1.8	C2
327	DNASE1	2.5	3.0	1.5	1.4	1.5	C4
328	HMOX1	2.5	2.0	2.3	1.4	5.8	C2
329	MAST1	2.5	1.7	1.4	0.9	1.3	C1
330	C7orf60	2.5	2.0	2.1	2.2	2.1	C2
331	JAG2	2.5	1.8	1.6	1.4	1.3	C1
332	KRT16	2.5	1.7	0.4	0.4	0.2	C1
333	PGAM2	2.5	2.2	2.0	1.7	2.4	C2
334	ARRDC3	2.5	2.4	1.3	1.2	1.5	C4
335	BCAS1	2.5	1.9	0.9	1.0	0.9	C1
336	KIAA1217	2.5	2.5	1.2	1.2	1.5	C4
337	C11orf49	2.5	2.2	1.5	1.4	1.5	C4
338	LOXL1	2.5	2.2	1.6	1.1	0.9	C4
339	TPI1	2.5	2.2	2.6	2.4	2.5	C2
340	SLC27A1	2.5	1.7	1.8	1.3	1.7	C2
341	LPCAT2	2.5	2.1	0.9	1.1	1.0	C4
342	NAT6	2.5	1.1	1.4	1.3	1.6	C1
343	GABARAPL1	2.5	2.6	2.0	1.5	3.2	C2
344	CDCA7L	2.5	1.9	2.5	2.3	2.2	C2
345	NTSR1	2.5	1.4	1.4	1.3	0.8	C1
346	PDGFRL	2.5	1.4	1.7	1.4	1.7	C2
347	DHRS13	2.5	1.4	2.3	1.9	2.1	C2
348	AMIGO2	2.5	2.2	2.0	1.6	1.6	C4
349	KIAA0195	2.5	2.8	1.8	1.5	1.9	C4
350	THAP8	2.5	1.8	2.1	2.0	2.0	C2

		Fold change (adjusted pvalue <0.05)					
		Hypoxia	DMOG	IOX2	BNS	BIQ	Cluster
351	BBX	2.4	2.2	2.6	2.0	2.3	C2
352	AC022400.2	2.4	2.3	4.4	1.7	3.8	C2
353	DHX40	2.4	1.9	1.9	1.7	1.9	C2
354	PCOLCE	2.4	1.2	1.5	1.2	1.3	C1
355	ZMYND8	2.4	0.6	1.1	1.1	1.0	C1
356	BRSK1	2.4	1.5	0.9	0.7	0.9	C1
357	BCAN	2.4	1.8	1.5	1.4	1.9	C2
358	DSCAM	2.4	1.6	1.2	1.1	1.2	C1
359	YPEL1	2.4	2.6	1.7	1.7	2.1	C4
360	PROS1	2.4	1.3	1.8	1.4	1.8	C2
361	CALCOCO1	2.4	2.0	1.6	1.5	2.1	C2
362	PROSAPIP1	2.4	1.8	1.6	1.2	1.6	C1
363	PTPRD	2.4	2.9	1.8	1.4	1.7	C4
364	DSC2	2.4	3.7	1.5	1.0	1.3	C4
365	SPRR1B	2.4	1.9	0.8	0.8	0.5	C4
366	C17orf107	2.4	1.3	1.6	1.3	1.6	C1
367	DDX41	2.4	1.5	2.1	1.7	1.9	C2
368	CSGALNACT1	2.4	2.4	1.1	0.9	1.1	C4
369	OOEP	2.4	1.2	1.8	1.6	1.6	C1
370	VIM	2.4	2.0	1.5	1.3	1.3	C4
371	EPHA6	2.4	1.6	1.8	1.7	1.8	C2
372	PPP2R2A	2.4	2.4	1.6	1.4	1.7	C4
373	SPOCK1	2.4	2.8	1.0	1.0	0.7	C4
374	LGALS1	2.4	1.4	1.5	1.3	1.5	C1
375	ITPR1	2.4	4.6	0.9	0.9	0.8	C4
376	SYNGR3	2.4	1.6	1.1	0.9	1.1	C1
377	C20orf96	2.3	1.6	1.7	1.2	1.4	C1
378	ELF3	2.3	1.6	1.2	1.3	1.4	C1
379	BCKDHA	2.3	1.8	1.9	1.8	1.9	C2
380	PLOD2	2.3	3.6	1.9	1.7	1.8	C4
381	FYN	2.3	1.9	1.7	1.6	1.5	C2
382	CD109	2.3	2.8	1.3	1.1	1.0	C4
383	TMEM105	2.3	1.5	1.2	1.1	1.2	C1
384	SEC14L2	2.3	2.7	1.1	1.2	1.1	C4
385	GPR132	2.3	2.0	0.8	0.8	0.7	C4
386	C2orf81	2.3	1.2	1.9	1.7	1.9	C2
387	GPER	2.3	1.9	1.5	1.5	1.1	C1
388	DPYSL2	2.3	1.8	1.4	1.3	1.2	C1
389	HMGCLL1	2.3	1.2	1.4	1.6	1.2	C1
390	TMBIM1	2.3	0.9	0.8	0.8	0.5	C1
391	TGFBI	2.3	3.0	1.1	1.1	1.3	C4
392	CHRNB4	2.3	1.5	1.4	1.4	1.9	C1
393	MGC20647	2.3	2.0	0.7	0.5	0.3	C4
394	GPR179	2.3	2.8	1.3	1.3	1.3	C4
395	ZNF185	2.3	1.8	1.3	1.2	1.0	C1
396	WBSCR27	2.3	1.3	1.9	1.7	2.4	C2
397	BRWD3	2.3	2.1	2.3	2.0	2.4	C2
398	HERC3	2.3	2.5	1.6	1.5	1.8	C4
399	FAM57A	2.3	2.0	2.6	2.1	2.1	C2
400	MTMR11	2.3	1.5	1.5	1.2	0.9	C1
401	PDLIM2	2.3	2.5	1.1	1.1	1.0	C4
402	KRT7	2.3	1.4	0.6	0.8	0.5	C1
403	IKBIP	2.3	2.1	2.0	2.1	2.0	C2
404	C1orf145	2.3	1.4	1.5	1.1	1.4	C2
405	S100A6	2.3	1.7	1.0	0.8	0.9	C1
406	LENEP	2.3	1.8	1.8	1.5	1.3	C2
407	BCL11B	2.3	1.3	2.0	1.7	1.5	C2
408	TRIOBP	2.3	1.8	1.3	1.1	1.3	C4
409	ANKRD9	2.3	1.9	2.2	1.4	1.6	C2
410	MAP3K8	2.3	1.6	2.0	1.4	2.1	C2
411	TNFSF10	2.3	0.9	0.8	1.5	0.9	C1
412	TUBA1A	2.3	2.3	1.4	1.2	1.5	C4
413	CDK18	2.3	1.2	1.4	1.1	1.0	C1
414	RP11-159G9.5	2.3	2.1	1.9	2.1	2.1	C2
415	SAT1	2.3	1.4	0.9	1.0	0.9	C1
416	WFDC2	2.3	1.5	2.0	1.0	1.6	C2
417	RAB11FIP5	2.3	1.9	1.9	1.5	1.6	C2
418	LTBP2	2.3	1.2	1.3	0.9	1.3	C1
419	FAM214B	2.3	1.6	1.3	1.1	1.2	C1
420	PDZD4	2.3	1.6	1.7	1.4	1.6	C2

		Fold change (adjusted pvalue <0.05)					
		Hypoxia	DMOG	IOX2	BNS	BIQ	Cluster
421	SORBS3	2.3	1.5	1.4	1.1	1.3	C1
422	PRSS27	2.3	0.9	1.0	1.3	0.8	C1
423	KLF7	2.3	2.6	1.3	1.3	1.2	C4
424	TIPARP	2.3	1.5	1.4	1.4	1.3	C1
425	BPNT1	2.3	1.4	1.8	1.5	1.6	C2
426	NUDT18	2.3	1.3	2.0	2.0	2.0	C2
427	SLC7A11	2.3	1.1	3.0	1.1	7.8	C2
428	SEMA4B	2.2	3.4	1.2	1.2	1.2	C4
429	CAV1	2.2	1.8	0.8	0.8	0.5	C4
430	ADA	2.2	2.4	1.6	1.1	1.2	C4
431	SLC25A45	2.2	1.3	1.1	1.1	1.2	C1
432	EMP3	2.2	1.6	1.8	1.6	2.0	C2
433	TM4SF19	2.2	1.8	0.8	1.1	0.9	C1
434	PHF21A	2.2	1.6	1.6	1.3	1.6	C1
435	SHC2	2.2	1.8	1.2	0.8	0.9	C1
436	PPP2R5B	2.2	2.1	1.9	1.6	1.6	C2
437	DGKD	2.2	2.7	1.2	1.1	1.3	C4
438	PLAGL1	2.2	2.8	1.9	1.6	1.9	C4
439	MDGA2	2.2	2.6	2.1	1.5	1.9	C4
440	RGS22	2.2	1.1	1.0	1.2	1.0	C1
441	CLMN	2.2	1.7	1.2	1.1	1.2	C4
442	C11orf35	2.2	1.3	1.8	1.4	1.5	C2
443	RELT	2.2	1.8	2.2	1.8	1.9	C2
444	NECAB2	2.2	1.4	1.0	0.9	1.2	C1
445	SEMA4G	2.2	1.2	1.4	1.1	1.3	C1
446	MYO15B	2.2	1.5	1.7	1.5	1.9	C2
447	NFATC4	2.2	0.7	1.2	0.8	0.8	C1
448	VEGFB	2.2	1.8	1.7	1.6	1.7	C2
449	TRIB2	2.2	1.8	1.2	1.2	0.8	C4
450	RNF223	2.2	1.5	2.0	1.4	1.7	C2
451	PGRMC2	2.2	1.8	1.7	1.5	1.8	C2
452	S100P	2.2	2.8	1.6	1.3	1.8	C4
453	EEF2K	2.2	1.8	1.6	1.3	1.5	C1
454	STAT6	2.2	1.2	1.2	0.9	0.8	C1
455	JUN	2.2	2.3	1.6	1.3	1.7	C4
456	NGEF	2.2	1.7	1.2	0.8	0.9	C1
457	TMSB10	2.2	1.8	1.5	1.4	1.5	C1
458	MPZL2	2.2	1.9	1.3	1.3	1.2	C4
459	MUC20	2.2	1.4	1.3	1.2	1.0	C1
460	PCDHB3	2.2	1.7	2.0	1.8	2.0	C2
461	IRS2	2.2	2.3	1.5	1.2	1.7	C4
462	KDM5B	2.2	1.8	1.7	1.5	1.6	C2
463	DBP	2.2	1.1	1.2	1.3	1.1	C1
464	CEACAM5	2.2	2.0	1.6	1.3	1.5	C4
465	C3orf67	2.2	1.3	1.6	1.7	1.9	C2
466	TMEM123	2.1	2.1	1.4	1.3	1.2	C4
467	RAB26	2.1	0.7	0.9	0.8	1.1	C1
468	HMGCL	2.1	1.3	1.9	1.7	2.0	C2
469	TMEM107	2.1	1.4	1.9	1.6	2.0	C2
470	FAM57B	2.1	0.9	1.3	1.2	1.4	C2
471	MXRA7	2.1	1.9	1.2	1.1	1.1	C4
472	MXD1	2.1	1.9	1.6	1.3	1.3	C4
473	IFI27L1	2.1	1.8	2.0	1.7	2.4	C2
474	RIOK3	2.1	1.7	1.7	1.6	1.6	C2
475	SRD5A3	2.1	2.6	1.6	1.3	1.6	C4
476	RBPJ	2.1	2.1	1.6	1.6	1.6	C4
477	KDM4C	2.1	1.9	2.0	1.8	2.0	C2
478	AMZ1	2.1	2.7	1.8	1.7	1.4	C4
479	GDF15	2.1	2.3	1.8	1.3	2.4	C2
480	SNTB1	2.1	1.9	2.2	1.3	1.8	C2
481	RLF	2.1	2.2	1.8	1.8	1.8	C2
482	MST1	2.1	1.0	1.5	1.3	1.3	C2
483	MEX3D	2.1	2.0	1.4	1.2	1.2	C4
484	MSANTD3	2.1	3.0	1.6	1.4	1.7	C4
485	PDK3	2.1	1.7	2.0	1.8	1.7	C2
486	FAM160A1	2.1	2.3	1.6	1.3	1.7	C4
487	FTL	2.1	1.7	1.8	1.7	2.5	C2
488	QPCTL	2.1	1.2	1.4	1.3	1.4	C1
489	GTF2IRD2B	2.1	2.4	1.8	1.4	1.7	C4
490	RNF208	2.1	1.4	1.5	1.4	1.4	C1

		Fold change (adjusted pvalue <0.05)					
		Hypoxia	DMOG	IOX2	BNS	BIQ	Cluster
491	FGFR3	2.1	1.4	0.8	0.9	0.8	C1
492	GPRC5A	2.1	2.5	1.1	1.1	1.1	C4
493	TSPO	2.1	1.7	1.3	1.1	1.1	C1
494	PXDN	2.1	2.2	1.4	1.1	1.2	C4
495	ANXA1	2.1	2.1	0.8	0.8	0.5	C4
496	PCSK4	2.1	1.1	1.0	1.0	1.2	C1
497	FAM117A	2.1	1.1	1.0	1.1	1.3	C1
498	HIST1H2BN	2.1	1.7	1.9	1.5	1.7	C2
499	CA4	2.1	2.0	1.3	1.1	1.4	C4
500	ZBTB25	2.1	1.7	1.9	1.5	1.8	C2
501	SCAPER	2.1	1.7	1.9	1.6	1.8	C2
502	TMEM8B	2.1	1.2	1.6	1.5	1.8	C2
503	RUNX1	2.1	2.5	1.4	1.2	1.3	C4
504	AP000350.4	2.1	2.0	1.8	2.0	1.8	C2
505	CCDC58	2.1	1.3	1.8	2.3	1.8	C2
506	CDKN1B	2.1	1.5	1.3	1.3	1.3	C1
507	SLC35E3	2.1	1.2	1.8	1.6	1.8	C2
508	DARS	2.1	1.9	1.7	1.8	1.7	C2
509	BAG1	2.1	1.0	1.0	1.0	0.9	C1
510	LMO7	2.1	2.0	1.1	1.0	0.9	C4
511	RAP2B	2.1	2.1	1.2	1.1	1.2	C4
512	NFIL3	2.1	2.1	1.6	1.4	1.5	C4
513	HLA-A	2.1	1.6	2.1	1.7	2.0	C2
514	FEM1C	2.1	2.0	1.8	1.7	1.8	C2
515	TMTC2	2.1	2.3	1.9	1.7	2.1	C2
516	TMEM102	2.1	1.6	1.2	1.2	1.2	C1
517	LAMB3	2.1	2.2	0.9	0.8	0.6	C4
518	TPM2	2.1	1.9	1.1	0.9	0.9	C4
519	FAM127A	2.1	1.6	2.1	1.9	2.2	C2
520	TMPRSS13	2.1	1.9	1.4	1.2	1.4	C4
521	PBXIP1	2.1	1.6	1.3	1.3	1.5	C1
522	ZNF84	2.1	1.8	1.5	1.4	1.6	C1
523	AHNAK	2.1	2.3	1.2	1.2	1.1	C4
524	NXPH4	2.1	1.8	1.7	1.3	1.2	C1
525	ECE1	2.1	2.3	1.0	1.1	0.8	C4
526	ZNF532	2.1	2.4	1.3	0.9	1.2	C4
527	DNAJC18	2.1	1.3	1.4	1.3	1.6	C2
528	HLA-C	2.0	1.9	2.0	1.9	1.9	C2
529	MAFF	2.0	3.2	1.1	0.8	1.0	C4
530	C17orf103	2.0	1.6	1.3	1.3	1.6	C1
531	LZTFL1	2.0	1.7	1.4	1.3	1.4	C2
532	CRIP1	2.0	1.9	1.0	1.4	1.1	C1
533	AL031666.2	2.0	0.6	0.8	1.0	0.9	C1
534	SBK2	2.0	0.9	0.4	0.6	0.2	C1
535	TSC22D2	2.0	2.7	1.3	1.2	1.2	C4
536	ACACB	2.0	1.0	1.6	1.6	1.8	C2
537	PPM1N	2.0	1.1	1.6	1.1	1.6	C2
538	FAM84A	2.0	1.6	1.7	1.4	2.1	C2
539	ANO6	2.0	2.6	1.2	1.1	1.1	C4
540	DKFZP686J19100	2.0	1.8	0.6	0.7	0.6	C4
541	KDM4B	2.0	2.4	1.7	1.7	1.6	C4
542	DDR1	2.0	1.5	1.1	1.0	1.0	C1
543	CTF1	2.0	0.8	1.0	0.8	1.0	C1
544	PGAM4	2.0	2.1	1.8	1.7	1.8	C2
545	ZNF449	2.0	1.3	1.7	1.3	1.7	C2
546	RNF39	2.0	2.1	1.5	1.3	1.5	C4
547	PCSK1N	2.0	1.6	2.8	1.5	2.4	C2
548	ZNF337	2.0	1.8	1.8	1.4	1.7	C2
549	IMMP2L	2.0	2.3	2.2	2.0	2.8	C2
550	EFHD1	2.0	1.3	1.1	1.1	0.7	C1
551	BTG1	2.0	2.1	1.4	1.3	1.4	C4
552	SH3RF2	2.0	0.9	0.6	0.6	0.3	C1
553	ZNF654	2.0	1.9	1.8	2.1	1.9	C2
554	SDK1	2.0	1.6	1.3	1.1	1.1	C1
555	ZC3HAV1L	2.0	2.1	2.2	1.8	1.9	C2
556	NARF	2.0	2.4	1.7	1.7	1.7	C4
557	SEMA6C	2.0	2.7	1.2	1.3	1.6	C4
558	TMEM143	2.0	1.4	1.3	1.3	1.4	C1
559	ZNF581	2.0	1.8	1.3	1.2	1.5	C4
560	ARHGAP4	2.0	1.1	1.4	1.2	1.3	C1
561	C9orf172	2.0	1.7	2.1	1.6	2.0	C2
562	COL1A1	2.0	1.3	1.2	1.1	1.2	C1
563	FAM219A	2.0	2.6	1.7	1.5	2.0	C4
564	MIF	2.0	2.1	1.8	1.7	1.7	C2
565	SAP30	2.0	2.1	2.3	2.1	2.2	C2

Appendix 3: Genes upregulated by hypoxia in both RNA-seq and microarray

		Fold change - RNA-seq (adjusted p-value < 0.05)						Fold change - microarray (adjusted p-value < 0.05)			
		Hypoxia	DMOG	IOX2	BNS	BIQ	Cluster	Hypoxia	DMOG	IOX2	IOX2FIHi
1	CA9	654.6	648.8	157.5	129.4	111.4	C4	9.3	7.3	1.9	9.3
2	LOX	66.4	23.0	27.9	11.0	22.6	C1	31.0	3.7	12.5	10.8
3	CYP1A1	50.3	4.1	3.3	3.5	5.6	C1	3.6	1.2	2.2	0.7
4	RNF183	47.4	25.3	23.0	18.7	20.1	C1	6.0	5.5	10.3	9.4
5	MAP7D2	46.9	43.8	5.6	5.0	5.1	C4	2.9	2.6	1.1	1.2
6	NDRG1	43.2	59.2	13.4	12.3	16.8	C4	11.3	8.5	4.7	7.6
7	ISM2	41.9	18.0	17.9	9.7	10.0	C1	3.8	2.2	3.1	2.7
8	PPFIA4	35.1	22.4	27.1	20.8	28.6	C2	24.9	18.4	25.0	28.7
9	ADM	32.6	29.4	13.1	9.3	13.0	C4	16.1	6.9	7.5	14.5
10	PFKFB4	24.5	21.7	12.8	11.0	11.9	C4	7.4	6.2	4.6	6.7
11	TLE6	20.4	9.4	9.5	5.3	6.6	C1	2.2	1.5	2.6	2.5
12	ALDOC	17.5	12.4	12.2	8.5	11.4	C2	12.8	6.7	7.5	8.6
13	PDK1	15.9	10.8	9.4	8.2	9.5	C2	2.1	2.2	1.7	1.5
14	IGFBP3	14.6	12.6	4.1	2.8	4.8	C4	9.0	4.8	2.2	9.7
15	PGM1	14.0	12.8	12.3	10.7	11.3	C2	3.1	4.1	3.9	2.8
16	UPK1A	13.6	3.7	3.0	2.2	2.5	C1	10.7	3.9	5.2	4.7
17	SH3GL3	13.3	9.7	5.4	4.1	5.8	C4	4.3	3.5	3.6	1.7
18	SCNN1B	13.1	9.9	3.0	2.2	1.7	C4	3.6	2.2	1.3	1.5
19	TMEM45A	13.1	12.3	6.3	5.0	6.4	C4	14.5	16.3	7.6	9.8
20	BNIP3	12.7	11.0	9.2	8.7	9.3	C2	5.2	6.2	5.4	3.3
21	ANGPTL4	12.1	13.5	5.7	3.2	5.3	C4	2.5	1.5	1.7	2.3
22	SYDE1	11.9	6.9	5.2	3.9	4.0	C1	2.8	1.8	2.6	4.8
23	SPAG4	11.7	6.8	8.7	6.6	7.7	C2	3.9	2.9	4.4	3.6
24	ANKRD37	11.1	13.4	5.3	4.8	5.6	C4	109.3	19.6	12.4	46.9
25	ENO2	11.0	9.9	6.0	4.3	5.7	C4	11.8	6.4	7.1	8.1
26	BNIP3L	10.3	8.9	5.7	5.1	5.8	C4	10.9	5.3	5.7	6.5
27	RNF165	10.2	4.5	6.8	4.6	5.7	C2	9.0	4.9	7.6	6.9
28	C1orf51	9.8	6.7	11.6	8.5	9.9	C2	4.0	4.3	7.4	6.4
29	SPRY1	9.2	8.1	8.0	6.9	9.1	C2	5.4	4.4	5.8	2.8
30	EFEMP2	9.0	3.1	3.8	2.9	3.1	C1	2.9	1.3	2.1	1.5
31	GPR146	9.0	6.9	7.6	5.2	7.4	C2	3.1	2.7	3.3	3.7
32	FAM162A	8.7	8.4	5.5	4.4	5.1	C4	7.5	5.1	4.5	5.1
33	PLIN2	8.5	3.9	4.7	2.2	3.2	C1	6.1	2.5	6.9	9.1
34	FOS	8.5	6.5	4.3	3.4	3.5	C4	7.2	3.3	3.7	5.5
35	RORA	8.0	7.6	5.0	4.0	5.2	C4	5.7	4.5	4.4	3.0
36	FAM13A	7.7	7.6	2.7	1.8	2.6	C4	3.5	2.1	1.5	2.0
37	DDIT4	7.6	5.4	3.5	3.3	3.4	C4	4.4	2.1	2.4	3.3
38	PGK1	7.0	7.2	4.7	4.3	4.4	C4	2.8	2.9	2.1	2.0
39	DPYSL4	6.7	3.8	4.5	3.6	3.5	C2	5.4	3.8	6.0	5.6
40	RRAGD	6.6	3.1	4.6	3.0	4.2	C2	3.8	1.7	3.5	3.1
41	MT1X	6.5	4.2	1.7	2.4	1.3	C1	4.8	1.9	1.8	4.0
42	INSIG2	6.5	5.4	3.1	2.8	3.4	C4	6.6	3.8	3.9	3.8
43	WSB1	6.4	3.6	2.5	1.9	2.3	C1	5.3	1.6	4.2	3.8
44	MXI1	6.3	5.5	4.1	3.0	4.0	C4	5.1	2.1	3.4	3.0
45	SMAD9	6.3	5.0	4.1	3.2	3.9	C4	2.5	1.9	1.7	1.3
46	ANKZF1	6.1	4.3	5.1	4.5	4.7	C2	3.0	2.0	2.6	2.6
47	HK2	6.1	8.6	3.6	3.8	3.6	C4	5.4	4.1	2.9	4.1
48	EGLN3	6.0	7.6	1.9	1.7	1.7	C4	2.5	2.9	1.2	2.8
49	WISP2	5.9	4.1	2.2	1.6	1.8	C1	4.5	2.1	2.2	3.7
50	ANG	5.9	6.0	3.7	2.8	4.6	C4	4.6	1.8	2.8	2.3
51	LDHA	5.8	6.8	5.1	5.1	4.8	C2	4.3	4.1	4.0	3.6
52	STYK1	5.7	3.6	2.7	2.2	3.8	C1	2.8	1.7	1.7	2.2
53	ERO1L	5.7	5.4	3.1	2.7	2.7	C4	5.4	4.1	3.4	3.3
54	FUT11	5.6	6.0	4.2	3.5	3.9	C4	7.7	3.9	4.4	4.4
55	PAM	5.5	5.5	4.8	3.5	4.6	C2	2.1	2.3	2.1	1.4
56	GBE1	5.5	5.9	4.0	4.1	4.1	C4	4.8	7.5	4.9	3.5
57	C1orf116	5.5	4.7	1.4	1.5	1.1	C4	2.0	1.8	1.1	1.8
58	C8orf58	5.3	5.0	3.1	2.9	2.8	C4	3.5	2.9	2.1	3.4
59	VLDLR	5.3	5.0	5.0	4.1	4.8	C2	6.4	5.0	6.8	5.1
60	PPP1R3E	5.1	3.3	3.0	2.4	3.2	C2	2.9	2.1	1.6	1.8

		Fold change - RNA-seq (adjusted p-value < 0.05)						Fold change - microarray (adjusted p-value < 0.05)			
		Hypoxia	DMOG	IOX2	BNS	BIQ	Cluster	Hypoxia	DMOG	IOX2	IOX2FIHi
61	ZNF395	5.1	4.7	2.8	2.5	2.5	C4	4.2	2.5	2.3	2.6
62	GYS1	5.0	3.4	4.0	3.4	3.9	C2	3.2	2.1	2.4	2.4
63	P4HA2	5.0	5.6	4.1	3.2	3.9	C4	3.4	3.7	2.9	2.7
64	P4HA1	4.9	8.0	3.7	3.6	4.0	C4	4.4	4.4	2.9	2.5
65	ERRFI1	4.8	6.5	2.1	1.4	2.0	C4	2.2	2.3	1.6	3.1
66	RNF122	4.7	3.2	3.5	3.1	3.5	C2	2.3	1.7	2.0	2.0
67	CCNG2	4.7	3.9	2.6	2.4	2.8	C4	6.2	4.3	3.0	2.2
68	HLA-B	4.7	2.2	3.6	3.0	3.1	C2	2.2	1.3	2.2	2.1
69	VEGFA	4.6	5.2	3.0	2.3	2.7	C4	4.5	2.9	2.9	4.4
70	KCTD11	4.5	5.9	2.5	2.3	2.4	C4	3.1	2.9	2.1	2.8
71	CCL28	4.4	2.5	3.9	3.0	3.5	C2	2.7	1.7	1.9	1.7
72	ALOXE3	4.4	3.0	2.5	1.6	1.7	C1	2.1	1.8	2.0	2.2
73	CYP1B1	4.4	1.2	1.5	1.5	1.4	C1	2.2	1.4	1.5	1.3
74	OLFML2A	4.3	3.4	1.7	1.4	1.5	C4	2.6	1.8	1.6	0.7
75	QSOX1	4.3	5.2	2.4	2.3	2.3	C4	2.1	2.1	1.4	1.9
76	RNASE4	4.3	3.6	2.9	2.0	3.8	C2	4.0	1.6	2.3	2.1
77	NOL3	4.2	2.7	2.5	2.1	2.6	C2	4.1	1.3	1.7	2.2
78	PFKFB3	4.2	5.4	2.6	2.7	2.6	C4	8.2	7.0	4.7	7.7
79	ITGA5	4.1	6.1	2.1	1.6	1.7	C4	2.2	2.1	1.3	3.2
80	KRT15	4.1	2.6	0.9	1.3	0.9	C1	3.1	1.9	1.2	2.3
81	EGLN1	3.9	4.4	3.6	3.3	3.8	C2	5.7	6.1	5.3	6.4
82	CKB	3.9	1.6	1.9	1.4	1.4	C1	2.1	1.0	0.9	0.8
83	CITED2	3.9	2.8	2.0	1.7	1.9	C1	5.2	2.5	3.7	3.6
84	PLEKHA2	3.7	2.3	2.4	2.3	2.2	C1	2.2	1.5	2.0	1.7
85	PTRF	3.7	2.6	3.6	2.7	3.0	C2	3.0	2.9	3.4	3.1
86	SOX9	3.5	4.7	1.2	1.4	1.5	C4	3.3	1.8	1.2	0.9
87	VPS37D	3.5	2.8	2.1	2.0	1.8	C4	2.6	1.6	1.6	2.1
88	SLC2A1	3.4	3.4	2.1	2.0	2.2	C4	4.1	2.4	2.4	3.2
89	CSRP2	3.4	2.2	3.6	2.7	2.9	C2	3.1	2.1	1.8	1.5
90	TCP11L2	3.4	3.4	2.0	1.8	2.2	C4	2.2	1.3	1.5	1.5
91	PIK3IP1	3.4	2.0	1.9	2.0	2.0	C1	2.7	1.6	2.1	1.4
92	P2RY11	3.4	2.9	2.0	2.0	2.4	C4	2.1	3.4	1.6	1.7
93	HLA-DRB1	3.3	3.1	2.5	2.6	2.0	C4	2.7	2.0	2.0	2.4
94	ALDOA	3.3	3.9	2.3	2.3	2.5	C4	2.1	1.9	1.5	2.0
95	TET1	3.3	1.7	1.3	1.5	1.2	C1	2.1	1.8	0.9	0.9
96	PFKP	3.3	3.5	2.8	2.6	2.6	C2	2.1	2.6	2.1	1.6
97	MPI	3.3	2.1	3.0	2.4	2.8	C2	2.3	1.4	2.3	1.6
98	PPP1R3C	3.3	3.7	2.7	2.6	2.4	C4	7.3	5.7	3.7	4.3
99	NUDT13	3.2	1.5	1.9	1.9	2.3	C2	2.3	1.5	1.9	1.7
100	STC1	3.2	2.8	2.8	2.6	2.3	C2	6.5	6.9	5.6	4.9
101	ZNF511	3.2	2.1	2.7	2.1	2.1	C2	4.2	2.4	3.3	3.2
102	ZNF404	3.1	2.0	2.8	2.1	2.8	C2	2.3	2.5	3.4	1.5
103	SGPP2	3.1	1.8	2.2	1.4	1.7	C1	2.3	1.8	3.1	1.8
104	KIAA1715	3.1	2.2	2.5	2.3	2.4	C2	2.6	2.2	2.7	2.5
105	YEATS2	3.0	3.6	2.5	2.2	2.5	C4	3.6	4.4	3.3	3.1
106	MAPT	3.0	1.8	2.4	1.9	2.2	C2	2.1	1.2	1.7	0.9
107	SH2B2	3.0	2.8	2.6	1.9	2.3	C2	3.0	3.0	2.5	3.5
108	NCKIPSD	2.9	2.7	2.7	2.1	2.4	C2	4.5	3.3	3.5	4.2
109	PGAM1	2.9	3.1	2.6	2.5	2.3	C2	7.2	6.8	5.8	4.9
110	RBM43	2.9	2.0	2.1	1.9	2.2	C2	2.2	1.4	1.9	1.7
111	STC2	2.9	2.5	1.7	1.6	1.4	C4	6.1	3.1	4.5	5.7
112	ADORA2B	2.9	1.8	2.0	1.5	1.5	C1	3.8	2.1	3.9	3.8
113	ATF3	2.8	6.5	1.5	1.4	2.0	C4	4.0	4.8	3.0	5.0
114	ULBP1	2.8	1.6	2.7	1.2	2.0	C2	2.1	2.3	3.2	3.5
115	HCFC1R1	2.7	1.4	1.3	1.3	1.1	C1	2.3	1.0	1.2	1.5
116	FAM110C	2.7	2.4	1.6	1.5	1.7	C4	2.9	1.8	2.7	3.2
117	DEGS2	2.7	1.9	1.6	1.5	1.3	C1	2.0	1.1	1.3	1.4
118	C3orf58	2.7	2.3	2.6	2.2	2.4	C2	3.0	2.8	3.3	1.4
119	PIM1	2.7	3.0	1.4	1.2	1.3	C4	4.6	2.3	2.7	1.7
120	TMEM45B	2.7	2.6	1.7	1.2	1.4	C4	2.6	1.3	2.0	1.7

		Fold change - RNA-seq (adjusted p-value < 0.05)						Fold change - microarray (adjusted p-value < 0.05)			
		Hypoxia	DMOG	IOX2	BNS	BIQ	Cluster	Hypoxia	DMOG	IOX2	IOX2FIHi
121	RPL7	2.7	0.6	0.6	0.7	0.7	C1	2.1	1.9	1.8	1.7
122	SCD	2.6	1.3	1.0	1.0	0.9	C1	3.0	1.6	1.6	1.6
123	FAM117B	2.6	1.9	2.0	2.0	1.8	C2	4.6	3.0	3.9	1.9
124	MMEL1	2.6	1.2	1.7	1.6	1.2	C1	5.7	2.1	3.4	5.3
125	RAB20	2.5	1.9	1.8	1.9	1.8	C2	2.1	1.4	1.7	1.3
126	DNASE1	2.5	3.0	1.5	1.4	1.5	C4	2.7	1.4	1.2	2.5
127	LOXL1	2.5	2.2	1.6	1.1	0.9	C4	2.1	2.2	1.5	2.0
128	TPI1	2.5	2.2	2.6	2.4	2.5	C2	3.2	2.6	3.3	2.5
129	NAT6	2.5	1.1	1.4	1.3	1.6	C1	2.0	0.6	1.6	2.2
130	DHRS13	2.5	1.4	2.3	1.9	2.1	C2	2.9	1.7	2.5	2.1
131	THAP8	2.5	1.8	2.1	2.0	2.0	C2	2.4	1.4	1.9	2.3
132	BBX	2.4	2.2	2.6	2.0	2.3	C2	2.5	2.0	2.3	2.1
133	YPEL1	2.4	2.6	1.7	1.7	2.1	C4	2.1	1.6	1.6	1.7
134	DDX41	2.4	1.5	2.1	1.7	1.9	C2	3.3	1.5	2.3	2.5
135	ELF3	2.3	1.6	1.2	1.3	1.4	C1	2.0	1.1	1.2	1.1
136	PLOD2	2.3	3.6	1.9	1.7	1.8	C4	3.7	2.9	2.4	2.2
137	FYN	2.3	1.9	1.7	1.6	1.5	C2	2.6	2.0	1.5	1.5
138	ZNF185	2.3	1.8	1.3	1.2	1.0	C1	2.0	1.8	1.4	1.4
139	BRWD3	2.3	2.1	2.3	2.0	2.4	C2	2.2	1.4	1.4	0.9
140	FAM57A	2.3	2.0	2.6	2.1	2.1	C2	3.3	3.7	6.4	4.7
141	IKBIP	2.3	2.1	2.0	2.1	2.0	C2	3.5	2.0	2.6	2.0
142	BCL11B	2.3	1.3	2.0	1.7	1.5	C2	2.6	2.3	2.0	1.0
143	TRIOBP	2.3	1.8	1.3	1.1	1.3	C4	2.1	0.9	1.6	2.4
144	MAP3K8	2.3	1.6	2.0	1.4	2.1	C2	3.1	3.7	3.7	3.6
145	RAB11FIP5	2.3	1.9	1.9	1.5	1.6	C2	3.3	2.1	2.2	3.2
146	TIPARP	2.3	1.5	1.4	1.4	1.3	C1	2.7	1.9	1.5	2.2
147	BPNT1	2.3	1.4	1.8	1.5	1.6	C2	2.5	1.4	1.8	1.6
148	ADA	2.2	2.4	1.6	1.1	1.2	C4	2.3	1.7	1.7	2.0
149	PHF21A	2.2	1.6	1.6	1.3	1.6	C1	2.0	1.2	1.4	0.9
150	JUN	2.2	2.3	1.6	1.3	1.7	C4	4.3	2.5	2.8	4.3
151	PCDHB3	2.2	1.7	2.0	1.8	2.0	C2	2.1	1.6	1.8	1.0
152	CEACAM5	2.2	2.0	1.6	1.3	1.5	C4	2.8	1.6	1.8	2.0
153	TMEM123	2.1	2.1	1.4	1.3	1.2	C4	5.3	3.3	3.2	2.4
154	MXD1	2.1	1.9	1.6	1.3	1.3	C4	3.8	1.4	1.7	2.4
155	RIOK3	2.1	1.7	1.7	1.6	1.6	C2	5.6	3.2	3.7	3.6
156	AMZ1	2.1	2.7	1.8	1.7	1.4	C4	2.1	1.4	1.2	3.0
157	RLF	2.1	2.2	1.8	1.8	1.8	C2	3.8	3.2	2.4	2.8
158	MEX3D	2.1	2.0	1.4	1.2	1.2	C4	2.9	2.0	2.0	2.2
159	PDK3	2.1	1.7	2.0	1.8	1.7	C2	3.5	2.3	3.1	2.7
160	QPCTL	2.1	1.2	1.4	1.3	1.4	C1	2.8	1.2	1.9	1.6
161	GTF2IRD2B	2.1	2.4	1.8	1.4	1.7	C4	2.9	2.6	2.0	2.8
162	CA4	2.1	2.0	1.3	1.1	1.4	C4	2.3	1.2	1.7	2.9
163	ZBTB25	2.1	1.7	1.9	1.5	1.8	C2	2.7	2.4	2.0	2.0
164	CCDC58	2.1	1.3	1.8	2.3	1.8	C2	2.8	2.5	2.8	2.7
165	NFIL3	2.1	2.1	1.6	1.4	1.5	C4	3.9	3.1	3.2	2.5
166	TMTC2	2.1	2.3	1.9	1.7	2.1	C2	2.1	3.1	2.6	1.4
167	LZTFL1	2.0	1.7	1.4	1.3	1.4	C2	2.2	1.1	1.4	1.4
168	TSC22D2	2.0	2.7	1.3	1.2	1.2	C4	4.0	3.2	2.5	2.6
169	ANO6	2.0	2.6	1.2	1.1	1.1	C4	2.2	2.0	1.6	1.4
170	PGAM4	2.0	2.1	1.8	1.7	1.8	C2	4.7	4.2	3.6	3.5
171	IMMP2L	2.0	2.3	2.2	2.0	2.8	C2	2.0	1.9	2.4	1.8
172	ZNF654	2.0	1.9	1.8	2.1	1.9	C2	4.8	4.3	4.2	3.2
173	SAP30	2.0	2.1	2.3	2.1	2.2	C2	2.5	1.6	2.0	1.4